BrJAC
Brazilian Journal of Analytical Chemistry
an International Scientific Journal

Special Edition of BrJAC on the

21st Brazilian Meeting on Analytical Chemistry and the 9th Ibero-American Congress of Analytical Chemistry

(21st ENQA and 9th CIAQA)

July – September 2026 Volume 13 Number 52

European Symposium on Analytical Spectrometry
August 30 – September 3, 2026
Budapest, Hungary

ESAS 2026
Budapest, Hungary

Atomic and molecular spectroscopy experts and exhibitors are all invited to participate in the ninth installment of this international conference series!

Chairs

Viktor Mihucz (ELTE)
Gábor Galbács (University of Szeged)

Plenary speakers

Vincent Motto-Ros
(Lyon, France)

Detlef Günther
(Zürich, Switzerland)

Volker Deckert
(Jena, Germany)

László Drahos
(Budapest, Hungary)

Focus topics

Inductively coupled plasma mass spectrometry
Laser-induced breakdown spectroscopy
Raman spectroscopy
Infrared spectroscopy
Mass spectroscopy
X-ray fluorescence spectroscopy
Inductively coupled plasma optical emission spectrometry
Atomic absorption spectrometry
Microwave induced plasma optical emission spectrometry
Fluorescence spectroscopy
Single cell and nanoparticle analysis
Chemical imaging
Qualitative discrimination analysis (machine learning)
Solid sampling
Trace analytical sample preparation
Microfluidics

Short courses

D. Clases (Austria): Single particle ICP-MS
T. Janáky (Hungary): Mass spectroscopy in proteomics
P. Fürjes (Hungary): Microfluidics in spectroscopy
B. Hufnagl (Austria): Machine learning in spectroscopy

MAGYAR KÉMIKUSOK EGYESÜLETE MKE HUNGARIAN CHEMICAL SOCIETY

ELTE EÖTVÖS LORÁND UNIVERSITY

SZTE UNIVERSITY OF SZEGED HUNGARY

For more information, look for the website at www.esas2026.hu

BrJAC

Brazilian Journal of Analytical Chemistry

VISÃO FOKKA - COMMUNICATION AGENCY

Aims & Scope

BrJAC is a double-blind peer-reviewed research journal, dedicated to the diffusion of significant and original knowledge in all branches of Analytical Chemistry and Bioanalytical Chemistry. It is addressed to professionals involved in science, technology, and innovation projects at universities, research centers and in industry. The **BrJAC welcomes** the submission of research papers reporting studies devoted to new and significant analytical methodologies, putting in evidence the scientific novelty, impact of the research, and demonstrated analytical or bioanalytical applicability. BrJAC **strongly discourages** those simple applications of routine analytical methodologies, or the extension of these methods to new sample matrices, unless the proposal contains substantial novelty and unpublished data, clearly demonstrating advantages over existing ones.

BrJAC is a quarterly journal that publishes original, unpublished scientific articles, reviews and technical notes. In addition, it publishes interviews, points of view, letters, sponsor reports, and features related to analytical chemistry.

For complete information on ethics and policies on conflicts of interest, copyright, reproduction of already published material, preprints, use of AI by authors and reviewers and studies involving biological material, in addition to the manuscript submission and peer review system, please visit 'About us' and 'Author Guidelines' at www.brjac.com.br.

ISSN 2179-3425 printed

ISSN 2179-3433 electronic

Indexing Sources

Scopus

CiteScore$_{2025}$ 1.9
SJR$_{2025}$ 0.216
SNIP$_{2025}$ 0.381
CiteScoreTracker$_{2026}$ 1.1
Last updated on June 8, 2026
Access source details

CiteScore trend

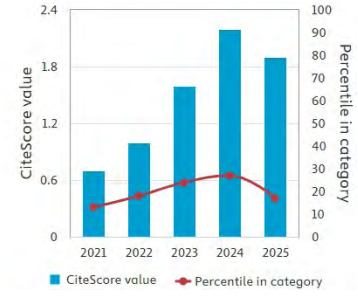

CLARIVATE ANALYTICS EMERGING SOURCES CITATION INDEX INDEXED

IF$_{2025}$ 1.0

CAPES QUALIS

BrJAC is in the Qualis B1 stratum
Period 2021-2024

Google scholar

Cited by

	All	Since 2021
Citations	1376	1168
h-index	17	16
i10-index	36	30

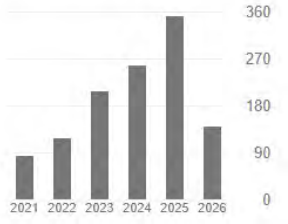

Last updated on June 15, 2026

BrJAC is associated to the Brazilian Association of Scientific Editors

BrJAC is published quarterly by:
Visão Fokka Communication Agency
Av. Washington Luiz, 4300 - Bloco G - 43
13042-105 – Campinas, SP, Brazil
contato@visaofokka.com.br
www.visaofokka.com.br

EDITORIAL BOARD

EDITORIAL ADVISORY BOARD

EDITORIAL ADVISORY BOARD (Continued)

CONTENTS

BrJAC

CONTENTS (Continued)

CONTENTS (Continued)

Brazilian Journal of Analytical Chemistry
2026, Volume 13, Issue 52, pp 1-3
doi: 10.30744/brjac.2179-3425.editorial.N52

EDITORIAL

21st ENQA & 9th CIAQA: First Edition Held in Northern Brazil

Kelly das Graças Fernandes Dantas[1,2*], Josué Carinhanha Caldas Santos[3,4], Wendell Karlos Tomazelli Coltro[4,5]

Guest Editors of this BrJAC Special Edition on the 21st ENQA and 9th CIAQA

[1]*Instituto de Ciências Exatas e Naturais, Universidade Federal do Pará, Belém, PA, Brazil*

[2]*Instituto Nacional de Ciência e Tecnologia em Ciências Moleculares (INCT-CiMol), Centro de Ciências Exatas e da Natureza, Universidade Federal da Paraíba, João Pessoa, PB, Brazil*

[3]*Instituto de Química e Biotecnologia, Universidade Federal de Alagoas, Maceió, AL, Brazil*

[4]*Instituto Nacional de Ciência e Tecnologia em Bioanalítica Lauro Kubota (INCTBio-LK), Instituto de Química, Universidade Estadual de Campinas, Campinas, SP, Brazil*

[5]*Instituto de Química, Universidade Federal de Goiás, Goiânia, GO, Brazil*

The ENQA is a rotating conference organized by the Analytical Chemistry Division of the Brazilian Chemical Society (SBQ) and has a history of more than 40 years. Its first edition took place in the early 1980s. Today, it stands as the largest and most important scientific conference in Analytical Chemistry in Brazil and one of the leading chemistry events in Latin America. The 21st National Meeting on Analytical Chemistry marked a defining moment in the conference's history, as it was the first edition ever held in Brazil's Northern region.

The 21st ENQA was jointly organized with the 9th Ibero-American Congress on Analytical Chemistry (CIAQA) and took place at the Hangar Convention and Exhibition Center of the Amazon, from September 15 to 18, 2024, in the city of Belém, Pará State, Brazil. Belém is a vibrant metropolis known for its distinctive culture and rich gastronomy, largely based on ingredients derived from the Amazon rainforest's diverse flora and fauna. Surrounded by rivers and islands, Belém is one of the most prominent cities in the Brazilian Amazon. Hosting the meeting in Belém, the host city of COP30, further underscored the relevance of Analytical Chemistry to environmental monitoring, climate studies, biodiversity conservation, and sustainable development. The Amazon region provides unique opportunities for analytical research involving biodiversity, environmental monitoring, food authenticity, natural products, and ecosystem preservation.

Following twenty previous editions held in other regions of the country, the 21st ENQA & 9th CIAQA represented an important milestone for science in Northern Brazil. Hosting the event in this region was fundamental to promoting inclusion and reducing inequalities in access to scientific activities. Furthermore, the meeting fostered the dissemination and visibility of regional and national scientific research through discussions on highly relevant topics presented during the event. The participation of international speakers addressing frontier themes also contributed significantly to the conference's internationalization.

In addition to the four-day scientific program, researchers, students, and professionals from across Brazil and abroad had the opportunity to interact with technical specialists from companies in Analytical Chemistry, learning about the latest advances in instrumentation and technological innovation. The scientific discussions highlighted emerging trends in analytical sciences, including artificial intelligence-assisted analytical

Cite: Dantas, K. G. F.; Santos, J. C. C.; Coltro, W. K. T. 21st ENQA & 9th CIAQA: First Edition Held in Northern Brazil. *Braz. J. Anal. Chem.* 2026, *13* (52), pp 1-3. https://doi.org/10.30744/brjac.2179-3425.editorial.N52

This Editorial is part of the BrJAC Special Issue dedicated to the 21st ENQA and 9th CIAQA.

methodologies, advanced mass spectrometry, microplastics monitoring, omics technologies, environmental sustainability, and point-of-care analytical systems. These topics reinforce the strategic role of Analytical Chemistry in addressing major societal challenges. As society faces increasingly complex environmental, health, and technological challenges, Analytical Chemistry continues to serve as a fundamental pillar for generating reliable information and supporting evidence-based decision-making.

The meeting received 538 submitted abstracts and welcomed more than 867 participants from 25 Brazilian states, the Federal District, and 17 other countries. The participation of researchers from 17 countries strengthened international collaboration and reinforced CIAQA's role as a major platform for scientific integration across Ibero-America. The conference theme, "*Analytical Chemistry and its Contributions to the Development of a Sustainable Society*," guided a comprehensive scientific program that included six short courses, six workshops, nine plenary lectures, a session with editors, eight themed sessions, thirteen technical presentations, forty-eight oral communications, three poster sessions, award and tribute ceremonies, ENQA in the Schools activities, a book session, and several social integration events. This edition reflected the increasing diversity of the analytical chemistry community, with women representing 53% of attendees and assuming prominent roles throughout the scientific program.

In this special edition, the Brazilian Journal of Analytical Chemistry (BrJAC) presents an interview with Professor Orlando Fatibello Filho from the Federal University of São Carlos (São Paulo State, Brazil), who has extensive experience in Analytical Chemistry, particularly in electroanalytical methods, bioanalytical chemistry, optical analytical methods in the UV-Vis region, and chemiluminescence.

This issue also includes two "Points of View" articles and one letter. The "Points of View" contributions were written by Professor Cassiana Montagner from the University of Campinas (São Paulo, Brazil), discussing microplastics studies in Analytical Chemistry, and by Professor Renato Zanella, addressing advances in Ibero-American Analytical Chemistry. In addition, Professor Maria Montes-Bayón from the University of Oviedo (Spain) contributes a letter discussing cisplatin resistance in cell models and alternative nano-delivery systems investigated using mass spectrometric platforms.

The research articles featured in this edition provide important contributions to the medical, biological, and food sciences, reaffirming the central role of Analytical Chemistry in advancing scientific knowledge and sustainable development.

The organizing committee gratefully acknowledges all sponsors and supporters, including funding agencies, companies, the Royal Society of Chemistry, the National Institutes of Science and Technology (INCTs), ABQ-PA, and CFQ-CRQs, whose contributions were essential in supporting the participation of invited national and international speakers.

Finally, the guest editors of this special BrJAC issue thank all authors for submitting their valuable contributions and all reviewers for dedicating their time and expertise to ensure the high quality of this edition dedicated to the 21st ENQA & 9th CIAQA. The editors also recognize the efforts of the organizing and scientific committees, as well as the entire event support team, whose dedication made this successful conference possible.

The success of the 21st ENQA & 9th CIAQA demonstrates the vitality of Analytical Chemistry in Brazil and Ibero-America and provides a strong foundation for future scientific cooperation to address global challenges through analytical innovation.

Kelly das Graças Fernandes Dantas is a Full Professor at the Institute of Exact and Natural Sciences of the Federal University of Pará in Belém, Pará, Brazil. She graduated in Chemistry from the Federal University of Viçosa (1999), Master in Chemistry (Analytical Chemistry) from the São Paulo State University (2001), Ph.D. in Science (Analytical Chemistry) from the Federal University of São Carlos (2005) with a visiting research period (2004) at the Faculty of Physical and Analytical Chemistry at the University of Oviedo in Spain, and postdoctoral from the Federal University of São Carlos (2006). Currently, she is Director of the Analytical Chemistry Division of the Brazilian Chemistry Society, member of the National Institute on

Science and Technology of Molecular Science (INCT-CiMol), and coordinator of the Applied Analytical Spectrometry Group (GEAAp). She has experience in Analytical Chemistry and her main research topics are sample preparation, emission and atomic spectrometry, chromatographic techniques, and speciation applied to foods, biological, and environmental samples of the Amazon region. CV

Josué Carinhanha Caldas Santos holds a degree in Chemistry from the State University of Bahia, as well as a master's degree in Organic Chemistry and a Ph.D. in Analytical Chemistry from the Federal University of Bahia, including a visiting research period at the Faculty of Pharmacy of the University of Porto (Portugal). He is the coordinator of the Laboratory of Instrumentation and Development in Analytical Chemistry (LINQA) at the Institute of Chemistry and Biotechnology of the Federal University of Alagoas (UFAL). His research focuses on Analytical Chemistry and its interfaces, with an emphasis on the interaction of (macro)molecules, such as proteins, enzymes, DNA, and humic substances, with metal ions, pharmaceuticals, and biologically active compounds; the development of sample preparation strategies; atomic and molecular fluorescence; the synthesis and application of nanomaterials and fluorescent or colorimetric probes for analytical purposes; and the development of analytical kits for detecting markers of interest in agriculture, health, and forensic sciences. For more information about the research group, follow the social media: **@linqaufal**. CV

Wendell Karlos Tomazelli Coltro is a Full Professor at the Institute of Chemistry and Vice-Rector for Research and Innovation at the Federal University of Goiás, Brazil. He obtained his B.Sc. in Chemistry from the State University of Maringá in 2002. He received his M.Sc. (2004) and Ph.D. (2008) in Analytical Chemistry from the University of São Paulo, at the Institute of Chemistry of São Carlos. In 2006, he was a visiting scholar at University of Kansas (USA), under the supervision of Susan C. Lunte. His research focuses on analytical instrumentation, microfabrication, microfluidics, electrophoresis, electrochemical detection, and forensic chemistry. His recent work includes the development of disposable analytical devices and microfluidic systems using 3D printing, with an emphasis on green methodologies. CV

Brazilian Journal of Analytical Chemistry
2026, Volume 13, Issue 52, pp 4-10
doi: 10.30744/brjac.2179-3425.interview.N52

INTERVIEW

Professor Orlando Fatibello Filho kindly granted an interview to BrJAC

Professor Fatibello holds a bachelor's degree in chemistry education from the Federal University of São Carlos (1976), a master's degree in Chemistry (Physical Chemistry) from the University of São Paulo (1980), and a PhD in Chemistry (Analytical Chemistry) from the Institute of Chemistry at the University of São Paulo (1985). He obtained his Habilitation (Livre Docência) in Analytical Chemistry from the Institute of Chemistry at the University of São Paulo in 2000. He completed a postdoctoral fellowship in the research group of George G. Guilbault at the Department of Chemistry, University of New Orleans, LA, USA (February 1987 to July 1989). He also served as a Visiting Full Professor in the Department of Chemistry at the Faculty of Sciences and Technology of the University of Coimbra, PT (March 2008 to February 2009).

Hired in December 1976 as an Assistant Professor, he has been a Full Professor at the Federal University of São Carlos since December 2003. He served as Director of the Analytical Chemistry Division of the Brazilian Chemical Society, was a member of the editorial board of the journal Química Nova, and has been a member of the editorial board of Analytical Letters since May 2005. He has been a Full Member of the Academy of Sciences of the State of São Paulo (ACIESP) since September 2012. In addition, he served as a member of the Chemistry Advisory Committee (CA) of the National Council for Scientific and Technological Development (CNPq) from July 2017 to July 2020.

He received second place in the Brazilian Association of University Presses (ABEU) Award with the book *Equilíbrio Iônico: Aplicações em Química Analítica* in the Natural and Mathematical Sciences category in November 2017. He was also a finalist for the Prêmio Jabuti in 2020 with the book *Potenciometria: Aspectos Teóricos e Práticos*. In 2025, he published the book *Problemas resolvidos do livro Equilíbrio Iônico: Aplicações em Química Analítica*.

He has published more than 378 scientific articles (h-index = 64), 9 book chapters, and 11 books. He has supervised 39 Master's students, 38 PhD students, and more than 90 undergraduate research students. In addition, he supervised 25 postdoctoral fellows. His former students are currently employed in several companies, the Brazilian Federal Police, and universities such as UFSCar, UNISANTOS, UEG, UFG, UFPR, UFBA, UFPA, UFPI, UFGD, UFMG, UFV, UEPG, UNESP, UEL, IFET Maranhão, UFRO, UNIP, and UNIOESTE, among others.

Professor Fatibello ranked 198th in the Ranking of Scientists in Brazilian Institutions according to the GSC Ranking Web of Universities, and is listed among the most influential Brazilian scientists worldwide in a study published in PLOS (10.1371/journal.pbio.3000918), as well as in the Brazil Top 10,000 Scientists – AD Scientific Index 2023 World Scientist and University Rankings.

He has extensive experience in Analytical Chemistry, with a strong focus on electroanalytical methods, bioanalytical chemistry, and optical analytical techniques in the UV-Vis region and chemiluminescence. His research encompasses flow injection analysis with electrochemical detection, UV-Vis spectrophotometry, turbidimetry, and chemiluminescence detection, as well as long optical path spectrophotometry.

Cite: Fatibello Filho, O. Professor Orlando Fatibello Filho kindly granted an interview to BrJAC**.** *Braz. J. Anal. Chem.* 2026, *13* (52), pp 4-10. https://doi.org/10.30744/brjac.2179-3425.interview.N52

This Interview is part of the BrJAC Special Issue dedicated to the 21st ENQA and 9th CIAQA.

His work also includes the development of biosensors based on plant extracts and tissues; modified carbon paste electrodes; electrodes modified with polymeric films containing carbon nanotubes and/or metallic nanoparticles; and boron-doped diamond electrodes. In addition, he has contributed to Green Analytical Chemistry and chemistry education, particularly through the development of low-cost experimental approaches using everyday materials.

In recent years, his research group has focused on the synthesis and application of deep eutectic solvents (DES) for solid-liquid and liquid-liquid microextraction of analytes from food, environmental, biological, and pharmaceutical samples. Following extraction and preconcentration, analytes are determined using spectrophotometry, smartphone-based digital image colorimetry, or electroanalytical techniques.

His research addresses the limitations of conventional separation and preconcentration methods, which typically require large volumes of organic solvents, generate significant waste, and are time-consuming. In this context, DES have been explored as greener and more sustainable alternatives to toxic and volatile organic solvents, offering advantages such as low cost, ease of preparation, and high atom economy.

He has also contributed to the application of DES in the synthesis of metallic nanoparticles for electrochemical sensing. Notably, his group has synthesized ultrasmall platinum nanoparticles (USPtNPs) with diameters on the nanometer scale, which were used to modify glassy carbon electrodes for the determination of riboflavin.

Furthermore, a variety of ultrasmall metal nanoparticles (USMNPs), including Au, Ir, Pt, Ag, CeO_2, Cu, Ni, and iron oxides (Fe_3O_4 and Fe_2O_3), have been synthesized using DES as reaction media and subsequently applied in the fabrication of electrochemical sensors for the determination of analytes in diverse matrices.

BrJAC: What early influences encouraged you to study chemistry? Did you have any influencers, such as a teacher?

Prof. Fatibello: Several early influences pushed me toward chemistry. In 1966, I worked in a chemical industry, and it was there that I decided to study chemistry. Also, the curiosity about how things work—why metals rust, why baking makes cakes rise, and why some reactions release heat—also played an important role. Experiences such as school laboratory experiments or even home activities (*e.g.* mixing vinegar and baking soda, cooking, growing crystals) helped to spark this interest. Another strong influence was my teachers. A passionate science teacher can make a significant difference by demonstrating engaging experiments, connecting chemistry to real-world applications (such as environmental issues, medicine, pharmaceuticals, and materials), and encouraging curiosity and independent thinking.

Exposure to renowned scientists also contributed to my motivation. Learning about figures such as Marie Curie—whose laboratory I had the opportunity to visit in Paris—and reading books by Linus Pauling, known for his work on chemical bonding, reinforced my perception of chemistry as a meaningful and impactful field.

In many cases, a single memorable experience—such as observing a color change in a reaction or successfully carrying out an experiment—can become a turning point, transforming chemistry from an abstract subject into an exciting and engaging discipline.

BrJAC: How was the beginning of your career in chemistry?

Prof. Fatibello: My career in chemistry began in March 1977, when I joined the Department of Chemistry at the Federal University of São Carlos as a professor of chemistry. Both experimental and theoretical classes were an inspiration to me, leading me to pursue analytical chemistry.

BrJAC: What has changed in your profile, ambitions, and performance since the time you started your career?

Prof. Fatibello: When I started my career, my profile was defined mainly by curiosity and a strong willingness to learn. I was focused on building technical skills, understanding how organizations work, and proving my value through consistency and effort. At that stage, my ambitions were relatively short-term: gaining experience, developing competence, and finding my place professionally.

Over time, my profile has evolved to become more strategic and results-oriented. I've developed greater confidence in decision-making, improved my communication skills, and learned to collaborate more effectively across teams. I now approach challenges with a broader perspective, considering not only immediate tasks but also long-term impact and sustainability.

My ambitions have also grown. Instead of focusing only on personal development, I'm now motivated by contributing to larger goals, leading initiatives, and creating meaningful impact within my organization. I aim to continue growing into roles where I can influence direction, mentor others, and help drive innovation.

In terms of performance, the most significant change has been consistency and efficiency. I've learned to prioritize better, manage my time effectively, and deliver higher-quality results under pressure. I'm also more proactive, taking ownership of projects and seeking continuous improvement.

Overall, the journey has been one of growth—from learning and adapting to leading and contributing with purpose.

BrJAC: Could you comment briefly on the recent evolution of analytical chemistry, considering your contributions?

Prof. Fatibello: The recent evolution of analytical chemistry has been marked by significant advances in sensitivity, speed, and data analysis capabilities. Modern techniques now allow for the detection of compounds at trace levels, often in highly complex matrices, while also reducing analysis time and improving reliability. The integration of automation, miniaturization, and digital tools has further enhanced efficiency and reproducibility, making analytical processes more robust and accessible.

In my work, I have contributed to this evolution by focusing on method development and optimization, particularly in ensuring accuracy and consistency under challenging conditions. I have also applied analytical techniques to address practical problems, with an emphasis on data quality and the interpretation of results to support decision-making. In addition, I have worked to streamline workflows and adopt new technologies, including deep eutectic solvents (DES), where appropriate, aligning my efforts with the broader trend toward more efficient and sustainable analytical practices.

Overall, my contributions reflect a commitment to precision, innovation, and the continuous improvement of analytical methodologies in line with the field's ongoing transformation.

BrJAC: What are your lines of research? You have published many scientific papers — would you highlight any of them?

Prof. Fatibello: As mentioned, I have recently contributed to the application of deep eutectic solvents in analytical chemistry and several papers have been published in this field. Please take a look at my **Lattes CV**.

BrJAC: What is your opinion about the current progress of chemistry research in Brazil? What are the recent advances and challenges in scientific research in Brazil?

Prof. Fatibello: The current state of chemistry research in Brazil is strong, with many scientists conducting high-quality research across a wide range of fields, often in close alignment with international developments. Recent advances and challenges vary depending on the specific area of chemistry. Given the breadth of the topic, it is not possible to cover all aspects in this interview.

BrJAC: For you, what have been the most important recent achievements in analytical chemistry research? What are the landmarks?

Prof. Fatibello: Recent achievements in analytical chemistry have been shaped by a convergence of advances in instrumentation, data science, and miniaturization, allowing scientists to measure chemical

systems with unprecedented sensitivity, selectivity, and speed. One of the most important landmarks is the continued evolution of high-resolution mass spectrometry, particularly techniques such as Orbitrap mass spectrometry and time-of-flight mass spectrometry, which enable precise identification of complex mixtures in fields ranging from environmental analysis to proteomics. Coupled with chromatographic separation, these tools have made it possible to detect trace-level contaminants and biomolecules that were previously inaccessible.

Another major milestone is the rise of single-cell and spatially resolved analysis. Techniques like single-cell analysis and mass spectrometry imaging allow researchers to probe chemical heterogeneity within tissues, revealing biological processes at an extraordinary level of detail. These approaches are transforming biomedical research, especially in cancer diagnostics and precision medicine.

The integration of artificial intelligence and machine learning into analytical workflows is also a defining recent achievement. Algorithms are now routinely used for spectral interpretation, pattern recognition, and predictive modeling, significantly accelerating data analysis and improving reproducibility. This is particularly impactful in omics sciences, where datasets are large and complex.

Miniaturization and portability represent another landmark. The development of lab-on-a-chip systems and portable sensors has enabled real-time, on-site analysis in environmental monitoring, food safety, and clinical diagnostics. Technologies such as microfluidics have reduced sample and reagent consumption while increasing throughput.

Finally, advances in electrochemical and optical sensing have led to highly selective and sensitive detection platforms, including biosensors capable of detecting disease markers at very early stages. The rapid development of diagnostic tools during global health crises, particularly those based on CRISPR-based detection, highlights how analytical chemistry continues to play a central role in addressing urgent societal challenges.

Together, these achievements mark a shift toward faster, more precise, and more accessible analytical techniques, expanding the impact of analytical chemistry across science, medicine, and industry.

BrJAC: There are, in Brazil and in the world, several conferences on chemistry. To you, how important are these meetings to the chemistry scientific community? How do you see the development of national chemistry meetings in Brazil?

Prof. Fatibello: Scientific conferences play a central role in the chemistry community, both in Brazil and worldwide. They are not just venues for presenting results, but spaces where ideas are tested, collaborations are formed, and emerging trends are identified. In a field as dynamic as chemistry, the opportunity to exchange knowledge face-to-face accelerates scientific progress in ways that publications alone cannot achieve. Conferences also allow researchers—especially students and early-career scientists—to engage directly with leading experts, receive feedback, and build professional networks that often shape their future careers.

Another important aspect is the interdisciplinary nature of modern chemistry. Meetings bring together specialists from analytical, organic, inorganic, physical, and materials chemistry, as well as related areas such as biology, physics, and engineering. This interaction fosters innovation, as many of today's scientific challenges—such as sustainability, energy, and health—require integrated approaches. In this sense, conferences act as catalysts for new research directions.

In Brazil, national chemistry meetings have shown significant development over the years, both in size and scientific quality. Events organized by institutions such as the Brazilian Chemical Society have become increasingly important platforms for showcasing the country's scientific production. These meetings reflect the growth of Brazilian research, with a strong presence of graduate programs and increasing international participation. They also play a key role in reducing regional inequalities by providing opportunities for researchers from different parts of the country to present their work and establish collaborations.

Looking ahead, the continued development of national meetings in Brazil will likely depend on sustained investment in science and education, as well as efforts to increase internationalization. Hybrid formats, combining in-person and virtual participation, may further expand access and visibility. Overall, these conferences are essential for strengthening the scientific community, promoting innovation, and ensuring that Brazilian chemistry remains connected to global advances.

BrJAC: What is the importance of awards for the development of science and new technologies?
Prof. Fatibello: Awards play an important role in the development of science and new technologies by recognizing excellence, motivating researchers, and giving visibility to impactful work. At an individual level, receiving a prestigious prize—such as the Nobel Prize or the Fields Medal—can significantly enhance a scientist's career, opening doors to funding opportunities, collaborations, and leadership positions. This recognition not only rewards past achievements but also encourages continued innovation and risk-taking.

"Awards also contribute to public engagement with science. High-profile recognitions bring scientific achievements into the spotlight, making them more accessible to society and helping to build trust in scientific research."

Beyond individual recognition, awards help shape the direction of scientific research. By highlighting specific discoveries or fields, they signal what is considered important or promising within the scientific community. For example, prizes in areas like renewable energy, biotechnology, or artificial intelligence can stimulate further investment and attract new researchers to these fields, accelerating technological development.

Awards also contribute to public engagement with science. High-profile recognitions bring scientific achievements into the spotlight, making them more accessible to society and helping to build trust in scientific research. This visibility is crucial for fostering a culture that values science and supports policies aimed at research and innovation.

In addition, awards can strengthen institutions and national scientific systems. When researchers or groups are recognized, their universities and research centers gain prestige, which can translate into increased funding and international collaboration. In countries like Brazil, national awards and recognitions are particularly important for highlighting local talent and reinforcing the relevance of domestic research on the global stage.

However, it is also important to acknowledge that awards should strive to be inclusive and representative, ensuring that recognition reflects the diversity of contributions across different regions, genders, and career stages. When well-structured and fairly distributed, awards serve as powerful tools to inspire excellence, guide scientific priorities, and drive the advancement of science and technology.

BrJAC: For you, what is the importance of the national funding agencies for the scientific development of Brazil?
Prof. Fatibello: National funding agencies are fundamental to the scientific development of Brazil, as they provide the financial and institutional support that sustains research, innovation, and the training of human resources. Organizations such as CNPq, CAPES, and FAPESP play a central role in enabling research projects, scholarships, and international collaborations across all areas of knowledge.

These agencies are essential not only for funding equipment and infrastructure, but also for supporting students and early-career researchers through scholarships and fellowships. This investment is crucial for building a qualified scientific workforce and ensuring continuity in research activities. Without consistent funding, laboratories struggle to operate, long-term projects are interrupted, and the country risks losing talent to institutions abroad.

Another important aspect is that funding agencies help define national research priorities. By launching strategic calls and thematic programs, they can stimulate research in areas of high social and economic impact, such as public health, renewable energy, agriculture, and environmental sustainability. In this way, they act as drivers of innovation and contribute directly to technological development and competitiveness.

In addition, these agencies promote internationalization by supporting exchanges, joint projects, and participation in global scientific networks. This integration strengthens the visibility of Brazilian science and facilitates access to cutting-edge knowledge and technologies.

However, the effectiveness of these agencies depends on stable and adequate investment. Fluctuations in funding can compromise scientific progress and reduce the country's ability to respond to emerging challenges. Therefore, strengthening national funding agencies is not only a matter of supporting science, but also of ensuring Brazil's long-term development, sovereignty, and capacity for innovation.

BrJAC: What advice would you give to a young scientist who wants to pursue a career in chemistry?
Prof. Fatibello: Pursuing a career in chemistry can be both challenging and deeply rewarding, but it requires curiosity, persistence, and a willingness to continuously learn. One of the most important pieces of advice for a young scientist is to build a strong foundation in the core areas of chemistry while remaining open to interdisciplinary approaches. Modern chemistry increasingly overlaps with fields such as biology, physics, materials science, and data science, so developing a broad scientific perspective can be a major advantage.

"Modern chemistry increasingly overlaps with fields such as biology, physics, materials science, and data science, so developing a broad scientific perspective can be a major advantage."

Equally important is gaining hands-on experience in the laboratory. Practical skills, problem-solving abilities, and familiarity with analytical techniques are essential for understanding how theory translates into real-world applications. At the same time, learning how to communicate science clearly—both in writing and in presentations—is crucial, as the impact of your work depends on how well it is shared with others.

Seeking mentorship and collaboration is another key step. Working with experienced researchers can provide guidance, open opportunities, and help you navigate challenges along the way. Participating in conferences, workshops, and research exchanges will also expand your network and expose you to new ideas and perspectives.

Resilience is fundamental in a scientific career. Experiments may fail, results may be unexpected, and progress can sometimes feel slow. However, these challenges are part of the process and often lead to the most meaningful discoveries. Staying motivated and maintaining a critical, yet optimistic mindset will help you move forward.

Finally, it is important to align your career with your interests and values. Chemistry offers opportunities in academia, industry, education, and entrepreneurship. Whether your goal is to advance fundamental knowledge or develop technologies that benefit society, maintaining a sense of purpose will make your journey more fulfilling and impactful.

BrJAC: For what would you like to be remembered?
Prof. Fatibello: If I were to answer that as a scientist, I would say I would like to be remembered not only for specific discoveries, but for the impact of my work on people and on the advancement of knowledge. Scientific results are important, but they are always part of a larger, collective effort. Contributing meaningful insights, helping to solve relevant problems, and advancing the field even in small steps are all part of a lasting legacy.

I would also hope to be remembered as someone who supported and inspired others—students, collaborators, and colleagues. Mentorship, generosity in sharing knowledge, and fostering a collaborative environment are just as important as publishing papers or receiving recognition. Science progresses through communities, not individuals alone.

Another aspect that matters is integrity. Being rigorous, honest, and responsible in conducting and communicating research is essential for building trust in science. A career marked by ethical commitment and respect for evidence leaves a more enduring contribution than any single achievement.

I would like to be remembered as someone who was curious, dedicated, and committed to making a positive difference through chemistry—whether by advancing scientific understanding, contributing to innovation, or helping others grow along the way.

Finally, my contribution to analytical chemistry has been strongly focused on teaching and on the development of educational resources that support the training of new scientists. Throughout my academic career, I have dedicated myself to helping students understand the fundamental principles of analytical chemistry and, more importantly, to connect theory with practical applications. I believe that a solid conceptual foundation is essential for students to confidently apply analytical methods in research, industry, and everyday problem-solving.

In addition to classroom teaching and laboratory supervision, I have also worked on producing didactic materials that make complex topics more accessible. This includes structured lecture content, laboratory guides, and problem-solving exercises designed to strengthen analytical thinking and experimental design skills. My goal has always been to encourage critical reasoning rather than memorization, helping students develop the ability to interpret data and evaluate analytical results independently.

A significant milestone in my academic journey has been the publication of a book in analytical chemistry. This work was developed with the intention of integrating theoretical concepts with practical examples, offering a comprehensive and updated perspective on the field. The book reflects both classical foundations and recent advances in analytical techniques, aiming to serve as a reference for undergraduate and graduate students as well as educators.

Through teaching and writing, I hope to contribute to the formation of well-prepared professionals who are capable of advancing the field of analytical chemistry. Education is one of the most lasting contributions a scientist can make, and I consider it a privilege to participate in the training of future generations of chemists.

Brazilian Journal of Analytical Chemistry
2026, Volume 13, Issue 52, pp 11-12
doi: 10.30744/brjac.2179-3425.PoV.RZ.N52

POINT OF VIEW

Advances in Ibero-American Analytical Chemistry

Renato Zanella

Departamento de Química, Universidade Federal de Santa Maria, Santa Maria, RS, Brazil

Analytical Chemistry in Latin American countries, Spain, and Portugal is characterized by strong scientific and technological integration among research groups, driven by conferences in the field and collaborative networks that seek to address contemporary challenges through integration. Ibero-American Analytical Chemistry has served as an essential pillar of economic development, particularly in health, food safety, and the environment, and is internationally recognized for its scientific excellence. The current situation in Latin America is marked by a growing international presence, consolidated by decades of investment in human resources and infrastructure, although it also faces structural and financial challenges. There remains a gap in access to state-of-the-art equipment and chronic difficulties with laboratory maintenance and the importation of supplies. Public universities have played a key role not only in academic research but also in supporting government and private-sector initiatives.

The Ibero-American community has distinguished itself in excellence in education, with strong and active scientific societies. Organizations such as the Spanish Society of Analytical Chemistry (SEQA) and the Brazilian Chemical Society (SBQ), through its Division of Analytical Chemistry, lead teaching and research efforts, promoting international scientific cooperation. The Ibero-American Congress of Analytical Chemistry (CIAQA), held since 2005, has been the main driver of cooperation within the Ibero-American scientific community. SEQA, established in the 1980s, coordinates Spanish efforts in the field and is part of the Analytical Chemistry Division of the European Chemical Society (EuChemS). Spain plays a prominent role in the field, having hosted globally prestigious events such as Euroanalysis 2025 in Barcelona. Analytical Chemistry in Portugal is characterized by strong networking and international cooperation, notably through its active participation in the Ibero-American community, demonstrating a high degree of technological sophistication. Research in the field is concentrated in major universities that maintain a considerable output of scientific research. The Analytical Chemistry Division of the Portuguese Chemical Society (SPQ) is also a member of EuChemS.

The state of Analytical Chemistry in Latin America is marked by significant growth, with a strong focus on areas such as environmental monitoring, agribusiness, and food quality control. Countries such as Brazil, Mexico, Chile, Argentina, and Colombia lead in scientific output in the field, driven by international collaborations and laboratory modernization, although challenges such as funding continuity and access to cutting-edge technologies still exist. Brazil leads in academic output in Latin America due to investment in public universities and graduate programs. The country has more than 10 prominent public universities with extensive scientific output in the field. The National Meeting on Analytical Chemistry (ENQA) is considered the most important analytical chemistry event in Latin America and is frequently organized in conjunction with CIAQA. These events bring together hundreds of researchers from Ibero-America and strengthen scientific exchange. Mexico has several research groups that collaborate with Ibero-American researchers. The country's scientific output is driven by a diverse network of universities and the Mexican Association of Analytical Chemistry (AMQA). Argentina has made significant scientific strides in this field, with research spread across several universities. The country maintains frequent collaborations with Ibero-

Cite: Zanella, R. Advances in Ibero-American Analytical Chemistry. *Braz. J. Anal. Chem.* 2026, *13* (52), pp 11-12. https://doi.org/10.30744/brjac.2179-3425.PoV.RZ.N52

This Point of View is part of the BrJAC Special Issue dedicated to the 21st ENQA and 9th CIAQA.

American nations through events such as the Argentine Congress of Analytical Chemistry (CAQA) and the CIAQA. Chile stands out in this field, particularly through researchers at the country's leading universities. Chile's Division of Analytical and Environmental Chemistry has organized the Meeting on Analytical and Environmental Chemistry (EQAA), bringing together professionals from various countries. The field gained recognition starting in the 1990s and is now vital to the export economy, ensuring food safety. Colombia also has prominent research groups at various universities that collaborate with Ibero-American researchers. In Colombia, technological progress stands out, with improvements in infrastructure despite limited financial support. The Colombian Society of Chemistry (SCCQ) organizes events that include topics in Analytical Chemistry. In Uruguay, analytical chemistry is limited to a few research groups, but the country is recognized as an active participant through the Uruguayan Congress of Analytical Chemistry (CUQA), a regular event that has previously been organized in conjunction with the CIAQA.

The Latin American Network for Environmental Quality Analysis (RACAL) has been strengthening cooperation through the Latin American Symposium on Environmental Analytical Chemistry (LASEAC), held since 1990 in various Latin American countries and attended by several Ibero-American researchers.

The strengthening of Analytical Chemistry in Latin America depends on continued investment and government policies that endure changes in administration. Initiatives such as CIAQA and the Brazilian Journal of Analytical Chemistry (BrJAC) aim to strengthen ties among Ibero-American researchers to create more robust research networks. Major international events such as the Analitica Latin America Congress, the Latin American Congress on Chromatography (COLACRO), and the Rio Symposium on Atomic Spectrometry (RSAS) regularly bring together hundreds to thousands of professionals, fostering a collaborative ecosystem.

COLACRO has been organized since 1986 and has already taken place in Brazil, Argentina, Mexico, Chile, Venezuela, and Portugal. The RSAS was launched in 1988 as an opportunity for Latin American students and scientists to interact with renowned scientists from around the world and has already been held in Brazil, Venezuela, Argentina, Mexico, and Chile. Another event that brings together hundreds of participants is the Ibero-American Conference on Mass Spectrometry (IberoMS), a field that has grown significantly over the past decade.

Despite these advances, the region still faces challenges, including the need for long-term sustainable investment, overcoming bureaucratic obstacles, and modernizing infrastructure in less developed areas. Cooperation among research groups in Ibero-America can be an effective way to promote the advancement of analytical chemistry in a broad and sustainable manner.

Renato Zanella is a Full Professor at the Federal University of Santa Maria, RS, Brazil. He holds a PhD in Analytical Chemistry from the Dortmund Universität (Germany) and completed a post-doctorate at the Free University of Amsterdam (Netherlands). He joined UFSM in 1994 and has served as a Full Professor since 2014. Coordinator since 2001 of the Laboratory of Pesticide Residue Analysis (LARP), an ISO/IEC 17025-accredited laboratory, and of the Chromatography and Mass Spectrometry Research Center (CPCEM) with a focus on residues and contaminants. Member of the CNPq Chemistry Advisory Committee (2020-2023) and the Fapergs Board of Directors (2017-2022). President Director of the Science and Technology Support Foundation (FATEC) since 2024. President of the *Red de Analises de La Calidad Ambiental en América Latina* (RACAL) from 2013 to 2024 and member of the Extended Executive Committee of the International Association of Environmental Analytical Chemistry (IAEAC) since 2013. Vice-coordinator of the National Institute of Science and Technology (INCT) in Food Analytical Chemistry. Director (2006-2008) and Vice-Director (2004-2006) of the SBQ/Division of Analytical Chemistry. CNPq Research Productivity Fellow level 1B, author of 234 papers and 18 book chapters, with 6191 citations and h-index 43. Supervisor of 52 master's and 30 doctoral studies. Associate editor of Food Analytical Methods since 2021. CV

Brazilian Journal of Analytical Chemistry
2026, Volume 13, Issue 52, pp 13-15
doi: 10.30744/brjac.2179-3425.PoV.CCM.N52

BrJAC

POINT OF VIEW

Microplastics: A Complex Research Field for Analytical Chemistry?

Cassiana C. Montagner

Laboratório de Química Ambiental, Instituto de Química, Universidade Estadual de Campinas, UNICAMP, Rua Monteiro Lobato, 270, 13083-862, Cidade Universitária, Campinas, SP, Brazil

In 2005, I began my master's project evaluating endocrine-disrupting compounds in surface waters.[1] This was among the first studies on emerging contaminants in Brazil, aligning with the strong international trend in Environmental Chemistry. Since then, I have closely followed the evolution of this field both in our country and worldwide.

Advances in methodologies for quantifying emerging contaminants, such as pharmaceuticals, personal care products, plasticizers, pesticides, etc., at nanogram-per-liter concentrations across different environmental matrices have significantly driven progress in sample preparation for organic substances. After starting with the technologies available in research laboratories, liquid chromatography coupled with tandem mass spectrometry (LC-MS/MS) has consolidated its role as the primary analytical tool, ensuring accuracy and precision in assessing the occurrence and transport of these contaminants in water and soil. Later, the advent of high-resolution mass spectrometry has further enhanced the evaluation of environmental scenarios, introducing untargeted analysis as a valuable approach to elucidate the fate and behavior of chemicals in surface water, groundwater, and drinking water supplies. However, this process has faced numerous barriers within the sphere of public policy, particularly when confronting large corporations. A paradigmatic example is the case of per- and polyfluoroalkyl substances (PFAS), extensively documented and brought to public attention through the film Dark Waters.

Approximately 10 years ago, attention was drawn to a new (or perhaps not entirely new) class of emerging contaminants: Microplastics! Remarkably, plastics began to be mass-produced around 60 years ago, and while they revolutionized lifestyle, healthcare, food production, and engineering, the environmental consequences of inadequate waste management have become increasingly evident. Society has played a key role in addressing this issue, driven by pressure from the scientific community, governmental agencies, and diverse stakeholders to develop solutions for plastic pollution. Unlike other categories of emerging contaminants, microplastic pollution is not an invisible problem; its tangible presence makes it easier to convey the urgency of understanding the environmental and health implications associated with plastics and, consequently, microplastics in the environment.

Omnipresent in our life, all polymers previously classified as particles with dimensions less than 5 mm, and more recently redefined as those with sizes between 1 and 1000 um, are microplastics.[2] However, we are not talking about one substance or a group of substances with the same characteristic. Size, format, color, type of polymer, level of degradation, additives, all that combination brings a particle, a different physical chemistry characteristic, behavior, toxicity, capacity to interaction with another contaminants, including microorganisms and biofilm formation. Consequently, assessing the risks associated with microplastics in the environment is an intrinsically complex task.[3]

Cite: Montagner, C. C. Microplastics: A Complex Research Field for Analytical Chemistry? *Braz. J. Anal. Chem.* 2026, *13* (52), pp 13-15. https://doi.org/10.30744/brjac.2179-3425.PoV.CCM.N52

This Point of View is part of the BrJAC Special Issue dedicated to the 21st ENQA and 9th CIAQA.

As observed in the beginning of research on other emerging contaminants, it was essential to understand how to quantify microplastics in environmental samples, as this provides an important foundation for future regulatory frameworks. Early studies began with traditional approaches that relied heavily on visual inspection under optical microscopy, which was time-consuming and prone to bias, for analyzing beach sand or other samples containing large microplastics (1-5 mm). Today, because of the advances in methodologies: from sampling and sample preparation (such as optimized digestion protocols and density separation techniques that help preserve particle morphology and minimize fragmentation) to instrumental analysis, we can detect and report the presence of microplastics across a wide range of matrices: water, soil, air, biological samples, tissues, organs, etc., opening new horizons for understanding the impacts of microplastics on ecosystems and human health.[4,5] The recent innovations in analytical methods aim to enhance the accuracy, efficiency, and representativeness of results, particularly in the detection of small microplastics and nanoplastics (<1 um).

Advanced spectroscopic techniques such as micro-attenuated total reflectance Fourier transform infrared spectroscopy (μ-ATR-FTIR), Raman microscopy, and near-infrared hyperspectral imaging (NIR-HSI) allow precise chemical characterization of particles at increasingly smaller scales. Among thermoanalytical techniques, gas chromatography pyrolysis coupled with mass spectrometry (Py-GC-MS) or flame ionization (Py-GC-FID) has emerged also as a powerful technique by retaining chemical signatures of the original material, including polymers, additives and other adsorbed compounds.

Then, automated scanning modules and chemometric tools have reduced analysis time while improving reproducibility, enabling simultaneous detection of multiple polymer classes directly on filters. Studies on behavior, degradation, and removal in environmental matrices, as well as the engineering of new materials, have begun to be explored in greater detail at the microscopic scale.

In other dimensions, classical molecular dynamics and density functional theory calculations have been used for advancing microplastic analysis providing a molecular-level understanding of contaminant interactions that cannot be fully captured by experimental methods alone. Molecular dynamics simulations allow researchers to model the dynamic behavior of microplastics in aqueous environments, revealing how parameters such as temperature, salinity, and pH influence sorption and desorption processes. Density functional theory complements these insights by quantifying the electronic and energetic aspects of interactions, such as hydrogen bonding, van der Waals forces, and electrostatic contributions, thereby clarifying the mechanisms that drive contaminant binding to polymer surfaces. Together, these are examples as computational approaches bridge experimental observations with theoretical predictions, enabling more accurate assessments of microplastic behavior across diverse environmental matrices.[6,7]

This explains why the number of publications on microplastics listed in the Web of Science (now exceeding 32,000) has grown exponentially over the past decade, reflecting the state of the art across multiple dimensions of this field. Most of these studies fall within Environmental Sciences, followed by Environmental Engineering, Marine and Freshwater Biology, Toxicology, and Analytical Chemistry. There is not a standardized method, nor an easy question to answer. This trend shows that concerns about microplastic contamination are driving innovation across disciplines, propelling scientific advancement on a global scale, with Analytical Chemistry playing a crucial role in this science. Thus, the complexity of the topic also represents an opportunity to further explore new analytical methodologies across different scientific fields.

REFERENCES

(1) Montagner, C. C.; Jardim, W. F. Spatial and Seasonal Variations of Pharmaceuticals and Endocrine Disruptors in the Atibaia River, São Paulo State (Brazil). *J. Braz. Chem. Soc.* **2011**, *22* (8), 1452-1462. https://doi.org/10.1590/S0103-50532011000800008

(2) International Organization for Standardization (ISO). *Plastics — Environmental aspects — State of knowledge and methodologies*. ISO Technical Report No. 21960:2020. Available at: https://www.iso.org/standard/72300.html (accessed May 07, 2026).

(3) Sodré, F F.; Arowojolu, I. M.; Canela, M. C.; Ferreira, R. S.; Fernandes, A. N.; Montagner, C. C.; Vidal, V.; Dias, M. A.; Abate, G.; da Silva, L. C.; et al. How natural and anthropogenic factors should drive

microplastic behavior and fate: The scenario of Brazilian urban freshwater. *Chemosphere* **2023**, *340*, 139813. https://doi.org/10.1016/j.chemosphere.2023.139813
(4) Montagner, C. C.; Dias, M. A.; Paia, E. M.; Vidal, C. Microplásticos: ocorrência ambiental e desafios analíticos. *Quim. Nova* **2021**, *44* (10), 1328-1352. http://dx.doi.org/10.21577/0100-4042.20170791
(5) Fernandes, A. N.; Bertoldi, C.; Lara, L. Z.; Stival, J.; Alves, N. M.; Cabrera, P. M.; Grassi, M. T. Microplastics in Latin America ecosystems: a critical review of the current stage and research needs. *J. Braz. Chem. Soc.* **2022**, *33* (4), 303-326. http://dx.doi.org/10.21577/0103-5053.20220018
(6) Dias, M. A.; Batista, P. R.; Ducati, L. C.; Montagner C. C. Insights into sorption and molecular transport of atrazine, testosterone, and progesterone onto polyamide microplastics in different aquatic matrices. *Chemosphere* **2023**, *318*, 137949. https://doi.org/10.1016/j.chemosphere.2023.137949
(7) Madeira, C. L.; Cho, J.; Gomez, R. D. B.; Montagner, C. C. Natural organic matter decreases the sorption capacity of fipronil and its degradation products onto polyethylene microplastics: combined experimental and theoretical insights. *ACS EST Water* **2025**, *5* (7), 3710-3718. https://doi.org/10.1021/acsestwater.4c01261

Acknowledgments

The São Paulo Research Foundation (FAPESP #2022/12104-4) and National Council for Scientific and Technological Development (CNPq #304993/2023-9).

Disclosure

To be truthful to the point of view, I declare that artificial intelligence was used to edit, improve, and proofread the text.

Cassiana Montagner is an Associate Professor at Institute of Chemistry / University of Campinas (IQ-UNICAMP), Coordinator of the **Environmental Chemistry Laboratory** in Brazil and the Thematic Fapesp Project Plast-Agrotox. She is Editor-in-Chief of *Química Nova* (PubliSBQ) and Topic Editor at *Environmental Science & Technology Letters* (ACS Publications). She specializes in Environmental Chemistry with emphasis on Water Security in urban regions and the Amazon, investigating emerging contaminants, microplastics, and pesticides to support Brazilian regulatory policies. She also develops and validates analytical methods for detecting these contaminants at trace levels, ensuring reliable monitoring and risk assessment. CV

Brazilian Journal of Analytical Chemistry
2026, Volume 13, Issue 52, pp 16-20
doi: 10.30744/brjac.2179-3425.Letter.N52

BrJAC

LETTER

Mass Spectrometric Platforms to Study Cisplatin Resistance in Cell Models and Alternative Nano-Delivery Systems

Maria Montes-Bayón[1,3]*, Lucía Gutiérrez Romero[1,3], Carlos López-Portugués[1,3], Paula Díez[2,3], Mario Corte-Rodriguez[1,3]

[1]*Department of Physical and Analytical Chemistry, Faculty of Chemistry, University of Oviedo, Oviedo, Spain*

[2]*Department of Functional Biology, Immunology Area, Faculty of Medicine and Health Sciences, University of Oviedo, Oviedo, Spain*

[3]*Health Research Institute of the Principality of Asturias (ISPA), Oviedo, Spain*

The positive chemotherapeutic effect of cisplatin in most cancers (e.g. ovarian, prostate, etc.) is hampered by the inherent and acquired drug resistance, a multifactorial and still not well characterized process. Several mechanisms have been suggested to participate in conferring platinum-resistant properties to a tumor cell that need to be carefully studied in order to provide therapeutic alternatives. In this Letter, two different aspects are addressed: 1) the evaluation of molecular mechanisms involved in cisplatin resistance by the use of combined multi-strategy platforms based on mass spectrometry, and 2) the search for therapeutic alternatives to enhance efficacy and selectivity of cisplatin based on the use of nanotransporters. Both approaches are briefly discussed from the point of view of the analytical chemistry contribution.

Cisplatin, a platinum-based chemotherapeutic agent, exerts its cytotoxic effects primarily through the formation of irreversible nuclear DNA lesions that interfere with replication and transcription, ultimately yielding cell death. However, accumulating evidence indicates that cisplatin cytotoxicity is multifactorial, extending beyond direct DNA damage, and involving modulation of cytoplasmic and nuclear signaling pathways that influence cell survival, stress response, and metabolic adaptation.[1] Multiple mechanisms have been also implicated in conferring cisplatin resistance, including altered drug uptake and efflux, enhanced DNA repair capacity, dysregulated apoptosis, autophagy induction, and metabolic adaptation. These mechanisms can be classified as **pre-target**, mostly associated to a decrease on the drug cellular uptake or increase efflux, **on-target**, related to a lower binding to DNA or to an efficient repair of the formed adducts and **post-target**, due to deficiencies on the apoptotic route. In this work we have tried to compartmentalize the three types of resistance by combining strategies based on mass spectrometry and some, at the individual cell level.

Resistance pre-target: single cell ICP-MS

For evaluation of the cellular incorporation of cisplatin in different cell models (sensitive and the resistant counterparts), an analytical strategy based on single cell ICP-MS was developed. Single cell analysis is crucial because it is now known that every cell can behave differently, also regarding cisplatin uptake, depending on many biological variables, such as cell type, cell cycle status, hypoxia, redox changes, etc. Therefore, cells were introduced individually into the ICP-MS using the instrumental approach shown in Figure 1, in which every cell containing Pt provided an independent cell event. Previous experiments revealed that

Cite: Montes-Bayón, M.; Gutiérrez Romero, L.; López-Portugués, C.; Díez, P.; Corte-Rodriguez, M. Mass Spectrometric Platforms to Study Cisplatin Resistance in Cell Models and Alternative Nano-Delivery Systems. *Braz. J. Anal. Chem.* 2026, *13* (52), pp 16-20. https://doi.org/10.30744/brjac.2179-3425.Letter.N52

This Letter is part of the BrJAC Special Issue dedicated to the 21st ENQA and 9th CIAQA.

most of the tested cells maintained an intact cellular morphology and stay in a monodisperse state during nebulization (only a low percentage of cells were disrupted during the transport and nebulization process), thus, each ICP-MS peak corresponds to the Pt in an individual cell.[2] Quantification of the cell-associated Pt content can be obtained by using inorganic Pt standards of increasing concentration to obtain a calibration curve. The mass of Pt per cell can be obtained using the equation plotted in Figure 1 where the transport efficiency of the inorganic standards into the plasma has to be calculated based on additional calculations. The obtained results in terms of Pt concentration revealed a heterogeneous behaviour among cell pairs (sensitive/resistant) revealing different molecular mechanisms governing resistance (see Figure 1).[3]

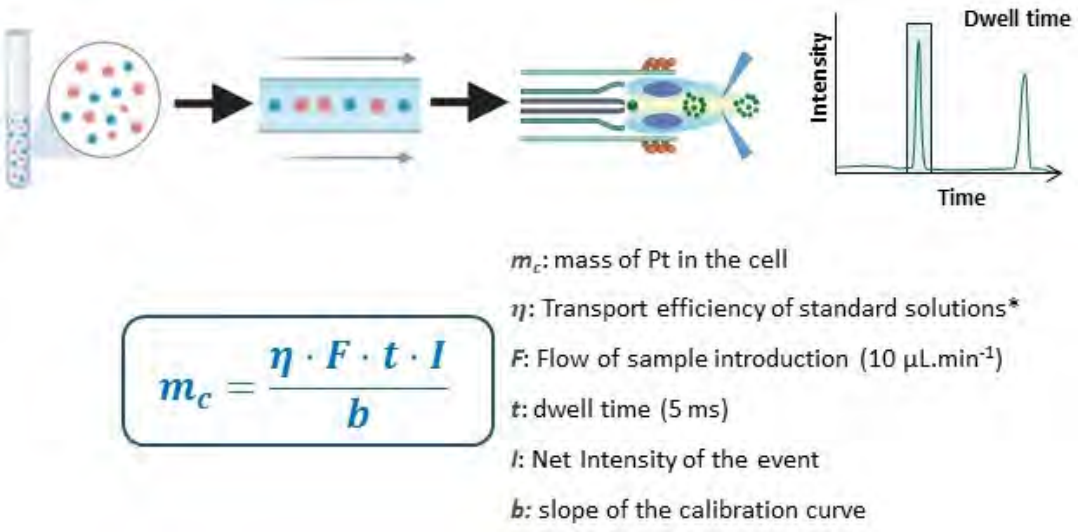

Figure 1. General scheme for single cell ICP-MS quantitative information.

Resistance on-target/post-target: ESI-MS for proteomics

Since the resistance mechanisms can be associated to molecular pathways beyond drug incorporation, it is important to establish if these correspond to newly acquired molecular adaptations (developed upon exposure) or from pre-existing proteomic states that predispose cells to tolerate genotoxic stress. For this aim, the sensitive/resistant pairs were also tested to address proteomics variations using ESI-Q-ToF that could serve as fingerprints of molecular resistance. Our results demonstrate that resistance emerges from heterogeneous adaptive mechanisms governed by intrinsic proteomic states and stress-tolerance programs. The experiments serve to identify pharmacokinetic-, repair-, tolerance-and mixed-dominant resistance phenotypes highlighting the mechanistic diversity underlying cisplatin response.

Alternative drug-delivery systems: the use of nanocarriers

The use of nanodelivery systems containing biocompatible components that are taken up by endocytosis instead of by specific cell transporters and preventing also the drugs from being recognized by efflux pumps is aimed. This would yield a higher intracellular cisplatin accumulation unaffected by the deregulation of specific membrane transporters. Cisplatin and also platinum(IV) prodrugs have been associated to nanoparticles as nanoplatforms for improving drug delivery to tumors and to promote preferential accumulation in cancer cells. Here, we explore the capabilities of the previously synthesized biocompatible ultrasmall iron oxide nanoparticles coated by tartaric and adipic acid, to be directly conjugated to the cisplatin(IV) prodrug cis-diamminetetrachloroplatinum(IV). The possibility of having a direct reaction between the two species dramatically simplifies the synthetic route. However, adequate analytical strategies that permit to quantitatively address the level of conjugation and release of the prodrug have to be developed to study the formation of these species. In this regard, the use of SDS-based reversed-phase chromatography

coupled to ICP-MS detection of Fe and Pt succeeded for this aim (see Figure 2 where Fe and Pt signals can be observed) confirming the elimination of the free drug and complemented with microscopy and light scattering experiments. Additionally, cellular uptake in ovarian cancer sensitive and resistant cell models was addressed at the individual cell level using single cell-ICP-MS strategies (see Figure 2) revealing the higher efficacy of the nanotransporter to increase the level of incorporation in both cell types.

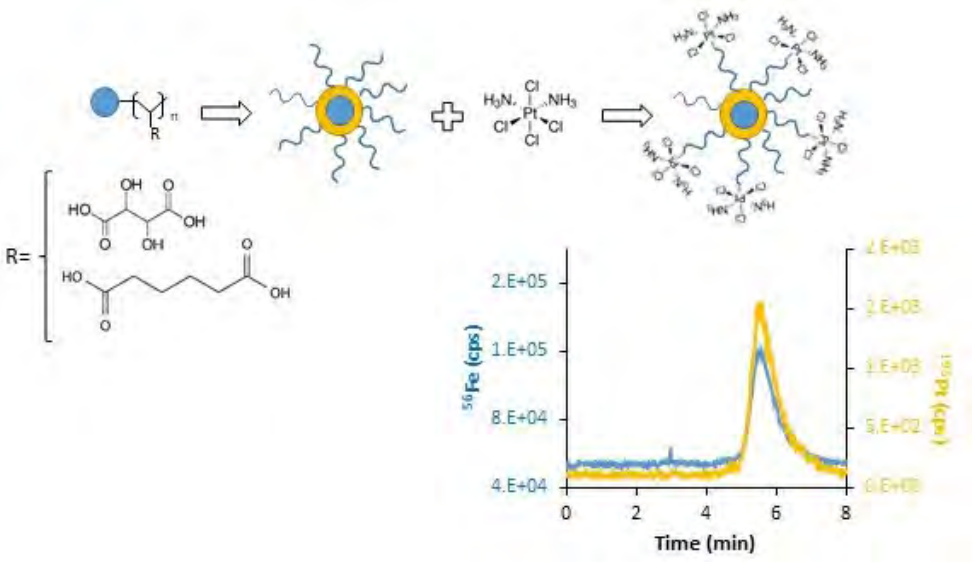

Figure 2. Drug delivery system for cisplatin(IV) transport into cells and assessment of the purity by HPLC-ICP-MS. (adapted from reference 3)

However, two-dimensional cell models do not seem to be the final stage to characterize the efficacy of newly designed drug delivery systems and the use of tri-dimensional cell models seem to be also required. Multicellular spheroids containing different number of cells (1000, 2000 and 4000 cells) were obtained using the “hanging-drop” procedure previously described. All of them were exposed to the Pt-loaded NPs and to the free cisplatin at the same concentration (20 µM Pt). To address the internal distribution of the different elements, the spheroids were sliced in thin sections (10 µm thickness). The elemental distribution maps of multiple elements obtained from a representative thin section of the spheroids after incubation with the different Pt compounds was obtained by laser ablation with ICP-MS detection. To obtain quantitative information of Pt profiles in the spheroids’ sections, gelatin embedded calibration standards of Pt were used according to previous publications. This work was conducted in collaboration with the laboratory of Prof. U. Karst (University of Münster, Germany). LA-ICP-MS analysis permitted to establish the penetration capabilities of the Pt-loaded nanoparticles in comparison to this of cisplatin, reflecting that the nanoparticulated form presented specific hot spots within 100-125 µm from the surface of the spheroid (outer shell and most proliferative) where highest Pt/Fe signals could be detected. This is also in agreement with previous publications revealing the size-dependent penetration capabilities of Au nanoparticles through spheroids.[4]

SUMMARY

Out of the presented results, the most important conclusion is that the complexity of cisplatin resistance requires the development of adequate analytical strategies that permit to tackle the problem from different viewpoints. The characterization of the response from the patient at the individual cell level as well as the proteome of the cells before initiating the therapy could help to predict the response and the outcome in patients. In addition, the use of Pt(IV)-loaded ultrasmall Fe oxide NPs allow efficient drug penetration into cells in both, two-dimensional and three-dimensional cell cultures as established using SC-ICP-MS and LA-ICP-MS.

REFERENCES

(1) Gutierrez-Romero, L.; Díez, P.; Montes-Bayón, M. Bioanalytical strategies to evaluate cisplatin nanodelivery systems: From synthesis to incorporation in individual cells and biological response. *J. Pharm. Biomed. Anal*. **2024**, *237*, 115760. https://doi.org/10.1016/j.jpba.2023.115760

(2) Rodríguez, M. C.; García, E. R. A-F.; Blanco, E.; Bettmer, J.; Montes-Bayón, M. Quantitative Evaluation of Cisplatin Uptake in Sensitive and Resistant Individual Cells by Single-Cell ICP-MS (SC-ICP-MS). *Anal. Chem*. **2017**, *89*, 11491-11497. https://doi.org/10.1021/acs.analchem.7b02746

(3) Turiel-Fernández, D.; Gutiérrez-Romero, L.; Corte-Rodriguez, M.; Bettmer, J.; Montes-Bayón, M. Ultrasmall iron oxide nanoparticles cisplatin (IV) prodrug nanoconjugate: ICP-MS based strategies to evaluate the formation and drug delivery capabilities in single cells. *Anal. Chim. Acta* **2021**, *1159*, 338356, https://doi.org/10.1016/j.aca.2021.338356

(4) Chen, W.; Wang, W.; Xie, Z.; Centurion, F.; Sun, B.; Paterson, D. J.; Tsao, S. C. H.; Chu, D.; Shen, Y.; Mao, G.; Gu, Z. Size-Dependent Penetration of Nanoparticles in Tumor Spheroids: A Multidimensional and Quantitative Study of Transcellular and Paracellular Pathways. *Small* **2023**, 2304693. https://doi.org/10.1002/smll.202304693

María Montes-Bayón is Full Professor of Analytical Chemistry at the Department of Physical and Analytical Chemistry, University of Oviedo, Spain. Her research focuses on ICP-MS-based analytical methodologies for single-cell analysis, metallodrug evaluation in chemotherapy, clinical biomarker determination, and biomedical applications of nanoparticles. She has authored numerous high-impact publications in analytical and bioanalytical chemistry and currently serves as President of the Spanish Society for Analytical Chemistry.

Lucía Gutiérrez Romero is a researcher at the Department of Physical and Analytical Chemistry, Faculty of Chemistry, University of Oviedo, Spain. Her research interests include bioanalytical chemistry, single-cell ICP-MS, nanoparticle-based drug delivery systems, and platinum-based anticancer therapies, with emphasis on analytical strategies for evaluating nanodelivery systems at the cellular level.

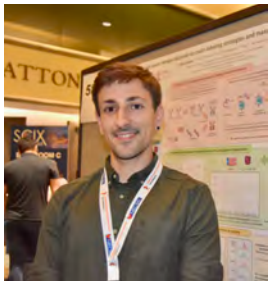

Carlos López-Portugués is a researcher affiliated with the Department of Physical and Analytical Chemistry at University of Oviedo, Spain. His research activities are focused on analytical and bioanalytical chemistry, particularly ICP-MS-based methodologies, nanoreporters, and biomarker quantification in clinical samples.

Paula Díez is a researcher at the Department of Functional Biology, Immunology Area, Faculty of Medicine and Health Sciences, University of Oviedo, Spain, and associated with the Health Research Institute of the Principality of Asturias (ISPA). Her research focuses on cancer biology, platinum resistance mechanisms, ovarian cancer biomarkers, and translational biomedical applications involving metallodrugs and nanomedicine.

Mario Corte-Rodríguez is Assistant Professor in Analytical Chemistry at the Department of Physical and Analytical Chemistry, University of Oviedo, Spain. His research is centered on mass spectrometry and ICP-MS applications in biomedical analysis, including metallodrugs, nanoparticle characterization, single-particle and single-cell analysis, and analytical approaches for studying cellular incorporation and reactivity of metal-based anticancer agents.

Brazilian Journal of Analytical Chemistry
2026, Volume 13, Issue 52, pp 21-39
doi: 10.30744/brjac.2179-3425.AR-184-2024

BrJAC

ARTICLE

Multivariate Assessment of Ground Coffee Samples from Bahia, Brazil on the Basis of Mineral Composition

Naiara dos Santos Brandão[1], Priscilla Carôso da Rocha[1], Victor Miranda Amazonas[1], Wilson da Silva Rocha[2], Nuno Avelar Nascimento[3], Márcio José Silva dos Santos[1], Allison Gonçalves Silva[2], Erik Galvão Paranhos da Silva[3], Marcos de Almeida Bezerra[1], Cleber Galvão Novaes*[1]

[1]Universidade Estadual do Sudoeste da Bahia (UESB), Rua José Moreira Sobrinho, S/N, Jequié, BA, 45208-091, Brazil

[2]Instituto Federal da Bahia (IFBA), Rodovia BR 367, Rua José Fontana, 1, Porto Seguro, BA, 45810-000, Brazil

[3]Universidade Estadual de Santa Cruz, Campus Soane Nazaré, Rodovia BR-415, Ilhéus, BA, 45662-900, Brazil

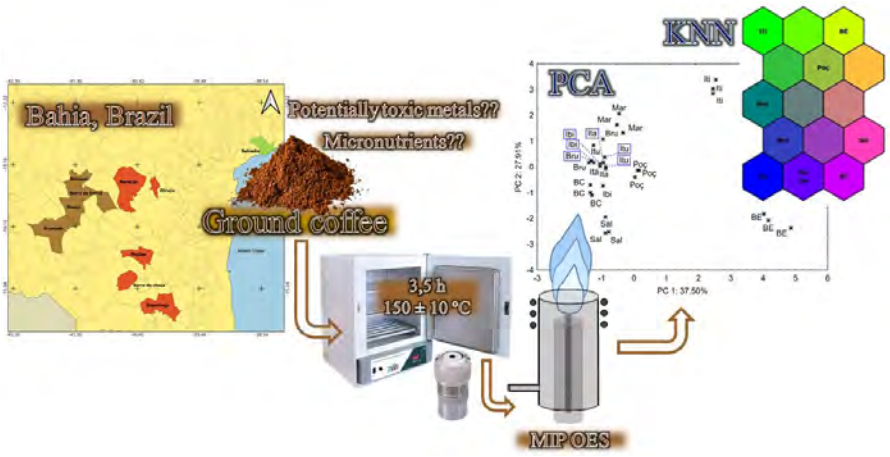

This study determined metals in ground coffee samples from different producing regions in Bahia and used Principal Component Analysis (PCA) and Kohonen neural networks as multivariate techniques to assess sample similarity based on their mineral composition. The samples were prepared using a decomposition method with dilute acid and hydrogen peroxide in a closed system under high pressure. Microwave Induced Plasma Optical Emission Spectrometry (MIP OES) was used to quantify the elements Al, Co, Cr, Cu, Fe, Mn, Ni, V and Zn. For all samples, the elements with the highest concentrations were Mn, Fe, Al, Zn and Cu; and the lowest concentrations were obtained for the elements Cr, Ni, Co and V. The results of this study provide and aggregate relevant nutritional information about coffee produced in the Southwest and Chapada Diamantina regions of Bahia.

Cite: Brandão, N. S.; da Rocha, P. C.; Amazonas, V. M.; Rocha, W. S.; Nascimento, N. A.; dos Santos, M. J. S.; Silva, A. G.; da Silva, E. G. P.; Bezerra, M. A.; Novaes, C. G. Multivariate Assessment of Ground Coffee Samples from Bahia, Brazil on the Basis of Mineral Composition. *Braz. J. Anal. Chem.* 2026, *13* (52), pp 21-39. https://doi.org/10.30744/brjac.2179-3425.AR-184-2024

Submitted: November 27, 2024; **Revised:** April 17, 2025; **Accepted:** August 18, 2025; **Published online:** August 29, 2025.

This article is part of the BrJAC Special Issue dedicated to the 21st ENQA and 9th CIAQA.

Keywords: Principal Component Analysis, Kohonen Neural Networks, Metals, Dilute acid, MIP OES

INTRODUCTION

Coffee is one of the most widely consumed beverages in the world and is produced from the roasted beans of the coffee tree. Arabica coffee (*Coffea arabica*) and conilon coffee (*Coffea canephora*) are the most widely cultivated species, and Arabica coffee is the most widely sold and consumed species, having a more appreciated aroma and flavor, while conilon, also called robusta coffee, has a more bitter flavor, containing a higher concentration of caffeine and antioxidants and a lower amount of sugar.[1]

Brazil currently occupies a prominent position as the largest coffee producer and exporter in the world.[2] The main producing regions are located in the states of Minas Gerais, Espírito Santo, São Paulo and Bahia. In the Bahia scenario, the southwest and Chapada Diamantina regions have attributes that contribute to a quality beverage, such as a mild climate, fertile soil and high altitude.[3]

Coffee seeds are rich in bioactive compounds such as chlorogenic acid, cafestol, caffeic acid and caffeine, a substance with psychostimulant properties.[4] They also have neuroprotective, antioxidant, thermogenic, anti-inflammatory, antidiabetic and antifibrotic activities. Regarding the elemental composition of coffee, this matrix contains essential macro and microelements (Ca, Mg, Fe, Co, Cu, Mn, Zn, etc.),[5] as well as potentially toxic elements (As, Cd, Hg and Pb) resulting from soil and water pollution and the uncontrolled use of inorganic fertilizers and pesticides.[6] Factors such as cultivated species, cultivation environment, production management, in addition to type of processing and storage contribute to the variation in the amount of these elements in coffee.

Essential micronutrients naturally present in coffee may present a potentially toxic character depending on their concentration levels. Copper is an important component of enzymes involved in the metabolism of amino acids, glucose, and cholesterol. On the other hand, several studies associate Wilson's disease with excessive copper accumulation in the body.[7] Zinc plays a crucial role in the development and functioning of the immune system. Conversely, chronic ingestion of zinc can increase levels of low-density lipoprotein (LDL) and decrease levels of high-density lipoprotein (HDL). The absorption of Zn can be influenced by the presence of Cu and Fe.[8] Iron is also an important essential element, necessary in the synthesis of hemoglobin, while the excess is stored as hemosiderin and ferritin proteins in the liver.[9]

Manganese is a micronutrient required for bone growth and acts in the regular metabolism of carbohydrates, proteins, and lipids. A dysfunction known as manganism, characterized by cognitive disabilities and motor disturbances, is caused by the excess of this element in the brain.[10] Cobalt is an essential element for forming vitamin B12, whereas other cobalt compounds present carcinogenic properties for the human body following excessive exposure.[11]

Aluminium is not essential for human metabolism; adversely, its toxicity disrupts hepatic energy metabolism and can be associated with Parkinson's and Alzheimer's diseases.[12] The essentiality of the element vanadium in human physiology has been a subject of great discussion. On the other hand, its excess can affect important cellular functions such as cell cycle, signaling pathways as well as cell survival mechanisms.[13] Chromium presents itself as a special case among the elements. In the human body, Cr(III) is essential for the metabolism of proteins, lipids, and glucose. In contrast, Cr(VI) is a potent carcinogen, with no recognized biological function.[14] Nickel is an essential trace element for several animal species, plants and micro-organisms. However, a deficiency state in humans is not very well established. The chronic exposure to nickel and its compounds can cause lung fibrosis, cardiovascular disease and cancer of the respiratory tract.[15]

Given the high global consumption and nutritional value of coffee, the study of the elemental composition of this matrix becomes important and necessary. To meet this demand, several analytical techniques have been used for quantification, such as atomic absorption spectrometry (AAS), direct mercury analyzer (DMA), inductively coupled plasma optical emission spectrometry (ICP OES), inductively coupled plasma mass spectrometry (ICP-MS), microwave induced plasma optical emission spectrometry (MIP OES), in addition to electroanalytical methods.[16]

Among the aforementioned techniques, MIP OES emerges as an interesting alternative for multielement analysis, since the instrument sensitivity is suitable for quantification in various food samples. Furthermore, the plasma generated in MIP OES is sustained by nitrogen taken from atmospheric air, which significantly reduces analysis costs.[17,18] However, this technique requires that the sample be in solution, a condition that can be achieved with the use of strong acids, a mixture of acids or a mixture of an acid and another auxiliary reagent. In this context, our study applied a previously validated decomposition procedure based on the application of diluted nitric acid and hydrogen peroxide, reducing the amount of reagents in the experiments, in accordance with the principles of green chemistry.[19]

Multielement techniques such as MIP OES, ICP OES and ICP-MS normally require multivariate data processing due to the large volume of information generated in the analyses, which can be obtained by applying Principal Component Analysis (PCA), an unsupervised technique based on a linear transformation that reduces the dimensionality of the original dataset while preserving the maximum possible variance. This reduction is achieved by generating new orthogonal variables, known as principal components (PCs), which retain most of the original information and allow the identification of patterns and similarities among samples. However, PCA is inherently limited to identifying linear correlations and may fail to reveal more complex, non-linear structures within the dataset. As an alternative, Artificial Neural Networks (ANN), particularly the Kohonen Self-Organizing Map (KSOM), have been increasingly applied for exploratory multivariate analysis. KSOM is an unsupervised, non-linear method capable of preserving the topological relationships of the input data, providing an intuitive and detailed visualization of sample similarities and variable contribution, and enabling the detection of subtle patterns that may not be identified by linear techniques such as PCA.[20,21]

This paper presents a current study on the concentrations of essential and potentially toxic elements in ground coffee samples grown in different producing regions of Bahia. KSOM and PCA were used as multivariate tools to assess the similarity of the samples based on the mineral composition quantified by MIP OES. The study also aimed to verify whether the levels of metals present in coffee are in accordance with those found in the literature. Our study is the first to determine the concentrations of metals in ground coffee from the vast majority of cities evaluated.

MATERIALS AND METHODS

Instrumentation

Multielement determination was performed using an MIP OES (4210, Agilent Technologies, Melbourne, Australia) axial mode, equipped with a OneNeb nebulizer, double-pass cyclonic nebulization chamber, Czerny-Turner monochromator and charge-coupled device (CCD) detection. Plasma was generated using nitrogen gas obtained from atmospheric air through an N_2 generator (4107, Agilent). The quantified elements with their respective analytical spectral lines and the instrumental parameters applied are presented in Table I.

Table I. Operating conditions used for the determination of metals by MIP OES

Parameter	Setting
Wavelength (nm)	Al 396.152 (I)*; Co 340.512 (I)*; Cr 425.433 (I)*; Cu 324.754 (I)*; Fe 371.993 (I)*; Mn 403.076 (I)*; Ni 352.454 (I)*; Pb 405.781 (I)*; V 437.923 (I)*; Zn 213.857 (I)*.
Nebulizer flow (L min^{-1})	Al 0.95; Co 0.75; Cr 0.90; Cu 0.70; Fe 0.65; Mn 0.90; Ni 0.70; Pb 0.75; V 0.50; Zn 0.45.
Applied plasma power (W)	1000
Reading time (s)	3
Number of replicas	3
Sample capture time (s)	15

(continued on next page)

Table I. Operating conditions used for the determination of metals by MIP OES (continued)

Parameter	Setting
Stabilization time (s)	15
Pump speed (rpm)	15
Background broker	Automatic
Sample introduction	Manual

*(I): Atomic line

Reagents, materials and solutions

The reagents used in the assays were of analytical grade and the solutions were prepared using ultrapure water (Millipore, Bedford, MA, USA; resistivity of 18.2 MΩ cm). Diluted nitric acid solutions were prepared from a 65% stock solution (Merck, Darmstadt, Germany). A 30% hydrogen peroxide solution (Synth, São Paulo, SP, Brazil) was used in the decomposition step. A multielement standard solution for calibration containing Al, Co, Cr, Cu, Fe, Mn, Ni, Pb, V and Zn was prepared from a stock solution (1000 μg mL^{-1}, Sigma-Aldrich, St. Louis, USA). Conventional glassware was decontaminated using 10% HNO_3 for at least 24 hours.

Sample acquisition and preparation

Ground coffee samples were purchased from supermarkets or directly from family farmers in nine cities in the Chapada Diamantina and Southwest regions of Bahia. The focus of the study was to evaluate two coffee producing regions and not just the cities; therefore, three samples were collected in each city. The sample collected in Salvador was included for comparison purposes only. Table II presents a description of the samples and Figure 1 shows a map of the collection sites.

To prepare the samples, approximately 0.2 g of coffee powder was subjected to decomposition in a high-pressure reactor with 1.75 mL of 7.0 mol L^{-1} nitric acid, 0.5 mL of 30% hydrogen peroxide and 2.25 mL of ultrapure water. The mixture was then subjected to an oven for 3.5 hours at 150 ± 10 ºC. After cooling the digests, they were made up with ultrapure water to a final volume of 10.0 mL and stored in the refrigerator until analysis. Analytical blank solutions were subjected to the same process as the samples.

Data processing

To obtain the geographic coordinates and altitude, a Global Positioning System (GPS, Garmin Etrex 30x) was used. The maps were created using the geographic information software QGIS 3.38. Spatial interpolation, where the geostatistical method of Ordinary Kriging (OK) was applied, used the SAGA GIS software version 7.8.2.

With the element concentration data, the basic statistical parameters were obtained using Excel®, and the multivariate parameters through PCA were obtained using Statistica® 12. For the treatment using Kohonen neural networks, a tool package developed by the Laboratory of Computer and Information Science (Helsinki University of Technology, Finland) was used, implemented using MatLab (version R2018b, MathWorks, USA). The implementation code was adapted by the research group from algorithms suggested in the literature (Haykin, 2009).[21] The Kohonen map was trained with the input data set using a batch training algorithm. The function that limited the neighborhood used in the training of the platform and for the network structure was hexagonal. Network architecture was evaluated based on qualitative indices such as quantization error (QE) and topological error (TE).

Table II. Information about the ground coffee samples and description of the locations where they were produced

Municipality of collection	Coffee (species)	Additional information
Salvador	Arabica	Supermarket purchase / Industrial processing without identification of production origin
*Barra do Choça	Arabica	Supermarket purchase / Organic coffee
*Itapetinga	No information on the label	Supermarket purchase / Industrial production
*Itiruçu	No information on the label	Supermarket purchase / Industrial production
*Maracás	Arabica	Acquisition at the planting site / Family farming production
*Poções	Arabica	Purchased at an open-air market / Family farming production
**Barra da Estiva	Arabica	Purchased directly from the producer / Family farming production
**Brumado	No information on the label	Supermarket purchase / Industrial production
**Ibicoara	Arabica	Supermarket purchase / Artisanal roasting / Agroecological coffee
**Ituaçu	Arabica	Supermarket purchase / Family farming production

Regions in Bahia: *Southwest; **Chapada Diamantina.

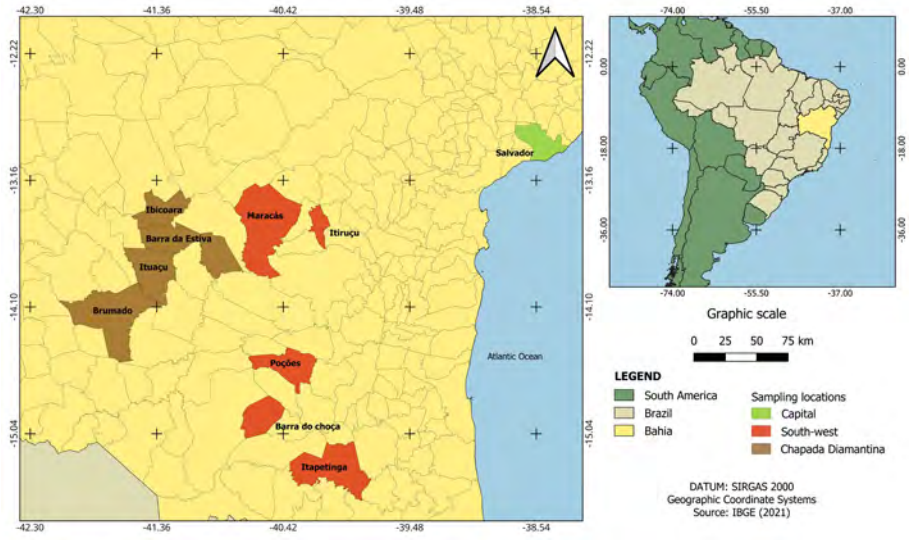

Figure 1. Map illustrating the municipalities localization where ground coffee samples were produced.

RESULTS AND DISCUSSION

Figures of merit

After preparing the ground coffee samples, Al, Co, Cr, Cu, Fe, Mn, Ni, V and Zn were quantified using MIP OES. The concentrations of the elements in the samples were calculated through linear regression obtained by least squares. The correlation coefficients were greater than 0.9988, which implies good linearity of the method; R^2 values greater than 0.998 are satisfactory, according to the National Institute of Metrology, Standardization and Industrial Quality (INMETRO).[22]

The limits of detection (LOD) and quantification (LOQ) were calculated by two methods: 1) by multiplying the standard deviation of ten analytical blank measurements by three and ten, respectively, and dividing the result by the slope of the analytical curve; 2) using the residual standard deviation of the regression line. The values obtained are presented in Table III. Although the values obtained by the second method are greater than the first, these limits were satisfactory for the quantification of the elements in ground coffee samples, with the exception of Pb, where the concentration value obtained was lower than the calculated LOQ for both methods and Cr, where the concentration of some samples was higher than the LOQ using the second method.

Intermediate precision (n=15) was evaluated by applying the same analytical methodology on different days considering the influence of random effects. The RSD (%) was in the range of 0.70 – 6.8 for the dataset, which indicates that the method has an acceptable intermediate precision, as shown in Table III.

Accuracy was evaluated by calculating the percent recovery of the analyte at three different concentration levels using spike tests (Table III). Recoveries ranging from 71.3 to 110% were obtained and are considered acceptable. Therefore, the method presents adequate precision and accuracy for the analysis of the nine metals in ground coffee samples.

Table III. Figures of merit obtained for the method applied in the analysis of ground coffee samples produced in municipalities of the Southwest and Chapada Diamantina regions of Bahia

Analyte	LOD (μg g^{-1})		LOQ (μg g^{-1})		Intermediate precision RSD (%)	Accuracy (Recovery - %)		
	Method I	Method II	Method I	Method II		Spike 1	Spike 2	Spike 3
Al	0.31	0.55	1.0	1.8	0.91	71.3	105	108
Co	0.090	0.11	0.30	0.36	3.0	88.4	91.7	84.8
Cr	0.17	0.21	0.57	0.70	1.7	80.0	96.8	96.0
Cu	0.53	1.0	1.7	2.3	0.80	73.7	80.2	81.3
Fe	1.1	1.7	3.6	5.7	0.91	74.3	96.2	94.2
Mn	0.35	0.66	1.2	2.3	3.0	77.9	94.4	85.0
Ni	0.070	0.10	0.23	0.34	1.0	110	100	98.9
Pb	0.081	0.19	0.26	0.61	6.8	75.4	95.3	94.1
V	0.032	0.037	0.10	0.11	3.7	93.0	85.8	79.2
Zn	0.45	0.99	1.4	3.1	0.70	82.1	87.9	87.7

LOD: Limit of Detection; LOQ: Limit of Quantification; RSD: Relative Standard Deviation; Method I: calculated by multiplying the standard deviation of analytical blank measurements; Method II: calculated using the residual standard deviation of the regression line.
Spike 1: 12.5 μg g^{-1} for Fe; 6.25 μg g^{-1} for Al, Ni, Pb, V and Zn; 1.25 μg g^{-1} for Co, Cr, Cu and Mn.
Spike 2: 200 μg g^{-1} for Fe; 125 μg g^{-1} for Al, Ni, Pb, V and Zn; 20.0 μg g^{-1} for Co, Cr, Cu and Mn.
Spike 3: 625 μg g^{-1} for Fe; 325 μg g^{-1} for Al, Ni, Pb, V and Zn; 312 μg g^{-1} for Co, Cr, Cu and Mn.

Application of the method in real samples

After obtaining the figures of merit for the method, Al, Co, Cr, Cu, Fe, Mn, Ni, V and Zn were quantified in ground coffee samples from ten municipalities in the State of Bahia. The results of the analyses obtained by MIP OES, represented as mean and standard deviation (n=3), are presented in Table IV and the interpolation maps with the mean concentrations are presented in Figure 2. The results for Pb were not presented, as the concentration values were below the LOQ of the technique for this element. Ultra-trace concentrations of Pb for food matrices represent relevant information, since Pb is a potentially toxic element.

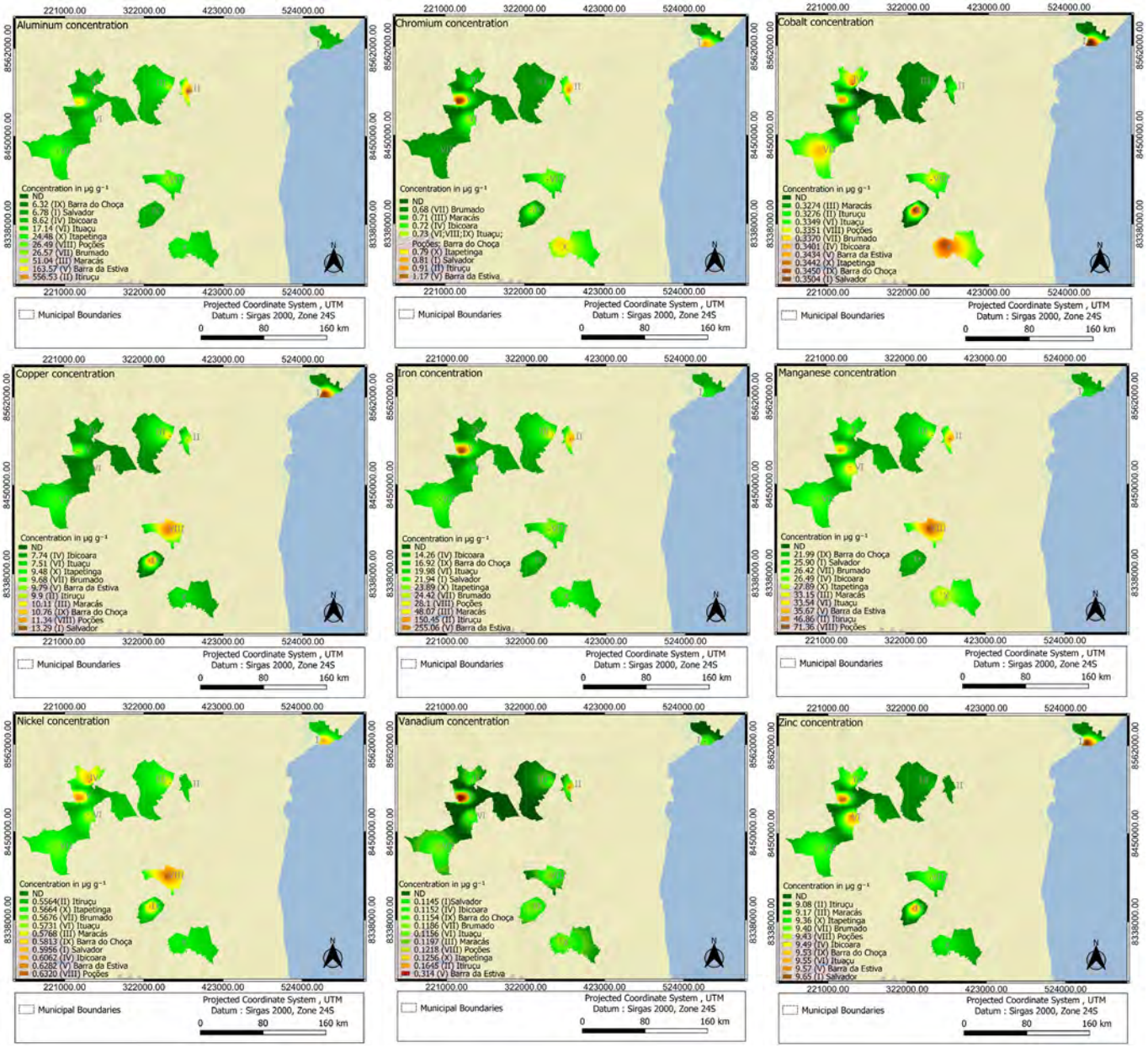

Figure 2. Interpolation maps with the mean concentrations obtained by analysis of ground coffee samples produced in municipalities of the Southwest and Chapada Diamantina regions of Bahia.

Table IV. Concentrations of elements quantified in ground coffee samples produced in municipalities of the Southwest and Chapada Diamantina regions of Bahia

Sample	Statistical parameters	Concentration (µg g^{-1})								
		Al	Co	Cr	Cu	Fe	Mn	Ni	V	Zn
Salvador	Mean	6.78	0.351	0.812	13.3	21.9	25.9	0.587	0.109	9.65
	SD	0.60	0.0030	0.051	0.38	3.7	1.6	0.0091	0.0031	0.050
	RSD (%)	8.8	0.85	6.3	2.9	17	6.2	1.6	2.8	0.52
*Barra do Choça	Mean	6.32	0.345	0.731	10.8	16.9	22.0	0.581	0.111	9.53
	SD	0.16	0.0030	0.010	0.21	0.58	0.57	0.0032	0.0012	0.10
	RSD (%)	2.5	0.87	1.4	1.9	3.4	2.6	0.55	1.1	1.1

(continued on next page)

Table IV. Concentrations of elements quantified in ground coffee samples produced in municipalities of the Southwest and Chapada Diamantina regions of Bahia (continued)

Sample	Statistical parameters	Concentration (μg g^{-1})								
		Al	Co	Cr	Cu	Fe	Mn	Ni	V	Zn
*Itapetinga	Mean	24.5	0.337	0.793	9.48	23.9	27.9	0.570	0.118	9.36
	SD	1.6	0.0011	0.023	0.13	1.9	0.44	0.0039	0.0012	0.038
	RSD (%)	6.5	0.23	2.9	1.4	7.9	1.6	0.68	1.1	0.41
*Itiruçu	Mean	556	0.328	0.912	9.90	150	46.9	0.558	0.161	9.08
	SD	20	0.0012	0.010	0.068	2.2	1.2	0.011	0.0032	0.041
	RSD (%)	3.6	0.37	1.1	0.69	1.5	2.6	2.0	2.0	0.45
*Maracás	Mean	51.0	0.335	0.711	10.1	48.0	33.2	0.582	0.122	9.17
	SD	2.1	0.0010	0.032	0.49	4.2	0.90	0.018	0.0010	0.078
	RSD (%)	4.1	0.30	4.5	4.9	8.8	2.7	3.1	0.82	0.85
*Poções	Mean	26.5	0.327	0.733	11.3	28.1	71.4	0.630	0.121	9.43
	SD	2.2	0.0011	0.011	0.73	1.1	0.71	0.011	0.0010	0.012
	RSD (%)	8.3	0.34	1.5	6.5	3.9	0.99	1.8	0.83	0.13
**Barra da Estiva	Mean	164	0.341	1.17	9.79	255	35.7	0.631	0.310	9.57
	SD	4.7	0.0012	0.040	0.14	18	0.54	0.051	0.021	0.038
	RSD (%)	2.9	0.35	3.4	1. 4	7.1	1.5	8.1	6.8	0.40
**Brumado	Mean	26.6	0.342	0.678	9.68	24.4	26.4	0.568	0.121	9.40
	SD	2.2	0.0042	0.031	0.051	0.47	0.62	0.0020	0.0012	0.081
	RSD (%)	8.3	1.2	4.6	0.53	1.9	2.4	0.35	1.0	0.86
**Ibicoara	Mean	8.62	0.340	0.719	7.74	14.3	26.5	0.612	0.109	9.49
	SD	0.53	0.011	0.023	0.42	0.59	0.40	0.022	0.0028	0.22
	RSD (%)	6.2	3.2	3.2	5.4	4.1	1.5	3.6	2.6	2.3
**Ituaçu	Mean	17.1	0.331	0.731	7.51	20.0	33.5	0.571	0.112	9.55
	SD	1.2	0.0010	0.060	0.12	0.47	0.60	0.0011	0.0010	0.068
	RSD (%)	7.0	0.30	8.2	1.6	2.4	1.8	0.19	1.0	0.71

Regions in Bahia: *Southwest; **Chapada Diamantina. SD: Standard Deviation; RSD: Relative Standard Deviation.

For aluminum, the highest concentration was 556 μg g^{-1} for the Itiruçu sample, followed by 164 μg g^{-1} for the Barra da Estiva sample. The lowest concentration (6.32 μg g^{-1}) was found for the Barra do Choça sample. The mean concentration obtained among the samples was 88.7 μg g^{-1}. For cobalt, the highest concentration was 0.351 μg g^{-1} for the Salvador sample, followed by 0.345 μg g^{-1} for the Barra do Choça sample. The lowest concentration (0.327 μg g^{-1}) was obtained for the Itiruçu sample. The mean concentration among the samples was 0.345 μg g^{-1}. In the case of chromium, the sample from Barra da Estiva presented the highest concentration (1.17 μg g^{-1}), followed by the sample from Itiruçu (0.912 μg g^{-1}). The sample acquired in Brumado had the lowest concentration (0.678 μg g^{-1}). The mean concentration obtained was 0.803 μg g^{-1}.

The Salvador sample had the highest concentration of copper (13.3 μg g^{-1}), followed by the Poções sample (11.3 μg g^{-1}). The lowest concentration (7.51 μg g^{-1}) was observed in the Ituaçu sample. The mean concentration obtained among the samples was 9.96 μg g^{-1}. For iron, the highest concentrations were 255 μg g^{-1} for the Barra da Estiva sample and 150 μg g^{-1} for the Itiruçu sample. The lowest concentration (14.3 μg g^{-1}) was detected in the Ibicoara sample. The mean concentration obtained among the samples was 60.3 μg g^{-1}.

For manganese, the coffee purchased in Poções had the highest concentration (71.4 μg g^{-1}) and 46.9 μg g^{-1} was found as the second highest value for the sample from Itiruçu. The lowest concentration was 22.0 μg g^{-1} for the sample from Barra do Choça and 34.9 μg g^{-1} was obtained as the mean concentration.

The highest concentration found for nickel was 0.631 μg g^{-1} for the samples from Barra da Estiva and Poções, followed by 0.612 μg g^{-1} for the sample from Ibicoara. The lowest concentration (0.558 μg g^{-1}) was found for the sample from Itiruçu and a mean concentration of 0.594 μg g^{-1} was found among the samples. For vanadium, the highest concentration was 0.310 μg g^{-1} for the samples from Barra da Estiva, followed by 0.161 μg g^{-1} for those from Itiruçu. The lowest concentration was 0.109 μg g^{-1} for the sample from Salvador. The mean concentration among the samples was 0.137 μg g^{-1}. Finally, the sample acquired in Salvador presented the highest zinc concentration (9.65 μg g^{-1}), followed by the sample from Barra da Estiva (9.57 μg g^{-1}). Itiruçu presented the lowest concentration (9.08 μg g^{-1}). The mean concentration among the samples was 9.42 μg g^{-1}.

In general, the concentrations found for each of the metals for the different samples are close to each other, with the exception of the values found for aluminum in the sample from Itiruçu (556 μg g^{-1}) and Barra da Estiva (164 μg g^{-1}) and for iron from Barra da Estiva (255 μg g^{-1}), which were much higher than in the other locations. For all samples, the elements with the highest concentrations were manganese, iron, aluminum, zinc and copper; and the lowest concentrations were observed for chromium, nickel, cobalt and vanadium. Table S1 (Supplementary material) presents the results organized in a decreasing concentration order. It is possible to verify that there is no single pattern obtained, mainly due to the differences in the origin of these samples. The similarity is present only for the elements found at lower concentrations, with the sequence Cr > Ni > Co > V being identified in all samples.

The variation in the concentration of metals in ground coffee is associated with different natural and anthropogenic factors, including atmospheric deposition; the chemical composition and pH of the soil; the form of management; contamination by fertilizers, correctives and pesticides used in cultivation; and even the proximity of plantations to large centers and highways.[23] In addition, the influence of the machinery used in the production and storage process should be taken into account which, depending on the conservation and maintenance conditions, can influence the quality of the final product.[24]

Several metals are essential for the development of plants, animals and humans. Copper, manganese, zinc and nickel are essential for the development of coffee crops, being increased via soil or leaves, which can, therefore, result in their presence in the beans. Furthermore, copper and zinc are indispensable in human metabolism and participate in enzymatic activities, while iron significantly contributes to the cellular reactions of the organism.[25,26] However, the metals studied in this research are considered potential contaminants. Factors such as concentration, route of exposure, as well as age, genetics and nutritional status of the exposed individuals are taken into consideration.[27] This further reinforces the need for studies on the concentrations present in food matrices, both for monitoring and nutritional reasons. It is also worth noting that recent information on the elemental composition of ground coffee samples in the regions studied is rare.

Data processing using multivariate analysis

A multivariate evaluation of the results obtained after the determination of the analytes by MIP OES (Table IV) was performed using principal component analysis and Kohonen neural networks. These mathematical treatments become an interesting alternative to improve the understanding and interpretation of the generated data, since it increases the understanding of the information by exploring the presence or absence of clusters among the samples.

Principal component analysis

A data matrix was initially created (10 samples × 9 variables) containing information regarding the ground coffee samples arranged in rows and information regarding the variables (individual element concentration values) arranged in columns. The Supplementary material (Table S2) presents the loading values that represent the importance of each variable to establish the principal components. Value above 0.60, highlighted in bold in the table, was considered a significant contribution.

The variables that most contribute to total variance (Al, Cr, Fe and V) presented significant values in PC1, highlighting that the first component represents 37.5% of data variance. The second principal component (PC2) accounts for 27.9% of data variance, with Co, Ni and Zn being the variables that present the highest values in PC. The third component (PC3) is responsible for 15.1% of the variance and is related to Mn. The fourth principal component (PC4) is responsible for only 10.6% of data variance and is related to Cu. The sum of the first four PCs accounts for 91.2% of data variance.

Data using PCA is interpreted through the axes of the principal components, where the score plot presents the coordinates of the samples on the new axes and the loading plot presents the eigenvectors, allowing data identification and expression, highlighting their similarities and differences. Figure 3a presents the score plot and Figure 3b presents the loading plot with the most significant PCs (PC1 × PC2). To include manganese in the evaluation, score plots (Figure 3c) and loading plots (Figure 3d) were generated using PC1 × PC3. These graphs allow the evaluation of the contribution of each variable in group separation.

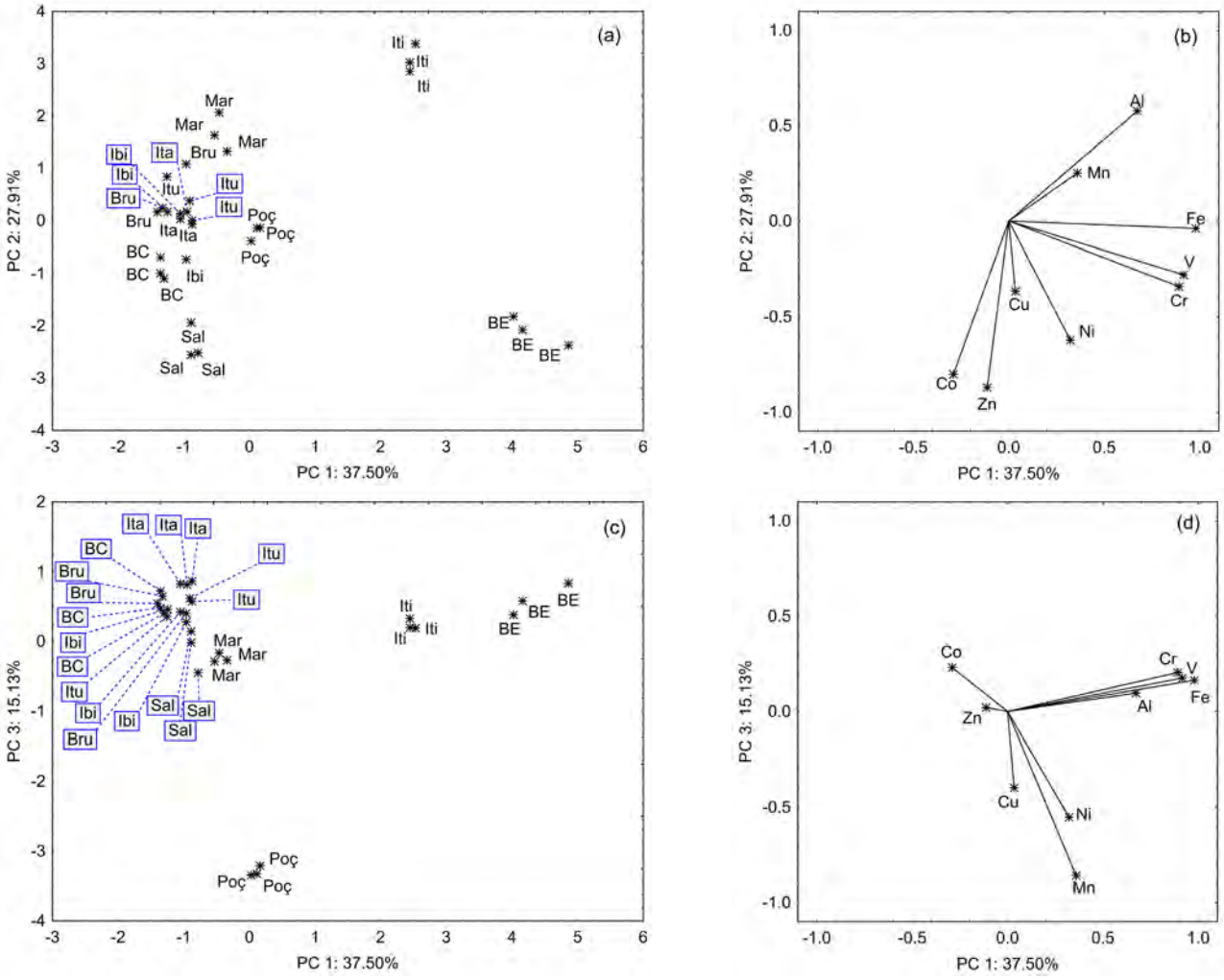

Figure 3. Plots generated from principal component analysis of the data obtained by analysis of ground coffee samples produced in municipalities of the Southwest and Chapada Diamantina regions of Bahia: (a) Score plot for PC1 × PC2; (b) Loading plot for PC1 × PC2; (c) Score plot for PC1 × PC3; and (d) Loading plot for PC1 × PC3.

Analyzing Figures 3a and 3b, it is possible to verify that the samples are separated into three parts, one consisting of the majority of the samples and the other two with isolated samples. There is a high similarity

between the samples from Barra do Choça, Brumado, Ibicoara, Itapetinga, Ituaçu, Maracás, Poções and Salvador. The grouping of these samples is due to the low concentrations of Al, Co, Cr, Fe, Ni, V and Zn. The sample from Itiruçu (present in the positive part of components 1 and 2) was isolated in the plot due to the higher concentration of Al in relation to the others. Likewise, the sample from Barra da Estiva (present in the positive part of component 1 and negative part of component 2) was isolated due to the higher concentration of Cr, Fe and V.

Analyzing Figures 3c and 3d, it is also possible to verify the formation of three clusters. The Poções sample was isolated in the plot due to the higher concentration of Mn present in relation to the other samples. Sample clustering of Barra da Estiva and Itiruçu is due both to the higher concentrations found for Al, Cr, Fe and V, and to the intermediate concentrations found for Mn. The main group observed in PC1 × PC2 is maintained when evaluating PC1 × PC3.

Neural networks

Kohonen self-organizing maps (KSOM) are an exploratory analysis tool that identifies sample groups and variables that constitute the generated maps, in addition to interpreting linear and nonlinear variables, unlike PCA, which is only applicable to linear variables. Due to its data modeling capacity, KSOM can be used to corroborate or disconfirm PCA data. In this context, KSOM was used to evaluate whether the pattern recognition capacity could be improved.

The 5 × 3-dimension map can be seen in Figure 4a, showing the best sample distribution according to their similarities. Each hexagon represents a neuron in the map, and each sample is represented by a neuron. Figure 4b presents the unified distance matrix where warm colors (red) indicate high distance values, while cold colors (blue) indicate low distance values and the highlighted neurons (hexagons) make up the position on the map (circle) of the samples.

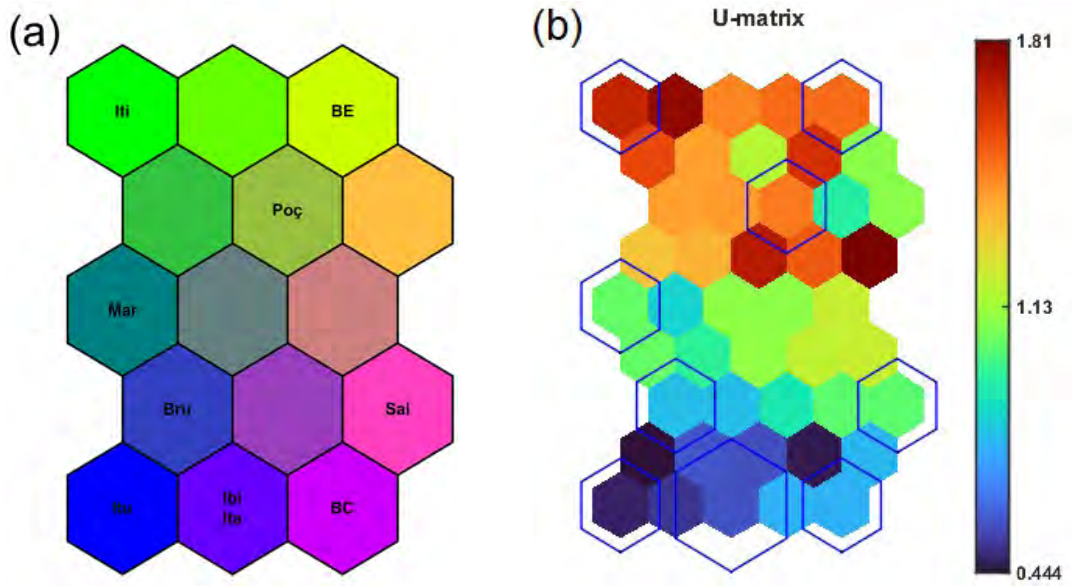

Figure 4. Graphs produced after Kohonen Self Organizing Maps application on the metal concentrations in ground coffee samples produced in municipalities of the Southwest and Chapada Diamantina regions of Bahia: (a) Best sampling distribution according to similarities and (b) Unified distance matrix.

Analyzing Figure 4, it is possible to observe a cluster formed by the cities of Poções and Barra da Estiva at first and then by Itiruçu, since both are located in the upper part on the right and left, respectively. It is also possible to see a large cluster in the lower part formed by the other cities: Barra do Choça, Brumado, Ibicoara, Itapetinga, Ituaçu, Maracás and Salvador.

The influence of variables on the formation of city clusters can be seen in the component maps (Figure 5). The position occupied by a sample on the dimensional map corresponds to the same position on the variable map. Warm colors (red) indicate high concentration values for the variable under study, while cold colors (blue) indicate low values.

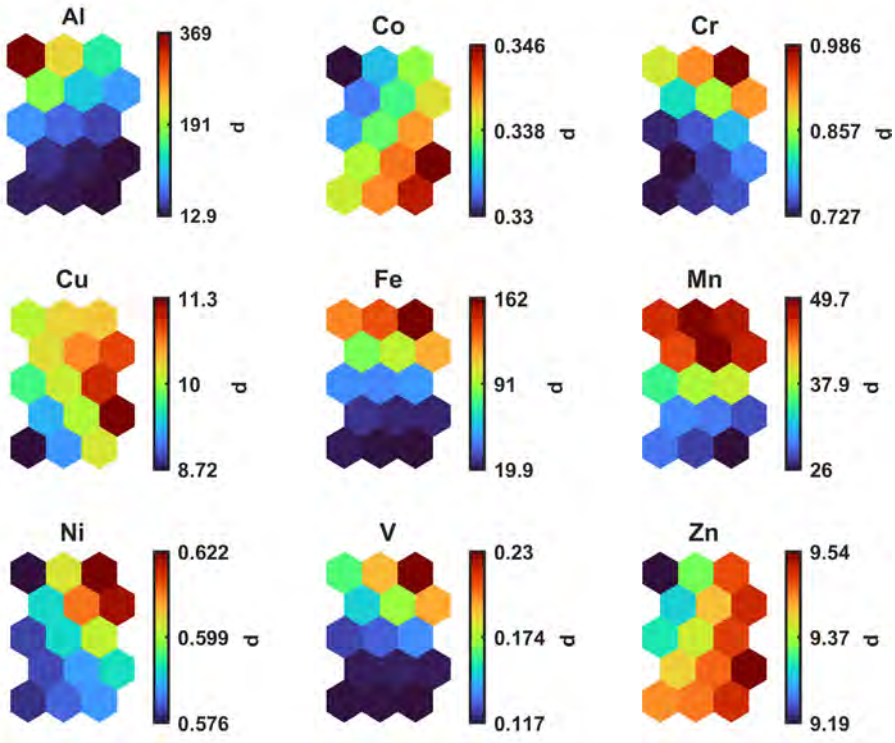

Figure 5. Neural maps showing as metals concentrations contribute in the neural modeling after Kohonen Self Organizing Maps application in data from ground coffee samples produced in municipalities of the Southwest and Chapada Diamantina regions of Bahia.

It can be seen that the cluster formed by Poções and Barra do Estiva refers to high concentrations of Fe, V and Cr and, secondly, the cluster formed with Itiruçu, is due to high concentrations of Al.

A comparative evaluation of the multivariate analyses performed using PCA (Figures 3a and 3b) and KSOM (Figures 4 and 5) reveals coherent and complementary information regarding the similarity patterns of the ground coffee samples assessed. Both PCA and KSOM indicated the formation of three distinct groups among the evaluated samples. In the PCA score plot (Figure 3a), most samples were clustered together, whereas two samples – Itiruçu and Barra da Estiva – were clearly separated due to their high concentrations of specific elements. A similar clustering pattern was observed in the KSOM map (Figure 4a), in which a cluster was formed by the samples from Poções and Barra da Estiva, followed by the isolated positioning of the Itiruçu sample. The remaining samples, collected from Barra do Choça, Brumado, Ibicoara, Itapetinga, Ituaçu, Maracás, and Salvador, were grouped together, suggesting a high degree of similarity in their mineral composition.

The variables responsible for sample separation were also consistent across both multivariate approaches. In the PCA loading plot (Figure 3b), aluminum, chromium, iron, and vanadium were identified as the main contributors to the isolation of the Itiruçu and Barra da Estiva samples. This behavior was corroborated by the KSOM component maps (Figure 4), in which high concentrations of these elements were highlighted in the corresponding clusters. Moreover, both methods consistently distinguished the sample from Poções due to its higher manganese content, as evidenced in the PCA score plot using PC1 × PC3 (Figure 3c) and in the neural network component maps (Figure 4).

Despite the convergence of results, the two multivariate techniques differ in their analytical approach and graphical representation. PCA is restricted to identifying linear relationships among variables and relies on the interpretation of score and loading plots. In contrast, KSOM enables the analysis of both linear and non-linear relationships, providing a more intuitive visualization of sample proximity and the influence of individual variables through the unified distance matrix and component maps.

Furthermore, KSOM allows for a clearer and more direct interpretation of variable contributions to sample grouping, as indicated by the color gradients in the distance matrix (Figure 4b) and in the component maps (Figure 5). In comparison, PCA does not visually express the distance magnitude between samples and is limited to the variance explained by the principal components.

Some additional insights can be realized by KSOM compared to PCA. Although PCA is limited to the identification of linear relationships, KSOM effectively captured both linear and non-linear patterns within the dataset, thereby enhancing the interpretation of complex data structures. Specifically, KSOM offered a topological representation of sample similarity through the unified distance matrix (U-Matrix), which visually quantified the degree of dissimilarity among samples. This characteristic provided an intuitive understanding of sample distribution, a level of detail not accessible in PCA score plots. Additionally, the component maps generated by KSOM facilitated a localized assessment of the influence of each variable on sample clustering, complementing the global overview offered by PCA loading plots.

The topology-preserving characteristic of KSOM ensured that samples with similar mineral profiles were positioned adjacently on the map, allowing the identification of subtle patterns that may not have been discernible through PCA alone. In summary, KSOM proved to be a valuable complementary tool to PCA, providing a more detailed and comprehensive visualization of sample similarity and variable contribution, as well as capturing complex, non-linear relationships within the ground coffee dataset.

The error check was made using (i) quantization error, representing the average of the distances between each data vector and the corresponding weight vector of the winning neuron. The quantization error does not have a standard value; however, the smaller the error, the better the winning neuron will define the input vectors and (ii) topographic error, which quantifies the ability of the map to describe the topology of the input data. It is calculated by checking all inputs, as well as which neuron is the best and which is the second best.[28] Likewise, the topographic error does not have a standard value, but it is better when the values tend to zero. In this study, the values of the quantization and topographic errors were equal to 1.360 and 0.000, respectively, evidencing good accuracy of the sample data to represent the topology of the obtained network.

The results obtained did not reveal any significant differences in the concentrations of the elements between the samples from artisanal processing (family farming) and those from industrial processing. High concentrations of Al and Fe were found in samples from cities (Barra da Estiva and Itiruçu) that process coffee differently. On the other hand, the sample from industrial processing located in Salvador presented the highest concentrations for Co, Cu and Zn, and the lowest for V. Further studies are necessary to assess whether there is a change in the elemental composition depending on the sample processing method.

In the current Brazilian legislation, there are no maximum consumption limits required for any the metals analyzed in this study. However, considering the maximum permitted limits (μg g^{-1}) in Decree No. 55,871 of March 26, 1965, revoked in 2019 (Cu: 30.0; Cr: 0.10; Ni: 5.0 and Zn: 50.0),[29] the average values found for chromium are above the limit. The other elements mentioned are below the maximum values established. The concentration values found in this study were compared to values described in the literature for the same analytes in different types of coffee, as shown in Table V.

Table V. Comparison of the values obtained for the ground coffee samples with other studies reported in the literature

Reference	Sample characteristics	Applied technique	Analyte	Observed concentration range in the literature (μg g^{-1})	Observed concentration range in this study using MIP OES (μg g^{-1})
Oleszczuk et al., 2007.[30]	Green coffee beans (Brazil)	ICP OES	Co	0.100 – 0.300	0.327 – 0.351
			Cu	10.0 – 16.0	7.51 – 13.3
			Mn	15.0 – 32.0	22.0 – 71.4
Habte et al., 2016.[31]	Green coffee beans (Ethiopia)	ICP OES ICP-MS	Al	4.23 – 173	6.32 – 556
			Co	0.0190 – 0.0610	0.327 – 0.351
			Cr	0.0710 – 0.255	0.678 – 1.17
			Cu	13.2 – 16.9	7.51 – 13.3
			Fe	21.1 – 127	14.3 – 255
			Mn	12.6 – 24.0	22.0 – 71.4
			Ni	0.139 – 0.509	0.558 – 0.631
			V	0.00500 – 0.102	0.109 – 0.310
			Zn	3.00 – 8.27	9.08 – 9.65
Semen et al., 2017.[32]	Green coffee beans (Turkey)	ICP-MS	Al	4.56 – 45.3	6.32 – 556
			Co	0.0900 – 0.250	0.327 – 0.351
			Cu	9.85 – 14.7	7.51 – 13.3
			Ni	0.270 – 0.810	0.558 – 0.631
			Zn	3.79 – 42.4	9.08 – 9.65
Pohl et al., 2022.[33]	Ready-to-drink coffee after infusion (Europe)	ICP OES	Cu	0.0261 – 0.0450	7.51 – 13.3
			Fe	0.0331 – 0.175	14.3 – 255
			Mn	0.257 – 0.451	22 – 71.4
			Zn	0.0233 – 0.0948	9.08 – 9.65
Barbosa et al., 2014.[34]	Organic coffee (Brazil)	ICP-MS	Al	3.80 – 16.4	6.32 – 556
			Co	0.0505 – 0.373	0.327 – 0.351
			Cr	1.10 – 1.80	0.678 – 1.170
			Mn	15.3 – 37.7	22.0 – 71.4
			Ni	0.220 – 0.990	0.558 – 0.631
			Zn	2.90 – 6.30	9.08 – 9.65
	Conventional coffee (Brazil)	ICP-MS	Al	8.30 – 118	6.32 – 556
			Co	0.00940 – 0.368	0.327 – 0.351
			Cr	1.00 – 1.70	0.678 – 1.170
			Mn	17.3 – 30.3	22.0 – 71.4
			Ni	0.0600 – 0.960	0.558 – 0.631
			Zn	3.80 – 28.4	9.08 – 9.65

(continued on next page)

Table V. Comparison of the values obtained for the ground coffee samples with other studies reported in the literature (continued)

Reference	Sample characteristics	Applied technique	Analyte	Observed concentration range in the literature (μg g^{-1})	Observed concentration range in this study using MIP OES (μg g^{-1})
Jarošová et al., 2014.[35]	Ground coffee (India, Kenya, Honduras, Colombia and Ethiopia)	ICP-MS	Cr	0.0200 – 0.850	0.678 – 1.17
			Cu	16.6 – 19.3	7.51 – 13.3
			Fe	23.9 – 47.7	14.3 – 255
			Mn	27.3 – 123	22.0 – 71.4
			Ni	0.0700 – 3.69	0.558 – 0.631
			Zn	1.71 – 7.12	9.08 – 9.65
Voica et al., 2016.[36]	No identification (various countries)	ICP-MS	Al	0.540 – 308	6.32 – 556
			Co	0.0400 – 1.05	0.327 – 0.351
			Cr	0.900 – 57.0	0.678 – 1.170
			Cu	0.460 – 151	7.51 – 13.3
			Fe	5.90 – 521	14.3 – 255
			Mn	7.57 – 70.1	22.0 – 71.4
			Ni	0.220 – 12.2	0.558 – 0.631
			Zn	1.68 – 22.4	9.08 – 9.65
Albals et al., 2021.[37]	Green and roasted coffee beans (Jordan)	ICP-MS	Al	70.90 – 182	6.32 – 556
			Co	0.27 – 0.970	0.327 – 0.351
			Cr	2.03 – 4.06	0.678 – 1.170
			Cu	24.85 – 30.8	7.51 – 13.3
			Fe	132.20 – 196	14.3 – 255
			Mn	45.10 – 86.2	22.0 – 71.4
			Ni	0.75 – 2.67	0.558 – 0.631
			V	0.72 – 1.62	0.109 – 0.310
			Zn	5.99 – 10.6	9.08 – 9.65

ICP OES: Inductively Coupled Plasma Optical Emission Spectrometry; ICP-MS: Inductively Coupled Plasma Mass Spectrometry; MIP OES: Microwave Induced Plasma Optical Emission Spectrometry.

In the comparisons presented in Table V, it can be observed that the variations in the concentrations found for aluminum and iron were also greater for Habte et al.,[31] Barbosa et al.,[34] Voica et al.[36] and Albals et al.,[37] indicating agreement with this study. Both the high concentrations of iron and aluminum can be directly associated with soil pH, since these elements have greater availability for plants in acidic soils.

Pohl et al.[33] determined the concentrations of copper, iron, manganese and zinc for ready-to-drink coffee after infusion, and the values found were much lower than those of the roasted and ground coffee samples in our study. This is justifiable, considering that not only is the concentration of the elements extracted in the aqueous infusion process of the beverage influenced by the initial concentrations of the elements present in the ground coffee used, but also by the preparation conditions of the beverage, the coffee matrix and the physical and chemical characteristics of the elements. The degree of leachability is different for each element and for each type of coffee, as a function of factors such as the nature and strength of the ion complexes of the elements formed with coffee constituents.

Barbosa et al.[34] conducted a comparative study between samples of conventionally grown and organically grown coffee. Aluminum and zinc levels in conventionally grown coffee samples were higher, while cobalt, chromium, manganese and nickel levels were similar between the two types of crops. These values are consistent with those observed in our study, with the exception of aluminum.

CONCLUSIONS

In this study, it was possible to efficiently apply a method for decomposing ground coffee samples using diluted acid and hydrogen peroxide. Samples from different regions of Bahia were analyzed and the results could be evaluated in relation to the content of Al, Co, Cr, Cu, Fe, Mn, Ni, V and Zn, quantified by MIP OES. Regarding Pb, MIP OES did not show quantification capacity for direct analysis.

The analyses performed through PCA and KSOM indicated the formation of three distinct groups among the evaluated samples. KSOM revealed specific zones with high concentrations of Co, Zn, and Cu, which contributed to the differentiation of certain sample clusters – information that was less evident in the PCA analysis. The use of multivariate techniques efficiently contributed to data analysis and interpretation, demonstrating that they are coherent and complementary.

In comparison with the literature, greater differences were observed in relation to aluminum and iron. The results presented in this study are important not only for nutritional and toxicological evaluation, but also to add value to coffee produced by small properties. Likewise, it provides relevant nutritional information about the coffee produced in Bahia. Such information are important for several areas of science, such as chemistry, agronomy, nutrition, health and food.

Conflicts of interest

The authors declare no conflict of interest.

Acknowledgements

The authors thank: "Fundação de Amparo à Pesquisa do Estado da Bahia" (FAPESB - INCITE grant number PIE0006/2022), "Conselho Nacional de Desenvolvimento Científico e Tecnológico" (CNPq - grant number 307904/2022-9) and "Coordenação de Aperfeiçoamento de Pessoal de Nível Superior" (CAPES - Finance Code 001).

REFERENCES

(1) Girma, B.; Wale, K. Analytical Methods for Determining Metals Concentrations in Coffee (*Coffea arabica L.*) in Ethiopia: A Review. *Am. J. Appl. Chem*. **2023,** *11* (4), 95-102. https://doi.org/10.11648/j.ajac.20231104.11

(2) Baqueta, M. R.; Diniz, P. H. G. D.; Pereira, L. L.; Almeida, F. L. C.; Valderrama, P.; Pallone, J. A. L. An overview on the Brazilian *Coffea canephora* scenario and the current chemometrics-based spectroscopic research. *Food Res. Int.* **2024**, *194*, 114866. https://doi.org/10.1016/j.foodres.2024.114866

(3) Leite, S. A.; Guedes, R. N. C.; Santos, M. P. D.; Costa, D. R. D.; Moreira, A. A.; Matsumoto, S. N.; Lemos, O. L.; Castellani, M. A. Profile of coffee crops and management of the neotropical coffee leaf miner, *Leucoptera coffeella*. *Sustainability* **2020,** *12* (19), 8011. https://doi.org/10.3390/su12198011
(4) Febrianto, N. A.; Zhu, F. Coffee bean processing: Emerging methods and their effects on chemical, biological and sensory properties. *Food Chem.* **2023,** *412*, 135489. https://doi.org/10.1016/j.foodchem.2023.135489
(5) Kargarghomsheh, P.; Tooryan, F.; Sharifiarab, G.; Moazzen, M.; Shariatifar, N.; Arabameri, M. Evaluation of trace elements in coffee and mixed coffee samples using ICP-OES method. *Biol. Trace Elem. Res.* **2024**, *202* (5), 2338-2346. https://doi.org/10.1007/s12011-023-03795-w
(6) Khaneghah, A. M.; Mahmudiono, T.; Javanmardi, F.; Tajdar-Oranj, B.; Nematollahi, A.; Pirhadi, M.; Fakhri, Y. The concentration of potentially toxic elements (PTEs) in the coffee products: A systematic review and meta-analysis. *Environ. Sci. Pollut. Res.* **2022***, 29*, 78152–78164. https://doi.org/10.1007/s11356-022-23110-9
(7) Gromadzka, G.; Grycan, M.; Przybyłkowski, A. M. Monitoring of Copper in Wilson Disease. *Diagnostics* **2023**, *13*, 1830. https://doi.org/10.3390/diagnostics13111830
(8) Schoofs, H.; Schmit, J.; Rink, L. Zinc Toxicity: Understanding the Limits. *Molecules* **2024**, *29*, 3130. https://doi.org/10.3390/molecules29133130
(9) Sun, B.; Tan, B.; Zhang, P.; Zhu, L.; Wei, H.; Huang, T.; Yang, W. Iron deficiency anemia: A critical review on iron absorption, supplementation and its influence on gut microbiota. *Food Funct*. **2024**, *15* (3), 1144-1157. https://doi.org/10.1039/D3FO04644C
(10) Frydrych, A.; Frankowski, M.; Jurowski, K. The toxicological analysis and assessment of essential elements (Cu, Fe, Mn, Zn) in Food for Special Medical Purposes (FSMP) dedicated to oncological patients available in Polish pharmacies. *Food Chem. Toxicol.* **2024**, *189*, 114768. https://doi.org/10.1016/j.fct.2024.114768
(11) Leyssens, L.; Vinck, B.; Van Der Straeten, C.; Wuyts, F.; Maes, L. Cobalt toxicity in humans—A review of the potential sources and systemic health effects. *Toxicology* **2017**, *387*, 43-56. https://doi.org/10.1016/j.tox.2017.05.015
(12) Bryliński, Ł.; Kostelecka, K.; Woliński, F.; Duda, P.; Góra, J.; Granat, M.; Flieger, J.; Teresiński, G.; Buszewicz, G.; Sitarz, R.; et al. Aluminium in the Human Brain: Routes of Penetration, Toxicity, and Resulting Complications. *Int. J. Mol. Sci*. **2023**, *24*, 7228. https://doi.org/10.3390/ijms24087228
(13) Amaral, L. M. P. F.; Moniz, T.; Silva, A. M. N.; Rangel, M. Vanadium Compounds with Antidiabetic Potential. *Int. J. Mol. Sci.* **2023**, *24*, 15675. https://doi.org/10.3390/ijms242115675
(14) Ferreira, S. L. C.; Porto, I. S. A.; Felix, C. S. A.; Dantas, S. V. A.; Chagas, A. V. B., Muller, T. P., Aleluia, A. C. M. Determination and Risk Assessment of Toxic Chemical Elements in Fish Samples - A Review. *Anal. Lett.* **2025,** *58* (6), 926–942. https://doi.org/10.1080/00032719.2024.2347455
(15) Rizwan, M.; Usman, K.; Alsafran, M. Ecological impacts and potential hazards of nickel on soil microbes, plants, and human health. *Chemosphere* **2024**, *357*, 142028. https://doi.org/10.1016/j.chemosphere.2024.142028
(16) dos Santos, H. D.; Boffo, E. F. Coffee beyond the cup: analytical techniques used in chemical composition research – a review. *Eur. Food Res. Technol*. **2021**, *247*, 749–775 https://doi.org/10.1007/s00217-020-03679-6
(17) Müller, A.; Pozebon, D.; Dressler, V. L. Advances of nitrogen microwave plasma for optical emission spectrometry and applications in elemental analysis: a review. *J. Anal. At. Spectrom.* **2020**, *35* (10), 2113-2131. https://doi.org/10.1039/D0JA00272K
(18) Balaram, V. Microwave plasma atomic emission spectrometry (MP-AES) and its applications – A critical review. *Microchem. J*. **2020**, *159*, 105483. https://doi.org/10.1016/j.microc.2020.105483
(19) Faiza, B. H.; Scott, C.; Winroth, S.; Ishida, H. Synthesis of Bio-Based and Intrinsically Flame-Retardant Benzoxazine Containing Dynamic Ester Bond that Quantitatively Satisfies All Twelve Principles of Green Chemistry. *ACS Sustain. Chem. Eng.* **2024**, *12*, 13525–13534. https://doi.org/10.1021/acssuschemeng.4c03838

(20) Souza, A. S.; Bezerra, M. A.; Cerqueira, U. M. F. M.; Rodrigues, C. J. O.; Santos, B. C.; Novaes, C. G.; Almeida, E. R. V. An introductory review on the application of principal component analysis in the data exploration of the chemical analysis of food samples. *Food Sci. Biotechnol.* **2024**, *33* (6), 1323-1336. https://doi.org/10.1007/s10068-023-01509-5

(21) Haykin, S. S. *Neural Networks and Learning Machines* (3rd Edition). Pearson Education India, 2009. ISBN: 0131293761, 9780131293762

(22) Instituto Nacional de Metrologia, Normalização e Qualidade Industrial (INMETRO). DOQCGCRE-008, *Orientação Sobre Validação de Métodos Analíticos*, Brazil, 2011. Updated in 2022/05/20. Available at: http://www.inmetro.gov.br/Sidoq/Arquivos/CGCRE/DOQ/DOQ-CGCRE-8_04.pdf (accessed 2022-06-11).

(23) Lima-Junior, D. P.; Lima, L. B.; Carnicer, C.; Zanella, R.; Prestes, O. D.; Floriano, L.; de Marco Júnior, P. Exploring the relationship between land-use and pesticides in freshwater ecosystem: A case study of the Araguaia River Basin, Brazil. *Environ. Adv.* **2024**, *15*, 100497. https://doi.org/10.1016/j.envadv.2024.100497

(24) Farghal, H. H.; Mansour, S. T.; Khattab, S.; Zhao, C.; Farag, M. A. A comprehensive insight on modern green analyses for quality control determination and processing monitoring in coffee and cocoa seeds. *Food Chem.* **2022**, *394*, 133529. https://doi.org/10.1016/j.foodchem.2022.133529

(25) Costa-Pinto, R.; Gantner, D. Macronutrients, minerals, vitamins and energy. *Anaesth. Intensive Care Med.* **2020**, *21* (3), 157-161. https://doi.org/10.1016/j.mpaic.2022.12.009

(26) Gui, J. Y.; Rao, S.; Huang, X.; Liu, X.; Cheng, S.; Xu, F. Interaction between selenium and essential micronutrient elements in plants: A systematic review. *Sci. Total Environ.* **2022**, *853*, 158673. https://doi.org/10.1016/j.scitotenv.2022.158673

(27) Anissa, Z.; Sofiane, B.; Adda, A.; Marlie-Landy, Joseph. Evaluation of trace metallic element levels in coffee by ICP-MS: a comparative study among different origins, forms, and packaging types and consumer risk assessment. *Biol. Trace Elem. Res.* **2023**, *201*, 5455–5467. https://doi.org/10.1007/s12011-023-03582-7

(28) Ritter, H.; Kohonen, T. Self-organizing semantic maps. *Biol. Cybern.* **1989**, *61*, 241–254. https://doi.org/10.1007/BF00203171

(29) Presidency of the Brazilian Republic, General Secretariat, Deputy Directorate for Legal Affairs. Decree N° 55871 of March 26th, Amends Decree Nº. 50040 of January 24, 1961. Concerning regulatory standards for the use of food additives, 1965, Brazil. Updated in 2022/07/06. Available at: https://www.planalto.gov.br/ccivil_03/decreto/1950-1969/D55871.htm (accessed 2022-08-17).

(30) Oleszczuk, N.; Castro, J. T.; da Silva, M. M.; Korn, M. G. A.; Welz, B.; Vale, M. G. R. Method development for the determination of manganese, cobalto and copper in green coffee comparing direct solid sampling electrothermal atomic absorption spectrometry and inductively coupled plasma optical emission spectrometry. *Talanta* **2007**, *73*, 862–869. https://doi.org/10.1016/j.talanta.2007.05.005

(31) Habte, G.; Hwang, I. M.; Kim, J. S.; Hong, J. H.; Hong, Y. S.; Choi, J. Y.; Nho, E. Y.; Jamila, N.; Khan, N.; Kim, K. S. Elemental profiling and geographical differentiation of Ethiopian coffee samples through inductively coupled plasma-optical emission spectroscopy (ICP-OES), ICP-mass spectrometry (ICP-MS) and direct mercury analyzer (DMA). *Food Chem.* **2016**, *212*, 512–520. https://doi.org/10.1016/j.foodchem.2016.05.178

(32) Şemen, S.; Mercan, S.; Yayla, M.; Açıkkol, M. Elemental composition of green coffee and its contribution to dietary intake. *Food Chem.* **2017**, *215*, 92–100. https://doi.org/10.1016/j.foodchem.2016.07.176

(33) Pohl, P.; Welna, M.; Szymczycha-Madeja, A.; Greda, K.; Jamroz, P.; Dzimitrowicz, A. Response surface methodology assisted development of a simplified sample preparation procedure for the multielement (Ba, Ca, Cu, Fe, K, Mg, Mn, Na, Sr and Zn) analysis of different coffee brews by means of inductively coupled plasma optical emission spectrometry. *Talanta* **2022**, *241*, 123215. https://doi.org/10.1016/j.talanta.2022.123215

(34) Barbosa, R. M.; Batista, B. L.; Varrique, R. M.; Coelho, V. A.; Campiglia, A. D.; Barbosa Jr, F. The use of advanced chemometric techniques and trace element levels for controlling the authenticity of organic coffee. *Food Res. Int.* **2014**, *61*, 246–251. https://doi.org/10.1016/j.foodres.2013.07.060
(35) Jarošová, M.; Milde, D.; Kuba, M. Elemental Analysis of Coffee: A Comparison of ICP-MS and AAS Methods. *Czech J. Food Sci.* **2014,** *32* (4), 354–359. https://doi.org/10.17221/399/2013-CJFS
(36) Voica, C.; Feher, I.; Iordache, A. M.; Cristea, G.; Dehelean, A.; Magdas, D. A.; Mirel, V. Multielemental Analysis of Coffee by Inductively Coupled Plasma-Mass Spectrometry. *Anal. Lett.* **2016**, *49* (16), 2627-2643. https://doi.org/10.1080/00032719.2015.1116003
(37) Albals, D.; Al-Momani, I. F.; Issa, R.; Yehya, A. Multi-element determination of essential and toxic metals in green and roasted coffee beans: A comparative study among different origins using ICP-MS. *Sci. Prog.* **2021**, *104*, 1–17. https://doi.org/10.1177/00368504211026162

SUPPLEMENTARY MATERIAL

Table S1. Elements quantified in ground coffee samples produced in municipalities of the Southwest and Chapada Diamantina regions of Bahia in decreasing concentration order

Sample	Elements in decreasing concentration order (μg g^{-1})
Salvador	Mn > Fe > Cu > Zn > Al > Cr > Ni > Co > V
*Barra do Choça	Mn > Fe > Cu > Zn > Al > Cr > Ni > Co > V
*Itapetinga	Mn > Al > Fe > Cu > Zn > Cr > Ni > Co > V
*Itiruçu	Al > Fe > Mn > Cu > Zn > Cr > Ni > Co > V
*Maracás	Al > Fe > Mn > Cu > Zn > Cr > Ni > Co > V
*Poções	Mn > Fe > Al > Cu > Zn > Cr > Ni > Co > V
**Barra da Estiva	Fe > Al > Mn > Cu > Zn > Cr > Ni > Co > V
**Brumado	Al > Mn > Fe > Cu > Zn > Cr > Ni > Co > V
**Ibicoara	Mn > Fe > Zn > Al > Cu > Cr > Ni > Co > V
**Ituaçu	Mn > Fe > Al > Zn > Cu > Cr > Ni > Co > V

Regions in Bahia: *Southwest; **Chapada Diamantina.

Table S2. Loading values that represent the importance of each variable related to metals concentration in ground coffee samples to establish the principal components

Parameter	PC1	PC2	PC3	PC4
Al	**0.673**	0.577	0.0970	-0.308
Co	-0.290	**-0.802**	0.231	-0.149
Cr	**0.891**	-0.341	0.205	-0.105
Cu	0.0350	-0.365	-0.397	**-0.821**
Fe	**0.979**	-0.0380	0.164	0.0121
Mn	0.359	0.252	**-0.858**	0.0881
Ni	0.322	**-0.622**	-0.552	0.350
V	**0.916**	-0.279	0.176	0.148
Zn	-0.113	**-0.869**	0.0202	0.0472

PC: principal component

Brazilian Journal of Analytical Chemistry
2026, Volume 13, Issue 52, pp 40-49
doi: 10.30744/brjac.2179-3425.AR-03-2025

ARTICLE

The Determination of Abietic Acid in Natural Resins and their Derived Products Using Assisted Ultrasonic Sample Preparation and Analysis by Liquid Chromatography

Thais Fukui de Sousa*, **Daniela Daniel**

AQiA – Química Inovativa. Rua Rosa Mafei,563. Bonsucesso, Guarulhos, SP, 07177-010, Brazil

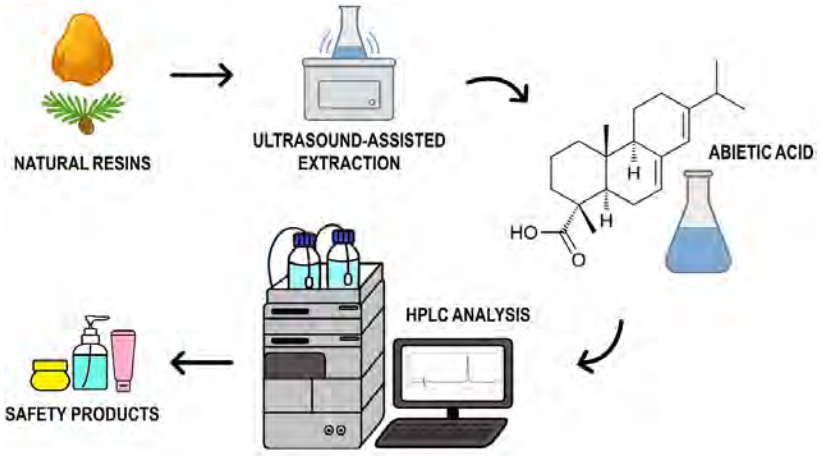

This study focused on the development and validation of a method for determining abietic acid in natural resins and derivative products using High-Performance Liquid Chromatography with spectrophotometric detection. A Pursuit PFP column (150 mm x 4.6 mm, 5.0 µm) was used to separate the abietic acid from other matrix compounds, using methanol:formic acid 0.1% (75:25) as mobile phase in isocratic elution mode at a flow rate of 0.7 mL min^{-1}. The sample analysis volume was set at 10 µL and the abietic acid was detected at a wavelength of 245 nm. The samples were prepared by ultrasonic assisted approach. The developed method showed a good linearity of the calibration curve with determination coefficient equal to 0.999. Validation parameters such as accuracy, precision, specificity, detection and quantitation limits, recovery and matrix effect were evaluated and displayed excellent reliability, accuracy and sensitivity. This method proved to be efficient to identify and quantify abietic acid in natural resins and its derivatives used as raw materials for cosmetic products.

Keywords: abietic acid, natural resins, high-performance liquid chromatography, cosmetic products, validation

INTRODUCTION

Natural resins are complex mixtures primarily composed of organic compounds, including terpenes, acids, and esters, among others. They are amorphous substances, odorless or with a slight aroma, translucent and with a color varying between yellow and dark brown, used for many years by different industries. In

Cite: de Sousa, T. F.; Daniel, D. The Determination of Abietic Acid in Natural Resins and their Derived Products Using Assisted Ultrasonic Sample Preparation and Analysis by Liquid Chromatography. *Braz. J. Anal. Chem.* 2026, *13* (52), pp 40-49. https://doi.org/10.30744/brjac.2179-3425.AR-03-2025

Submitted: January 13, 2025; **Revised:** May 2, 2025; July 7, 2025; **Accepted:** August 18, 2025; **Published online:** September 5, 2025.

This article is part of the BrJAC Special Issue dedicated to the 21st ENQA and 9th CIAQA.

cosmetics, for example, it is present in mascaras, blushes and lipsticks, helping the makeup hold together, under the name “colophonium” by INCI. It is also commonly found in dental floss, sunscreen and depilatory cream.[1,2]

The composition of natural resins can vary depending on the species of plant or tree, environmental conditions and extraction methods, and although there are variations in the composition, the major components are the same. Common components found in all natural resins are the resins acids (90%) and neutral compounds (10%). Resin acids are diterpenoid acids, of which the abietane-type structures (abietic, palustric, levopimaric and dehydroabietic acids) and pimarane-type structures (pimaric, isopimaric and sandarapimaric acids) are the most abundant. Neutral substances are composed of terpenes, terpene alcohols, sesquiterpene and diterpene hydrocarbons, aldehydes and alcohols.[3,4]

Natural resins are a common cause of allergic contact dermatitis due to their widespread usage and skin sensitizing capacity, of which the main allergenic components are abietane-type resin acids oxidized by air exposure.[5] Abietic acid is the major substance present in resins and its oxidation occurs via a free radical chain reaction, producing allergenic compounds, such as 15-hydroperoxyabetic acid, considered the major sensitizer in natural resins.[6,7] Given this situation, it is important to determinate the concentration of abietic acid, especially when you want to incorporate natural resins into a cosmetic formulation, mainly aiming to protect consumer safety.

There are several analytical methods in the literature to quantify the abietic acid in different matrices. In the beginning the analysis of abietic acid was carried out by gas chromatography (GC), however the high temperature used in the analysis leads to abietic acid isomerization and consequently to inaccurate results. The high-performance liquid chromatography (HPLC) coupled to ultraviolet or fluorescence detector has been widely developed as a better alternative to GC for high-temperature susceptible analytes, such as abietic acid. To increase the detection limit of HPLC-based methods, it is necessary to preconcentrate or derivatize the samples. However, this approach increases the number of tedious and time-consuming operational steps, raising the possibility of errors due to analyte loss or sample contamination.[8]

Ultrasound-assisted extraction (UAE) enhances the interaction between the solid matrix and the solvent by increasing local pressure, thereby promoting more efficient solvent penetration. As it operates at relatively low temperatures, UAE is suitable for extracting heat-sensitive compounds. Compared to conventional extraction methods, it offers several advantages, including operational simplicity, reduced extraction time, lower solvent consumption, and the capability for simultaneous processing of multiple samples. Additionally, UAE conditions are relatively easy to optimize, as the process depends on a limited number of parameters (primarily matrix moisture content, solvent characteristics, and extraction time) making it a practical and efficient alternative for sample preparation.[9]

Table I presents a comparison of various analytical methods reported in the literature for the determination of abietic acid by HPLC. Although several methods have been previously described, none integrates the same combination of sample selection, sample preparation, and analytical conditions as the method developed in this study. This unique combination results in improved efficiency, reliability, and applicability for routine analysis. Additionally, the proposed method was validated in accordance with INMETRO guidelines and is currently implemented in the routine quality control laboratory of our manufacturing unit, allowing the quantification of abietic acid in natural resins and their derivatives used as raw materials in cosmetic formulations.

Table I. Analytical methods for abietic acid determination reported in literature

Author	Method	Matrice	Sample treatment	Linear Range (ppm)	LOD (ppm)	LOQ (ppm)
Zhu, Y. 2014[7]	HPLC-PAD	Duck meat	SPE-C18*	0.05 – 5.0	0.015	0.05
Liu, J. 2014[8]	HPLC-FLD-MS/MS	Cosmetics	UCSED**	0.075 – 3.0	0.0082	0.0267

(continued on next page)

Table I. Analytical methods for abietic acid determination reported in literature (continued)

Author	Method	Matrice	Sample treatment	Linear Range (ppm)	LOD (ppm)	LOQ (ppm)
Mitani, K. 2007[10]	LC-MS	Food	On-line SPME	0.0005 – 0.05	0.0003	0.0005
Mckeon, L. 2014[11]	CE-DAD	Rosin	Dissolution	5.0 – 1000.0	0.15	0.5
Lee, B. L. 1994[12]	HPLC-PAD	Adhesive	SPE-C18*	0.025 – 1.0	0.025	0.05
Sarria-Villa, R. A. 2021[13]	HPLC-PAD	Rosin	SPE-C18*	10.0 – 100.0	0.091	0.304
Hroboňová, K. 2006[14]	HPLC-DAD-MS	Propolis	Liquid extraction with methanol	0.2 – 1.0	0.1	0.2
Sakunpak, A. 2024[15]	HPLC-DAD	Oral spray	Dissolution and filtration	31.3 – 1000.0	10.9	33.2
This report	HPLC-DAD	Natural Resins	Ultrasonic extraction and filtration	1.0 -100.0	0.15	0.5

*SPE-C18: Solid-phase extraction using C18 cartridges. **UCSED: Ultrasonic-assisted closed in-syringe extraction and derivatization.

MATERIALS AND METHODS

Materials and chemicals

Abietic acid, ultrapure water and methanol HPLC grade were purchased from Sigma-Aldrich (USA) while formic acid was purchased from Neon (Brazil). To carry out the analysis a stock solution abietic acid standard was prepared diary dissolving 1.0 g of abietic acid in 10 mL of methanol. Working standards for calibration curve were prepared immediately before use in mobile phase.

Pine and Mastic naturals resins are commercially sold and were acquired from local producers or imported. The raw material for cosmetics produced from these natural resins were manufactured by the company Aqia Química Inovativa Ltda.

Apparatus

An LC-2030 HPLC system (Shimadzu) with DAD detector set at the wavelength of 245 nm and a Pursuit PFP column (150 mm x 4.6 mm, 5.0 µm, Agilent) was used to analyze the abietic acid. The best composition of the methanol:formic acid mobile phase was determined based on tests varying the concentration of formic acid (0.05 - 1%) and different proportions between the solvents (70:30, 75:25 or 80:20). To determine the best analysis conditions, flow rates (0.5 - 0.7 mL min^{-1}), temperatures (25 ºC - 50 ºC) and injection volumes (1 - 50 µL) were tested. Data acquisition was performed on LabSolution® software. A SSBuc 10L ultrasonic bath (SolidSteel, Brazil) was used for the extractions of the samples.

Sample preparation

In this study the abietic acid was determined in two natural resins (pine and mastic resin) and six cosmetic raw material samples. The natural resin samples and their derivative products were prepared before the HPLC analysis by ultrasonic-assisted liquid extraction. A precisely weighed mass of 100.0 mg of sample was added into 15-mL centrifuge tube, followed by addition of 10 mL methanol. The tube was capped and shaken in an ultrasonic batch. For the extraction of abietic acid from diverse samples, different times into ultrasonic batch were investigated (2, 5, 10, 20 and 30 minutes) to determine which would promote better extraction. After appropriate dilution with methanol (1:10, v/v), samples were filtered through a 0.45 µm nylon syringe filter prior to injection into HPLC system.

Method validation

The validation of the analytical method for determination of abietic acid in natural resins and their derivatives products was performed through range, linearity, accuracy, precision, limits of detection (LOD) and quantification (LOQ) and matrix effect.

RESULTS AND DISCUSSION

Chromatographic conditions

Abietic acid is a weak organic acid and its retention on reverse phase HPLC-based method can be improved by using some additives in mobile phase, such as formic acid, acetic acid, phosphoric acid, etc., as well by its composition. In the present study, 03 different concentrations of formic acid, ranging from 0.05 to 1% were evaluated at same mobile phase composition (75:25, v/v). The best compromise between retention time and peak area was obtained for concentration of 0.1% of formic acid.

To choose the best mobile phase composition, mixtures of methanol and formic acid 0.1% were tested in different proportions: 80:20 (v/v), 75:25 (v/v) and 70:30 (v/v), and the better response considering the retention time and peak shape was obtained using a solution methanol/formic acid 0.1% in the proportion of 75:25 (v/v), as can be seen in Figure 1A.

Flow rate, ranging from 0.5 to 0.7 mL min^{-1}, temperature, from 25 to 50 °C, and injected sample volume, from 1 to 20 µL, were also parameters evaluated in the chromatographic method optimization, and the chromatograms obtained are shown in Figures 1B, C and D. The comprehensive evaluation of chromatographic parameters enabled the identification of the best analytical conditions for the determination of abietic acid, summarized in Table II, resulting in improved sensitivity, accuracy, analysis time, and overall robustness of the developed method.

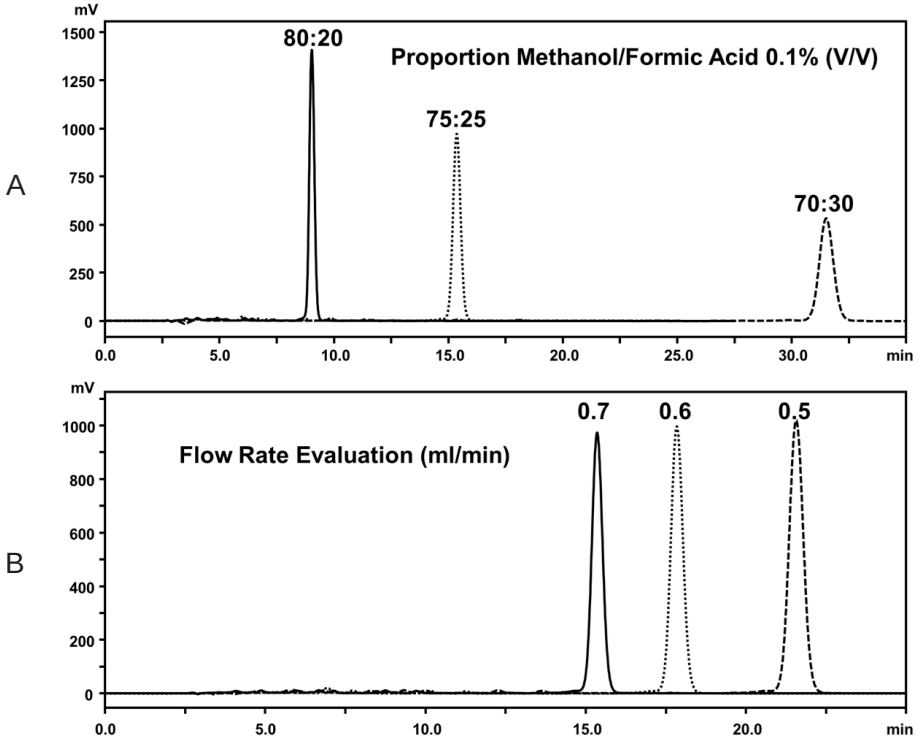

Figure 1. Influence of chromatographic parameters on method performance: (A) Mobile phase composition; (B) Flow rate; (C) Temperature and (D) Injection volume. (continued on the next page)

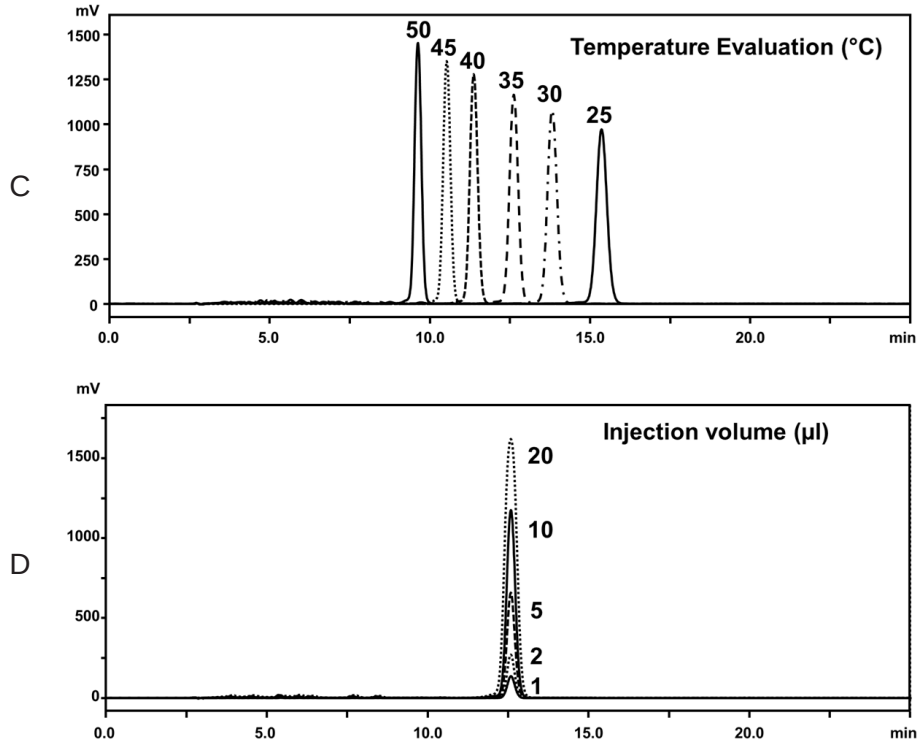

Figure 1. Influence of chromatographic parameters on method performance: (A) Mobile phase composition; (B) Flow rate; (C) Temperature and (D) Injection volume. (continued)

Table II. Chromatographic conditions of the developed method for determination of abietic acid

Instrument	Shimadzu LC-2030
Column	Pursuit PFP (150 mm x 4,6 mm, 5,0 µm)
Detector	UV, 245 nm
Flow rate	0.7 mL min^{-1}
Temperature	35 ºC
Injection volume	10 µL
Mobile phase	Methanol:formic acid 0.1% (75:25)
Elution	Isocratic
Run time	20 minutes

Sample preparation

The ultrasonic-assisted liquid extraction of abietic acid from natural resins was investigated submitting the samples to times ranging from 2 to 30 minutes in an ultrasonic bath, monitoring the peak area result. Pine resin samples in methanol were analyzed in triplicate and results are presented in Figure 2. Just ten minutes provided the best abietic acid extraction, and it was adopted as analysis parameter.

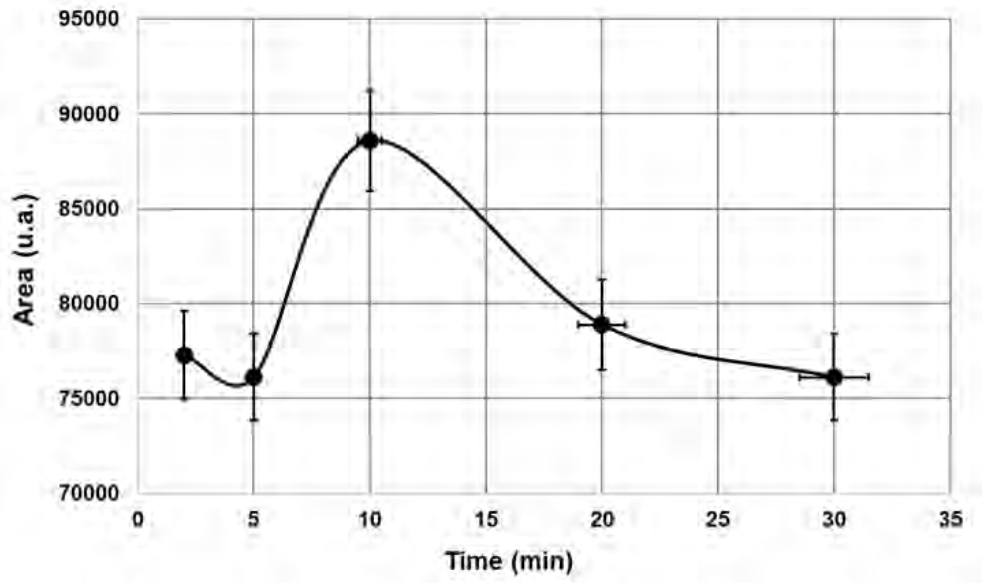

Figure 2. Ultrasonic-assisted liquid extraction time of abietic acid in pine vs peak area.

Method validation

Linearity, Matrix Effect and Limits of detection and quantitation

The linearity was determined in triplicate at six different concentration levels, range 1 – 100 ppm, prepared in methanol. The different concentrations of abietic acid were plotted against their respective peak areas. The linear regression equation, obtained by the least squares method, is y = 35525.6x – 3175.08 with determination coefficient (r^2) equal to 0.999. The chromatograms and linearity curve are presented in Figure 3, while the ANOVA results (at 95% confidence level) for the calibration curves are presented in Table III. The p-value obtained was greater than 0.05, indicating that there is no significant difference between the calibration curves. The residual analysis, used to assess homoscedasticity, revealed a random distribution of the residuals, confirming that the homoscedasticity assumption was satisfied and that the linear model is adequate.

The limit of detection (LOD) and quantitation (LOQ) of the analytical method were calculated according to INMETRO guidance (DOQ-CGCRE-008),[16] based on the standard deviation of the response and slope of the calibration curve. LOD and LOQ for abietic acid was found 0.3 ppm and 1.0 ppm, respectively.

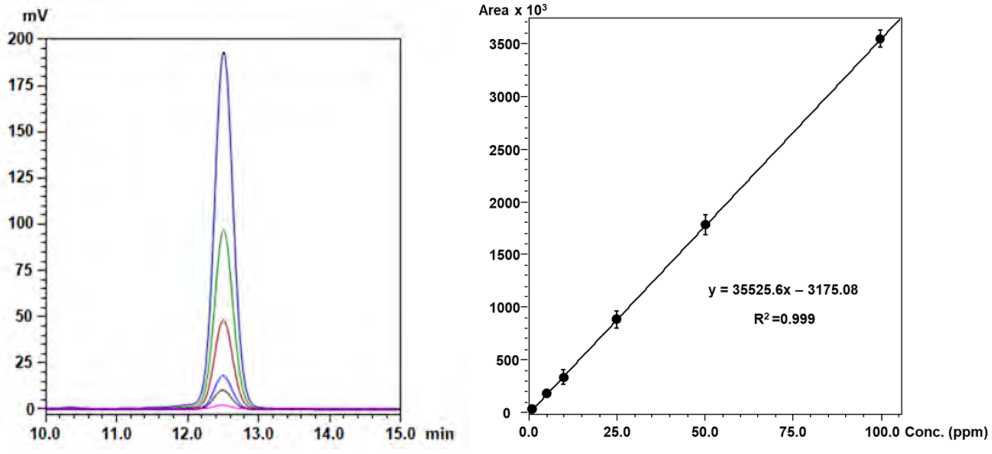

(A) (B)

Figure 3. (A) Chromatograms of abietic acid standards. (B) Linearity of abietic acid determined at 245 nm.

Table III. Results of ANOVA test for the calibration curves data

Source of Variation	DF	SS	MS	*F* ratio	Prob > *F*
Between groups	5	29,008,809,914,920.3	5,801,761,982,984.1	1952.85	< 0.0001
Within group	12	35,651,109,807.3	2,970,925,817.28		
Total	17	29,044,461,024,727.6			

DF = degrees of freedom; SS = sum of squares; and MS = mean square; $p < 0.05$.

To evaluate matrix effects on the quantification of abietic acid, matrix-matched curves calibration curves were prepared at the same concentrations levels as those prepared in solvent. For this purpose, abietic acid standards were spiked into natural pine and mastic resin samples prior to ultrasound-assisted extraction. The matrix effect (ME) was calculated using Equation (1):

$$ME\ (\%) = 100 \times \left[\left(\frac{Slope\ matrix}{Slope\ solvent}\right) - 1\right] \qquad (1)$$

The matrix effect was determined to be 2.6% for mastic resin and 1.9% for pine resin. These values do not significantly impact on the accuracy and precision of the analytical results and can therefore be considered negligible. Consequently, sample quantification was performed using a calibration curve prepared in methanol.

Accuracy and Precision

The accuracy of the analytical method was evaluated through recovery tests by spiking samples with known amount of abietic acid standard at four different concentrations levels (1, 10, 50 and 100 ppm), analyzing in triplicate and then calculating the recovery percentage. The values of the recovery rate were above 96% to all concentration levels, in accordance with INMETRO acceptance criteria (DOQ-CGCRE-008).[16]

The precision was evaluated through intra-day and interday precision. Each sample was analyzed five times within a day (intra-day) and three consecutive days (inter-day). The precision was calculated as percent relative standard deviation (% RSD). The relative standard deviation values of the abietic acid were less than 7.3%. The results demonstrating the accuracy and precision of the proposed method are presented in Table IV.

Table IV. Intra- and inter-day accuracy and precision of abietic acid at four concentration levels (*n*=5)

Concentration (ppm)	Intra-day		Inter-day		Recovery (%)
	Mean+SD	Precision (RSD%)	Mean+SD	Precision (RSD%)	
1	0.95 ± 0.1	6.8	0.96 ± 0.1	7.3	96
10	10.37 ± 0.1	0.7	10.72 ± 0.4	3.9	107
50	49.38 ± 0.2	0.5	50.95 ± 1.9	3.7	102
100	103.94 ± 1.4	1.3	107.27 ± 3.0	2.8	107

Application of the method

The abietic acid standard and the samples were analyzed by HPLC established method. The retention time of abietic acid was 12.5 minutes, which allowed its unequivocal identification in the samples. The chromatograms of the standard abietic acid and samples are shown in Figure 4. As expected, the concentration of abietic acid in pine resin is higher than in raw material obtained from it, while mastic gum doesn't contain any trace of abietic acid its composition.[17] The results obtained are summarized in Table V.

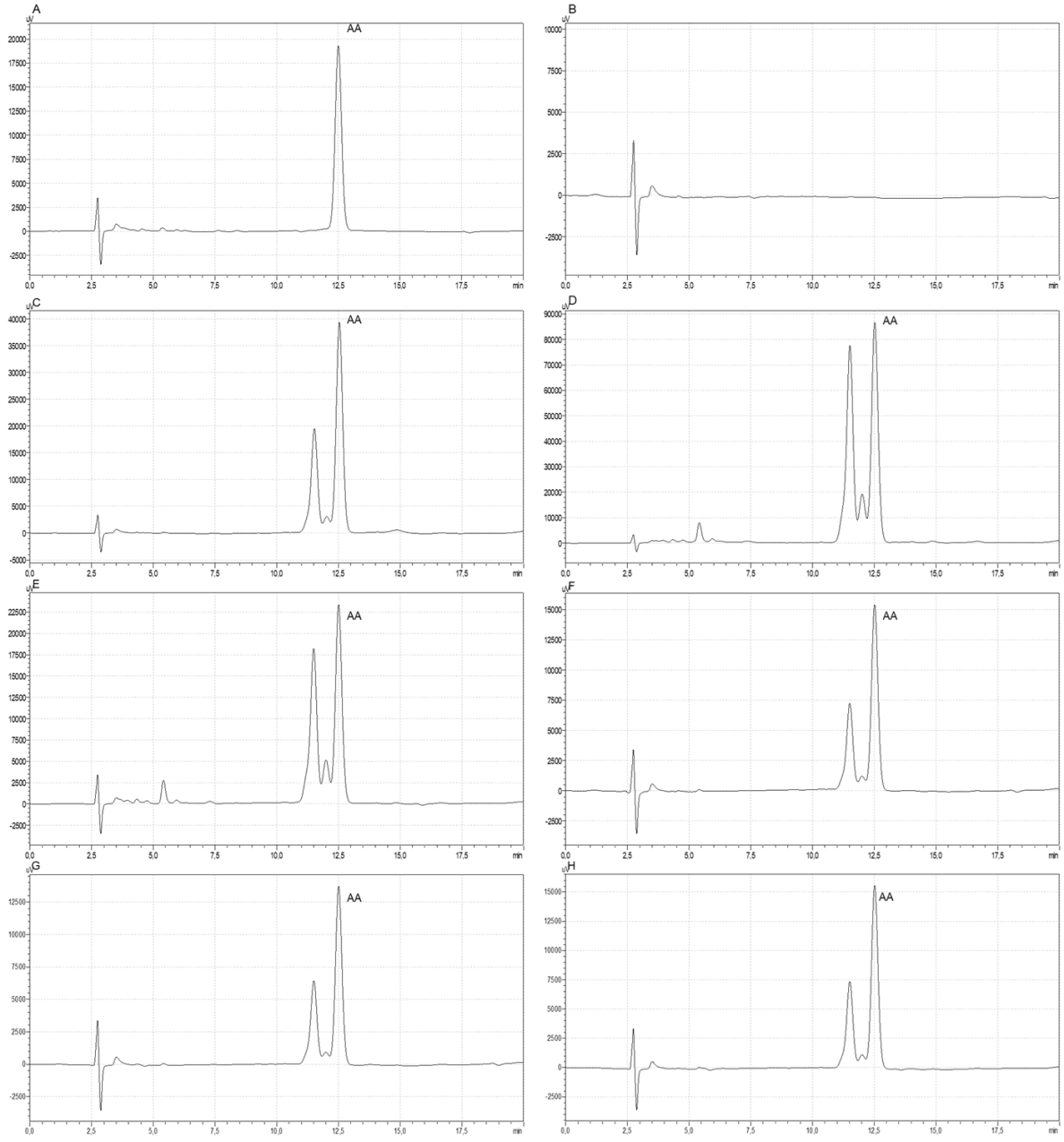

Figure 4. Chromatogram of abietic acid (**AA**). Standard solution **(A)**, mastic resin **(B)**, pine resin **(C)** and cosmetic raw material **(D – H)**.

Table V. Concentration of abietic acid in natural resins and cosmetic raw materials

Sample	Concentration (ppm)
Pine resin	145.0 ± 4.3
Mastic gum	ND
Raw material 1	39.5 ± 1.2
Raw material 2	108.9 ± 3.3
Raw material 3	75.9 ± 2.3
Raw material 4	68.4 ± 2.0
Raw material 5	77.4 ± 2.3

CONCLUSIONS

The proposed method for analyzing the concentration of abietic acid in natural resins and raw material was successfully developed and validated. The method is simple, selective, with good resolution, excellent linearity (> 0.999), and low limit of detection (0.15 ppm). Furthermore, accuracy, precision, recovery, and repeatability for the determination of abietic acid meet the INMETRO criteria for validation of analytical methods. Although several HPLC methods for the determination of abietic acid have been described in previous studies, none of them offer the same combination of cost-efficiency and rapid analysis as the method presented in this study.

The developed method was effectively applied to determination of abietic acid in seven samples of interest, including natural resins and cosmetic raw material, proving to be a useful tool for monitoring abietic acid and in the quality control of cosmetic raw material.

Conflicts of interest

The authors declare that there are no conflicts of financial interest or otherwise.

Acknowledgements

This work was supported by the company AQiA Química Inovativa, Ltda.

REFERENCES

(1) Gigante, B. Resinas naturais. *Conservar Patrimonio* **2005**, *1*, 33-46. https://doi.org/10.14568/cp1_4
(2) Hamstra, A. A.; Jacob, S. E. A review of colophonium. *The Dermatologist* **2015**, *23* (8), 38-41.
(3) Downs, A. M. R.; Sansom, J. E. Colophony allergy: a review. *Contact Dermatitis* **1999**, *41* (6), 305-310. https://doi.org/10.1111/j.1600-0536.1999.tb06178.x
(4) Karlberg, A. T.; Hagvall, L. Colophony: Rosin in unmodified and modified form. In: John, S. M.; Johansen, J. D.; Rustemeyer, T.; Elsner, P.; Maibach, H. I. (Eds). *Kanerva's Occupational Dermatology*. Springer, 2020. Chapter 41, pp 607-624. https://doi.org/10.1007/978-3-319-68617-2
(5) Eriksson, K.; Wiklund, L.; Larsson, C. Dermal exposure to terpenic resin acids in Swedish carpentry workshops and sawmills. *Ann. Occup. Hyg.* **2004**, 48, 267-275. https://doi.org/10.1093/annhyg/meh013
(6) Karlberg, A. T.; Albadr, M. H.; Nilsson, U. Tracing colophonium in consumer products. *Contact dermatitis* **2021**, *85* (6), 671-678. https://doi.org/10.1111/cod.13944
(7) Zhu, Y.; Zhang, S.; Geng, Z.; Wang, D.; Liu, F.; Zhang, M.; Bian, H.; Xu, W. Simultaneous determination of abietic acid and dehydroabietic acid residues in duck meat by HPLC-PAD-FLD. *Food Anal. Methods* **2014**, *7*, 1627-1633. https://doi.org/10.1007/s12161-014-9798-6

(8) Liu, J.; Liu, M.; Li, X.; Lu, X.; Chen, G.; Sun, Z.; Li, G.; Zhao, X.; Zhang, S.; Song, C.; *et al*. Development of ultrasonic-assisted closed in-syringe extraction and derivatization for the determination of labile abietic acid and dehydroabietic acid in cosmetics. *J. Chromatogr. A* **2014**, *1371*, 20-29. http://dx.doi.org/10.1016/j.chroma.2014.10.059

(9) Picó, Y. Ultrasound-assisted extraction for food and environmental samples. *TrAC, Trends Anal. Chem.* **2013**, *43*, 84-99. https://doi.org/10.1016/j.trac.2012.12.005

(10) Mitani, K.; Fujioka, M.; Uchida, A.; Kataoka, H. Analysis of abietic acid and dehydroabietic acid in food samples by in-tube solid-phase microextraction coupled with liquid chromatography–mass spectrometry. *J. Chromatogr. A* **2007**, *1146* (1), 61–66. http://dx.doi.org/10.1016/j.chroma.2007.01.118

(11) Mckeon, L.; Regan, F.; Burns, B.; Leonard, R. Determination of resin acid composition in rosin samples using cyclodextrin-modified capillary electrophoresis. *J. Sep. Sci.* **2014**, *37*, 2791–2796. https://doi.org/10.1002/jssc.201400014

(12) Lee, B. L.; Ong, H. Y.; Koh, D.; Ong, C. N. High-performance liquid chromatographic method for determination of dehydroabietic and abietic acids, the skin sensitizers in bindi adhesive. *J. Chromatogr. A* **1994**, *685* (2), 263-269. https://doi.org/10.1016/0021-9673(94)00691-1

(13) Sarria-Villa, R. A.; Gallo-Corredor, J. A.; Benítez-Benítez, R. Characterization and determination of the quality of rosins and turpentines extracted from *Pinus oocarpa* and *Pinus patula* resin. *Heliyon* **2021**, *7* (8), e07834. https://doi.org/10.1016/j.heliyon.2021.e07834

(14) Hrobonová, K.; Lehotay, J.; Skačáni, I.; Čižmárik, J. HPLC determination and MS identification of dehydroabietic acid and abietic acid in propolis. *J. Liq. Chromatogr. Relat. Technol.* **2005**, *28*, 1725-1735. https://doi.org/10.1081/JLC-200060463

(15) Sakunpak, A.; Saingam. W. HPLC-DAD method validation for quantification of dehydroabietic acid and abietic acid in oral spray containing *Pinus merkusii* heartwood extract and its antibacterial effects on clinically isolated *Streptococcus mutans*. *Acta Chromatogr.* **2024**, *36* (3), 228-236. https://doi.org/10.1556/1326.2023.01149

(16) Instituto Nacional de Metrologia, Qualidade e Tecnologia (INMETRO), *DOQ-CGCRE-008: Orientação sobre validação de métodos analíticos*, *2020*. Updated in 2024/08/06. Available at: https://www.gov.br/cdtn/pt-br/assuntos/documentos-cgcre-abnt-nbr-iso-iec-17025/doq-cgcre-008/view (accessed 2024-06-12).

(17) Modugno, F.; Ribechini, E. GC/MS in the Characterization of Resinous Materials. In: Colombini, M. P.; Modugno, F. (Eds). *Organic Mass Spectrometry in Art and Archaeology*. Wiley, 2009. Chapter 8, pp 215- 235. https://doi.org/10.1002/9780470741917.ch8

Brazilian Journal of Analytical Chemistry
2026, Volume 13, Issue 52, pp 50-71
doi: 10.30744/brjac.2179-3425.AR-04-2025

BrJAC

ARTICLE

Evaluation of Volatile and Non-Volatile Compounds in Specialty and Traditional Coffees from the *Circuito das Águas Paulista* Region

Bruna Luiza Duarte Guedes[1], Winston P. C. Gomes[2], Gabriela Maria R. N. de Alcantara[2], Gisele G. Bortoleto[3], Wanessa R. Melchert[1]*

[1]*Escola Superior de Agricultura Luiz de Queiroz, Universidade de São Paulo, PO Box 9, Piracicaba, SP, 13418-970, Brazil*

[2]*Centro de Energia Nuclear na Agricultura da Universidade de São Paulo (CENA/USP), Av. Centenário, 303, Piracicaba, SP, 13416-000, Brazil*

[3]*Centro Estadual de Educação Tecnológica Paula Souza/CEETEPS, Escola Técnica de Piracicaba Deputado Roque Trevisan, Piracicaba, SP, 13414-141, Brazil*

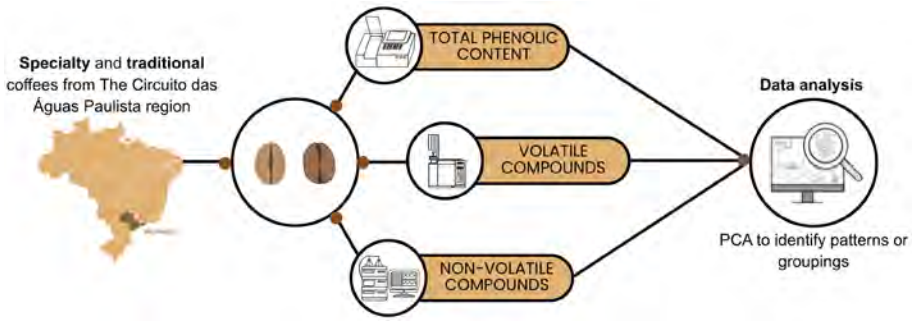

Coffee, renowned for its aroma and flavor, ranks second in global consumption. Key compounds in coffee beans significantly influence their sensory properties in green and roasted forms. Brazil, a leading coffee producer and exporter, benefits from the adaptability of coffee plants due to its diverse geographical features. The *Circuito das Águas Paulista* region, in particular, provides an ideal environment for high-quality coffee cultivation, producing coffees that surpass the 80-point threshold needed to attain specialty coffee status. This study evaluated 17 roasted *Coffea arabica* samples: 12 from the 2020/2021 harvest (six specialty and six traditional) and 5 from the 2022/2023 harvest. Chemical composition was assessed using UV-Vis spectrophotometry, HPLC, GC-FID, and chemometric tools. Total phenolic content, measured by the Folin-Ciocalteu method, ranged from 3371 to 3968 milligrams of gallic acid equivalents per 100 grams (mg GAE 100 g^{-1}). Caffeine and chlorogenic acid contents (507–1006 mg 100 g^{-1} and 453–1004 mg 100 g^{-1}, respectively) were determined by HPLC. Volatile compounds such as diacetyl (37.01–108.28 µg 100 g^{-1}) and 2-methylpyrazine (2.41–3.38 µg 100 g^{-1}) were quantified by GC-FID with headspace sampling. Significant differences were found between specialty and traditional coffees, particularly in diacetyl, which was more abundant in specialty samples and may act as a marker. Principal component analysis effectively distinguished the two groups, with 2-methylpyrazine playing a key role in traditional coffees. Comparison between harvests

Cite: Guedes, B. L. D.; Gomes, W. P. C.; de Alcantara, G. M. R. N.; Bortoleto, G. G.; Melchert, W. R. Evaluation of Volatile and Non-Volatile Compounds in Specialty and Traditional Coffees from the *Circuito das Águas Paulista* Region. *Braz. J. Anal. Chem.* 2026, *13* (52), pp 50-71. https://doi.org/10.30744/brjac.2179-3425.AR-04-2025

Submitted: January 20, 2025; **Revised:** July 2, 2025; September 23, 2025; **Accepted:** November 5, 2025; **Published online:** November 27, 2025.

This article is part of the BrJAC Special Issue dedicated to the 21st ENQA and 9th CIAQA.

revealed notable variations in caffeine, gallic acid, chlorogenic acid, 3,4-dihydroxybenzoic acid, and 2-methylpyrazine, suggesting that environmental conditions, such as frost, can affect coffee chemistry and quality. The analytical advance of this work resides in the integration of complementary analytical techniques with chemometric analysis, providing a robust approach to discriminate coffee categories and evaluate environmental influences on their chemical composition.

Keywords: specialty coffees, chromatography, volatile compounds, phenolic compounds, chemometrics

INTRODUCTION

Coffee is a widely recognized stimulant beverage known for its distinctive aroma and flavor, ranking second globally in consumption, just behind water.[1,2] In the global coffee trade, Brazil leads in production and export. This leadership can be attributed to the adaptability of coffee plants to Brazil's diverse environmental conditions, including varied altitudes, latitudes, climates, and terrains.[3]

According to CONAB (*Companhia Nacional de Abastecimento*) in 2022, the Brazilian states with the highest coffee production rates are Minas Gerais, Espírito Santo, São Paulo, Paraná, Bahia, Rondônia, Rio de Janeiro, Goiás, Mato Grosso, Amazonas, and Pará. The *Circuito das Águas Paulista* region is particularly notable for its favorable geography and the differentiated quality/composition of its waters, which support the cultivation of high-quality coffee.[4-6] Therefore, due to these unique edaphoclimatic conditions, altitude, nutrient-rich soils, water, and mild microclimates, it is essential to map the chemical profile of the coffees produced in this region in detail.

The designation of specialty coffee is determined through sensory evaluations, such as cupping scores, following guidelines established by the Specialty Coffee Association of America.[7] Coffee must score at least 80 points and have certified traceability to be classified as a specialty. Therefore, many producers seek certifications from specialized evaluation entities to demonstrate the quality and excellence of the coffee's sensory characteristics.[5,8]

Sensory characteristics can be directly related to the compounds (volatile and non-volatile) present in the composition of coffee beans, as they influence the beverage's aroma and flavor, thereby enhancing its appeal and consumer acceptance. The chemical composition of coffee includes carbohydrates, lipids, proteins, minerals, amino acids, and bioactive compounds. Additionally, edaphoclimatic factors can influence this set of elements, with altitude and exposure to light being significant factors.[9-11]

Caffeine, chlorogenic acid, gallic acid, 5-hydroxymethylfurfural (5-HMF), and 3,4-dihydroxybenzoic acid are bioactive compounds commonly found in coffee, each with distinct nutritional significance and contributing significantly to the sensory richness and uniqueness of coffee.[9-11] Caffeine has a psychoactive stimulant effect, but high doses can lead to adverse effects like insomnia and tachycardia.[12,13] Chlorogenic acid and gallic acid are antioxidants with anti-inflammatory potential, and are often used in functional foods and nutraceuticals; both are generally considered safe at dietary levels.[14–17] 5-HMF, formed during thermal processing, is valued as a quality marker but may be linked to potential mutagenic effects.[18,19] Meanwhile, 3,4-dihydroxybenzoic acid shows antioxidant activity with low toxicity reported at low doses.[20,21]

Recent research in the literature has employed high-performance liquid chromatography (HPLC) and gas chromatography (GC) to evaluate the non-volatile and volatile compounds in coffee, respectively. However, few studies still focus on evaluating specialty and traditional coffees, particularly roasted ones, using uniform standards for roasting, extraction, and preparation with beans from the same species and region, and correlating these aspects with sensory analysis parameters.[22,23] In this field, the works of Alcantara *et al*. and Abreu *et al.* stand out.[24,25]

In light of this, the present study aimed to analyze and compare the chemical composition of specialty and traditional coffees from cities of the *Circuito das Águas Paulista* region employing chromatographic, spectrophotometric, and chemometric techniques. Only through in-depth knowledge of the chemical signatures that reflect the local terroir will it be possible, in subsequent studies, to establish comparative criteria with other producing regions and demonstrate the peculiarities of this region. Thus, this study establishes an

analytical framework that will enable us to evaluate, in future stages, regional differences and support specific quality claims for coffees from the *Circuito das Águas Paulista*. Furthermore, the specific objectives of this study were to quantify the total phenolic compounds (TPC) in samples of specialty and traditional coffees, identify and quantify non-volatile compounds based on retention time and established analytical standards, and obtain the chromatographic profile of these non-volatile compounds. It also aimed to identify and quantify volatile compounds in the samples and establish correlations between the results obtained and the sensory scores, cultivation altitude, and classification of the coffee samples.

The novelty of this study lies in the integrated application of complementary analytical techniques (UV-Vis spectrophotometry, HPLC, GC-FID with headspace sampling) combined with chemometric tools. This analytical strategy enabled a comprehensive chemical characterization of roasted coffee, allowing the identification of discriminant compounds between specialty and traditional samples and the evaluation of environmental influences across harvests. In this sense, the work contributes to advancing coffee quality assessment and authentication by demonstrating the potential of established methods when applied in an integrative and systematic approach.

MATERIALS AND METHODS

Reagents and equipment

For all analyses, deionized water (conductivity of 18.2 MΩ·cm at 25 ºC) and analytical-grade reagents from Sigma-Aldrich (≥99% purity), including acetic acid, methanol, acetonitrile, gallic acid, Folin-Ciocalteu reagent, caffeine, 3,4-dihydroxybenzoic acid, chlorogenic acid, 5-hydroxymethylfurfural, sodium carbonate, acetaldehyde, acetone, methanol, ethanol, diacetyl, and 3-methyl-butanol, were used.

The following types of equipment were utilized during the analyses: an ultrasonic bath (Ultra Cleaner, model 1450), an analytical balance (Mettler Toledo, model ME104), a UV-Vis spectrophotometer (Agilent, model Cary 60), a high-performance liquid chromatography (Agilent, model 1100), and a gas chromatograph (PerkinElmer, model Clarus 600).

Sample preparation

Twelve samples of Arabica coffee beans were obtained from producers in the *Circuito das Águas Paulista* region during the 2020/2021 period, including the cities of Serra Negra, Socorro, Águas de Lindóia, and Monte Alegre do Sul, all located in the state of São Paulo, Brazil (Table I). Subsequently, all samples underwent a roasting process for uniformity. The coffee beans were ground using an analytical mill (Tecnal, model TE-631/4) and passed through a 20-mesh sieve for proper standardization, according to protocol by the Specialty Coffee Association.[7] Subsequently, five additional samples of Arabica coffee beans from the 2022/2023 harvest were collected from the same region for further comparison.

Table I. Specialty and traditional coffee samples

Samples	Classification	Plant variety	City	Altitude (m)	SCAA* Score
S1	Specialty	*Arara*	Socorro	1000 - 1200	80.175
S2	Specialty	*Bourbon Amarelo*	Monte Alegre do Sul	900	83.325
S3	Specialty	*Mundo Novo*	Monte Alegre do Sul	1100	80.15
S4	Specialty	*Mundo Novo*	Serra Negra	1150	80.275
S5	Specialty	*Bourbon Amarelo*	Socorro	1300	81.6
S6	Specialty	*Arara*	Serra Negra	1100	84.175
T1	Traditional	*Arara, Mundo Novo*	Serra Negra	825	78.975
T2	Traditional	*Catuaí Vermelho*	Serra Negra	680	78.625

(continued on next page)

Table I. Specialty and traditional coffee samples (continued)

Samples	Classification	Plant variety	City	Altitude (m)	SCAA* Score
T3	Traditional	*Catuaí*	Águas de Lindóia	1200	78.425
T4	Traditional	NOS**	Serra Negra	720	77.7
T5	Traditional	*Catuaí*	Serra Negra	1120	79.075
T6	Traditional	*Mundo Novo*	Serra Negra	1100	73.925

*Specialty Coffee Association of America. **Not otherwise specified.

In the spectrophotometric analyses performed, the beverage was prepared using the infusion method described in the coffee sensory analysis protocol by the Specialty Coffee Association of America.[7] In this process, 1.37 g of ground coffee was brought into contact with 25 mL of water at a temperature of 90 ºC for 5 minutes. After this time, the beverage was filtered using conventional filter paper and then diluted with water at a 1:50 (v/v) ratio.

The beverage preparation was carried out using the percolation method, adapted from Alcantara, Spíndola, and Melchert, for the chromatographic analyses of non-volatile compounds.[24] In this process, 15 mL of preheated water at 90 ºC was poured over 1.0 g of ground coffee. Subsequently, the mixture was filtered using conventional filter paper. The resulting extract was filtered using a 0.45 µm PTFE syringe filter for future injection into the chromatograph.

Determination of total phenolic compounds

Total phenolic compounds were determined using the Folin-Ciocalteu method with a UV-Vis spectrophotometer (Agilent, model Cary 60) equipped with a 1 cm path length cuvette for reading, and gallic acid was used as the analytical standard.[26]

A 600 µL aliquot of the diluted sample (1:50, v/v) was transferred to a Falcon® tube. Subsequently, 3000 µL of 10% (v/v) Folin-Ciocalteu reagent solution was added. After 5 minutes, 2250 µL of a 4% (w/v) sodium carbonate solution was added. The resulting mixture was kept at room temperature and protected from light for 2 hours. Subsequently, the spectrophotometer measured the solution at a wavelength of 770 nm.[26]

The analytical curve was established in a concentration range of 10 to 50 mg L^{-1} of gallic acid (GAE). The results were expressed in milligrams of GAE per 100 g of ground-roasted coffee. All analyses were performed in triplicate to ensure greater precision in the results.[26-28]

Determination of non-volatile compounds

Non-volatile compounds were separated using a high-performance liquid chromatograph (Agilent, model 1100) equipped with a UV detector (Agilent, model VWD G1314A). A 30 µL sample was injected into a reverse-phase C18 column (Agilent, model Eclipse XDB, 4.6 x 250 mm, 5 µm). The mobile phase consisted of solvent A (5% v/v acetic acid in water) and solvent B (acetonitrile), using isocratic elution with a composition of 95% A and 5% B. The flow rate was set at 0.8 mL min^{-1}, with a total run time of 55 minutes.[28,29]

Signals were measured and identified by comparing the chromatographic profile with that of analytical standards at 280 nm for caffeine, 5-hydroxymethylfurfural, 3,4-dihydroxybenzoic acid, and gallic acid, and 320 nm for chlorogenic acid.

Determination of volatile compounds

Volatile compounds were determined using a gas chromatograph (PerkinElmer, model Clarus 600) equipped with a flame ionization detector (FID) and an automatic headspace sampler (CTC Analytics, Pal System). The column used was NOVA-WAX (Nova Analytics), with dimensions of 30 m in length, 0.25 mm in diameter, and a stationary phase of 0.25 µm.[23,30,31] In the headspace method, a sample weighing 0.55 g

was placed in a 20 mL vial. Heating occurred for 5 minutes at an oven temperature of 80 °C, with agitation at 500 rpm. The collected and injected volume was 1.5 mL, injected at a speed of 500 µL s^{-1} with a split ratio of 1:30.[23,30,31] Additionally, the injector temperature was maintained at 150 °C, and the detector at 300 °C. The column temperature was initially programmed to 45 °C for 3 minutes. It was then gradually increased at a rate of 7.5 ºC min^{-1} until reaching 60 ºC, followed by a rate of 15 ºC min^{-1} up to 165 °C, with a total run time of 12 minutes. High-purity gases (99.999%) were employed, including nitrogen at a flow rate of 1.2 mL min^{-1}, hydrogen at 45 mL min^{-1}, and synthetic air at 450 mL min^{-1}.[23,30,31]

The identification of the compounds (acetaldehyde, acetone, methanol, ethanol, diacetyl, 3-methyl-butanol alcohol and 2-methylpyrazine) was based on the comparison of the retention time with the injection of the analytical standards and by the values obtained from the linear retention indexes (LRI), which were determined according to Equation (1).

$$LRI = 100 \times \left(\frac{t_c - t_n}{t_{n+1} - t_n} + n \right) \quad (1)$$

where:

t_c is the retention time of the compound of interest

t_{n+1} is the retention time of the subsequent hydrocarbon

n is the number of carbons of the previous hydrocarbon

To calculate the LRI, the retention times of linear alkanes (C7-C40, Sigma-Aldrich, 49452-U) were obtained under the same experimental conditions. The values obtained were compared with the literature and with the NIST Chemistry WebBook.[32-38]

Furthermore, the ethanol/methanol ratio was calculated using the concentration values of the compounds as reported by Gibson apud Flament.[39] Since this ratio presents a flavor known as “Solai,” a higher ratio is associated with higher-quality coffees.[39]

Limit of detection (LOD) and quantification (LOQ)

For both total phenolic compounds and volatile and non-volatile compounds, the limit of quantification (LOQ) was calculated using the minimum concentration of each sample, and the limit of detection (LOD) was determined using Equation (2).[40]

$$LOD = 3.3 \times \frac{s}{b} \quad (2)$$

where:

s is the estimate of the standard deviation of the regression curve

b is the slope of the analytical calibration curve

Calibration curve precision was assessed by the percentage relative standard deviation (RSD) of triplicate signals at each concentration level. All RSD values were below 20%.[41]

Statistical analysis

The obtained contents of the evaluated compounds were subjected to the unpaired Student’s *t*-test with a significance level of 95% (α = 0.05). The Shapiro-Wilk, Mann-Whitney, and Levene tests were also applied to verify the normality and homogeneity of the results. In addition, patterns or groupings that could differentiate specialty coffees from traditional coffees were investigated using principal component analysis (PCA). All analyses were performed using **OriginPro® 2024b software**.

RESULTS AND DISCUSSION

Total phenolic compounds

The analytical curve for the total phenolic compounds (TPC) analysis is described as follows: for concentrations ranging from 10 to 50 mg L^{-1}, the regression equation is *A*bs = 0.006 + 0.0088 C, with a coefficient of determination (R^2) of 0.999. The LOD and LOQ were estimated at 0.3 and 10 mg L^{-1}, respectively. Table II presents the content of total phenolic compounds for all coffee samples, including both specialty and traditional varieties.

Table II. Total phenolic compounds content in specialty and traditional coffee samples

Sample	Mean content (mg GAE 100 g^{-1} of coffee)
S1	3490 ± 129
S2	3751 ± 28
S3	3856 ± 68
S4	3638 ± 96
S5	3831 ± 49
S6	3584 ± 108
Mean	3692 ± 106a (RSD 3%)
T1	3377 ± 25
T2	3968 ± 29
T3	3673 ± 86
T4	3666 ± 79
T5	3371 ± 34
T6	3806 ± 40
Mean	3643 ± 207a (RSD 6%)

Note: means followed by the same letter in the column do not differ by Student's *t*-test at the 95% confidence level (α = 0.05). RSD = Relative Standard Deviation.

The mean content of GAE in mg 100 g^{-1} of roasted coffee was 3692 ± 145 for specialty and 3643 ± 236 for traditional. The samples with the highest and lowest concentrations of TPC were the traditional samples T2 and T5, with 3968 and 3371 mg GAE 100 g^{-1} of coffee, respectively. Furthermore, the results of the Student's *t*-test at 95% confidence did not indicate a statistically significant difference between the coffees due to standardized roasting processes, as more intense roasts tend to degrade phenolic compounds, as stated by Alcantara, Dresch, and Melchert.[24]

The average values of total phenolic compounds obtained fall within the range reported by Alcantara, Dresch, and Melchert[24] which ranged from 1368 to 4332 mg GAE 100 g^{-1} of roasted coffee. The study by Almeida and Benassi[42] reported a range of 1910 ± 40 to 3550 ± 40 mg GAE 100 g^{-1} of roasted coffee for total phenolics in commercial traditional coffees, with values in this study falling at the upper end of that range. It is noteworthy that neither study standardized the roasting process.

Furthermore, it is noted that the relative standard deviation (RSD - Table II) for the Special samples was 3%, while for the Traditional samples it was 6%, demonstrating that the traditional samples have a greater dispersion in their phenolic composition. The greater variability of the traditional samples is likely due to less standardized agricultural practices and edaphoclimatic factors, which differ from those observed and practiced in samples of specialty coffees.

Non-volatile compounds

Table III presents the retention time, regression equations, correlation coefficients, LODs, and LOQs for each non-volatile compound analyzed. The chromatographic analysis enabled the identification and quantification of the following non-volatile compounds in specialty and traditional coffee samples: caffeine, chlorogenic acid, gallic acid, 5-HMF, and 3,4-dihydroxybenzoic acid (Table IV). When evaluating the RSD range observed in Table IV (13–22% for the Special samples and 14–36% for the Traditional samples), it essentially reflects the intrinsic heterogeneity of the coffee samples, since the grinding and roasting procedure were standardized. Factors such as origin, cultivar, and post-harvest conditions will significantly impact the concentration of these compounds.

Table III. Analytical parameters of non-volatile compounds

Compounds	Retention time (min)	Concentration (mg L^{-1})	Regression equation	R^2	LOQ (mg L^{-1})	LOD (mg L^{-1})
Caffeine	21.6	200 – 950	Area = -355 + 88.2 C	0.999	200	6.1
Chlorogenic acid	12.6	100 – 1000	Area = 380.3 + 59.7 C	0.999	100	13.2
Gallic acid	4.2	10 – 100	Area = 720.2 + 70.4 C	0.992	10	9.0
5-hydroxymethylfurfural	6.2	2 – 40	Area = 15.9 + 261 C	0.999	2.0	0.3
3,4-dihydroxybenzoic acid	7.1	12.5 – 200	Area = -11.1 + 57.2 C	0.999	12.5	1.0

Table IV. Non-volatile compound content in specialty and traditional coffees

Sample	Mean of non-volatile compounds ± standard deviation (mg 100 g^{-1} of ground roasted coffee)				
	Caffeine	Chlorogenic acid	Gallic acid	5-HMF	3,4-dihydroxybenzoic acid
S1	871 ± 12	1004 ± 11	24 ± 1	31 ± 1	122 ± 2
S2	881 ± 43	969 ± 41	23 ± 2	31 ± 1	111 ± 6
S3	607 ± 31	755 ± 44	12 ± 1	28 ± 2	84 ± 5
S4	909 ± 79	910 ± 81	19 ± 1	27 ± 3	102 ± 14
S5	939 ± 31	729 ± 45	28 ± 1	18 ± 1	87 ± 5
S6	1006 ± 87	965 ± 31	28 ± 4	36 ± 1	112 ± 5
Mean	860 ± 144a (RSD 17%)	889 ± 118a (RSD 13%)	23 ± 5a (RSD 22%)	28 ± 6a (RSD 21%)	103 ± 15a (RSD 15%)
T1	507 ± 35	453 ± 15	6 ± 1	15 ± 4	47 ± 13
T2	759 ± 90	645 ± 83	16 ± 5	18 ± 2	82 ± 12

(continued on next page)

Table IV. Non-volatile compound content in specialty and traditional coffees (continued)

Sample	Mean of non-volatile compounds ± standard deviation (mg 100 g^{-1} of ground roasted coffee)				
	Caffeine	Chlorogenic acid	Gallic acid	5-HMF	3,4-dihydroxybenzoic acid
T3	642 ± 16	595 ± 35	12 ± 1	20 ± 1	71 ± 5
T4	670 ± 11	570 ± 10	18 ± 1	16 ± 1	69 ± 2
T5	540 ± 5	505 ± 37	11 ± 1	11 ± 1	65 ± 4
T6	748 ± 42	544 ± 99	20 ± 2	15 ± 3	65 ± 11
Mean	635 ± 104b (RSD 16%)	558 ± 78b (RSD 14%)	14 ± 5b (RSD 36%)	16 ± 3b (RSD 19%)	66 ± 13b (RSD 20%)

Note: means followed by the same letter in the column do not differ by Student's *t*-test at the 95% confidence level (α = 0.05).
RSD = Relative Standard Deviation.

According to the results obtained for caffeine concentrations, traditional coffees generally had lower caffeine content compared to specialty coffees, as shown in Table IV, with mean values of 860 ± 144 and 635 ± 104 mg 100 g^{-1} for specialty and traditional coffees, respectively. The specialty and traditional coffee samples showed a statistically significant difference when performing the Student's *t*-test at a 95% confidence level. These resulting values were slightly below those found by Kitzberger, Scholz, and Benassi,[43] whose caffeine variation ranged from 1038 to 1386 mg 100 g^{-1}, and by Duarte, Pereira, and Farah,[44] who reported a variation from 990 to 1540 mg 100 g^{-1}. In both studies, the analyzed coffees were classified as traditional and belonged to the Arabica species, having undergone different post-harvest treatments. On the other hand, when analyzing non-volatile compounds in roasted and ground Brazilian coffees, Alcantara, Dresch, and Melchert[24] obtained an average of 3440 mg 100 g^{-1} for specialty coffees and 4890 mg 100 g^{-1} for traditional coffees to caffeine content. Preparation methods, grain grinding type, and the origin and variety of the coffee may influence differences between the values found in the literature. It is worth noting that caffeine is present in higher amounts in the *Coffea canephora* species. Furthermore, commercially marketed coffees are typically composed of blends that combine the species *C. canephora* and *C. arabica*.[45-47]

Regarding chlorogenic acid, specialty coffees exhibited a range of 729 ± 45 to 1004 ± 12 mg 100 g^{-1}, resulting in an average of 889 ± 118 mg 100 g^{-1}. For traditional coffees, the range for this compound was from 453 ± 15 to 645 ± 83 mg 100 g^{-1}, with an average of 558 ± 78 mg 100 g^{-1}. According to the Student's *t*-test analysis with a 95% confidence level, specialty and traditional coffees exhibited statistically significant differences. The values obtained for this compound were slightly lower than those found by Alcantara, Dresch, and Melchert,[24] whose range was from 1502 ± 5 to 2276 ± 19 mg 100 g^{-1} for specialty coffees and from 559 ± 24 to 1237 mg 100 g^{-1} for traditional coffees. Similarly, both coffee categories showed statistically significant differences, with the specialty category showing higher levels of chlorogenic acid. The presence of chlorogenic acids significantly influences the sensory qualities of coffee due to their considerable thermal degradation during the roasting process. This process leads to the formation of volatile compounds that are crucial to the beverage's flavor characteristics. However, severe roasting conditions can result in substantial losses of chlorogenic acids, with only 5% of the compound potentially remaining. Moreover, chlorogenic acids are also associated with parameters such as acidity, astringency, and bitterness, playing an essential role in the overall acceptance and quality of the beverage.[48-50]

Like caffeine, sample T1 was also the traditional category sample with the lowest amount of gallic acid, at 6 ± 1 mg 100 g^{-1}. The highest value for this acid (28 ± 4 mg 100 g^{-1}) was found in specialty sample S6. The average for specialty samples was 23 ± 5 mg 100 g^{-1}, while for traditional samples, it was 14 ± 5 mg 100 g^{-1}. The Student's *t*-test results at a 95% confidence level indicated statistical differences

between the two classifications. The results obtained in this study were consistent with those presented by Alkaltham *et al*.[51] In their investigation of the effects of different roasting methods, the researchers quantified the presence of gallic acid in samples of green coffee, microwave-roasted coffee, and oven-roasted coffee. The values found were 7 mg 100 g^{-1} for green coffee, 16 mg 100 g^{-1} for microwave-roasted coffee, and 20 mg 100 g^{-1} for oven-roasted coffee.

Regarding the results obtained for the 5-HMF compound, the average from chromatographic analyses was 28 ± 6 mg 100 g^{-1} for specialty coffees and 16 ± 3 mg 100 g^{-1} for traditional coffees. As observed with non-volatile compounds evaluated earlier, specialty sample S6 exhibited the highest content, while the lowest was found in traditional sample T5. The range for 5-HMF varied from 12 ± 1 to 51 ± 5 mg 100 g^{-1}, and according to the Student's *t*-test at a 95% confidence level, specialty and traditional coffees were statistically different. The 5-HMF content for specialty coffee samples was lower than that obtained by Alcantara, Dresch, and Melchert,[24] whose range was approximately 80 to 120 mg 100 g^{-1}, and no detectable levels of 5-HMF were found in traditional samples. On the other hand, the resulting values fall within the range obtained in the study by Vignoli *et al*.,[29] where the highest content of 5-HMF reached 230 mg 100 g^{-1} when evaluating the effects of roasting processes on various bioactive compounds of Arabica coffee. Three traditional coffee samples were evaluated by Francisco *et al*.[52] obtained 72, 58, and 26 mg 100 g^{-1} of this compound. The variation in 5-HMF quantification in the literature can be explained by the degree of roast used in each sample, as 5-HMF is considered a thermal marker and is present in lower quantities at the beginning of this process.[29] Murkovic and Bornik[53] observed an approximately 160% increase in 5-HMF after a roasting process lasting 3 minutes at 240 °C.

For 3,4-dihydroxybenzoic acid, the analyzed samples ranged from 87 ± 5 to 122 ± 2 mg 100 g^{-1} of ground roasted coffee. Among the specialty samples, S1 exhibited the highest content of this compound, averaging 103 ± 15 mg 100 g^{-1}. Traditional coffee samples had an average of 66 ± 13 mg 100 g^{-1}, with sample T1 showing the lowest content of 3,4-hydroxybenzoic acid. Statistically, these two coffee classifications differed after applying for the Student's *t*-test at a 95% confidence level. These values were lower than those found by Alkaltham *et al*.[51] who analyzed the effects of different roasting methods and obtained quantifications of 463 mg 100 g^{-1} for 3,4-hydroxybenzoic acid in green coffee, 599 mg 100 g^{-1} for microwave-roasted coffee, and 617 mg 100 g^{-1} for oven-roasted coffee. For Brazilian coffees, research conducted by Uslu[54] observed variations in levels of 3,4-hydroxybenzoic acid ranging from 15 to 40 mg 100 g^{-1} of coffee. Similarly, in Colombian coffees, this substance exhibited an even wider range, varying from 13 to 61 mg 100 g^{-1}. These variations were noted during the investigation of the influences of different extraction methods and times on the phenolic compound content in coffee beans, and were significantly smaller than those obtained in the current study. Among specialty coffees, sample S6 exhibited the highest quantities of caffeine and 5-hydroxymethylfurfural, while sample S5 had the highest levels of gallic acid. Sample S1 showed the highest amount of 3,4-hydroxybenzoic acid. On the other hand, traditional coffee samples such as T1 and T5 generally showed the lowest quantities of these compounds.

Volatile compounds

The calculated linear retention index (LRI) values were systematically compared with those reported in the literature for columns of similar polarity to ensure the identification and characterization of volatile compounds. Seven compounds (Table V) were identified by GC-FID using external standards and validated with LRI values referenced in previous studies. The LRI values obtained in this study for each compound analyzed showed strong agreement with the values established in the literature, highlighting the reliability of the identification process.

Table V. Compounds identified in coffee samples by GC-FID and comparison of linear retention indices (LRI) with literature values

Compound	LRI experimental	LRI literature	Ref. literature	LRI NIST	Ref. NIST
Acetaldehyde	706	702	37	700	
Acetone	823	823	37	814	
Methanol	915	915	33	911	
Ethanol	952	944	34	950	38
Diacetyl	990	985	32	988	
3-methyl-butanol	1229	1229	36	1229	
2-methylpyrazine	1296	1297	35	1288	

Table VI presents the linear regression equations, correlation coefficients, LODs, and LOQs for each volatile compound analyzed. Through chromatographic analysis, the following volatile compounds were identified and quantified in samples of both traditional and specialty coffees: acetaldehyde, acetone, methanol, ethanol, diacetyl, 3-methyl-butanol, and ethanol/methanol. These results are detailed in Table VII, in which the average density of 0.343 g mL^{-1} for roasted coffee beans[55,56] was adopted to express the concentrations in µg 100 g^{-1} of coffee samples. Furthermore, the RSD values in Table VII reflect the intrinsic variability of volatile compounds between the batches of the *Circuito das Águas Paulista*, even with standardized roasting and grinding, evidencing the strong influence of edaphoclimatic factors (altitude, microclimate, and seasonal events) on the aromatic composition.

Table VI. Analytical parameters of volatile compounds

Compounds	Concentration (mg L^{-1})	Regression equation	R^2	LOQ (mg L^{-1})	LOD (mg L^{-1})
Acetaldehyde	0.25 – 40	Area = -0.56 + 89.52 C	0.999	0.25	0.07
Acetone	0.25 – 40	Area = -2.07 + 83.04 C	0.999	0.25	0.08
Methanol	5 – 900	Area = -0.95 + 3.82 C	0.997	5.00	2.63
Ethanol	0.5 – 100 100 – 750	Area = 1.82 + 16.39 C Area = 1241.24 + 6.93 C	0.999 0.992	0.50	0.10
Diacetyl	0.5 – 20	Area = -7.76 + 26.12 C	0.978	0.50	0.26
3-methyl-butanol	0.01 – 0.5 0.5 – 2.5	Area = 0.58 + 62.39 C Area = 0.27 + 63.82 C	0.999 0.999	0.01	0.009
2-Methylpyrazine	1.99 – 100	Area = -4.77 + 9.17 C	0.999	1.99	0.18

The result of the Student's *t*-test at a 95% confidence level indicated no statistically significant difference between the mean acetaldehyde content in samples of specialty and traditional coffees (Table VII). In the specialty coffee group, the variation ranged from 0.04 ± 0.01 to 0.29 ± 0.15 µg 100 g^{-1} of coffee, while in the traditional coffee group, it ranged from 0.12 ± 0.01 to 0.16 ± 0.03 µg 100 g^{-1} of coffee. These values were lower than those obtained by Kalschne *et al*.,[57] who evaluated the influence of steam treatment to

improve the volatile compound profile of defective roasted robusta coffees, obtaining a range of 32.74 to 57.59 µg 100 g^{-1} for acetaldehyde content. Discrepancies in results compared to the literature may be attributed to variations in coffee bean quality. Acetaldehyde can be considered an indicator of quality, as it is found in lower concentrations in higher-quality coffee beverages and is characterized by a pungent and putrid odor.[58,59] On the other hand, when comparing specialty and traditional green coffees, Gomes, Bortoleto, and Melchert[60] found statistically significant differences between the samples. With variations from 3.66 ± 0.25 to 37.68 ± 1.90 µg 100 g^{-1} for specialty green coffees and from 1.27 ± 0.30 to 11.73 ± 1.05 µg 100 g^{-1} for traditional green coffees, with acetaldehyde present in higher quantities in some specialty coffee samples. Despite contradicting the findings of Rodriguez *et al*.,[58] this difference in acetaldehyde content can be justified by climate characteristics, altitude, and the extraction process.[61,62]

Despite evaluating volatile compounds in green coffees, Gomes, Bortoleto, and Melchert[23] also did not obtain statistically significant values in differentiating between specialty and traditional coffees based on acetone quantification. The variation observed from 1.52 ± 0.15 to 60.54 ± 9.65 µg 100 g^{-1} in specialty coffee samples and from 6.08 ± 1.68 to 35.07 ± 1.42 µg 100 g^{-1} in traditional ones. These values were higher than those obtained in the present study, where the acetone content in roasted coffees was evaluated. The variation in acetone levels may be related to the extraction method used during beverage preparation. For instance, in a study conducted by Chavez, Mendoza, and Caetano,[39] where five different infusion methods were tested, this volatile compound was detected only in coffee prepared through the French press method. This suggests that the extraction method may play a significant role in determining the chemical composition of coffee, including the presence or absence of certain volatile compounds, such as acetone. Additionally, the quantification of this compound may also be influenced by the type of grain processing (wet or dry) and milder climatic conditions.[39,63]

Table VII. Content of volatile compounds in specialty and traditional coffees

Sample	Mean of volatile compounds ± standard deviation (μg 100 g^{-1} of coffee samples)							
	Acetaldehyde	**Acetone**	**Methanol**	**Ethanol**	**Ethanol/ Methanol Ratio**	**Diacetyl**	**3-methyl-butanol**	**2-Methylpyrazine**
S1	0.04 ± 0.01	0.21 ± 0.01	5.16 ± 4.10	3.92 ± 1.04	1.42 ± 0.02	108.28 ± 8.44	7.28 ± 0.11	2.56 ± 0.29
S2	0.04 ± 0.01	0.20 ± 0.02	8.00 ± 0.99	0.93 ± 0.03	0.11 ± 0.02	91.83 ± 2.29	6.63 ± 0.71	2.67 ± 0.09
S3	0.18 ± 0.04	0.20 ± 0.05	17.02 ± 0.75	0.87 ± 0.05	0.07 ± 0.03	97.23 ± 7.48	7.49 ± 0.63	2.41 ± 0.30
S4	0.14 ± 0.09	0.17 ± 0.02	18.18 ± 0.37	3.18 ± 0.06	0.21 ± 0.06	82.14 ± 13.35	13.45 ± 1.00	3.14 ± 0.06
S5	0.19 ± 0.02	0.24 ± 0.02	2.17 ± 0.73	0.44 ± 0.12	0.15 ± 0.03	81.31 ± 14.05	6.11 ± 0.51	2.57 ± 0.18
S6	0.29 ± 0.15	0.29 ± 0.01	10.99 ± 1.26	28.52 ± 0.45	2.61 ± 0.26	102.88 ± 15.43	8.91 ± 0.51	2.75 ± 0.29
Mean	0.15 ± 0.09a (RSD 60%)	0.22 ± 0.04a (RSD 18%)	10.34 ± 6.28a (RSD 61%)	6.31 ± 10.97a (RSD 174%)	0.76 ± 1.04a (RSD 18%)	93.94 ± 10.95a (RSD 12%)	8.31 ± 2.69a (RSD 32%)	2.68 ± 0.28a (RSD 10%)
T1	0.14 ± 0.02	0.18 ± 0.02	14.81 ± 1.19	1.10 ± 0.09	0.07 ± 0.01	37.01 ± 3.29	8.60 ± 0.72	2.80 ± 0.07
T2	0.15 ± 0.01	0.19 ± 0.01	10.49 ± 0.45	1.00 ± 0.04	0.10 ± 0.01	57.81 ± 2.49	6.98 ± 0.94	2.98 ± 0.16
T3	0.16 ± 0.03	0.19 ± 0.04	10.85 ± 0.95	1.00 ± 0.07	0.09 ± 0.01	51.60 ± 6.41	6.93 ± 0.94	2.68 ± 0.23
T4	0.13 ± 0.01	0.17 ± 0.01	9.18 ± 0.63	1.00 ± 0.06	0.11 ± 0.01	43.80 ± 0.73	7.29 ± 0.30	2.51 ± 0.10
T5	0.12 ± 0.01	0.17 ± 0.01	7.83 ± 1.20	0.91 ± 0.00	0.11 ± 0.01	44.18 ± 5.11	7.51 ± 0.45	2.41 ± 0.13
T6	0.16 ± 0.01	0.24 ± 0.01	8.03 ± 0.13	1.09 ± 0.02	0.14 ± 0.01	64.14 ± 4.69	7.41 ± 0.20	3.38 ± 0.19
Mean	0.14 ± 0.02a (RSD 14%)	0.19 ± 0.02a (RSD 11%)	10.20 ± 2.57a (RSD 25%)	1.02 ± 0.07a (RSD 105%)	0.10 ± 0.02a (RSD 14%)	49.76 ± 10.04b (RSD 20%)	7.45 ± 0.61a (RSD 8%)	2.79 ± 0.35a (RSD 13%)

Note: means followed by the same letter in the column do not differ by Student's *t*-test at the 95% confidence level (α = 0.05), RSD = Relative Standard Deviation.

Methanol and ethanol are the alcohols most frequently identified in the volatile fraction of roasted coffees.[64] For methanol, specialty samples ranged from 2.17 ± 0.73 to 18.18 ± 0.37 μg 100 g^{-1}, while traditional samples varied from 7.83 ± 1.20 to 14.81 ± 1.19 μg 100 g^{-1}. Compared to the literature, these values were lower than those reported by Rhoades,[65] whose average methanol content was 83.0 μg 100 g^{-1} in beverages made with fresh coffee beans. Regarding ethanol, traditional coffees ranged from 0.87 ± 0.05 to 28.52 ± 0.45 μg 100 g^{-1} and did not follow a normal distribution, as indicated by the Shapiro-Wilk test. Ethanol showed a narrow range in traditional coffees, with samples ranging from 0.91 ± 0.0 to 1.10 ± 0.09 μg 100 g^{-1}. Moreover, this compound's quantification was closer to that of Rhoades[65] where the resulting averages ranged from 2.2 to 3.2 μg 100 g^{-1}. The variation in this compound may be related to coffee bean processing, with higher quantities found in wet processing.[66] The results obtained in the present study for both compounds also did not show statistically significant differences when comparing specialty and traditional coffee groups, as determined by the Mann-Whitney test and Student's *t*-test at a 95% confidence level.

Diacetyl was the only volatile compound evaluated that showed a statistically significant difference between the two coffee classifications, as determined by Student's *t*-test at a 95% confidence level. As shown in Table VII, mean values of 93.94 ± 10.95 μg 100 g^{-1} and 49.76 ± 10.04 μg 100 g^{-1} were found for specialty and traditional coffees, respectively. These results suggest the potential use of this volatile compound to differentiate between specialty and traditional coffees. Conversely, Toci and Farah[67] identified higher quantities of this compound in coffees made from defective beans, as its presence is generally undesired in other food types, such as beer.[68] However, these values were lower than those obtained in the study conducted by Procida *et al*.,[69] diacetyl concentrations ranged from 195.9 to 881.8 μg 100 g^{-1} in roasted coffees of robusta and arabica species from various geographic regions. The coffee bean roasting process can influence the diacetyl content. Hyong *et al.*[70] observed that the concentration of this compound significantly increased as roasting temperature and time increased. The quantification of diacetyl may also be influenced by the method of beverage preparation.[71]

Specialty coffee samples showed a variation range of 6.11 ± 0.51 to 13.45 ± 1.00 μg 100 g^{-1} for 3-methyl-butanol content with a resulting mean of 8.31 ± 2.69 μg 100 g^{-1}, while traditional coffee samples ranged from 6.93 ± 0.94 to 8.60 ± 0.72 μg 100 g^{-1} with a mean of 7.45 ± 0.61 μg 100 g^{-1}. Despite the higher mean of specialty samples, there was no significant difference between these two classifications when applying the Student's *t*-test at a 95% confidence level.

3-methyl-butanol is associated with coffee processing, especially wet processing, and its presence is linked to microbial metabolic reactions during the process, being found in higher quantities in green coffees.[43] However, the results obtained in this study for roasted coffees were relatively close to those obtained by Gomes, Bortoleto, and Melchert[60] for green coffees, the variation in specialty samples was from 2.57 ± 0.48 to 7.67 ± 0.5 μg 100 g^{-1} and from 0.33 to 16.89 ± 2.28 μg 100 g^{-1} in traditional samples.

In the specialty coffee group, concentrations of 2-methylpyrazine ranged from 2.41 ± 0.30 to 3.14 ± 0.06 μg 100 g^{-1}, resulting in a mean of 2.68 ± 0.28 μg 100 g^{-1}. Meanwhile, in the traditional coffee group, the variation was from 2.41 ± 0.13 to 3.38 ± 0.19 μg 100 g^{-1}, with a mean of 2.79 ± 0.35 μg 100 g^{-1}. Upon conducting a Student's *t*-test at a 95% confidence level to compare the means between the two sample groups, it was found that there was no significant difference in the levels of 2-methylpyrazine between specialty and traditional coffees.

Based on the comparison of the results obtained in this study with data found in the literature, it was observed that the values of 2-methylpyrazine were significantly lower compared to those reported by Wang *et al*.[72] The range for this compound varied between 2041 and 3418 μg g^{-1} when evaluating the chemical composition of roasted coffee beans from 12 different cultivars.

Similarly, the results for 2-methylpyrazine were considerably lower than those obtained by Cheong *et al.*,[73] who evaluated Arabica coffees from various geographical regions. Thus, the discrepancy in 2-methylpyrazine levels may be related to the geographical origin of the coffee beans, as evidenced in the study by Toledo *et al.*[74] In that study, the use of 2-methylpyrazine as a marker for geographical origin achieved approximately 90.9% correct classifications, highlighting the importance of geographical context in the chemical composition

and sensory characteristics of the analyzed coffees. No statistically significant differences were found in the quantification of the most volatile compounds investigated in this study between traditional and specialty coffee samples.

Principal Component Analysis (PCA)

The analysis incorporated various variables, including non-volatile compounds: caffeine (CAF), chlorogenic acid (CGA), gallic acid (EGA), 5-hydroxymethylfurfural, and 3,4-hydroxybenzoic acid (3,4-HB); and volatile compounds: acetaldehyde (AcH), acetone, methanol (MeOH), ethanol (EtOH), ethanol/methanol ratio, diacetyl, 3-methyl-butanol (3-MeB), and 2-methylpyrazine (2-MeP).

Additionally, altitude and cupping scores were considered. PCA was conducted to identify patterns or groupings that differentiate specialty coffees from traditional ones based on these chemical and sensory variables. Figure 1 displays the plot from principal component analysis encompassing the variables of non-volatile compounds, altitude, and cupping scores.

When analyzing the plots from Figure 1, two distinct groups were formed between specialty and traditional coffees based on non-volatile compounds, altitude, and cupping scores (Figure 1a), except for samples S3 and T2. Coffee sample S3 stood out among the specialty coffees, positioned on the negative side of the x-axis. The behavior of this sample in PCA can be attributed to its lower levels of caffeine, gallic acid, and 3,4-hydroxybenzoic acid, resulting in a lower score compared to other specialty coffees. Additionally, sample S3 has the second lowest altitude (after S6) and the second lowest levels of chlorogenic acid and 5-hydroxymethylfurfural.

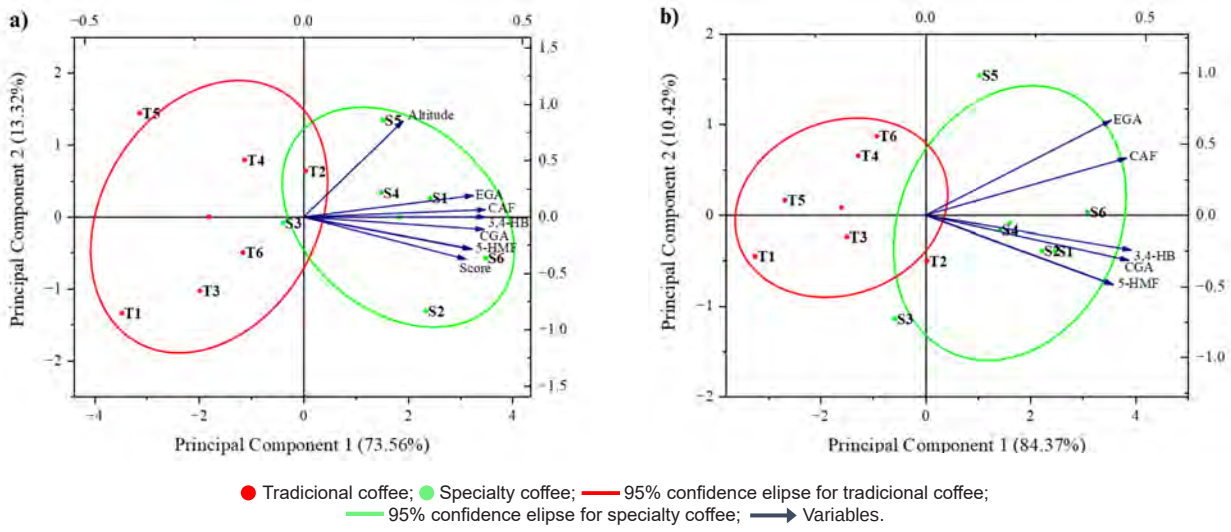

Figure 1. Biplot of the first two principal components with non-volatile compound variables, altitude, and scores (a) and (b), considering only non-volatile compounds for specialty and traditional coffees. (caffeine – CAF, chlorogenic acid – CGA, gallic acid – EGA, 5-hydroxymethylfurfural – 5HMF, and 3,4-hydroxybenzoic acid – 3,4-HB).

To provide a comprehensive evaluation, additional principal component analyses were conducted to investigate the impact of volatile compounds, considering both altitude and cupping scores. Furthermore, the relationship between these volatile and non-volatile compounds was examined; the results of these analyses are depicted in Figure 2.

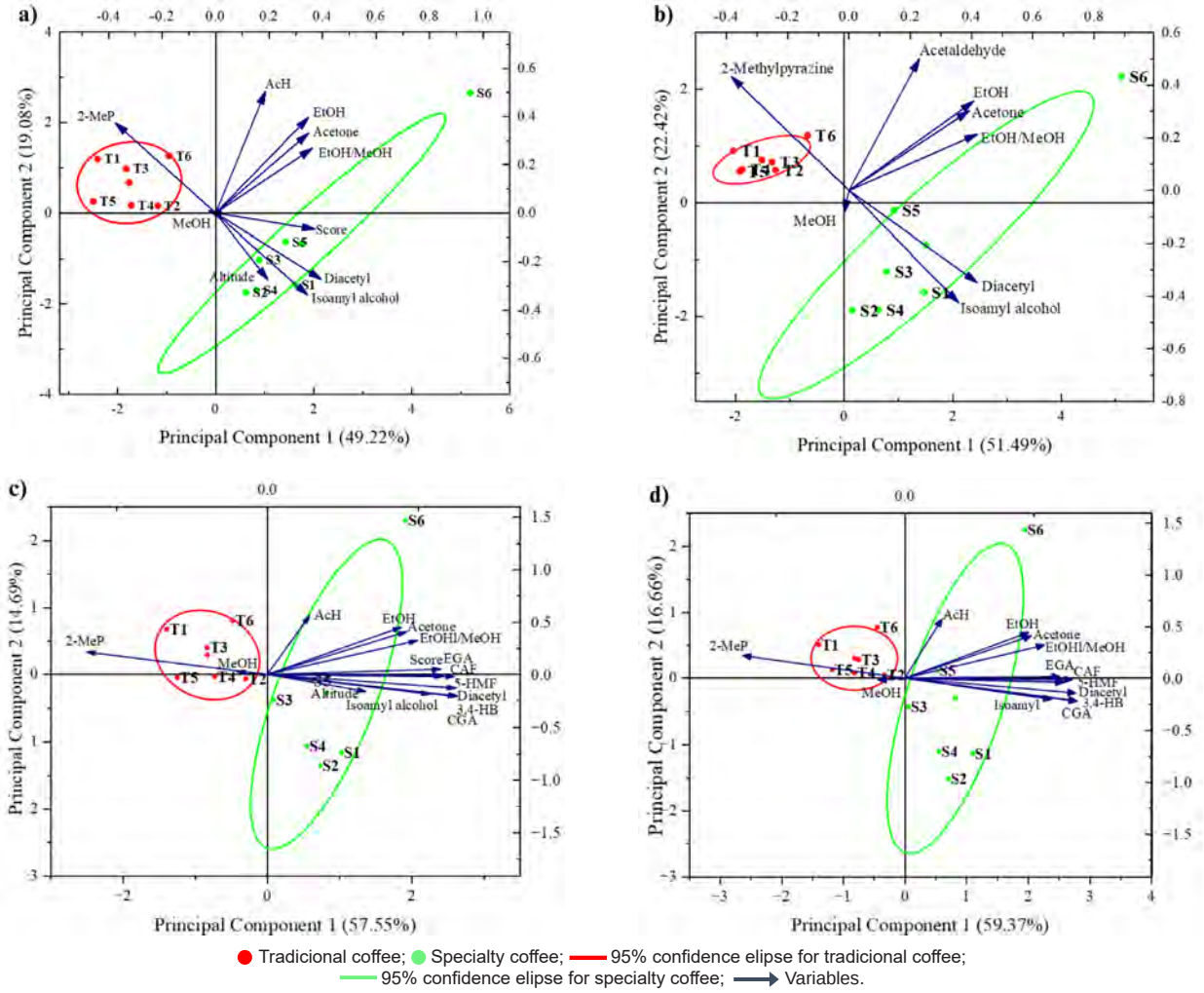

Figure 2. Biplot of the first two principal components with volatile compound variables, altitude, and scores (a); volatile compounds excluding altitude and ratings (b); all evaluated variables (c); and all evaluated variables excluding altitude and ratings (d) for specialty and traditional coffees. (caffeine – CAF, chlorogenic acid – CGA, gallic acid – EGA, 5-hydroxymethylfurfural – 5HMF, 3,4-hydroxybenzoic acid – 3,4-HB, acetaldehyde – AcH, methanol – MeOH, ethanol – EtOH, 3-methyl-butanol – 3-MeB, and 2-methylpyrazine – 2-MeP).

The analysis of Figure 2 reveals the identification of two distinct clusters: one formed by specialty coffee samples (in green) and another by traditional coffee samples (in red), with no overlapping samples. This separation is most pronounced along the first principal component (PC1), essential in distinguishing the two coffee categories. Optimal clustering was achieved without including altitude and cupping scores, with PC1 accounting for 51.49% (Figure 2b) and 59.37% (Figure 2d) of the total variance.

Notably, the volatile compound 2-methylpyrazine was particularly influential in traditional coffee samples, suggesting its significant role in differentiating these coffees, which may be due to variations in processing methods. Although prior studies indicate a stronger association between 2-methylpyrazine and wet-processed specialty coffees, this study also highlights its relevance in traditional coffee samples.[43]

Further, diacetyl and 3-methyl-butanol appear to characterize specialty coffee samples. While diacetyl is typically deemed undesirable in food products,[67,68] 3-methyl-butanol is consistent with findings linking it to wet processing, commonly employed in specialty coffee production.[75]

Comparison between harvests

To assess the impact of the frost that occurred during the 2020/2021 harvest period, five samples were collected from the same local producers during a non-frost harvest period (2022/2023), following the same methodology for total phenolic compounds, non-volatile compounds, and volatile compounds. These comparisons provide insight into how environmental stressors, such as frost, affect coffee quality and sensory characteristics.

Table VIII quantifies the total phenolic content and non-volatile and volatile compounds in coffee from the 2020/2021 and 2022/2023 harvests. The analysis shows that 5-hydroxymethylfurfural, acetone, and ethanol were the only compounds that did not exhibit statistically significant differences between the two harvest periods, as determined by a *t*-test at a 95% confidence level. In contrast, caffeine, along with other compounds, showed significant variations between the two periods, suggesting a potential correlation to the occurrence of frost. These findings highlight the impact of environmental stress on the chemical composition of coffee.

Table VIII. Compounds content by harvest

	mg 100 g^{-1} of coffee sample	
Compounds	**2020/2021**	**2022/2023**
TPC	3626 ± 166a	4314 ± 174b
5-hydroxymethylfurfural	21 ± 8a	25 ± 4a
3,4-dihydroxybenzoic acid	77 ± 23a	161 ± 17b
Chlorogenic acid	678 ± 181a	1189 ± 103b
Caffeine	758 ± 209a	3489 ± 126b
Gallic acid	19 ± 9a	11 ± 1b
	µg 100 g^{-1} of coffee sample	
Compounds	**2020/2021**	**2022/2023**
Acetaldehyde	0.18 ± 0.07a	0.43 ± 0.17a
Acetone	0.21 ± 0.03a	0.40 ± 0.16a
Methanol	7.88 ± 3.45a	1.78 ± 0.21b
Ethanol	1.99 ± 2.43a	3.07 ± 0.71a
Diacetyl	69.47 ± 19.07a	0.05 ± 0.03b
3-methyl-butanol	7.31 ± 0.78a	0.004 ± 0.001b
2-Methylpyrazine	2.90 ± 0.44a	1.16 ± 0.23b

Note: means followed by the same letter in the line do not differ by Student's *t*-test at the 95% confidence level (α = 0.05).

Figure 3 illustrates the Biplot of the first two principal components, including volatile and non-volatile compound variables, for specialty and traditional coffees from both harvest periods. PC1 accounts for 46.65% and PC2 for 21.38%. The samples identified by the letter N correspond to those obtained in the 2022/2023 harvest. When analyzing the plots from Figure 3, two distinct groups were formed between specialty and traditional coffees based on volatile and non-volatile compounds, except for sample N5, standing out among the specialty coffees, positioned on the negative side of the x-axis.

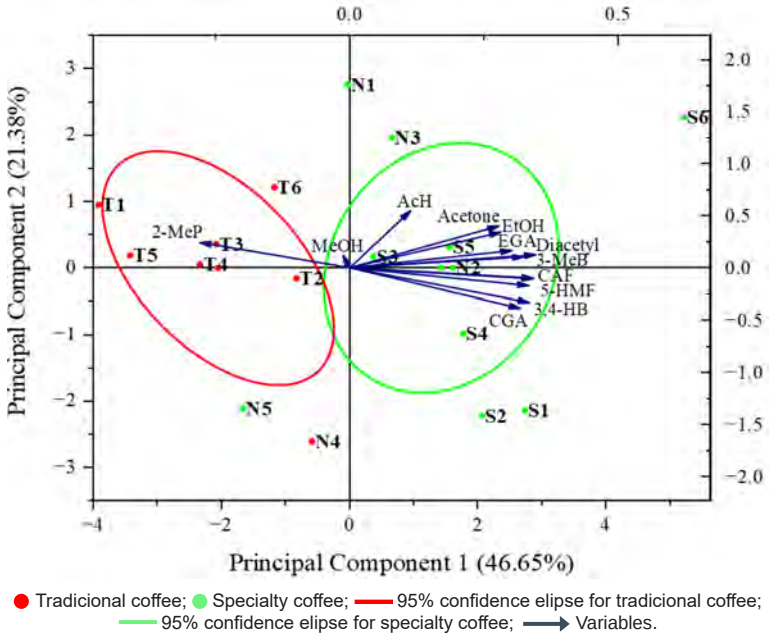

Figure 3. Biplot of the first two principal components with volatile and non-volatile compound variables for specialty and traditional coffees of both harvest periods. (caffeine – CAF, chlorogenic acid – CGA, gallic acid – EGA, 5-hydroxymethylfurfural – 5HMF, 3,4-hydroxybenzoic acid – 3,4-HB, acetaldehyde – AcH, methanol – MeOH, ethanol – EtOH, 3-methyl-butanol – 3-MeB, and 2-methylpyrazine – 2-MeP).

CONCLUSIONS

The chromatographic analysis of non-volatile compounds provided deeper insights into the distinctive characteristics between specialty and traditional coffees. This approach revealed significant differences in quantifying all evaluated non-volatile compounds: caffeine, chlorogenic acid, gallic acid, 5-hydroxymethylfurfural, and 3,4-hydroxybenzoic acid. These results highlight the chemical complexity of these samples and underscore the importance of examining a range of non-volatile compounds for a comprehensive understanding of the chemical profile and its relationship to the sensory aspects of coffee.

Regarding volatile compounds, diacetyl stood out as the only volatile compound assessed that showed statistically significant differences between the two coffee categories, according to the Student's *t*-test at a 95% confidence level. These findings suggest that diacetyl plays a crucial role in differentiating between specialty and traditional coffees.

PCA analysis proved to be extremely relevant for differentiating between specialty and traditional coffees. When addressing non-volatile compounds, including or excluding sensory scores and altitude, PCA showed a slight overlap of the confidence ellipses. However, this distinction became possible when volatile compounds were analyzed independently in a PCA encompassing all variables considered in this study. In both cases, analyses were conducted with and without sensory scores and altitude, yielding better results when these parameters were excluded. The volatile compound 2-methylpyrazine stood out in samples of coffees categorized as traditional, thus indicating a possible marker for lower-quality coffees from the *Circuito das Águas Paulista* region.

Combining chemical analyses with statistical tools played a prominent role in exploring the chemical composition of volatile and non-volatile species present in coffee. This approach facilitated correlating chemical composition with beverage classification, identifying clustering based on the similarity between specialty and traditional coffees.

Conflicts of interest

The authors declare no conflicts of interest regarding the publication of this article.

Acknowledgements

The authors appreciate the financial support of the National Council for Scientific and Technological Development (CNPq grant numbers 142474/2020-7, 141002/2024-7, and 305538/2022-5), Coordination of Improvement of Higher Education Personnel (CAPES, financial code 001), Luiz de Queiroz Agricultural Studies Foundation (FEALQ), and São Paulo Research Foundation (FAPESP).

REFERENCES

(1) Associação Industrial e Comercial do Café (AICC). *Origem*. Available from: http://aicc.pt/origem/ (accessed 2023-10-18).
(2) United States Department of Agriculture (USDA). *Coffee: World Markets and Trade*, 2023.
(3) Companhia Nacional de Abastecimento (CONAB). *Acompanhamento da Safra Brasileira de Café.* Brasília, 2023. Available from: https://www.conab.gov.br/info-agro/safras/cafe2 (accessed 2023-10-14).
(4) Sepúlveda, W. S.; Chekmam, L.; Maza, M. T.; Mancilla, N. O. Consumers' Preference for the Origin and Quality Attributes Associated with Production of Specialty Coffees: Results from a Cross-Cultural Study. *Food Res. Int.* **2016**, *89*, 997–1003. https://doi.org/10.1016/J.FOODRES.2016.03.039
(5) Cafés Especiais do Circuito das Águas Paulista são atrativos da Região. *Circuito das Águas Paulista.* Available from: https://www.circuitodasaguaspaulista.sp.gov.br/noticia/postagem/25/cafes-especiais-do-circuito-dasaguas-paulista-sao-atrativos-da-regiao (accessed 2023-11-19).
(6) Circuito das Águas Paulista e suas águas maravilhosas. *Circuito das Águas Paulista.* Available from: https://www.circuitodasaguaspaulista.sp.gov.br/noticia/postagem/58/circuito-das-aguas-paulista-e-suas-aguas-maravilhosas (accessed 2025-06-16).
(7) Specialty Coffee Association (SCA). *Protocols & Best Practices*. Available from: https://sca.coffee/research/protocols-best-practices (accessed 2023-10-14).
(8) Belchior, V.; Botelho, B. G.; Oliveira, L. S.; Franca, A. S. Attenuated Total Reflectance Fourier Transform Spectroscopy (ATR-FTIR) and Chemometrics for Discrimination of Espresso Coffees with Different Sensory Characteristics. *Food Chem.* **2019**, *273*, 178–185. https://doi.org/10.1016/j.foodchem.2017.12.026
(9) Nascimento, P. M. *Estudo da composição química, atividade antioxidante e potencial odorífico de um café conillon, em diferentes graus de torrefação e análise comparativa com café arábica*. Thesis for a Master's degree, Federal University of Uberlândia, Uberlândia, MG, BRA, 2006. https://repositorio.ufu.br/handle/123456789/17427
(10) Jeszka-Skowron, M.; Zgoła-Grześkowiak, A.; Grześkowiak, T. Analytical Methods Applied for the Characterization and the Determination of Bioactive Compounds in Coffee. *Eur. Food Res. Technol.* **2015**, *240*, 19–31. https://doi.org/10.1007/s00217-014-2356-z
(11) Tofalo, R.; Renda, G.; De Caterina, R.; Suzzi, G. Coffee: Health Effects. In: Caballero, B.; Finglas, P. M.; Toldrá, F. (Eds.). *Encyclopedia of Food and Health*. Academic Press, 2016, pp 237–243. https://doi.org/10.1016/B978-0-12-384947-2.00182-3
(12) Cappelletti, S.; Daria, P.; Sani, G.; Aromatario, M. Caffeine: Cognitive and Physical Performance Enhancer or Psychoactive Drug? *Curr. Neuropharmacol.* **2015**, *13* (1), 71–88. https://doi.org/10.2174/1570159X13666141210215655
(13) Saraiva, S. M.; Jacinto, T. A.; Gonçalves, A. C.; Gaspar, D.; Silva, L. R. Overview of Caffeine Effects on Human Health and Emerging Delivery Strategies. *Pharmaceuticals* **2023**, *16* (8), 1–35. https://doi.org/10.3390/ph16081067
(14) Santana-Gálvez, J.; Cisneros-Zevallos, L.; Jacobo-Velázquez, D. A. Chlorogenic Acid: Recent Advances on Its Dual Role as a Food Additive and a Nutraceutical against Metabolic Syndrome. *Molecules* **2017**, *22*, 1–21. https://doi.org/10.3390/molecules22030358

(15) Kahkeshani, N.; Farzaei, F.; Fotouhi, M.; Alavi, S. S.; Bahramsoltani, R.; Naseri, R.; Momtaz, S.; Abbasabadi, Z.; Rahimi, R.; Farzaei, M. H.; Bishayee, A. Pharmacological Effects of Gallic Acid in Health and Disease: A Mechanistic Review. *Iran. J. Basic Med. Sci.* **2019**, *22* (3), 225–237. https://doi.org/10.22038/ijbms.2019.32806.7897

(16) Behne, S.; Franke, H.; Schwarz, S.; Lachenmeier, D. W. Risk Assessment of Chlorogenic and Isochlorogenic Acids in Coffee By-Products. *Molecules* **2023**, *28*, 5540. https://doi.org/10.3390/molecules28145540

(17) Variya, B. C.; Bakrania, A. K.; Madan, P.; Patel, S. S. Acute and 28-Days Repeated Dose Sub-Acute Toxicity Study of Gallic Acid in Albino Mice. *Regul. Toxicol. Pharmacol.* **2019**, *101*, 71–78. https://doi.org/10.1016/J.YRTPH.2018.11.010

(18) Kowalski, S.; Lukasiewicz, M.; Duda-Chodak, A.; Zięc, G. 5-Hydroxymethyl-2-Furfural (HMF) -Heat-Induced Formation, Occurrence in Food and Biotransformation - A Review. *Pol. J. Food Nutr. Sci.* **2013**, *63* (4), 207–225. https://doi.org/10.2478/v10222-012-0082-4

(19) Monien, B. H.; Engst, W.; Barknowitz, G.; Seidel, A.; Glatt, H. Mutagenicity of 5-Hydroxymethylfurfural in V79 Cells Expressing Human SULT1A1: Identification and Mass Spectrometric Quantification of DNA Adducts Formed. *Chem. Res. Toxicol.* **2012**, *25* (7), 1484–1492. https://doi.org/10.1021/tx300150n

(20) Kakkar, S.; Bais, S. A Review on Protocatechuic Acid and Its Pharmacological Potential. *Int. Scholarly Res. Not.* **2014**, 1–9. https://doi.org/10.1155/2014/952943

(21) Di Nunzio, M.; Valli, V.; Tomás-Cobos, L.; Tomás-Chisbert, T.; Murgui-Bosch, L.; Danesi, F.; Bordoni, A. Is Cytotoxicity a Determinant of the Different in Vitro and in Vivo Effects of Bioactives? *BMC Complementary Altern. Med.* **2017**, *17* (1), 1–14. https://doi.org/10.1186/s12906-017-1962-2

(22) Belguidoum, K.; Amira-Guebailia, H.; Boulmokh, Y.; Houache, O. HPLC Coupled to UV-Vis Detection for Quantitative Determination of Phenolic Compounds and Caffeine in Different Brands of Coffee in the Algerian Market. *J. Taiwan Inst. Chem. Eng.* **2014**, *45* (4), 1314–1320. https://doi.org/10.1016/j.jtice.2014.03.014

(23) Gomes, W. P. C.; Bortoleto, G. G.; Melchert, W. R. Spectrophotometry and Chromatography Analyses Combined with Chemometrics Tools to Differentiate Green Coffee Beans into Special or Traditional. *J. Food Sci.* **2023**, *88* (12), 5012–5025. https://doi.org/10.1111/1750-3841.16807

(24) Alcantara, G. M. R. N.; Dresch, D.; Melchert, W. R. Use of Non-Volatile Compounds for the Classification of Specialty and Traditional Brazilian Coffees Using Principal Component Analysis. *Food Chem.* **2021**, *360*, 1–6. https://doi.org/10.1016/j.foodchem.2021.130088

(25) Abreu, M. B.; Marcheafave, G. G.; Bruns, R. E.; Scarminio, I. S.; Zeraik, M. L. Spectroscopic and Chromatographic Fingerprints for Discrimination of Specialty and Traditional Coffees by Integrated Chemometric Methods. *Food Anal. Methods* **2020**, *13* (12), 2204–2212. https://doi.org/10.1007/s12161-020-01832-1

(26) Alcantara, G. M. R. N.; Spíndola, G. B. F.; Melchert, W. R. Extraction of Non-Volatile Chemical Compounds in High-Quality and Traditional Coffee. *Braz. J. Anal. Chem.* **2023**, *10* (40), 76–89. https://doi.org/10.30744/BRJAC.2179-3425.AR-106-2022

(27) Singleton, V. L.; Orthofer, R.; Lamuela-Raventós, R. M. Analysis of Total Phenols and Other Oxidation Substrates and Antioxidants by Means of Folin-Ciocalteu Reagent. *Methods Enzymol.* **1999**, *299*, 152–178. https://doi.org/10.1016/S0076-6879(99)99017-1

(28) Martins, L. C. Otimização da extração assistida por micro-ondas de compostos bioativos de frutas. Final Course Project (Undergraduate), Escola Superior de Agricultura Luiz de Queiroz, Universidade de São Paulo, Piracicaba, 2020. Available from: https://bdta.abcd.usp.br/directbitstream/07cc6e01-9e01-4d99-8df5-c8d66832a093/TCCLuisClaudioMartins.pdf (accessed MM/YY).

(29) Vignoli, J. A.; Viegas, M. C.; Bassoli, D. G.; Benassi, M. de T. Roasting Process Affects Differently the Bioactive Compounds and the Antioxidant Activity of Arabica and Robusta Coffees. *Food Res. Int.* **2014**, *61*, 279–285. https://doi.org/10.1016/j.foodres.2013.06.006

(30) Lee, K.-G.; Shibamoto, T. Analysis of Volatile Components Isolated from Hawaiian Green Coffee Beans (*Coffea arabica* L.). *Flavour Fragrance J.* **2002**, *17* (5), 349–351. https://doi.org/10.1002/ffj.1067
(31) Bandeira, R. D. C. C.; Toci, A. R.; Trugo, L. C.; Farah, A. Composição Volátil Dos Defeitos Intrínsecos Do Café Por CG/Em-Headspace. *Quim. Nova* **2009**, *32* (2), 309–314. https://doi.org/10.1590/S0100-40422009000200008
(32) Ayseli, M. T.; Kelebek, H.; Selli, S. Elucidation of Aroma-Active Compounds and Chlorogenic Acids of Turkish Coffee Brewed from Medium and Dark Roasted Coffea Arabica Beans. *Food Chem.* **2021**, *338*, 1–10. https://doi.org/10.1016/J.FOODCHEM.2020.127821
(33) Devanthi, P. V. P.; Linforth, R.; Onyeaka, H.; Gkatzionis, K. Effects of Co-Inoculation and Sequential Inoculation of Tetragenococcus Halophilus and Zygosaccharomyces Rouxii on Soy Sauce Fermentation. *Food Chem.* **2018**, *240*, 1–8. https://doi.org/10.1016/J.FOODCHEM.2017.07.094
(34) Gonzalez-Rios, O.; Suarez-Quiroz, M. L.; Boulanger, R.; Barel, M.; Guyot, B.; Guiraud, J. P.; Schorr-Galindo, S. Impact of "Ecological" Post-Harvest Processing on the Volatile Fraction of Coffee Beans: I. Green Coffee. *J. Food Compos. Anal.* **2007**, *20* (3–4), 289–296. https://doi.org/10.1016/J.JFCA.2006.07.009
(35) Herawati, D.; Loisanjaya, M. O.; Kamal, R. H.; Adawiyah, D. R.; Andarwulan, N. Profile of Bioactive Compounds, Aromas, and Cup Quality of Excelsa Coffee (*Coffea liberica* ar. *dewevrei*) Prepared from Diverse Postharvest Processes. *Int. J. Food Sci.* **2022**, *2022*, 1–10. https://doi.org/10.1155/2022/2365603
(36) Ochiai, N.; Tsunokawa, J.; Sasamoto, K.; Hoffmann, A. Multi-Volatile Method for Aroma Analysis Using Sequential Dynamic Headspace Sampling with an Application to Brewed Coffee. *J. Chromatogr. A* **2014**, *1371*, 65–73. https://doi.org/10.1016/J.CHROMA.2014.10.074
(37) Viegas, M. C.; Bassoli, D. G. Utilização do Índice de Retenção Linear Para Caracterização de Compostos Voláteis em Café Solúvel Utilizando GC-MS e Coluna HP-Innowax. *Quim Nova* **2007**, *30* (8), 2031–2034. https://doi.org/10.1590/S0100-40422007000800040
(38) National Institute of Standards and Technology (NIST). Wallace, W. E. Retention Indices. *NIST Chemistry WebBook Standard Reference Database Number 69*. Gaithersburg MD, 2024. https://doi.org/10.18434/T4D303
(39) Flament, I. *Coffee Flavor Chemistry*. John Wiley & Sons, 2002.
(40) Miller, J. N.; Miller, J. C. *Statistics and Chemometrics for Analytical Chemistry*, 5th ed. Pearson/Prentice Hall, UK, 2005.
(41) Marasco Júnior, C. A.; da Silva, B. F.; Lamarca, R. S.; Gomes, P. C. F. L. Automated Method to Determine Pharmaceutical Compounds in Wastewater Using On-Line Solid-Phase Extraction Coupled to LC-MS/MS. *Anal. Bioanal. Chem.* **2021**, *413* (20), 5147–5160. https://doi.org/10.1007/s00216-021-03481-7
(42) Almeida, M. B.; Benassi, M. Atividade Antioxidante e Estimativa do Teor de Melanoidinas em Cafés Torrados Comerciais. *Semina:Cienc. Agrar.* **2011**, *32* (4-S1), 1893–1900. https://doi.org/10.5433/1679-0359.2011v32n4Sup1p1893
(43) Kitzberger, C. S. G.; Scholz, M. B. dos S.; Benassi, M. de T. Bioactive Compounds Content in Roasted Coffee from Traditional and Modern *Coffea arabica* Cultivars Grown under the Same Edapho-Climatic Conditions. *Food Res. Int.* **2014**, *61*, 61–66. https://doi.org/10.1016/j.foodres.2014.04.031
(44) Duarte, G. S.; Pereira, A. A.; Farah, A. Chlorogenic Acids and Other Relevant Compounds in Brazilian Coffees Processed by Semi-Dry and Wet Post-Harvesting Methods. *Food Chem.* **2010**, *118* (3), 851–855. https://doi.org/10.1016/j.foodchem.2009.05.042
(45) de Mejia, E. G.; Ramirez-Mares, M. V. Impact of Caffeine and Coffee on Our Health. *Trends Endocrinol. Metab.* **2014**, *25* (10), 489–492. https://doi.org/10.1016/j.tem.2014.07.003
(46) Oestreich-Janzen, S. Chemistry of Coffee. In: Liu, H-W.; Mander, L. (Eds.). *Comprehensive Natural Products II*. Elsevier 2010. Volume 3 (3.25), 1085–1096. https://doi.org/10.1016/B978-008045382-8.00708-5

(47) Olechno, E.; Puścion-Jakubik, A.; Zujko, M. E.; Socha, K. Influence of Various Factors on Caffeine Content in Coffee Brews. *Foods* **2021**, *10* (6). https://doi.org/10.3390/foods10061208
(48) Nogueira, M.; Trugo, L. C. Distribuição de Isômeros de Ácido Clorogênico e Teores de Cafeína e Trigonelina em Cafés Solúveis Brasileiros. *Food Sci. Technol.* **2003**, *23* (2), 296–299. https://doi.org/10.1590/S0101-20612003000200033
(49) Farah, A.; Donangelo, C. M. Phenolic Compounds in Coffee. *Braz. J. Plant Physiol.* **2006**, *18* (1), 23–36. https://doi.org/10.1590/S1677-04202006000100003
(50) Belay, A.; Gholap, A. V. Characterization and Determination of Chlorogenic Acids (CGA) in Coffee Beans by UV-Vis Spectroscopy. *Afr. J. Pure Appl. Chem.* **2009**, *3* (11), 234–240. Available from: https://academicjournals.org/journal/AJPAC/article-full-text-pdf/0E5B4BA1938
(51) Alkaltham, M. S.; Özcan, M. M.; Uslu, N.; Salamatullah, A. M.; Hayat, K. Effect of Microwave and Oven Roasting Methods on Total Phenol, Antioxidant Activity, Phenolic Compounds, and Fatty Acid Compositions of Coffee Beans. *J. Food Process. Preserv.* **2020**, *44* (11). https://doi.org/10.1111/jfpp.14874
(52) Francisco, K. C. A.; Lobato, A.; Tasic, N.; Cardoso, A. A.; Gonçalves, L. M. Determination of 5-Hydroxymethylfurfural Using an Electropolymerized Molecularly Imprinted Polymer in Combination with Salle. *Talanta* **2022**, *250*, 123723. https://doi.org/10.1016/j.talanta.2022.123723
(53) Murkovic, M.; Bornik, M. A. Formation of 5-Hydroxymethyl-2-Furfural (HMF) and 5-Hydroxymethyl-2-Furoic Acid during Roasting of Coffee. *Mol. Nutr. Food Res.* **2007**, *51*, 390–394. https://doi.org/10.1002/mnfr.200600251
(54) Uslu, N. The Influence of Decoction and Infusion Methods and Times on Antioxidant Activity, Caffeine Content and Phenolic Compounds of Coffee Brews. *Eur. Food Res. Technol.* **2022**, *248* (8), 2021–2030. https://doi.org/10.1007/s00217-022-04027-6
(55) Franca, A. S.; Mendonça, J. C. F.; Oliveira, S. D. Composition of Green and Roasted Coffees of Different Cup Qualities. *LWT - Food Sci. Technol.* **2005**, *38* (7), 709–715. https://doi.org/10.1016/J.LWT.2004.08.014
(56) Franca, A. S.; Oliveira, L. S.; Mendonça, J. C. F.; Silva, X. A. Physical and Chemical Attributes of Defective Crude and Roasted Coffee Beans. *Food Chem.* **2005**, *90* (1–2), 89–94. https://doi.org/10.1016/J.FOODCHEM.2004.03.028
(57) Kalschne, D. L.; Viegas, M. C.; De Conti, A. J.; Corso, P.; Benassi, M. de T. Steam Pressure Treatment of Defective Coffea Canephora Beans Improves the Volatile Profile and Sensory Acceptance of Roasted Coffee Blends. *Food Res. Int.* **2018**, *105*, 393–402. https://doi.org/10.1016/j.foodres.2017.11.017
(58) Rodriguez, D. B.; Frank, H. A.; Yamamoto, H. Y. Acetaldehyde as a possible indicator of spoilage in green kona (Hawaiian) coffee. *J. Sci. Food Agric.* **1969**, *20*, 15–17. https://doi.org/10.1002/jsfa.2740200105
(59) Bassoli, D. G. Impacto Aromático dos Componentes Voláteis do Café Solúvel: Uma Abordagem Analítica e Sensorial. Doctoral Thesis, Departamento de Tecnologia de Alimentos e Medicamentos, Universidade Estadual de Londrina, PR, 2006. https://repositorio.uel.br/handle/123456789/11008
(60) Gomes, W. P. C.; Bortoleto, G. G.; Melchert, W. R. Spectrophotometry and Chromatography Analyses Combined with Chemometrics Tools to Differentiate Green Coffee Beans into Special or Traditional. *J. Food Sci.* **2023**, *88* (12), 5012-5025. https://doi.org/10.1111/1750-3841.16807
(61) Bertrand, B.; Boulanger, R.; Dussert, S.; Ribeyre, F.; Berthiot, L.; Descroix, F.; Joët, T. Climatic Factors Directly Impact the Volatile Organic Compound Fingerprint in Green Arabica Coffee Bean as Well as Coffee Beverage Quality. *Food Chem.* **2012**, *135* (4), 2575–2583. https://doi.org/10.1016/j.foodchem.2012.06.060
(62) Bunzel, M.; Schendel, R. R. Determination of (Total) Phenolics and Antioxidant Capacity in Food and Ingredients. In: Nielsen, S. (Ed.). *Food Analysis, Food Science Text Series*. Springer International Publishing, 2017, pp 455–468. https://doi.org/10.1007/978-3-319-45776-5_25

(63) Bertrand, B.; Boulanger, R.; Dussert, S.; Ribeyre, F.; Berthiot, L.; Descroix, F.; Joët, T. Climatic Factors Directly Impact the Volatile Organic Compound Fingerprint in Green Arabica Coffee Bean as Well as Coffee Beverage Quality. *Food Chem.* **2012**, *135* (4), 2575–2583. https://doi.org/10.1016/j.foodchem.2012.06.060

(64) Moreira, R. F. A.; Trugo, L. C.; de Maria, C. A. B. Componentes voláteis do café torrado. Parte II. Compostos alifáticos, alicíclicos e aromáticos. *Quim. Nova* **2000**, *23* (2). https://doi.org/10.1590/S0100-40422000000200010

(65) Rhoades, J. W. Analysis of the Volatile Constituents of Coffee. *J. Agric. Food Chem.* **1960**, *8* (2), 136–141. https://doi.org/10.1021/jf60108a019

(66) Cardoso, W. S.; Agnoletti, B. Z.; de Freitas, R.; Pereira, R. R. Biochemical Aspects of Coffee Fermentation. In: Pereira, L. L.; Moreira, T. R. (Eds.). *Quality Determinants In Coffee Production. Food Engineering Series.* Springer Nature Switzerland, 2021, pp 149–208. https://doi.org/10.1007/978-3-030-54437-9

(67) Toci, A. T.; Farah, A. Volatile Fingerprint of Brazilian Defective Coffee Seeds: Corroboration of Potential Marker Compounds and Identification of New Low Quality Indicators. *Food Chem*. **2014**, 298-314. https://doi.org/10.1016/j.foodchem.2013.12.040

(68) Costa, G. P. Imobilização de α-acetolactato descarboxilase e aplicação processo de maturação de cervejas. Doctoral Thesis, Universidade Federal do Rio Grande do Sul, Porto Alegre, 2019. http://hdl.handle.net/10183/197086

(69) Procida, G.; Lagazio, C.; Cateni, F.; Zacchigna, M.; Cichelli, A. Characterization of Arabica and Robusta Volatile Coffees Composition by Reverse Carrier Gas Headspace Gas Chromatography–Mass Spectrometry Based on a Statistical Approach. *Food Sci. Biotechnol.* **2020**, *29* (10), 1319–1330. https://doi.org/10.1007/s10068-020-00779-7

(70) Hyong, S.; Chu, M.; Park, H.; Park, J.; Lee, K.-G. Analysis of α-Dicarbonyl Compounds and 4-Methylimidazole in Coffee Made with Various Roasting and Brewing Conditions. *LWT* **2021**, *151*. https://doi.org/10.1016/j.lwt.2021.112231

(71) Parenti, A.; Guerrini, L.; Masella, P.; Spinelli, S.; Calamai, L.; Spugnoli, P. Comparison of Espresso Coffee Brewing Techniques. *J. Food Eng.* **2014**, *121* (1), 112–117. https://doi.org/10.1016/j.jfoodeng.2013.08.031

(72) Wang, Y.; Wang, X.; Hu, G.; Hong, D.; Bai, X.; Guo, T.; Zhou, H.; Li, J.; Qiu, M. Chemical Ingredients Characterization Basing on ^{1}H NMR and SHS-GC/MS in Twelve Cultivars of *Coffea arabica* Roasted Beans. *Food Res. Int.* **2021**, *147*, 110544. https://doi.org/10.1016/j.foodres.2021.110544

(73) Cheong, M. W.; Tong, H.; Jian, J.; Ong, M.; Liu, S. Q.; Curran, P.; Yu, B. Volatile Composition and Antioxidant Capacity of Arabica Coffee. *Food Res. Int.* **2013**, *51* (1), 388-396. https://doi.org/10.1016/j.foodres.2012.12.058

(74) de Toledo, P. R. A. B.; de Melo, M. M. R.; Pezza, H. R.; Toci, A. T.; Pezza, L.; Silva, C. M. Discriminant Analysis for Unveiling the Origin of Roasted Coffee Samples: A Tool for Quality Control of Coffee Related Products. *Food Control* **2017**, *73*, 164–174. https://doi.org/10.1016/J.foodcont.2016.08.001

(75) Elhalis, H.; Cox, J.; Frank, D.; Zhao, J. The Role of Wet Fermentation in Enhancing Coffee Flavor, Aroma and Sensory Quality. *Eur. Food Res. Technol.* **2021**, *247* (2), 485–498. https://doi.org/10.1007/s00217-020-03641-6

Brazilian Journal of Analytical Chemistry
2026, Volume 13, Issue 52, pp 72-86
doi: 10.30744/brjac.2179-3425.AR-22-2025

BrJAC

ARTICLE

Fabrication of an Electrochemically Synthesized Nanoporous Gold Electrode for *In-Situ* Ascorbic Acid Determination in Fruit Samples

Eduarda Soldi Sartori Seixas, Pedro Henrique Alves Damasceno, Gilberto José Silva Junior*, Mauro Bertotti

Departamento de Química Fundamental, Instituto de Química, Universidade de São Paulo
Av. Prof. Lineu Prestes, 748, São Paulo, SP, 05508-000, Brazil

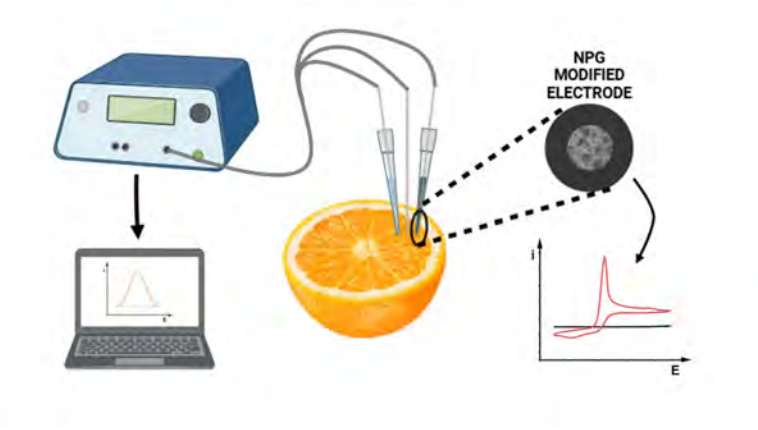

In this report, we present the development of a nanoporous gold (NPG) modified electrode fabricated through a mold-assisted electrodeposition technique, wherein a gold film was deposited onto a gold microfiber substrate. This modified electrode was subsequently employed for the *in-situ* determination of ascorbic acid (AA) in orange and lime juice samples. The NPG-modified electrode exhibited a high edge density, which contributes to an enhanced electrochemically active surface area, promoting a favorable electrocatalytic effect for the anodic oxidation of AA and resulting in a significantly lowered oxidation potential. Differential pulse voltammetry (DPV) measurements revealed a detection limit of 10 µmol L^{-1} and a quantification limit of 30 µmol L^{-1}. The NPG-modified electrode demonstrated outstanding analytical performance, displaying both high sensitivity and selectivity for AA determination in a complex matrix (orange and lime juice). The voltammetric data were corroborated with coulometric experiments, further validating the reliability of the electrochemical determination of AA using the NPG-modified electrode. Thus, this work highlights the potential of this novel electrochemical sensor, presenting a straightforward and efficient approach for NPG sensor fabrication, and underscoring its substantial promise for *in-situ* analytical applications.

Keywords: nanoporous gold electrode, *in-situ* analysis, ascorbic acid, electrocatalytic effect, food samples

INTRODUCTION

Fruits and vegetables are extensively recommended by health professionals for human consumption due to their rich nutritional profiles.[1] Beyond their nutritional value, these foods contain bioactive compounds that exhibit antioxidant properties, critical in mitigating oxidative stress and protecting against natural degenerative

Cite: Seixas, E. S. S.; Damasceno, P. H. A.; Silva Junior, G. J.; Bertotti, M. Fabrication of an Electrochemically Synthesized Nanoporous Gold Electrode for *In-Situ* Ascorbic Acid Determination in Fruit Samples. *Braz. J. Anal. Chem.* 2026, *13* (52), pp 72-86. https://doi.org/10.30744/brjac.2179-3425.AR-22-2025

Submitted: April 3, 2025; **Revised:** July 11, 2025; **Accepted:** August 18, 2025; **Published online:** September 17, 2025.

This article is part of the BrJAC Special Issue dedicated to the 21st ENQA and 9th CIAQA.

processes associated with premature aging and different diseases. Among the primary phytochemicals recognized for their antioxidant properties is vitamin C, also known as ascorbic acid (AA).[2,3]

AA is an antioxidant and water-soluble vitamin. Under certain physiological conditions, it also exists in its anionic form (ascorbate), which has a hexanoic sugar acid structure and contains two dissociable protons with pKa values of 4.04 and 11.34.[4] In addition to its antioxidant properties, AA facilitates the collagen synthesis, a critical component for maintaining healthy cartilage, skin, and bone tissue. Furthermore, it modulates cytokine production, enhances the rate of wound healing, and increases the synthesis of antibodies within the organism, among other physiological functions.[5,6]

In this context, the daily intake of foods rich in ascorbic acid is essential for maintaining bodily health. Among the fruits that serve as sources of ascorbic acid, certain varieties are particularly prominent for their high content, such as Barbados cherry, strawberry, lemon, and orange.[7] This study will specifically focus on determining AA in orange samples, as oranges are among the foods with the highest concentrations of vitamin C and are commonly consumed in daily diets. Factors such as climate, harvesting method, storage, and processing of fruits can cause variability in the AA content in foods.[8] In this regard, a rapid, simple, and effective method for determining vitamin C in food samples with high sensitivity and selectivity is highly desirable.

Different analytical techniques have been reported for detecting AA in various food samples. Among the more traditional instrumental methods, the literature highlights AA determination via fluorescence,[9,10] capillary electrophoresis coupled to mass spectroscopy,[11] high-performance liquid chromatography coupled to a colorimetric device[12] or to an UV-VIs detector,[13] etc. While these techniques offer high sensitivity for AA detection, they necessitate sophisticated, bulky, and expensive instrumentation, often associated with prolonged analysis times and the consumption of reagents. In this context, the development of electrochemical sensors for AA detection becomes highly advantageous, given their cost-effectiveness, miniaturization, and exceptional sensitivity and selectivity.

To enhance the sensitivity and selectivity of analytical determinations, the modification of electrode surfaces with materials possessing high surface area represents a straightforward and effective strategy. For instance, various nanomaterials have been prepared using different approaches and extensively used for several applications.[14-17] Among the various nanomaterials, NPG has gained prominence in the field due to its advantageous properties, such as excellent chemical stability, high surface area, outstanding electrical conductivity, and catalytic properties, which can enhance the determination of AA in fruit samples.[18]

Recent studies have focused on the fabrication of NPG-modified electrodes using approaches such as dealloying gold-containing alloys,[19,20] anodic corrosion of gold surfaces,[21] and synthesizing of hybrid films containing gold nanoporous and carbon-based materials for different applications.[22] Kumar and colleagues further reported their efforts in developing an NPG-modified electrode via mold-assisted electrodeposition to determine AA in biological samples.[23] However, it is noteworthy that, to date, no efforts have been reported on the fabrication of NPG-modified electrodes via electrodeposition for in-situ analysis in orange juice.

Paixão et al.[24] previously reported the use of a lab-made platinum microelectrode for mapping ascorbic acid in oranges. Their study focused on potential concentration differences of ascorbic acid across various fruit regions. In contrast, our research is centered on the development of a sensitive platform that facilitates the anodic oxidation of ascorbic acid, leveraging the physicochemical properties of nanoporous gold films. In this context, we present a rapid amperometric strategy for fabricating an NPG film on a lab-made gold microsensor surface for the determination of AA in natural orange juice samples. NPG-modified electrodes were fabricated using the Dynamic Hydrogen Bubble Template (DHBT) method,[25] and to optimize the platform, a comprehensive study was conducted by adjusting the experimental electrodeposition parameters to prepare NPG films under ideal conditions. In addition to the aforementioned advantages, the electrode developed in this work also presents a low fabrication cost, estimated at approximately USD 4.00 per device, which qualifies it as a low-cost analytical platform.

Notably, the electrochemical data obtained from the new amperometric microsensor based on NPG were found to be in excellent agreement with coulometric measurements in the same samples, thus validating the effectiveness and reliability of this novel approach.

MATERIALS AND METHODS

Chemicals

$HAuCl_4 \cdot 3H_2O$, ascorbic acid (AA), citric acid, folic acid, and glutamic acid were acquired from Sigma-Aldrich (St. Louis, MI, USA). Acetic acid, sodium acetate, potassium iodide, sodium sulfate, potassium chloride, D-(+)-glucose, and sulfuric acid (H_2SO_4) were purchased from Merck (Darmstadt, Germany), and soluble starch from Reagen (Paraná, Brazil). All the reagents were analytical grade and used without further purification unless otherwise stated. The solutions were prepared using Milli-Q water with 18 MΩ cm resistivity.

Experimental apparatus

Electrochemical measurements were conducted using an Autolab PGSTAT128N potentiostat interfaced with NOVA 2.0 software. The experiments were performed in a three-electrode configuration, employing a gold microelectrode, Ag/AgCl (saturated KCl), and a platinum wire as the working, reference, and counter electrodes, respectively. The gold electrode was polished with alumina powder (0.05 µm), rinsed with large quantities of distilled water, and subjected to ultrasonic cleaning for several seconds. Subsequently, the electrochemical behavior was assessed in a 0.5 mol L^{-1} H_2SO_4 solution, and the cleaning procedure was repeated until a reproducible gold electrochemical response was achieved. Surface morphology images of nanoporous gold were acquired using field emission-scanning electron microscopy (FE-SEM) with a JOEL JSM-7401F (30 kV) instrument. The coulometric system consists of a cell with a platinum net (anode) immersed in 50 mL of acetate buffer (pH 4.0) with 2 g of KI, 1 mL of a starch indicator, and 0.5 mL of the sample. Another platinum electrode kept inside a protection tube filled with a 0.5 mol L^{-1} Na_2SO_4 solution was used as a cathode. The protection tube was in contact with the rest of the cell through a membrane, and the starch indicator was prepared by adding 1 g of soluble starch in 100 mL of boiling distilled water.

Fabrication of bare Au and NPG-modified electrodes

The bare gold microelectrode was prepared from a gold fiber (99.99%, 0.025 mm, GoodFellow®) sealed in the tip of a micropipette using Araldite® epoxy glue. The interior of the pipette tip was filled with carbon black to ensure electrical contact and a nickel-chromium wire was inserted. The pipette tip was sealed with Parafilm paper. The fabricated electrode was polished using 600-grit sandpaper to remove excess glue, followed by 1200-grit sandpaper to expose the gold fiber.

The electrodic surface modification step was carried out using a mold-assisted electrodeposition approach known as DHBT. The microelectrode prepared in the previous step was immersed in a 5.0 mmol L^{-1} $HAuCl_4$ solution in 0.5 mol L^{-1} H_2SO_4, and using an amperometric approach, a potential of -3 V was applied during 100 s, forming a highly porous structure, the NPG-modified electrode. The potential and deposition time values were properly optimized. After each step, the electrochemical characterization was performed by cyclic voltammetry (CV) in a 0.5 mol L^{-1} H_2SO_4 solution.

Analytical parameters for AA determination

The analytical curve was obtained in a 30 to 100 µmol L^{-1} AA concentration range in acetate buffer (pH 4.0) using the DPV technique. Acetate buffer in this pH was chosen because such a value is close to the one found in natural orange juice (pH around 4.2). The AA anodic response was recorded in the potential range from -0.2 to 0.6 V (vs. Ag/AgCl sat. KCl), and the optimized parameters were determined as pulse amplitude 50 mV, step potential 5 mV, and scan rate 50 mV s^{-1}. Measurements were performed in triplicate for each concentration to estimate the precision.

The AA concentration in natural orange juice and in natural lime juice was determined using the standard addition method where 60 µL of a 0.1 mol L^{-1} AA in acetate buffer (pH 4.0) solution was added five times to the juice. After each addition, measurements were done using DPV, and three replicates were performed to estimate the precision. Coulometry titration was employed as a validation method using a constant current of 0.01 A.[26]

Pretreatment of natural orange juice and natural lime juice samples

The oranges and limes employed in these experiments were from the *Citrus sinensis* and *Citrus latifolia* species, respectively. The samples were prepared by squeezing the fruits separately and filtering the juice using qualitative filter paper. The analyses were conducted on the same day the samples were prepared.

RESULTS AND DISCUSSION

Morphological characterization

The both bare and NPG-modified electrodes' structural morphology study was performed using Field Emission Scanning Electron Microscopy (FE-SEM) images (Figure 1). A gold microfiber was immersed halfway into a 5.0 mmol L^{-1} $HAuCl_4$ in 0.5 mol L^{-1} H_2SO_4 solution to obtain the NPG film, enabling a clear comparison between the bare and modified microfiber regions (Figures 1A, 1E). Amplified images of both areas (Figures 1B, 1F) highlight their differences. The bare gold microfiber (Figures 1A, 1B) shows a smooth surface, with only a few tiny traces inherent to the commercial microfiber. The NPG-modified microfiber, obtained on the day of image acquisition, displays a porous film over the fiber, showing increased surface area and roughness with nanoporous structures (Figures 1E, 1F).

SEM images of the bare and NPG-modified electrodes surfaces were also obtained (Figures 1C, 1D, 1G, 1H). The bare electrode images (Figures 1C, 1D) show the shape of a cross-sectional area of the microfiber. The amplified image (Figure 1D) reveals a smooth surface without significant roughness. In contrast, the SEM images of the NPG-modified electrode (Figures 1G, 1H) show the nanostructures obtained. The SEM images of the NPG-modified electrode surface were obtained on an electrode modified ten days before the images were taken. Even after ten days, the NPG morphology remains, demonstrating mechanical stability. The amplified image of the NPG-modified electrode (Figure 1H) also shows the nanometer-sized pores obtained.

In all NPG images, the honeycomb-like formation of the NPG film on the material's surface is visible. This formation leads to an increase in the surface area due to the gold deposition assisted by the hydrogen bubbles formed and an increase in roughness, as seen in the formation of the porous structure.[18,27-29]

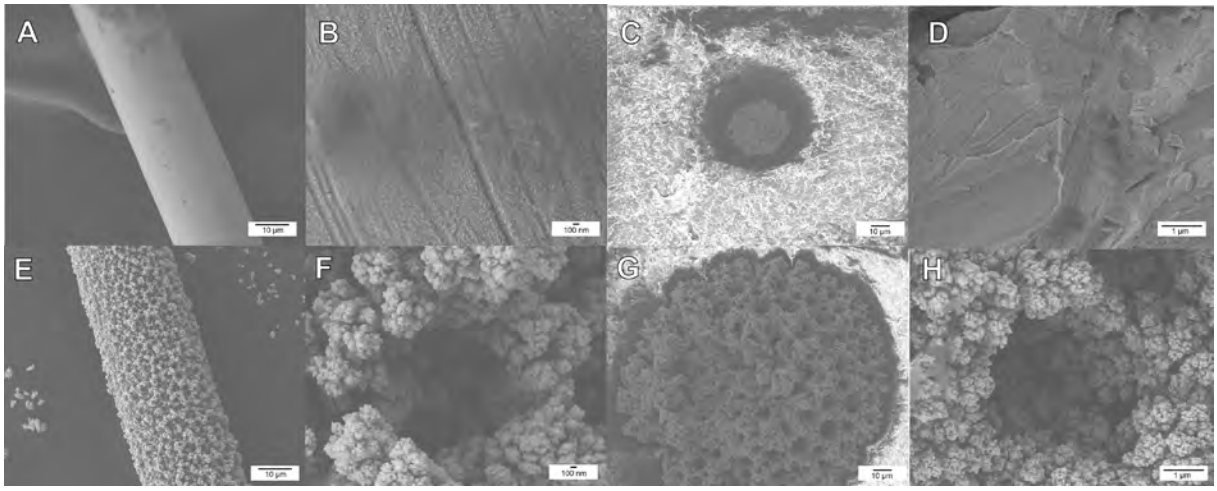

Figure 1. SEM images of a bare gold microfiber 1400X magnified (A) and 30000X magnified (B), a gold bare microelectrode 750X magnified (C) and 16000X magnified (D), a modified microfiber with NPG 1400X magnified (E) and 30000X magnified (F), an NPG-modified electrode 750X magnified (G) and 16000X magnified (H).

Electrochemical characterization

The electrochemical characterization was carried out by CV using the bare and NPG-modified electrodes in a 0.5 mol L^{-1} H_2SO_4 solution, and the results are shown in Figure 2. As one can see, distinct voltammetric

profiles were obtained for the bare and the NPG-modified electrodes. A single anodic current peak was observed at E = 1.4 V for the bare microelectrode. In contrast, the voltammogram for the NPG-modified electrode shows two anodic peaks at E = 1.2 V and E = 1.4 V. The difference between the profiles obtained on the different surfaces and the two oxidation peaks on the NPG-modified electrode are attributed to the formation of new crystalline planes of the deposited gold during the electrode surface modification.[27]

During the reverse scan, a remarkable cathodic current peak (E = 0.9 V) is noticed for the NPG-modified electrode. Hence, the electrochemically active surface area (ECSA) was determined according to the Equations (1) and (2):[25]

$$Charge\ (C) = \frac{Cathodic\ peak\ area}{Scan\ rate\ (Vs^{-1})} \quad (1) \qquad ECSA\ (cm^{-2}) = \frac{Charge}{390\ \mu C\ cm^{-2}} \quad (2)$$

The modified electrode ECSA increased about 1500-fold when compared to the bare electrode. This area increase is attributed to changes in surface morphology promoted by the gold electrodeposition, as shown in the SEM images of the surface (Figure 1).

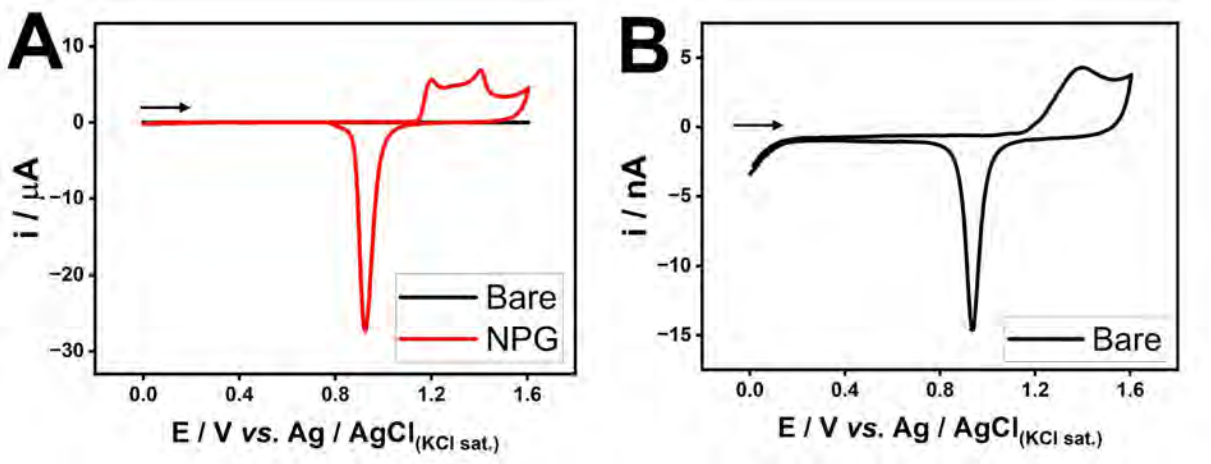

Figure 2. CVs of bare (black curve) and NPG-modified (red curve) electrodes recorded in a 0.5 mol L^{-1} H_2SO_4 solution (A) and magnified CV of the bare microelectrode (B). (Scan rate:100 mV s^{-1}).

Electrochemical behavior of ascorbic acid (AA)

AA undergoes oxidation to dehydroascorbic acid (DA) through a two-electron electrochemical reaction.[4,25,29]

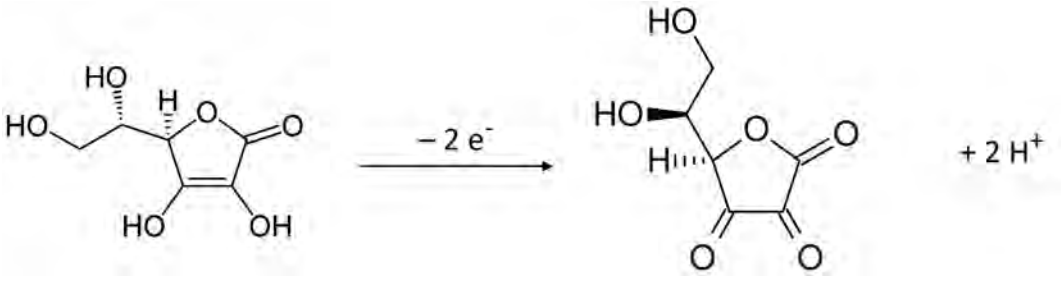

The electrochemical behavior of AA was investigated by CV in a potential window from 0.6 to -0.2 V in a 3.0 mmol L^{-1} AA solution in acetate buffer (pH 4.0) and the obtained CVs for both bare and NPG-modified electrodes are shown in Figure 3. The voltammetric profile obtained using the bare microelectrode (Figure 3B) clearly demonstrates the anodic current generated during the oxidation of ascorbic acid in comparison to the background signal.

Figure 3A shows the comparative study of the electrochemical behavior of AA using both bare and NPG-modified electrodes. The CV recorded with the NPG-modified electrode (red curve) presented a maximum current that is 42-fold higher than the bare Au electrode and a clear anticipation of the onset potential. The observed increase in anodic current can be attributed to the significant enhancement of the ECSA. The NPG film allows AA to penetrate the pores; hence, a larger area is available for the electrochemical reaction, and a pre-concentration occurs within the pores, as evidenced by the first cycle of CV. In subsequent cycles, a slight decrease in anodic current is observed due to the fast electron transfer, leading to the oxidation of AA to DA without significant diffusion through the NPG film (Figure 1S).

The potential shift associated with the anodic process toward less positive values can be explained by the formation of new crystalline planes in the deposited gold film.[27, 28] These new surfaces allow different mechanisms associated with the AA oxidation, resulting in a more facile electron transfer process.[25,27] Additionally, the species nanoconfinement in the pores increases the probability of the reaction occurrence, as the species are close to the electrode surface. The NPG film also enables better coordination between the electroactive species and the gold atoms, especially at the edges of the structures, facilitating better contact between the species and the electrode surface. Finally, the nanostructured defects enhanced the synergy between AA and the electrode surface.[27,28]

The AA anodic oxidation at the NPG-modified electrode presents a sharp peak at around 0.15 V (Figure 3A). This voltammetric shape reflects the fast electron transfer occurring at the NPG surface, and because AA is rapidly oxidized to DA, such electroactive species is rapidly depleted and generates a peak that is unusual for a microelectrode at conventional scan rates. Such behavior also reveals that AA in the bulk of the solution takes longer to penetrate the pores.

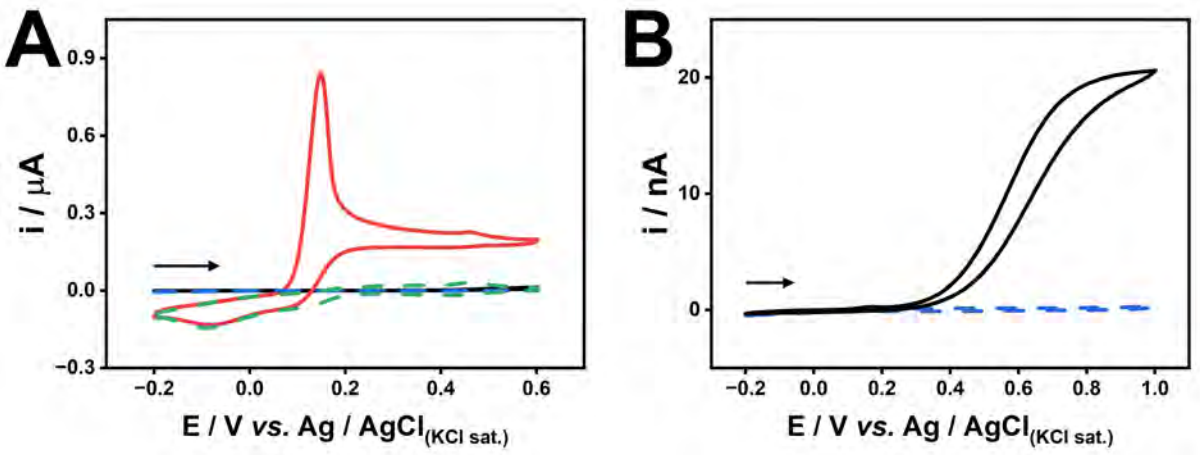

Figure 3. CVs recorded in a 3.0 mmol L^{-1} AA solution in acetate buffer (pH 4.0) using bare (black curve) and NPG-modified (red curve) electrodes (A) and CVs recorded in acetate buffer (pH 4.0) solution using bare (blue curve) and NPG-modified (green curve) electrodes (A). Magnified CVs recorded using the bare electrode (B). (Scan rate: 100 mV s^{-1}).

Analytical performance

Analytical parameters

To determine the limit of detection (LOD) and the limit of quantification (LOQ), calculated according to the IUPAC recommendations,[30] an analytical curve between 30 and 100 µmol L^{-1} was recorded in acetate buffer (pH 4.0) using the NPG-modified electrode (Figure 2S). A correlation coefficient of 0.9933 was found, the LOD was determined as 10 µmol L^{-1}, and the LOQ was determined as 30 µmol L^{-1}.

A comparison of key analytical parameters between the sensor developed in this work and other electrochemical sensor reported in the literature is presented in Table I. Compared to previously reported methods, the strategy developed in this work achieves a low limit of detection, which are either superior or comparable to those reported for other electrochemical sensors. Importantly, this level of sensitivity is achieved through a simple electrochemical deposition process completed in only 100 seconds. In contrast, many existing approaches rely on multi-step fabrication procedures, including nanomaterial synthesis, thermal treatment, or sequential deposition steps, all of which increase the complexity, cost, and duration of electrode preparation.

The sensor developed herein is based on a direct electrochemical modification using low-cost and commercially available materials, without requiring additional chemical synthesis, drop-casting, or sophisticated instrumentation. The linear concentration range obtained, along with the low detection limit, is fully suitable for the determination of the target analyte in fruit juice samples. These features highlight the practical applicability of the proposed sensor and support its potential as a reliable and efficient platform for routine electrochemical analyses.

Table I. Comparison of different modified electrodes and electroanalytical techniques for AA

Surface	Technique	Linear range μmol L^{-1}	LOD μmol L^{-1}	Sample	Ref.
PdNPs/rGO/GCE	DPV	300 – 30000	100	Human serum	31
NPG	DPV	320 – 3400	63	FBS	32
e-NCNF	AMP	50 – 1000	20	Rat brain microdialysates	33
ITO-rGO-AuNPs	LSV	20 – 150	9.4	Milk, fruit juice, urine	34
AuNPs/PAN	AMP	10 – 1000	8.8	–	35
erGO/TiS_2//GCE	AMP	0.1 – 1	0.03	Vit C tablets	36
ITO/gC_3N_4/NC@GC/h-ATS	DPV	0.05 – 200	0.02	Urine	37
NPG	DPV	30 – 100	10	Fruit juice	This work

Interference study

A study was performed to understand the response of AA in the presence of possible interferents commonly found in orange juices, including folic acid (FA), glutamic acid (GA), citric acid (CA), and glucose (GLU). Experiments were performed by fixing the AA concentration at 1 mmol L^{-1} and adding the other compounds in the same proportion they can be found in orange juices (1:0.003 for AA:FA, 1:0.6 for AA:GA, 1:10 for AA:CA, and 1:30 for AA:GLU).[38] Based on the results presented in Figure 4, it can be concluded that none of the tested species significantly influenced the AA quantification, with interference remaining at 5% for GA, 7% for GLU, and no interference was observed for the other species studied. One can conclude that the synergistic effect of the NPG film on the electron transfer rate involved in the AA anodic oxidation makes the proposed sensor highly selective for determining this analyte in orange samples.

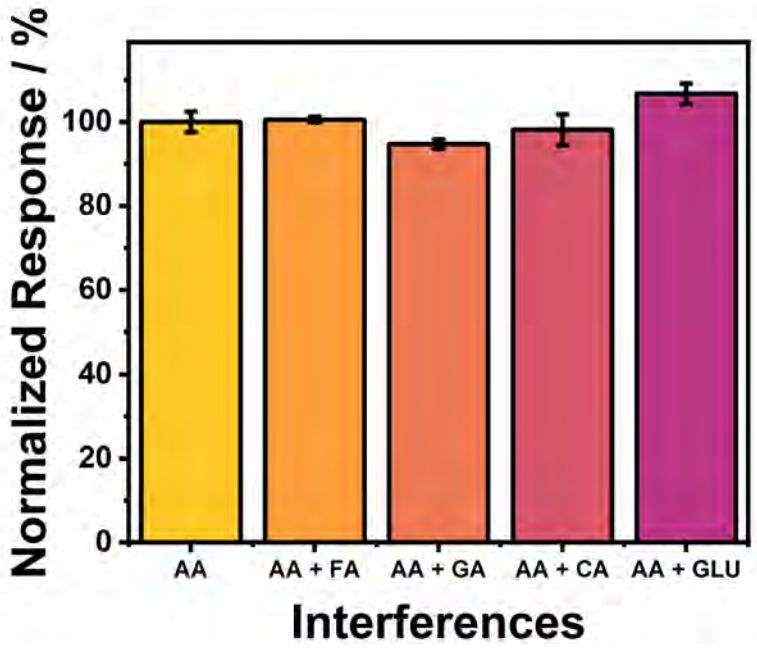

Figure 4. Interference study performed in solutions containing 1.0 mmol L^{-1} AA in the absence and presence of the possible interfering species: folic acid (FA), glutamic acid (GA), citric acid (CA), and glucose (GLU) using the NPG electrode.

Real samples

The developed NPG-modified electrode was applied to quantify AA in a natural orange juice sample. Due to a matrix effect, which can be caused by the presence of interferences such as GA and GLU, along with the differences in viscosity and conductivity, the AA signal obtained in the juice and by inserting the electrode into the fruit differed from that obtained in buffer solutions, as shown in Figure 5. Therefore, the juice's background signal was obtained by adding slices of *Cucumis sativus*, a species of cucumber known for its two peroxidases that degrade AA,[39] to a previously separated sample of the juice and leaving it in agitation for five hours.

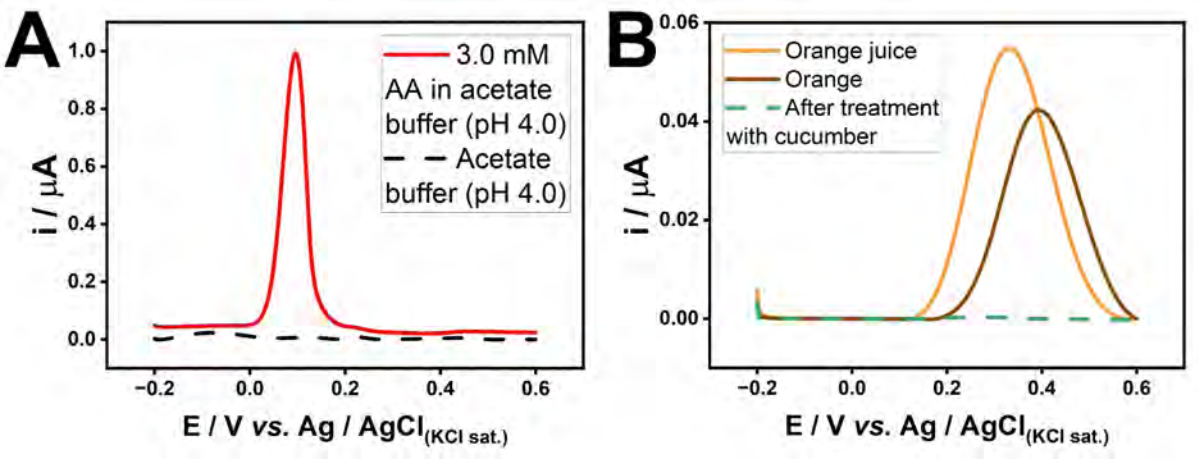

Figure 5. DPVs recorded in 3.0 mmol L^{-1} AA solution in acetate buffer (pH 4.0) and acetate buffer (pH 4.0) solution (A) and in natural orange juice, directly in an orange and after treatment with cucumber (B), using NPG-modified gold electrodes.

Due to this difference, the AA determination was carried out using the standard addition method, as shown in Figure 6. The results were compared to those obtained through coulometry, a comparative method for AA determination[26] performed on the same sample (Table II).

Table II. AA concentration determined in natural orange juice using DPV and coulometry

Method	AA Concentration mmol L^{-1}	RSD %
DPV	1.7 ± 0.1	5.9
Coulometry	1.6 ± 0.1	6.2

The proposed sensor's attractive features (selectivity and small size) made it possible to record the AA response directly in an orange (the same one used to prepare the orange juice, CV shown in Figure 5B, brown curve). The obtained signal was compared to the background corrected standard addition curve, shown in Figure 6C, and the concentration found in the orange was 1.1 ± 0.2 mmol L^{-1}.

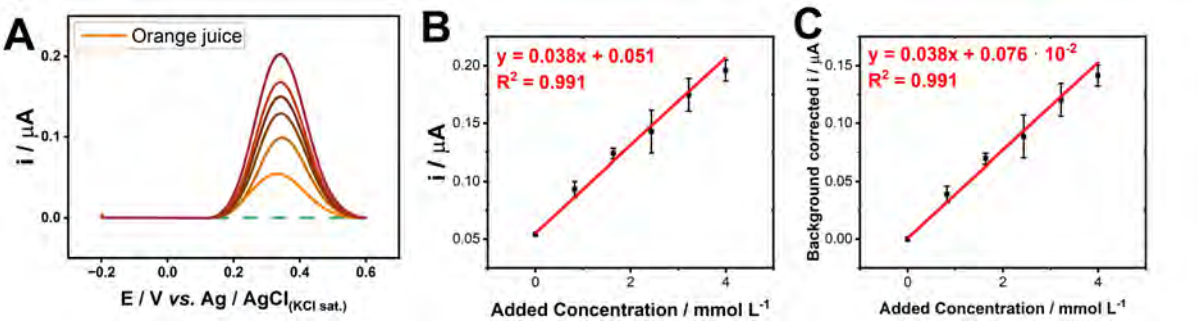

Figure 6. DPVs recorded in natural orange juice before and after additions of a standard 100 mmol L^{-1} AA solution in acetate buffer (pH 4.0) (A). Standard addition curve (B) and background corrected standard addition curve (C).

The developed sensor was also applied to quantify AA in natural lime juice by following the same steps used to quantify AA in natural orange juice. The standard addition curve is presented in Figures 7A and 7B, and the background-corrected standard addition curve is shown in Figure 7D. Results were compared to those obtained through coulometry for the same sample and are shown in Table III. The response was also recorded directly in the lime (Figure 7C), and the concentration was found to be 2.1 ± 0.1 mmol L^{-1}.

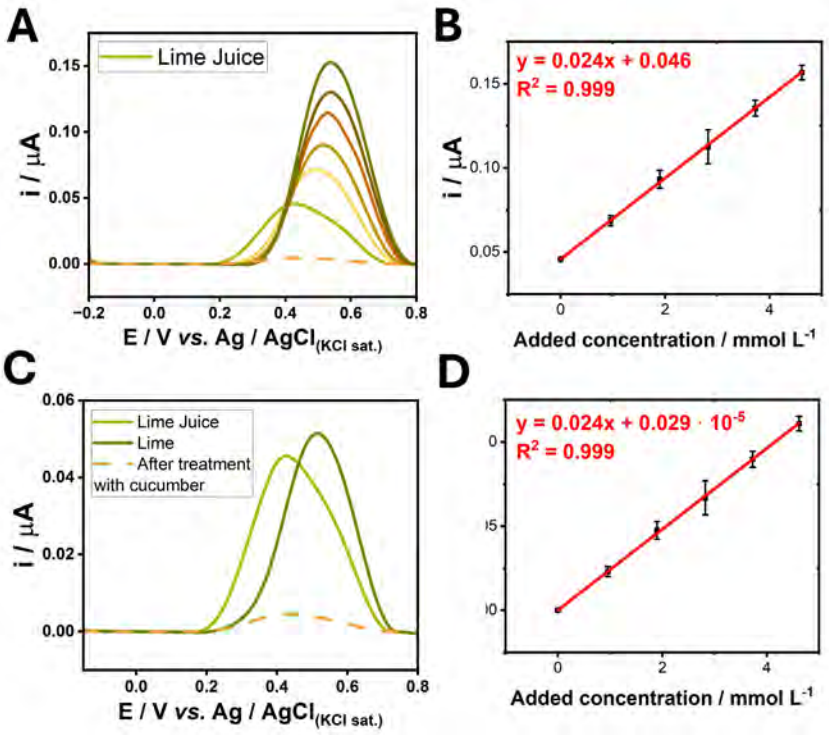

Figure 7. DPVs recorded in natural lime juice before and after additions of a standard 100 mmol L^{-1} AA solution in acetate buffer (pH 4.0) (A). Standard addition curve (B). DPVs recorded in natural lime juice, directly in the lime and after treating the natural juice with cucumber (C). Background corrected standard addition curve (D).

Table III. AA concentration determined in natural lime juice using DPV and coulometry

Method	AA Concentration mmol L^{-1}	RSD %
DPV	1.9 ± 0.2	10.5
Coulometry	1.5 ± 0.2	13.3

Coulometry titration can be a fast analysis but, as mentioned in the *Experimental apparatus* section of this article, besides having a visual end point that can be susceptible to human error, its system requires the use of 1 mL of starch indicator, 2 g of KI, and 50 mL of acetate buffer for this kind of analysis. Coulometry is known for the capability of sequential analysis using the same cell. However, since natural juices are colorful, it was necessary to prepare a new cell for each measurement in order to maintain the same endpoint, which significantly increased the reagent waste. Our study also showed that in cases of natural orange juice and in natural lime juice, coulometry RSD was higher.

The response stability of the NPG-modified electrode was also examined. If manipulated and stored under proper conditions, i.e., without physical impacts on the surface, stored in a 0.5 mmol L^{-1} H_2SO_4 solution, and electrochemically cleaned before and after each day of use (by recording 100 cycles of CV with a 500 mV s^{-1} scan rate in a 0.5 mol L^{-1} H_2SO_4 solution), the response can last about a month without significant loss, presenting less than 10% decrease after 25 days. After this time, the NPG-modified electrode no longer presents an ideal electrochemical behavior. Stability study results are presented in the supplementary material (Figure 3S). Results of a memory effect study, where sequential voltammograms recorded in

a solution without AA after keeping the electrode in solution containing AA, were also performed, and negligible signals can be noticed (Figure 4S). This confirms the absence of memory effects.

CONCLUSIONS

We have reported a novel approach to using NPG-modified electrodes, whose surface was modified by a rapid amperometric strategy, for detection and quantification using differential pulse voltammetry of AA in natural orange juice, natural lime juice, and for *in situ* analysis within an orange and a lime. The fast protocol of modifying the electrode surface significantly enhances the sensor's sensitivity and selectivity toward AA detection due to an electrocatalytic effect promoted by the nanoporous structure. We also demonstrated that the NPG-based electrode retains its electrochemical performance and structural integrity even when applied directly within fresh fruit tissue (a slightly rigid and heterogeneous matrix) without any pre-treatment or sample preparation. Further studies are of interest to better understand the matrix effect responsible for a significant change in the AA response in such a sample. The results showed that the obtained LOD is way lower than the AA concentration found in the fruits and the juices, justifying the use of the NPG-modified electrode for this approach. The proposed sensor yielded reliable results regarding the AA content in oranges and limes, besides being simple, cheaper, wasting fewer reagents, and not requiring sophisticated, bulky, and expensive instrumentation. Finally, we also reported the proper conditions for manipulating and storing the NPG-modified electrode, giving the modification a long service life.

Conflicts of interest

The authors declare that there are no known competing financial interests or personal relationships that could have appeared to influence the work reported in this paper.

Acknowledgements

The authors would like to thank the financial support from the São Paulo State Research Foundation, FAPESP [Grant numbers 2023/00246-1, 2022/03643-9, 2025/00748-2], and the National Council for Scientific and Technological Development, CNPq [Grant Number: 103418/2024-5].

REFERENCES

(1) Kitts, D. D. An evaluation of the multiple effects of the antioxidant vitamins. *Trends Food Sci. Technol.* **1997**, *8* (6), 198-203. https://doi.org/10.1016/S0924-2244(97)01033-9

(2) Aishwarya, K. D.; Nayaka, Y. A.; Pradeepa, E.; Sahana, H. R. Electrochemical determination of ascorbic acid using sensitive and disposable methylene blue modified pencil graphite electrode. *Anal. Biochem.* **2025**, *698*, 115733. https://doi.org/10.1016/j.ab.2024.115733

(3) Yaacob, S. F. F. S.; Din, S. N. M.; Suah, F. B. M. Ascorbic acid sensor using modified pencil graphite electrodes: a preliminary study. *Russ. J. Electrochem*. **2024**, *60*, 392-399. https://doi.org/10.1134/s1023193524050094

(4) Pisoschi, A. M.; Pop, A.; Serban, A. I.; Fafaneata, C. Electrochemical methods for ascorbic acid determination. *Electrochim. Acta* **2014**, *121*, 443–460. https://doi.org/10.1016/j.electacta.2013.12.127

(5) Tajima, S.; Pinnell, S. R. Ascorbic acid preferentially enhances type I and III collagen gene transcription in human skin fibroblasts. *J. Dermatol. Sci.* **1996**, *11* (3), 250-253. https://doi.org/10.1016/0923-1811(95)00640-0

(6) Desneves, K. J.; Todorovic, B. E.; Cassar, A.; Crowe, T. C. Treatment with supplementary arginine, vitamin C and zinc in patients with pressure ulcers: A randomised controlled trial. *Clin. Nutr.* **2005**, *24* (6), 979-987. https://doi.org/10.1016/j.clnu.2005.06.011

(7) Bechthold, A. New reference values for Vitamin C intake. *Ann. Nutr. Metab*. **2015**, *67* (1), 13-20. https://doi.org/10.1159/000434757

(8) Ogiri, Y.; Sun, F.; Hayami, S.; Fujimura, A.; Yamamoto, K.; Yaita, M.; Kojo, S. Very low vitamin C activity of orally administered L-dehydroascorbic acid. *J. Agric. Food Chem.* **2002**, *50*, 227-229. https://doi.org/10.1021/jf010910f

(9) Zhang, S. Q.; Wen, J.; Li, H. Y.; Chen, M. L. Iron modified hydrogen-bonded organic framework as fluorescent sensor for ascorbic acid detection. *Spectrochim. Acta, Part A* **2024**, *317*, 124393. https://doi.org/10.1016/j.saa.2024.124393

(10) Lu, X. C.; Wang, Z.; Wang, J. X.; Li, Y.; Hou, X. Q. Ultrasensitive Fluorescence Detection of Ascorbic Acid Using Silver Ion-Modulated High-Quality CdSe/CdS/ZnS Quantum Dots. *ACS Omega.* **2024**, *9* (25), 27127-27136. https://doi.org/10.1021/acsomega.4c01045

(11) Legrand, P.; Gahoual, R.; Benattar, R.; Toussaint, B.; Roques, C.; Mignet, N.; Goulay-Dufaÿ, S.; Houzé, P. Comprehensive and quantitative stability study of ascorbic acid using capillary zone electrophoresis with ultraviolet detection and high-resolution tandem mass spectrometry. *J. Sep. Sci.* **2020**, *43* (14), 2925-2935. https://doi.org/10.1002/jssc.202000389

(12) Sil, B. K.; Jamiruddin, M. R.; Haq, M. A.; Aekwattanaphol, N.; Ananth, K. P.; Salendra, L.; Paliwal, H.; Paul, P. K.; Buatong, W.; Srichana, T. Nanolevel of detection of ascorbic acid using horse-radish peroxidase inhibition assay. *Helioyn* **2024**, *10* (10), e30715. https://doi.org/10.1016/j.heliyon.2024.e30715

(13) Hasan, M. M.; Abu Reza, M.; Haque, A. Detection and Quantification of Ascorbic Acid in Citrus macroptera Fruit Pulp Juice by High Performance Liquid Chromatography. *Anal. Chem. Lett.* **2021**, *11* (2), 284-288. https://doi.org/10.1080/22297928.2021.1908911

(14) Huang, D.; Li, X.; Chen, M.; Chen, F.; Wan, Z.; Rui, R.; Wang R.; Fan S.; Wu, H. An electrochemical sensor based on a porphyrin dye-functionalized multi-walled carbon nanotubes hybrid for the sensitive determination of ascorbic acid. *J. Electroanal. Chem*. **2019**, *841*, 101-106. https://doi.org/10.1016/j.jelechem.2019.04.041

(15) Mohammadnezhad, K.; Ahour, F.; Keshipour, S. Electrochemical determination of ascorbic acid using palladium supported on N-doped graphene quantum dot modified electrode. *Sci. Rep.* **2024**, *14*, 5982. https://doi.org/10.1038/s41598-024-56231-x

(16) Li, N.; Nan, C.; Mei X.; Sun, Y.; Feng H.; Li Y. Electrochemical sensor based on dual-template molecularly imprinted polymer and nanoporous gold leaf modified electrode for simultaneous determination of dopamine and uric acid. *Microchim. Acta* **2020**, *187*, 496. https://doi.org/10.1007/s00604-020-04413-5

(17) Gutiérrez, A.; Ramírez-Ledesma, M. G.; Rivas, G. A.; Luna-Bárcenas, G.; Escalona-Villalpando, R. A.; Ledesma-García, J. Development of an electrochemical sensor for the quantification of ascorbic acid and acetaminophen in pharmaceutical samples. *J. Pharm. Biomed. Anal.* **2024**, *249*, 116334. https://doi.org/10.1016/j.jpba.2024.116334

(18) Silva Junior, G. J.; Selva, J. S. G.; Sukeri, S.; Gonçalves, J. M.; Regiart, M.; Bertotti, M. Fabrication of dendritic nanoporous gold via a two-step amperometric approach: Application for electrochemical detection of methyl parathion in river water samples. *Talanta* **2021**, *226*, 122130. https://doi.org/10.1016/j.talanta.2021.122130

(19) Chu, Y.; Zhou, H.; Wang, X.; Zhang, H.; Zhao, L.; Xu, T.; Yan, H.; Zhao, F. A flexible and self-supported nanoporous gold wire electrode with a seamless structure for electrochemical ascorbic acid sensor. *Microchem. J.* **2023**, *186*, 108259. https://doi.org/10.1016/j.microc.2022.108259

(20) Silva, T. A.; Khan, M. R. K.; Fatibello-Filho, O.; Collinson, M. Simultaneous electrochemical sensing of ascorbic acid and uric acid under biofouling conditions using nanoporous gold electrodes. *J. Electroanal. Chem*. **2019**, *846*, 113160. https://doi.org/10.1016/j.jelechem.2019.05.042

(21) Lins, R. S. O.; Sukeri, A.; Bertotti, M. A home-made nanoporous gold microsensor for lead(ii) detection in seawater with high sensitivity and anti-interference properties. *Anal. Methods* **2024**, *16*, 4415-4420. https://doi.org/10.1039/D4AY00698D

(22) Sakthivel, P.; Ramachandran, K.; Maheshvaran, K.; Senthil, T. S.; Manivel, P. Simultaneous electrochemical detection of ascorbic acid, dopamine and uric acid using Au decorated carbon nanofibers modified screen printed electrode. *Carbon Lett*. **2024**, *34* (9), 2325-2341. https://doi.org/10.1007/s42823-024-00759-5

(23) Kumar, A.; Furtado, V. L.; Gonçalves, J. M.; Bannitz-Fernandes, R.; Netto, L. E. S.; Araki, K.; Bertotti, M. Amperometric microsensor based on nanoporous gold for ascorbic acid detection in highly acidic biological extracts. *Anal. Chim. Acta* **2020**, *1095*, 61-70. https://doi.org/10.1016/j.aca.2019.10.022
(24) Paixão, T. R. L. C.; Lowinsohn, D.; Bertotti, M. Use of an Electrochemically Etched Platinum Microelectrode forAscorbic Acid Mapping in Oranges. *J. Agric. Food Chem*. **2006**, *54*, 3072-3077. https://doi.org/10.1021/jf052874g
(25) Kumar, A.; Gonçalves, J. M.; Furtado, V. L.; Araki, K.; Angnes, L.; Bouvet, M.; Meunier-Prest, R. Mass Transport in Nanoporous Gold and Correlation with Surface Pores for EC 1 Mechanism: Case of Ascorbic Acid. *ChemElectroChem* **2021**, *8* (11), 2129–2136. https://doi.org/10.1002/celc.202100440
(26) Bertotti, M.; Vaz, J. M.; Telles, R. Ascorbic Acid Determination in Natural Orange Juice: As a Teaching Tool of Coulometry and Polarography. *J. Chem. Educ.* **1995**, *72*, 445-447. https://doi.org/10.1021/ed072p445
(27) Veselinovic, J.; AlMashtoub, S.; Nagella, S.; Seker, E. Interplay of Effective Surface Area, Mass Transport, and Electrochemical Features in Nanoporous Nucleic Acid Sensors. *Anal. Chem.* **2020**, *92* (15), 10751-10758. https://doi.org/10.1021/acs.analchem.0c02104
(28) Mohd Zaki, M. H.; Mohd, Y.; Chin, L. Y. Surface Properties of Nanostructured Gold Coatings Electrodeposited at Different Potentials. *Int. J. Electrochem. Sci.* **2020**, *15* (11), 11401–11415. https://doi.org/10.20964/2020.11.41
(29) Sakthivel, P.; Ramachandran, K.; Maheshvaran, K.; Senthil, T. S.; Manivel, P. Simultaneous Electrochemical Detection of Ascorbic Acid, Dopamine and Uric Acid Using Au Decorated Carbon Nanofibers Modified Screen Printed Electrode. *Carbon Lett.* **2024**, *34* (9), 2325–2341. https://doi.org/10.1007/s42823-024-00759-5
(30) Currie, L. A. Nomenclature in Evaluation of Analytical Methods including Detection and Quantification Capabilities. *Anal. Chim. Acta* **1999**, *391*, 105-126. https://doi.org/10.1016/S0003-2670(99)00104-X
(31) Wei, Y.; Liu, Y.; Xu, Z.; Wang, S.; Chen, B.; Zhang, D.; Fang, Y. Simultaneous Detection of Ascorbic Acid, Dopamine, and Uric Acid Using a Novel Electrochemical Sensor Based on Palladium Nanoparticles/Reduced Graphene Oxide Nanocomposite. *Int. J. Anal. Chem*. **2020**, *2020*, 8812443. https://doi.org/10.1155/2020/8812443
(32) Silva, T. A.; Khan, M. R. K.; Fatibello-Filho, O.; Collinson, M. M. Simultaneous Electrochemical Sensing of Ascorbic Acid and Uric Acid under Biofouling Conditions Using Nanoporous Gold Electrodes. *J. Electroanal. Chem*. **2019**, *846*, 113160. https://doi.org/10.1016/j.jelechem.2019.05.042
(33) Cao, F.; Zhang, L.; Tian, Y. A Novel N-Doped Carbon Nanotube Fiber for Selective and Reliable Electrochemical Determination of Ascorbic Acid in Rat Brain Microdialysates. *J. Electroanal. Chem*. **2016**, *781*, 278–283. https://doi.org/10.1016/j.jelechem.2016.10.027
(34) Mazzara, F.; Patella, B.; Aiello, G.; O'Riordan, A.; Torino, C.; Vilasi, A.; Inguanta, R. Electrochemical Detection of Uric Acid and Ascorbic Acid Using r-GO/NPs Based Sensors. *Electrochim. Acta* **2021**, *388*, 138652. https://doi.org/10.1016/j.electacta.2021.138652
(35) Chu, W.; Zhou, Q.; Li, S.; Zhao, W.; Li, N.; Zheng, J. Oxidation and Sensing of Ascorbic Acid and Dopamine on Self-Assembled Gold Nanoparticles Incorporated within Polyaniline Film. *Appl. Surf. Sci*. **2015**, *353*, 425–432. https://doi.org/10.1016/j.apsusc.2015.06.141
(36) Pal, P.; Bhattacharjee, S.; Das, M. P.; Shim, Y.-B.; Neppolian, B.; Cho, B. J.; Veluswamy, P.; Das, J. Design of Electrochemically Reduced Graphene Oxide/Titanium Disulfide Nanocomposite Sensor for Selective Determination of Ascorbic Acid. *ACS Appl. Nano Mater*. **2021**, *4* (10), 10077–10089. https://doi.org/10.1021/acsanm.1c01464
(37) Krishnan, S.; Tong, L.; Liu, S.; Xing, R. A Mesoporous Silver-Doped TiO_2–SnO_2 Nanocomposite on g-C_3N_4 Nanosheets and Decorated with a Hierarchical Core−Shell Metal–Organic Framework for Simultaneous Voltammetric Determina-tion of Ascorbic Acid, Dopamine and Uric Acid. *Microchim. Acta* **2020**, *187* (1), 82. https://doi.org/10.1007/s00604-019-4045-x
(38) Robards, K.; Antolovich, M. Methods for Assessing the Authenticity of Orange Juice. A review. *The Analyst* **1995**, *120*, 1-28. https://doi.org/10.1039/an9952000001

(39) Battistuzzi, G.; D'Onofrio, M.; Loschi, L.; Sola, M. Isolation and Characterization of Two Peroxidases from *Cucumis sativus*. *Arch. Biochem. Biophys.* **2001**, *388*, 100-112. https://doi.org/10.1006/abbi.2001.2281

SUPPLEMENTARY MATERIAL

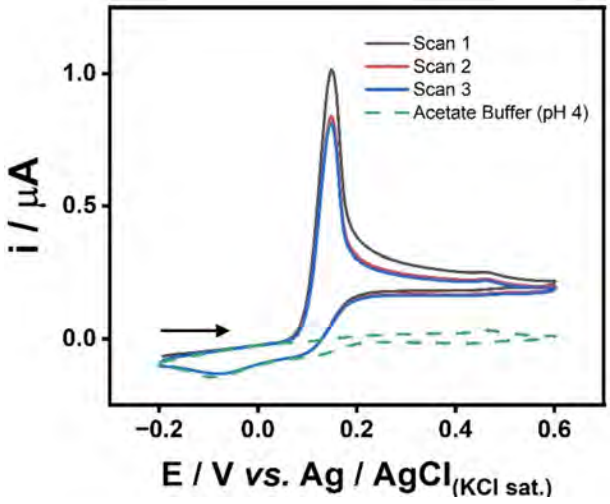

Figure 1S. Different CV cycles recorded in a 3.0 mmol L^{-1} AA in acetate buffer (pH 4.0) solution (black, red and blue curve) and a CV recorded in acetate buffer (pH 4.0) solution (green curve) using an NPG-modified electrode. Scan rate: 100 mV s^{-1}.

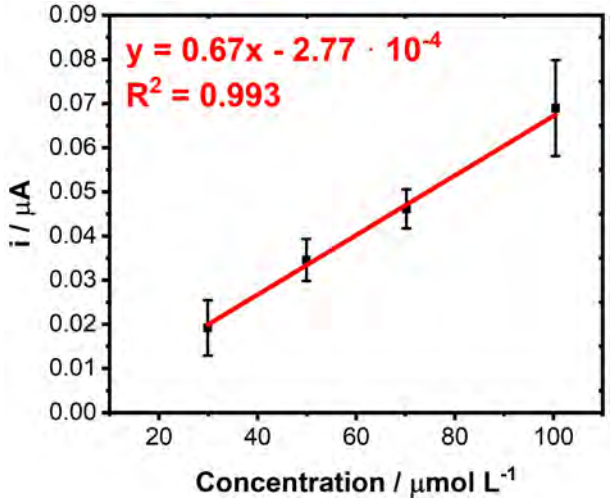

Figure 2S. Analytical curve between AA 30 and 100 µmol L^{-1} recorded in acetate buffer (pH 4.0) solutions using the NPG-modified electrode.

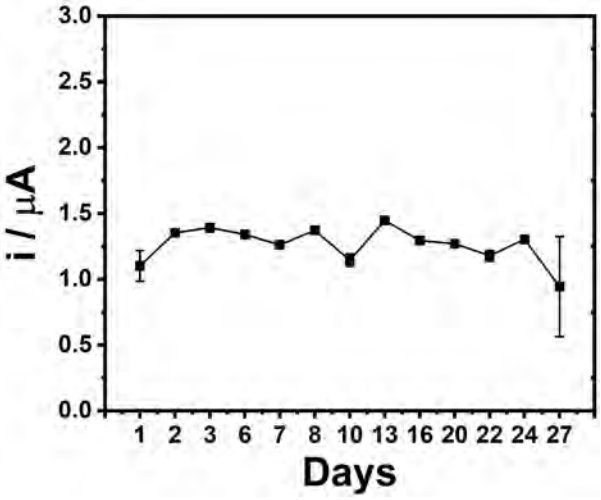

Figure 3S. Stability study results. Current was obtained by inserting the same NPG- modified electrode into a 3.0 mmol L^{-1} AA solution in acetate buffer (pH 4.0).

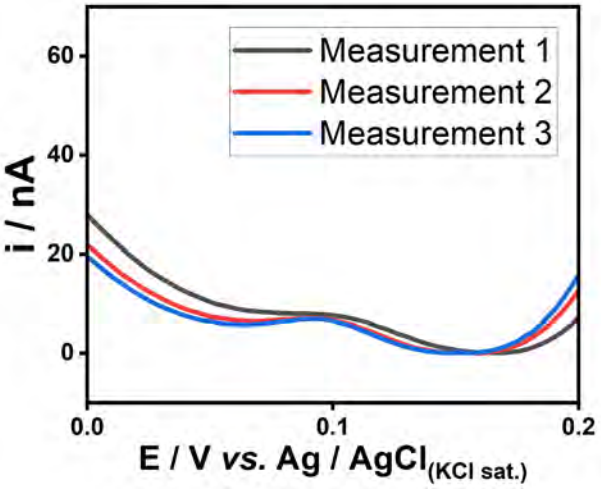

Figure 4S. Consecutive DPVs recorded in acetate buffer (pH 4) solution using an NPG-modified electrode. Between measurements, the sensor was kept in a solution containing AA to examine the memory effect.

Brazilian Journal of Analytical Chemistry
2026, Volume 13, Issue 52, pp 87-101
doi: 10.30744/brjac.2179-3425.AR-45-2025

BrJAC

ARTICLE

Analysis of Benzodiazepines in Urine Samples by Solvent Bar Microextraction using HPLC-UV

Viviana Andrea Morales-Sanchez[1], Wilson Largo-Taborda[1], Eleazar Vargas-Mena[1], Carlos Moreno[2], Milton Rosero-Moreano[1]*

[1]*Grupo de Investigación en Cromatografía y Técnica Afines, Facultad de Ciencias Exactas y Naturales, Universidad de Caldas ROR. Departamento de Caldas, Manizales, P.O. 170001, Colombia*

[2]*Departamento de Química Analítica, Facultad de Ciencias del Mar y Ambientales, Instituto de Investigaciones Marinas (INMAR), Universidad de Cádiz ROR. 11510 Puerto Real, Cádiz, Spain*

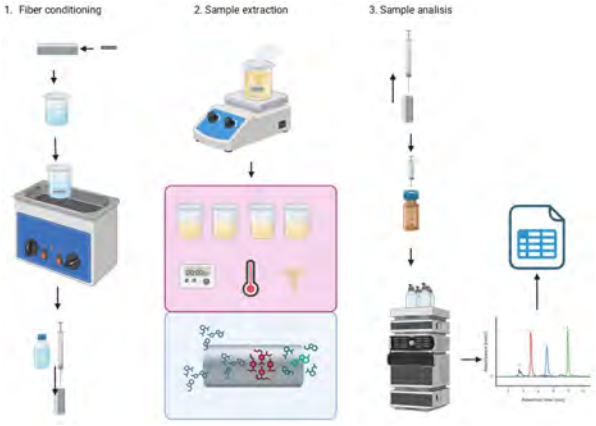

The identification of benzodiazepines (BZDs) in forensic samples has become a significant focus globally due to their increasing abuse in recent years. These compounds are readily assimilated by the body, leading to their increased use not only as over-the-counter medication but also in drug-facilitated sexual assaults. Consequently, this study investigated the behavior of selected BZDs in aqueous and spiked urine samples. Following method validation, real forensic urine samples were analyzed. To achieve this, a hollow fiber solvent bar microextraction (SBME) method was developed and optimized for the analysis of carbamazepine, nitrazepam, temazepam, and diazepam. The methodology involved the evaluation of factors such as microextraction time, temperature, agitation speed, and salt concentration. The optimization of the microextraction method was performed using a one-variable-at-a-time (OVAT) approach with an N + (N-1) design, considering each treatment with its respective replicates and the concentrations of the four standards. The optimal conditions for SBME were determined to be a temperature of 30 °C, a stirring speed of 400 rpm, a microextraction time of 30 min, and a salt concentration of 10% w/v. The analytical method was evaluated for sensitivity, linearity, precision, and accuracy, yielding RSD values below to 5%, in accordance with the guidelines for the validation of analytical methodologies. Finally, the developed method for the analysis of BZDs in urine by HPLC-UV following SBME was validated against more robust methods, including liquid chromatography-mass spectrometry, for final confirmation, demonstrating high performance in tests with forensic samples. The hollow fiber solvent bar microextraction technique allows for rapid analysis with small sample quantities, low costs, high recovery rates (86-96%), low detection (3.9-5.4 ng mL^{-1}) and quantification limits (in the range of 13.0 to 18.0 ng mL^{-1}), more efficient results, and greater eco-efficiency. This provides clear data for consumer protection and aids in clarifying criminal cases.

Cite: Morales-Sanchez, V. A.; Largo-Taborda, W.; Vargas-Mena, E.; Moreno, C.; Rosero-Moreano, M. Analysis of Benzodiazepines in Urine Samples by Solvent Bar Microextraction using HPLC-UV. *Braz. J. Anal. Chem.* 2026, *13* (52), pp 87-101. https://doi.org/10.30744/brjac.2179-3425.AR-45-2025

Submitted: May 30, 2025; **Revised:** September 25, 2025; November 13, 2025; **Accepted:** November 30, 2025; **Published online:** December 20, 2025.

This article is part of the BrJAC Special Issue dedicated to the 21st ENQA and 9th CIAQA.

Keywords: drugs of abuse, solvent bar, benzodiazepines, microextraction, SBME

INTRODUCTION

In the 60s, benzodiazepines (BZDs) began to be used gradually and displaced barbiturates due to their greater safety, therapeutic range, and pharmacological efficiency. Since then, more than 2000 different benzodiazepine-type drugs have been synthesized.[1] They are an essential class of drugs commonly used as minor tranquilizers, hypnotics, muscle relaxants, and anticonvulsants. The usefulness of BZD varies considerably because there are significant differences in the selectivity between these drugs.[2] They are among the drugs most frequently prescribed for the treatment of anxiety, sleep disorders, and status epilepticus.[3]

In addition, BZDs are used in the treatment of alcohol withdrawal, to relieve tension in the preoperative phase, for amphetamine-type drug overdose, and to induce anesthesia in surgical procedures. The over-the-counter use of these drugs is linked to different drug-facilitated sexual assaults (DFSA). It can potentially lead to dependence or adverse events like sudden death, respiratory depression, and coma.[4] Clinical and forensic toxicology laboratories, therefore, frequently receive requests for the determination of BZD in plasma, urine, or gastric fluids.[5] The analysis of BZD in biological fluids is laborious due to the diversity of these commercially available drugs and the fact that each product has a particular therapeutic and toxic range.[6] The concentration can also change due to post-mortem phenomena of redistribution or degradation.[1,7]

Their presence in forensic samples is usually associated with scenarios such as kidnappings, drug-facilitated crimes, recreational use, unintentional abuse associated with over-the-counter or self-administration, and replacement therapy in opioid withdrawal or to clinically treat the adverse effects of psychostimulant drug intoxication (e.g., cocaine overdose).[8] It has been proposed that criminal and violent acts produced under the effects of BZD may be related to low levels of serotonin through GABAergic effects.[9] Due to the partial transformation of BZD in the organism, different chemical adducts or metabolites appear, which leads to the need for updating information for the development of sufficiently sensitive and specific laboratory techniques for the reliable detection of BZDs in biological matrices. Clinical and forensic laboratory methodologies for BZD confirmation include a preliminary confirmation using liquid chromatography with ultraviolet detection (LC-UV), based on the comparison of the retention time and absorbance between a standard and real samples at a given wavelength. Immunoassay techniques such as fluorescent polarization immunoassay (FPIA), enzyme immunoassay (EIA), or multiplied enzyme immunoassay (EMIT) are also used; they are based on a competitive link between enzymatically labeled drugs (antigen) and the drugs in the analyzed matrix by the specific antibodies. The analytical principle is that a negative result indicates that when the drug is not present in the matrix, the antigen binds to the antibody and the substrate cannot bind to the enzyme; in this case, there are no changes in absorbance over time. However, when the drug is present in the analyzed matrix, the antigen is free to interact with the substrate and generates NADH, which absorbs at 340 nm; therefore, the concentration of the drug has a relatively proportional relationship to the absorbance.[10,11] Confirmatory analysis uses two focuses: 1-untargeted and qualitative assays based on structural identification, which regularly use gas chromatography coupled to mass spectrometry GC-MS, and liquid chromatography coupled to tandem mass spectrometry LC-MS/MS in full scan mode. 2-targeted (qualitative or quantitative) assays, which regularly use GC-MS or LC-MS in tandem mass spectrometry setup that uses a triple quadrupole (QqQ) or ion traps as mass filters, and the acquisition mode in selection reaction monitoring (SIM), multiple reaction monitoring (MRM), or target mode. The main goal of confirmatory assays is the univocal structural characterization, based on the match between the retention time, isotope ratio, and mass fragmentation patterns between the sample, drug certified reference standards, and spectral libraries.[8]

The solvent bar microextraction (SBME) was first introduced in 2004 by Jiang and Lee as an improvement on hollow fiber liquid-phase microextraction.[12] In this configuration, the fiber ends are sealed prior to use, allowing the fiber to move freely in contact with the sample during extraction. Its advantages include a simplified procedure, which enhances portability, and improved mass transfer from the sample to the fiber lumen, which reduces extraction times and allows for simultaneous extractions. Since its introduction, it has rapidly gained interest as a promising alternative in sample preparation for both inorganic and organic analysis, with applications in environmental, medical, and food analytical chemistry.[13]

SBME is a sample preparation technique that enables a high rate of mass transfer between phases, resulting in high recovery percentages. It is a rapid enrichment method with low interference, as the hollow fiber acts as a barrier. It can be easily integrated with various chromatographic systems, particularly HPLC, GC, and Capillary Electrophoresis (CE).[14,15]

Due to the different uses of BZD, their commitment to criminal acts in some cases, and in order to contribute to the implementation of modern methods of forensic analysis, it is necessary to develop a rapid, reliable, economical and environmentally friendly extraction method, as the membrane microextraction in solvent bar SBME in doped and forensic samples for the determination of four BZD. Its corresponding comparison with the usual method of analysis in the Legal Medicine laboratories, solid-phase extraction (SPE), will support whether there are significant differences in the recovery percentages between the two methodologies. The hollow membrane microextraction in solvent bar combines sampling, cleaning and enrichment of the sample in a single step, uses small amounts of solvent with a simple, easy, potentially automated sample preparation assembly and sequentially coupled to a separation procedure and detection for the determination of emergent pollutants in raw plastic industrial materials and forensic samples.[13,14]

Given the diverse applications of BZDs, their involvement in criminal activities, and the need to optimize forensic analysis methods, it is crucial to develop extraction techniques that are faster, more reliable, cost-effective, and environmentally friendly. This study aims to evaluate hollow fiber-supported liquid-phase microextraction for the detection of four BZDs in forensic samples, with the potential for use in legal medicine laboratories as a routine practice. The implementation of this methodology will help determine if significant differences exist in recovery rates compared to current techniques and will contribute to the modernization of forensic toxicology analytical processes.[15]

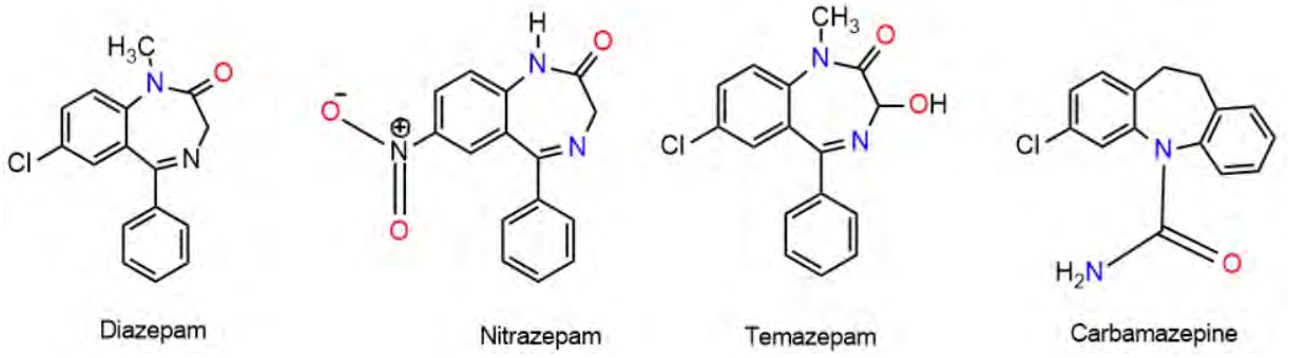

Figure 1. Molecular structure of target BZD.

MATERIALS AND METHODS

To implement the method, BZD standards were used in spiked samples, forensic samples, and the protocol applied for the technique. The method used for SBME-are also presented.

Reagents and solutions

All reagents and standards were acquired from Sigma-Aldrich Company through authorized distributors in Colombia (Quimirel Ltda and Commercial Outsourcing). Standard stock solutions of nitrazepam, carbamazepine, temazepam, and diazepam were prepared separately at a concentration of 1000 ng mL^{-1} in 10 mL of ultrapure Type I water (obtained from a Milli-Q purifier system). From these stock solutions, a 5 mL diluted mixture of the four analytes was prepared at a concentration of 30 ng mL^{-1} for proof-of-concept tests of the SBME procedure. All stock and working solutions were stored at 4 °C.

Sample collection and preparation

This research was approved by the Bioethics Committee of the Facultad de Ciencias Exactas y Naturales, Universidad de Caldas, Manizales, Colombia, where the study was conducted, with approval issued on June 14, 2022. Blank urine samples were obtained from healthy individuals with no prior exposure to medications or BZDs, as confirmed by a survey. The real forensic sample was voluntarily donated by a patient undergoing cancer treatment who had been administered morphine and diazepam intravenously 8 hours before sampling. The samples were hydrolyzed as follows: 500 µL of the forensic sample was mixed with 4450 µL of Type I water and 50 µL of β-glucuronidase. The mixture was incubated at 56 °C for 2.5 hours with gentle shaking. After hydrolysis, the urine pH was adjusted to 9 by adding a tetraborate buffer. The SBME was then performed under the optimized conditions, and the sample was analyzed by HPLC-UV.[4]

Instrumentation

HPLC-UV system

Chromatographic analysis was performed on a Thermo U-Dionex HPLC system equipped with an ultraviolet (UV) detector. An Agilent SB-C18 column (50 mm × 2.1 mm ID, 1.8 µm particle size) was used at 40 °C under isocratic conditions. The mobile phase consisted of a 5 mM KH_2PO_4/K_2HPO_4 buffer solution (pH 6.0), methanol, and diethyl ether (55:40:5 v/v/v) at a flow rate of 0.5 mL min^{-1} (the optimal flow was determined using the Van Deemter curve procedure). UV detection was performed at 245 nm. The analysis time was 5 min, and the injection volume was 20 µL. For corroboration of all results, two robust systems were used.

GC-MS system

An Agilent Technologies 7890A gas chromatograph equipped with a 5975C mass detector was used. The detector temperature was set at 250 °C. The column was an Rtx®-5 (30 m × 250 µm × 0.25 µm ID). The oven temperature program was as follows: initial temperature of 80 °C held for 3 min, then increased by 15 °C per minute to 200 °C, held for 5.33 min, then increased by 10 °C per minute to 300 °C, and maintained for 12 min. The total run time was 38.33 min. The injector temperature was 270 °C, operating in pulsed splitless mode at 20 PSI. The injection volume was 1 µL. The carrier gas was helium (99.999% purity).[16,17]

LC-MS system

Corroborative analysis of forensic samples was performed by HPLC-MS/MS on an Agilent Technologies 1120 liquid chromatograph coupled in tandem with a quadrupole filter and a 6200 series time-of-flight mass spectrometer. Analyte separation was carried out on a Zorbax Eclipse Plus C18 column (2.1 mm ID × 100 mm, 1.8 µm particle size), using 5 mM ammonium formate in 0.01% formic acid (A) and chromatography-grade acetonitrile (B) as mobile phases. The general source settings for positive electrospray ionization (ESI) were: capillary voltage, 3500 V; ion transfer tube temperature, 320 °C; and vaporizer temperature, 350 °C. The flow rate was 0.4 mL min^{-1}, the injection volume was 20 µL, and the scanned mass range was 80–1000 AMU. Data was analyzed using Agilent MassHunter Qualitative software with a lab-developed method for deconvolution and identification using dynamic combinatorial libraries (PDCL).

Calibration curve

To quantify the amount of BZD, a calibration curve was made with an external standard, in which the concentration versus the peak area of each of the standards worked was related. For nine concentration levels, three replications were made, for a total of 27 data points to estimate the relationship between concentration and area. A simple linear regression was performed by the least squares method, and the assumptions of normality, independence and homoscedasticity were verified for the four analytes studied. After verifying the assumptions of the model, the variance analysis of the regression was performed. This analysis was made taking into account all the replicates by concentration level and not by the average of each level, in order to a better adjustment of the model to the real situation according to the data shown in Figure 2.

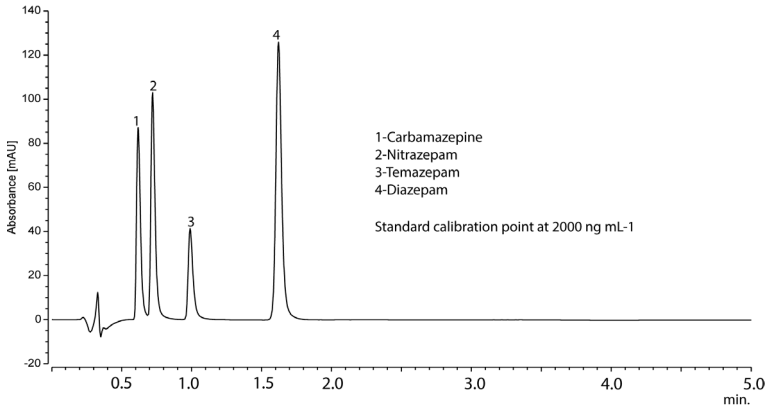

Figure 2. Chromatogram of the calibration curve. 1: carbamazepine (0.610 min), 2: nitrazepam (0.708 min), 3: temazepam (0.973) and 4: diazepam(1.598 min).

Solvent bar microextraction (SBME) procedure

Polypropylene Accurel PP S6/2 hollow fibers (Membrana, Wuppertal, Germany) were used as the support for the SBME experiments. The fibers had an inner diameter of 1,800 µm, a wall thickness of 450 µm, an average pore size of 0.2 µm, and a porosity of 72%. For each experiment, a 25 mm segment of the fiber was used. A metal pin was inserted into the fiber to allow it to be used as a magnetic stirrer. The SBME device was prepared by adding 30 µL of 1-octanol into the fiber lumen. The fiber was then immersed in 1-octanol to fill the pores and improve analyte transfer (two-phase mode). Both ends of the fiber were mechanically sealed to ensure that mass transfer occurred only through the membrane pores. The prepared SBME device was then introduced into a 5 mL vial containing the urine sample for extraction. Filtration of the matrix was not necessary, as this is facilitated by the membrane.

Optimization of SBME

The optimization of the SBME system was performed using a one-variable-at-a-time method[18] to study the effects of extraction temperature, stirring speed, extraction time, and the salting-out effect. An experimental design based on N + (N-1) was used, with four control variables, each at three levels. This design resulted in a maximum of nine experiments, which were conducted with a minimum of three repetitions for the four BZDs to establish the optimal operating conditions for the SBME system, as shown in Table I. The study was conducted using a One-Variable-at-a-Time (OVAT) approach to optimize the main factors affecting the response. For each factor investigated (e.g., temperature, time, stirring speed), a series of experiments was conducted where the level of that single factor was varied while all other factors were held constant at a baseline level. Each specific experimental condition (i.e., each level) was performed in triplicate (n=3) to ensure the reproducibility of the results and to calculate the mean and standard deviation for that point (see the errors bar in the Figures 4A-D).

Table I. Desing of Experiments N+(N-1)

Assay	Extraction temperature (°C)			Stirring speed (rpm)			Extraction time (min)			Salting out effect (w/v)		
Number	**10**	**20**	**30**	**400**	**700**	**1000**	**10**	**20**	**30**	**10**	**15**	**20**
1	+				+				+	+		
2		+			+				+	+		
3			+		+				+	+		

(continued on next page)

Table I. Desing of Experiments N+(N-1) (continued)

Assay	Extraction temperature (ºC)			Stirring speed (rpm)			Extraction time (min)			Salting out effect (w/v)		
Number	**10**	**20**	**30**	**400**	**700**	**1000**	**10**	**20**	**30**	**10**	**15**	**20**
4			+	+					+	+		
5			+			+			+	+		
6			+		+		+			+		
7			+		+			+		+		
8			+		+				+		+	
9			+		+				+			+

The levels for each factor were selected based on a combination of preliminary screening experiments and established findings in the relevant literatura.[19] The goal was to select a range that was known to be effective and relevant for this type of analysis.

While the levels were not always perfectly equidistant, they were chosen to adequately explore the operational range and identify the optimal working conditions. For example, if preliminary tests showed a sharp change between two points, we selected levels closer together in that region to better define the peak of the response curve. The term “9 experiments” referred to the total number of conditions tested for four factors (N-1) less 1 why one of them always keep constant with three levels each one ($3 \times (4 - 1) = 9$ conditions), with each condition being replicated three times.

SBME procedure

Unlike other modalities, both ends of the fiber are mechanically or thermally sealed after introducing the metal pin and the extraction solvent into the lumen, immobilizing the latter within the pores of the hollow membrane. Finally, the solvent bar is inserted into the sample, and once the extraction is complete, one end is opened to recover the acceptor phase.[6]

The complete procedure consists of cutting the membrane and the metal pin, then conditioning the membrane with acetone. After this, the lumen (hollow space) is filled with the appropriate solvent, and both ends are sealed using mechanical pressure. Next, the hollow fiber is functionalized as a magnetic stirrer by inserting a metal pin inside. The SBME system is then placed inside the doped sample container. After extraction, the SBME system is removed by cutting one end of the membrane, recovering the extract using a 30 µL Hamilton syringe. Finally, 30 µL of the extract is injected into the liquid chromatograph with the mobile phase,[7] as shown in Figure 3.

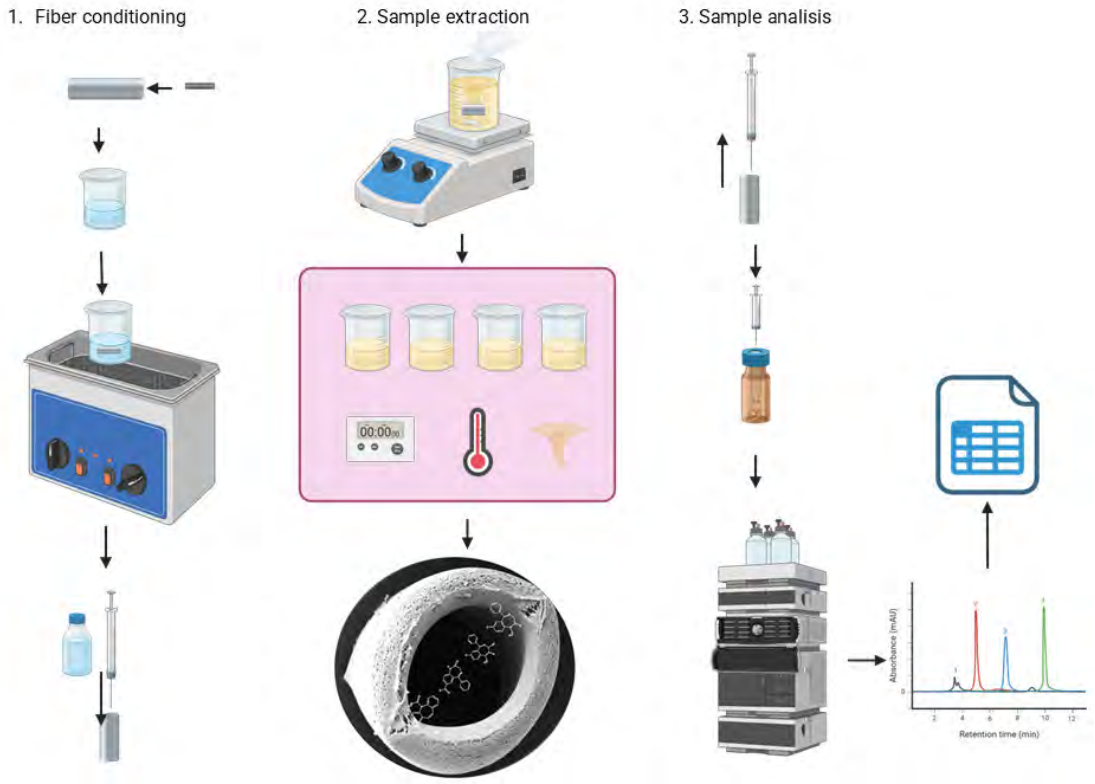

Figure 3. Flow diagram of the developed Solvent Bar Microextraction (SBME) system.

Calibration and statistical analysis

To quantify the BZDs, an external standard calibration curve was constructed by plotting concentration versus peak area for each of the four analytes. Nine concentration levels were prepared, with three replications for each, for a total of 27 data points. A simple linear regression was performed using the least squares method. The assumptions of normality (Shapiro-Wilks test), independence (Durbin-Watson test), and homoscedasticity (Bartlett's test) were verified for the four analytes under study. After verifying the model's assumptions, an analysis of variance (ANOVA) of the regression was performed. This analysis was conducted using all replicates for each concentration level, rather than the average of each level, to ensure a better fit of the model to the real data, as shown in Figure 2.

The SBME calibration curve was constructed using the four standards: carbamazepine, temazepam, nitrazepam, and diazepam. Spiked samples were prepared at six concentration levels: 100, 300, 500, 700, 900, and 1100 ng mL^{-1}, corresponding to typical concentrations found in the working matrix. Each sample was treated using the SBME procedure described above. Data analysis was conducted using SPSS and Statgraphics Centurion XI in demo mode.

RESULTS AND DISCUSSION

In this section, the setup and validation of the chromatographic methods used to quantify the analytes under study are presented, as well as the optimization of sample preparation methods with experiments, showing critical variables, as well as the best conditions for SPE with their recovery percentages. Also, the conditions for SBME are described, including the effect of microextraction speed, temperature, time, and the addition of NaCl, with their respective recovery percentages for both spiked and forensic samples. An analysis is performed using GC-MS and a corroboration of the case study by LC-MS/MS, demonstrating the reliability of the developed method.

Chromatographic method validation and analyte identification

Reversed-phase HPLC was chosen for the identification of the standards and analytes under study. The validation method involved the analysis of two blanks, two points from the calibration curve (200 ng mL^{-1} and 1100 ng mL^{-1}), a urine sample spiked with 1000 ng mL^{-1}, and an unspiked sample. Finally, the validation curve was analyzed. All analyses were performed in duplicate over five days to ensure thorough verification of the validation method.

The optimal separation conditions were established by alternating injections (20 µL) of standard, spiked, and unspiked samples, using an Agilent ZORBAX RRHD SB-C18 column (50 mm × 2.1 mm ID, 1.8 µm particle size). To determine the optimal mobile phase, tests were conducted based on previous work that performed chromatographic runs in isocratic mode at a flow rate of 0.5 mL min^{-1}. The optimal wavelength for analyte detection was determined by performing a spectral scan of the standard from 190 nm to 400 nm, which revealed the highest signal intensity at 254 nm. This is consistent with bibliographic references for BZD analysis. The optimal flow rate for chromatographic separation was determined using the Van Deemter curve, which shows the relationship between the linear velocity (u) of the mobile phase and the height equivalent to a theoretical plate (HETP). This curve was generated by injecting the four standards at flow rates ranging from 0.2 mL min^{-1} to 1.0 mL min^{-1}, using the optimal mobile phase described above. The lowest HETP (0.0025 mm) was obtained at a flow velocity of 0.05 cm s^{-1}, which corresponds to a flow rate of 0.5 mL min^{-1}. Therefore, this flow rate was determined to be optimal for the analysis of standards and samples.

Optimization of SBME conditions

To apply the SBME technique to the analysis of real samples, several variables were optimized. The pH of the samples was adjusted to and maintained at 7.0 prior to extraction. This pH was strategically chosen because the target analytes (carbamazepine, diazepam, temazepam, and nitrazepam) are all weak bases with p*K*a values significantly different from this pH. At a neutral pH, these compounds exist predominantly in their un-ionized, most hydrophobic form, which is essential for achieving maximum and reproducible extraction efficiency. These variables are discussed below.

Effect of extraction temperature

Temperature is a critical parameter in microextraction as it influences both the transfer rate and the partition coefficients of the analytes by affecting the kinetics and thermodynamics of the analyte adsorption process. The effect of temperature was evaluated at 10 °C, 20 °C, and 30 °C (see Table I and Figure 4A).

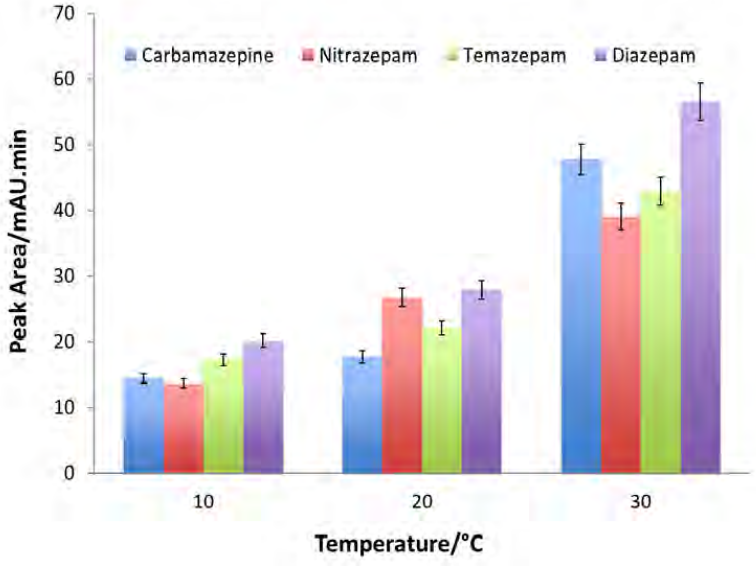

Figure 4A. Efect of extraction temperature.

It was observed that an increase in temperature enhances the microextraction of analytes, although some compounds are extracted at a higher rate. In general, the partition coefficient of some analytes can be improved with increasing temperature, and no significant increases were observed at 10 °C. Therefore, the optimal temperature was determined to be 30 °C.[14]

Effect of stirring speed

In the SBME system, stirring increases the transfer of analytes from the donor phase to the acceptor phase by reducing the thickness of the Nernst diffusion film. However, a very high stirring speed can cause significant loss of the extraction solvent or the formation of air bubbles in the pores of the SBME, which would prevent phase exchange. This is a limiting factor for the extraction. Stirring speeds of 400, 700, and 1000 rpm were evaluated (see Table I and Figure 4B). The best extraction results were obtained at 400 rpm, as significant losses of the organic solvent occurred at 700 and 1000 rpm.[19,20]

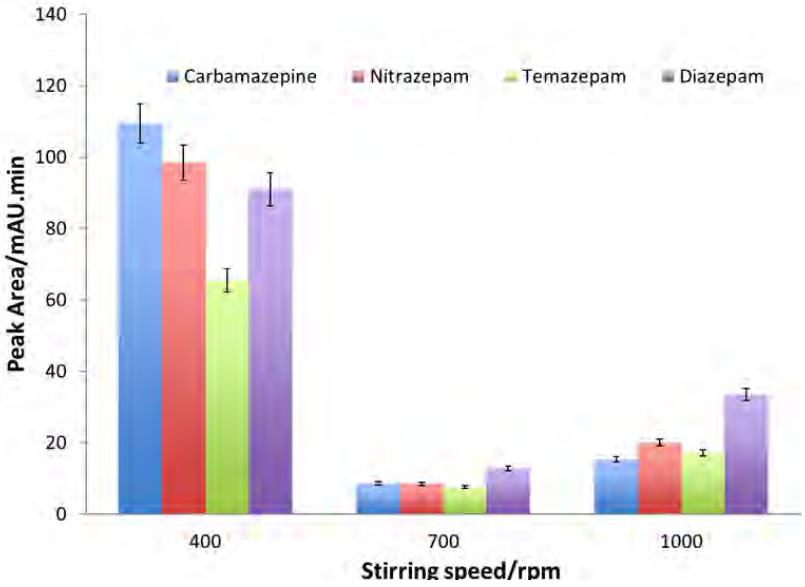

Figure 4B. Effect of stirring speed.

Effect of extraction time

The goal is to achieve system distribution equilibrium in the shortest possible time to extract the maximum amount of analyte. Extending the extraction time beyond equilibrium is futile, as the microextraction rate becomes constant and may even lead to loss of the organic solvent. The extraction time was evaluated at 10, 20, and 30 min (see Table I and Figure 4C). At an extraction temperature of 30 °C and a stirring speed of 400 rpm, the extraction rate increased up to approximately 30 minutes. Longer extraction times did not result in substantial improvements and could cause solvent loss, especially with this new type of hollow fiber arrangement.[21]

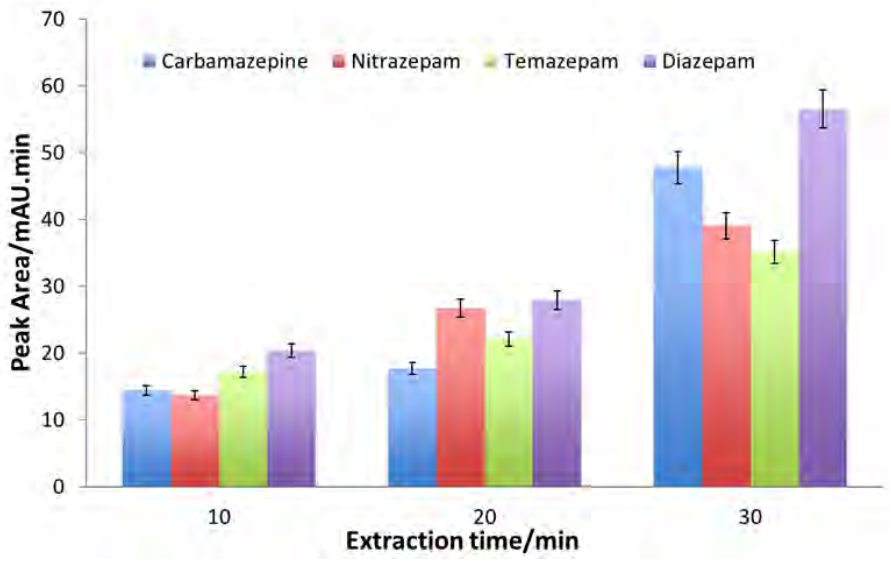

Figure 4C. Effect of extraction time.

Effect of NaCl addition

The ionic strength of the sample is a crucial parameter in any microextraction system, as it can significantly enhance the concentration of analytes. The effect of salt addition was evaluated at concentrations of 1%, 5%, and 10% NaCl (see Table I and Figure 4D). It was observed that increasing the ionic strength improves the solubility of the analyte in the organic phase. However, higher salt concentrations increase the viscosity of the solution and reduce mass transfer. Therefore, 10% NaCl was selected as the optimal concentration.[22]

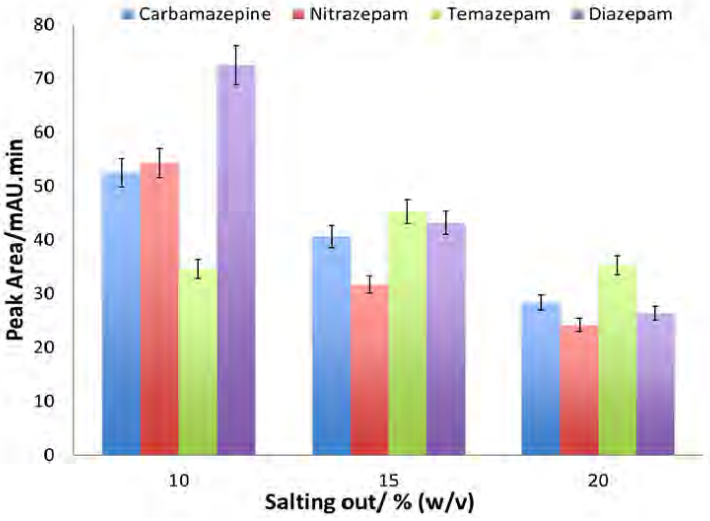

Figure 4D. Effect of salting out.

As shown, nine experiments were conducted with three levels and four control variables. Each experiment was replicated three times to determine the highest recovery percentage. Recovery percentages above 80% were obtained in experiment number 4 (see Table II), which had the following optimal conditions: 30 °C, 400 rpm, 30 minutes of stirring, and a 10% salt concentration.[23]

Table II summarizes the equations applied to calculate the validation parameters, namely the limit of detection (LOD), limit of quantification (LOQ), calibration features (slope, intercept and determination coefficient), accuracy, precision and enrichment factor (EF). The calculated values for carbamazepine, nitrazepam, temazepam, and diazepam were derived from the regression model parameters (intercept, slope, and their standard deviations). These results demonstrate the accuracy and sensitivity of the calibration model for each analyte.[24]

Table II. Calibration, sensitivity, accuracy, precision and preconcentration features

Analyte	Intercept	Slope	R^2	LOD ng mL^{-1}	LOQ ng mL^{-1}	Recovery %	RSD %	EF
Carbamazepine	0.0336	0.0013	0.9997	5.4	17.8	93.3	9.9	156
Nitrazepam	0.0494	0.0017	0.9992	4.0	13.2	85.9	9.7	143
Temazepam	0.0219	0.0008	0.9991	4.2	13.9	90.9	12.0	152
Diazepam	0.1103	0.0030	0.9994	3.9	12.9	95.9	15.9	160

Analysis of spiked and real samples by SBME

After optimizing the parameters of this novel microextraction technique, it was applied to real samples, yielding high performance (recoveries >85%) for both forensic and spiked sample analysis. This method allowed for the detection of these compounds using a simple, fast, robust, and cost-effective technique compared to the conventional SPE methods currently used in all Colombian forensic laboratories.

A standard mixed solution at 1000 ng mL^{-1} was injected as a reference to determine the recovery percentages for each microextraction. Subsequently, a 6 ng mL^{-1} standard solution mixture was prepared, considering that the membrane has a concentration factor of 167 (50 mL/0.03 mL). Therefore, the final concentration after extraction should be approximately 1000 ng mL^{-1} (167 × 6 ng mL^{-1}). Three beakers were prepared, each containing 5 mL of the 6 ng mL^{-1} standard solution mixture. Additionally, 0.5 g of NaCl was added to each beaker to enhance extraction (10% w/v). A direct injection of the 1000 ng mL^{-1} standard mixture was performed to calculate the recovery percentage for the microextracted samples.

Analysis of forensic samples

An analysis was performed on forensic urine samples containing the following substances: 1) Diazepam-Morphine FAB1; 2) Diazepam-Morphine FAB2; and 3) Interlaboratory Diazepam 20 µg mL^{-1}. The samples were first hydrolyzed and then extracted using SBME. A calibration curve was prepared using hydrolyzed spiked samples at six concentration points: 100, 300, 500, 700, 900, and 1100 ng mL^{-1}.

Chromatographic runs of forensic urine samples containing diazepam were performed to confirm the mass spectra of the peak eluting at the retention time of diazepam. Figures 5 and 6 show the chromatogram and mass spectrum of a sample, where the molecular ion (*m/z* 284), the base peak (*m/z* 256), and characteristic ions (*m/z* 242 and 165) are observed. To determine the sample concentrations, the area results were interpolated on the calibration curve. The calculated concentrations of the forensic samples are shown in Table III.

Table III. Concentration of Forensic Diazepam Samples in (Urine) Microextracted and Hydrolyzed

Forensic urine samples	Peak areas (mAU)	Interpolated value x	Concentration (µg mL^{-1})
ME-ILAB 1	0.419	2005.62	17.19
ME-FAB 13	0.213	718.125	6.15

(continued on next page)

Table III. Concentration of Forensic Diazepam Samples in (Urine) Microextracted and Hydrolyzed (continued)

Forensic urine samples	Peak areas (mAU)	Interpolated value x	Concentration (μg mL^{-1})
ME-FAB 21	0.122	149.375	1.28
ME-FAB 22	0.226	799.375	6.85

ILAB means Interlaboratoryal sample, and FAB means Forensic Analysis Batch; both correspond to an internal identification laboratory code for anonymized samples.

According to Table III, the calculated diazepam concentration for the interlaboratory sample using the developed SBME method is close to the certified concentration value (20 μg mL^{-1}), which demonstrates the good recovery performance of the method. The diazepam concentration values for the samples from the oncology patient show good precision, with the exception of sample FAB 21.

Confirmation analysis by GC-MS and LC-MS

To confirm the presence of diazepam in the forensic samples, they were injected into a GC-MS system. The SBME method was applied under the previously optimized conditions, and four trials were conducted. A diluted reference mixture solution (1000 ng mL^{-1}) was used to determine the recovery percentage. The SBME method was performed on urine samples diluted to 6 ng mL^{-1}, considering the theoretical concentration factor of 167. The results were then compared with a 1000 ng mL^{-1} diluted mixture solution of the four standards, yielding the recovery percentages shown in Table IV. The analysis of the forensic urine samples by GC-MS showed a peak with a retention time of 22.3 minutes, which corresponds to the signal of diazepam.

Table IV. Recovery Percentage of Urine Samples Microextracted by SBME GC-MS

BDZ	Diazepam MIX area 1000 ng mL^{-1}	Retention time (min)	Microextracted area (mAU)	Recovery (%)
DIAZEPAM 1	5168198	22.3	4562589	88
DIAZEPAM 2		22.3	4632300	90
DIAZEPAM 3		22.3	3898610	75
DIAZEPAM 4		22.3	3953481	76

To further confirm the presence of diazepam, sample injections were performed using an LC-QTOF system. The identification of diazepam by LC-MS/MS showed a signal for this analyte with a retention time of 6.04 minutes (Figure 5).[8]

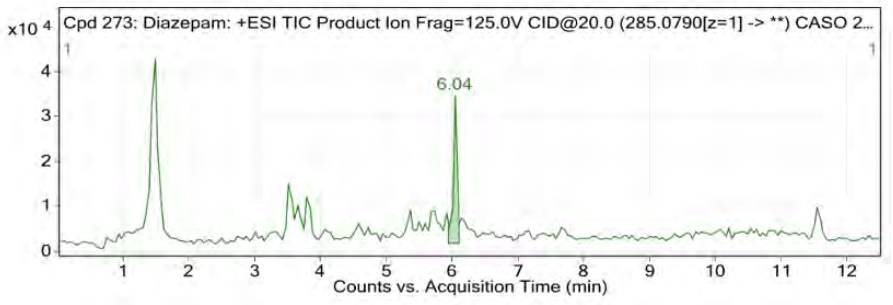

Figure 5. Chromatogram of Diazepam by LC-MS.

The mass spectrum of the diazepam molecule was obtained (Figure 6), confirming that the fragments correspond to the analyte of interest. These analyses confirm that the developed methodology is appropriate for the identification of diazepam, as it allows for differentiation between the analyte and other matrix compounds. Therefore, this method is reliable for use in future studies. The mass spectra of classic drugs and BZD monitored in the study, corresponding to central nervous system depressants and stimulants, which could have been consumed together with benzodiazepine-type drugs, are displayed in the Supplementary Material.

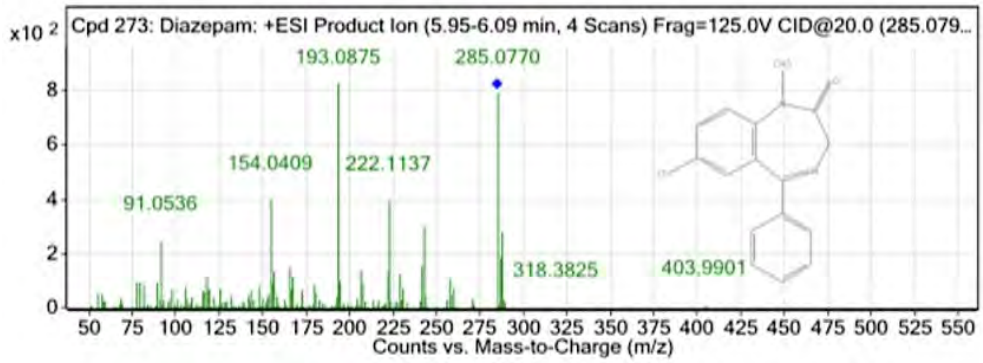

Figure 6. Mass spectrum of diazepam obtained by LC-MS.

In today's society, the analysis of BZD has gained great importance, making analytical testing increasingly significant. This is the case for the hollow fiber solvent bar microextraction technique, which allows for rapid analysis with small sample quantities, low costs, high recovery rates, low detection and quantification limits, more efficient results, and greater eco-efficiency compared to conventional techniques such as solid-phase extraction, which require longer response times. This provides clear limits for consumers or aids in clarifying criminal cases.[9]

For the identification of BZD, a robust technique such as high-performance liquid chromatography with ultraviolet detection (HPLC-UV) is used,[25] and it is further confirmed with even more robust techniques such as gas chromatography-mass spectrometry (GC-MS) and liquid chromatography-tandem mass spectrometry (LC-MS).[25] The extracted ion chromatogram for diazepam is shown in Figures 5-6, while the chromatograms for all other analytes can be found in the Supplementary Information (Figure SI-02).

CONCLUSIONS

The implementation of hollow fiber solvent bar microextraction (SBME) represents a significant advancement in the detection of BZDs in forensic samples. This method improves recovery rates and reduces interference, making it a viable alternative to more costly and labor-intensive sample preparation methods, such as solid-phase extraction (SPE). The ease of integration of SBME with chromatographic techniques like HPLC and GC-MS makes it a promising option for routine analysis in forensic toxicology laboratories.

SBME offers a more cost-effective, environmentally friendly, and accessible alternative to conventional extraction methods. This advancement has great potential in forensic toxicology, as it can facilitate the detection of compounds in biological matrices with greater speed and accuracy, thereby reducing the time and costs associated with forensic analyses.

The continuous evolution of detection and analytical techniques is essential to keep pace with the development of new BZDs and their derivatives. Research into the improvement of analytical methods, including microextraction and advanced chromatography techniques, plays a crucial role in forensic investigations and contributes to a more efficient and accurate approach to the analysis of controlled substances in biological samples.

Finally, in a great effort to understand better the intearactions between the key variables in the extraction processs, the follow-up study using a response surface methodology (RSM) or a full factorial design would be the logical next step to build a comprehensive statistical model.

Conflicts of interest

The authors don´t have any conflicts of interest

Acknowledgements

The authors M. Rosero-Moreano and V. Morales are grateful to the “Vicerrectoría de Investigaciones y Posgrados" of the University of Caldas for the financial support on the project code 0340920. V. Morales thanks to Colombian MinCiencias and the SGR Science, Technology, and Innovation Fund for supporting her doctoral studies through project BPIN 2021000100028. C. Moreno acknowledges the financial support from the Spanish Ministry of Economy and Competitiveness (Project PID2021-128642OB-I00 and Network RED2022-134079-T).

REFERENCES

(1) Melo, P.; Bastos, M. L.; Teixeira, H. M. Benzodiazepine stability in postmortem samples stored at different temperatures. *J. Anal. Toxicol.* **2012,** *36* (4), 52–60. https://doi.org/10.1093/jat/bkr008

(2) Nicholls, J.; Masterton, W.; Falzon, D.; McAuley, A.; Carver, H.; Skivington, K.; Dumbrell, J.; Perkins, A.; Steele, S.; Trayner K. Parkes, T. The implementation of safer drug consumption facilities in Scotland: a mixed methods needs assessment and feasibility study for the city of Edinburgh. *Harm. Reduct. J.* **2025,** *22* (6), 231-234. https://doi.org/10.1186/s12954-024-01144-1

(3) Carfora, A.; Campobasso, C. P.; Cassandro, P.; Petrella, R. Borriello, R. Long-Term Detection in Hair of Zolpidem, Oxazepam and Flunitrazepam in a Case of Drug-Facilitated Sexual Assault. *J. Anal. Toxicol.* **2022**, *46*, E16–E20. https://doi.org/10.1093/jat/bkaa174

(4) Kinani, S.; Bouchonnet, S.; Milan, N.; Ricordel, I. A sensitive and selective method for the detection of diazepam and its main metabolites in urine by gas chromatography-tandem mass spectrometry. *J. Chromatogr. A* **2007***, 1141* (1), 131–137. https://doi.org/10.1016/j.chroma.2006.12.008

(5) Andruch, V.; Kalyniukova, A.; Yordanova, T.; Płotka-Wasylka, J.; Vojteková, V.; Zengin, G. Microextraction by packed sorbent: Uncommon detection techniques, sorbents, samples and analytes. *TrAC, Trends Anal. Chem.* **2024**, *176*, 117769. https://doi.org/10.1016/j.trac.2024.117769

(6) Borges, K. B.; Freire, E. F.; Martins, I.; de Siqueira, M. E. P. B. Simultaneous determination of multibenzodiazepines by HPLC/UV: Investigation of liquid-liquid and solid-phase extractions in human plasma. *Talanta* **2009**, *78*, 233–241. https://doi.org/10.1016/j.talanta.2008.11.003

(7) Liu, F.; Zhang, Y.; Wang, J. Ji; J. Rapid detection of 10 benzodiazepines and metabolites in blood and urine using DART-MS/MS. *Drug Test. Anal.* **2024**, *16*, 817–826. https://doi.org/10.1002/dta.3576

(8) Shanks, K. G.; Kurtz, S. A. K.; Behonick, G. S. Detection of the benzodiazepine bromazolam by liquid chromatography with quadrupole time of flight mass spectrometry in postmortem toxicology casework and prevalence in Indiana (2023). *J. Anal. Toxicol.* **2024,** *48*, 582–590. https://doi.org/10.1093/jat/bkae053

(9) Karden, A.; Fragner, T.; Feichtinger, C.; Strizek, J.; McDermott, D. T.; Grabovac, I. Utilization of drug checking services in Austria: a cross-sectional online survey. *Harm. Reduct. J.* **2025**, *22*. https://doi.org/10.1186/s12954-025-01168-1

(10) Melanson, S. E. The Utility of Immunoassays for Urine Drug Testing. *Clin. Lab. Med*. **2012**, *32* (3), 429-47. https://doi.org/10.1016/j.cll.2012.06.004

(11) Bertol, E.; Vaianoa, F.; Furlanetto, S.; Mari, F. Cross-reactivities and structure–reactivity relationships of six benzodiazepines to EMIT® immunoassay. *J. Pharm. Biomed. Anal.* **2013**, *84*, 168-172. http://dx.doi.org/10.1016/j.jpba.2013.05.026

(12) Jiang, X.; Lee, H. K. Solvent bar microextraction. *Anal. Chem.* **2004**, *76* (18), 5591–5596. https://doi.org/10.1021/ac040069f

(13) López-López, J. A.; Mendiguchía, C.; Pinto, J. J.; Moreno, C. Application of solvent-bar microextraction for the determination of organic and inorganic compounds. *TrAC, Trends Anal. Chem.* **2019**, *110* (5), 57–65. https://doi.org/10.1016/j.trac.2018.10.034
(14) Rosero-Moreano, M.; Canellas, E.; Nerín, C. Three-phase hollow-fiber liquid-phase microextraction combined with HPLC-UV for the determination of isothiazolinone biocides in adhesives used for food packaging materials. *J. Sep. Sci.* **2014**, *37*, 272–280. https://doi.org/10.1002/jssc.201300840
(15) Ebrahimzadeh, H.; Mirbabaei, F.; Asgharinezhad, A. A.; Shekari, N.; Mollazadeh, N. Optimization of solvent bar microextraction combined with gas chromatography for preconcentration and determination of methadone in human urine and plasma samples. *J. Chromatogr. B* **2014**, *947–948*, 75–82. https://doi.org/10.1016/j.jchromb.2013.12.011
(16) Saito, K.; Kikuchi, Y.; Saito, R. Solid-phase dispersive extraction method for analysis of benzodiazepine drugs in serum and urine samples. *J. Pharm. Biomed. Anal.* **2014**, *100*, 28–32. https://doi.org/10.1016/j.jpba.2014.07.020
(17) Gautam, L.; Sharratt, S. D.; Cole, M. D. Drug facilitated sexual assault: Detection and stability of benzodiazepines in spiked drinks using gas chromatography-mass spectrometry. *Plos One* **2014**, *9* (2), e89031. https://doi.org/10.1371/journal.pone.0089031
(18) Sun, T.-T. Excessive trust in authorities and its influence on experimental design. *Nat. Rev. Mol. Cell Biol.* **2004**, *5*, 577–581. https://doi.org/10.1038/nrm1429
(19) Correa, L.; Fiscal, J.; Ceballos, S.; de la Ossa, A.; Taborda, G.; Nerin, C.; Rosero-Moreano, M. Hollow-fiber solvent bar microextraction with gas chromatography and electron capture detection determination of disinfection byproducts in water samples. *J. Sep. Sci.* **2015**, *38*, 3945–3953. https://doi.org/10.1002/jssc.201500324
(20) Ladino, J. A. F.; Chacón, S. L. C.; Loaiza, S. C.; Salcedo, A. O.; Ocampo, G. T.; Nerin, C.; Rosero-Moreano, M. Development of a new liquid phase microextraction method with hollow fiber HF-SBME for the analysis of the organochlorine compounds in water samples by GC-ECD. *Scientia Chromatographica* **2014,** *6* (4), 241–250.
(21) Rosero-Moreano, M.; Aguirre, M.; Pezo, D.; Taborda, G.; Dussán, C.; Nerin, C. Solventless Microextraction Techniques for Determination of Trihalomethanes by Gas Chromatography in Drinking Water. *Water, Air, Soil Pollut.* **2012***, 223*, 667–678. https://doi.org/10.1007/s11270-011-0891-9
(22) Obando, M.; Cárdenas, V.; Casanova, H.; Montaño, D.; Giraldo, L. F.; Cardona, W.; Rosero-Moreano, M. Arcillas naturales funcionalizadas con líquidos iónicos para micro-extracción de ocratoxina A por membrana hueca empacada. *Scientia Chromatographica* **2016**, *8* (2), 129-136.
(23) Vergel, C.; Guerrero, E. J.; Mendiguchía, C.; Moreno, C. Determination of Organochloride and Triazine Pesticides in Natural Waters by Solvent Bar Microextraction. *Anal. Lett.* **2014**, *47* (5), 2209–2220. https://doi.org/10.1080/00032719.2014.902462
(24) Laloup, M.; Fernandez, M. M. R.; De Boeck, G.; Wood, M.; Maes, V.; Samyn, N. Validation of a liquid chromatography-tandem mass spectrometry method for the simultaneous determination of 26 benzodiazepines and metabolites, zolpidem and zopiclone, in blood, urine, and hair. *J. Anal. Toxicol.* **2025**, *29* (7), 616–626. https://doi.org/10.1093/jat/29.7.616
(25) Mena, E. V.; Giraldo, E. R. H.; Castaño, J. A. G. Insights into the Silylation of Benzodiazepines Using N,O-Bis(trimethylsilyl)trifluoroacetamide (BSTFA): In Search of Optimal Conditions for Forensic Analysis by GC-MS. *Molecules* **2024**, *29* (24), 5884. https://doi.org/10.3390/molecules29245884

SUPPLEMENTARY MATERIAL

The Supplementary Material of this article is available at **https://doi.org/10.30744/brjac.2179-3425.AR-45-2025-SM**

Brazilian Journal of Analytical Chemistry
2026, Volume 13, Issue 52, pp 102-118
doi: 10.30744/brjac.2179-3425.AR-61-2025

BrJAC

ARTICLE

Hibiscus sabdariffa calyces: Evaluation of use in a Magnetic Solid Phase Extraction System for Cobalt Ions Preconcentration

Ana Alice Silva, Eduarda Garcia Santana, Weida Rodrigues Silva*, Amanda das Graças Barbosa, James Michael Silva, Vanessa Nunes Alves

Instituto de Química, Universidade Federal de Catalão, Catalão, GO, 75704-020, Brazil

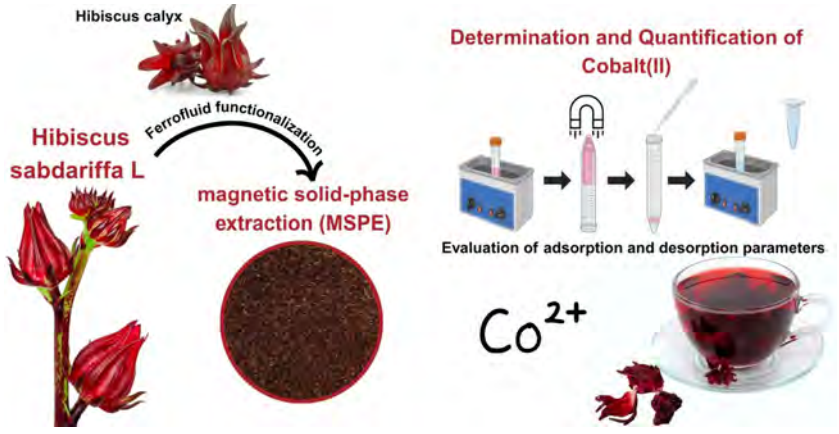

Cobalt (Co) is an industrially important metal, and its determination at low concentrations is essential due to its biological and toxicological relevance, requiring sensitive analytical methods, often involving preconcentration steps. The magnetic solid phase extraction (MSPE) becomes an efficient and sustainable alternative. In this study, a method based on MSPE was developed for the extraction and preconcentration of cobalt ions in aqueous systems, with determination by flame atomic absorption spectrometry, using the calyces of the *Hibiscus sabdariffa* flower, after a magnetization process. The material was prepared by washing and magnetization with iron oxide nanoparticles. Energy dispersive X-ray fluorescence (EDXRF) characterization confirmed the high incorporation of iron (≈88%), and X-ray diffraction (XRD) indicated the presence of magnetite/hematite. The pH at the point of zero charge (pH_{PZC}) increased from 2.0 (natural hibiscus) to 3.0 (magnetized). The percentage of Co(II) adsorption was significantly higher for the magnetized material at pH 7 and 8 (≈57–58% of extraction). The MSPE conditions were optimized using factorial design and Doehlert matrix, defining the adsorbent mass (≈51 mg), contact time (≈7.5 min), and eluent (0.1 mol L^{-1} HCl). The developed method showed a linear range of 0.440–10.0 mg L^{-1} (r = 0.990), with a detection and quantification limit of 0.132 mg L^{-1} and 0.440 mg L^{-1}, respectively. Recovery tests in aqueous samples (coconut water, swimming pool water, tap water, calcium-rich hard water, and *cachaça*—a Brazilian spirit distilled from sugarcane juice) showed variable recoveries (47.3% to 118%), indicating that accuracy is matrix-dependent, with challenges observed in complex samples (calcium-rich hard water and cachaça). The proposed method, using a low-cost, natural, and magnetized adsorbent, shows potential for the determination of Co(II), particularly in simpler matrices, aligning with the principles of green analytical chemistry.

Cite: Silva, A. A.; Santana, E. G.; Silva, W. R.; Barbosa, A. G.; Silva, J. M.; Alves, V. N. *Hibiscus sabdariffa* calyxes: Evaluation of use in a Magnetic Solid Phase Extraction System for Cobalt Ions Preconcentration. *Braz. J. Anal. Chem.* 2026, *13* (52), pp 102-118. https://doi.org/10.30744/brjac.2179-3425.AR-61-2025

Submitted: July 15, 2025; **Revised:** January 13, 2026; March 3, 2026; **Accepted:** April 22, 2026; **Published online:** May 18, 2026.

This article is part of the BrJAC Special Issue dedicated to the 21st ENQA and 9th CIAQA.

Keywords: adsorption, cobalt, hibiscus, magnetic solid phase microextraction, preconcentration

INTRODUCTION

Cobalt (Co) is a metal of great industrial importance, used in the manufacture of alloys, batteries, pigments in make-up and hair dye, cosmetic products, antimicrobial agents and catalysts for the oil industry.[1–3] However, Co is recognized as a skin allergen and is one of the main causes of allergic contact dermatitis.[4,5] In the environment, the most common form of Co present in soil is the Co^{2+} ion, although Co^{3+} can also be found in coordination compounds, $[CoOH]^+$ and $[Co(OH)_3]^-$. In plant and animal tissues, Co is present in relatively low concentrations, generally below 0.1 μg g^{-1} on a dry weight basis.[6–9] In biological systems, small amounts of Co(II) are essential, as it is a central component of vitamin B12, which is indispensable for preventing pernicious anemia by stimulating the production of red blood cells.[5] However, ingesting large quantities can cause adverse health effects, such as pulmonary disorders, vasodilation, flushing, cardiomyopathy, asthma and skin irritation.[4–6] Thus, the quantitative determination of cobalt at trace levels plays a crucial role in areas such as environmental analysis, industrial process control and medicine, requiring sensitive analytical methods to monitor its presence, especially in individuals exposed to this metal.[10–13]

In the investigation of cobalt in different matrices, traditional analytical approaches have been employed, including spectrophotometry,[14] flame atomic absorption spectrometry (FAAS),[15] graphite furnace atomic absorption spectrometry (GFAAS)[16] and inductively coupled plasma optical emission spectrometry (ICP-OES)[17] and electroanalytical methods.[18] Although these techniques have improved sensitivity and selectivity, effective quantitative analysis often requires the preconcentration of cobalt ions, given its low concentration and the complexity of real samples. In this context, it is necessary to use sample preparation techniques such as liquid-liquid extraction (LLE) and, above all, solid-phase extraction (SPE). Compared to LLE, SPE offers advantages: it uses a small number of solvents and shows good recovery with high enrichment factors; in addition, it allows greater flexibility in the choice of adsorbents, is easy to automate, has low operating costs and makes it possible to reuse the adsorbent material and also allows the miniaturization of the procedure, reducing the generation of waste.[19–21]

Although synthetic adsorbents such as activated carbon, modified silica and ion exchange resins are widely used because of their selectivity and high adsorption capacity, they have disadvantages related to high costs, difficulties in disposal, risks of cross-contamination and low biodegradability.[22] In this scenario, natural adsorbents have emerged as more economical and sustainable alternatives, often derived from industrial waste.[23,24] Various materials can be used as adsorbents, and the choice will depend on the specific application; examples include *Moringa oleifera* seeds,[25,26] coffee husks[27] and banana peel flour.[28] These alternative adsorbents are expected to offer lower cost, good chemical resistance, high specific area and high adsorption capacity compared to traditional materials. In addition, their surfaces can be chemically modified through magnetic derivatization,[29] a process which gives the adsorbent magnetic properties and facilitates separation and filtration procedures.[30–32] This modification enhances adsorption efficiency, simplifies solid phase separation and makes it possible to miniaturize methods, contributing to a reduction in reagent and sample consumption.[20,33,34]

Among the alternative materials with the potential to be used as a solid phase is *Hibiscus sabdariffa* L. (roselle), an edible flower grown in tropical and subtropical regions. Its calyces are widely used in the production of teas, iced drinks, jams, flavorings and herbal medicines. The extract from these calyces, which are rich in antioxidants and bioactive substances such as phenolic and organic acids and anthocyanins, shows various biological activities and is used in the pharmaceutical and food industries.[35–37] In addition to the studies showing its health benefits, the literature already reports studies using this plant in green nanoparticle synthesis to remove Pb^{2+}, in the synthesis of carbon dots for Cr^{6+} sensors and in the bioremediation of Cr^{6+} using its calyces.[38-40] However, the use of *Hibiscus sabdariffa* L. as an adsorbent material for the development of analytical methods is still explored little.

An alternative to conventional SPE is magnetic solid phase extraction (MSPE), which uses magnetized adsorbents to form magnetic solid phases. This technique is based on magnetic interaction: initially, a

magnetic material is used to adsorb the analytes, and after a defined contact time, an external magnet is used to separate the material from the solution, entraining the components of interest. The analytes are then released by desorption into a separate container. This procedure, which eliminates the need for an extraction column, is remarkably fast and efficient, as it relies on the interaction between the magnetic adsorbent and the analyte, which is significantly influenced by the eluent and the pH of the medium. In column-based solid-phase extraction systems, in addition to the influence of the medium's pH, and the type and concentration of the eluent, the elution flow rate also becomes a crucial factor, further increasing the complexity of the process. Thus, MSPE has stood out as a promising approach, combining cost-effectiveness, sustainability and high analytical efficiency in the extraction of metal ions.[22,30,34]

Based on the ideas presented, the aim of this work is to develop an analytical method using MSPE and magnetized hibiscus calyx as a solid phase for the determination of Co(II) in aqueous samples by FAAS. The proposal for this study is based on the high efficiency, speed and sustainability provided by MSPE, combined with the adsorbent potential of magnetized hibiscus calyx, which allows for the rapid separation of analytes. In this way, it is hoped to improve sensitivity and precision in the quantification of cobalt, promoting an economical analytical approach in line with the principles of green analytical chemistry.

MATERIALS AND METHODS

Chemicals, reagents, and sample

The solutions used were prepared with ultrapure water obtained from a Milli-Q system (Millipore, Merck, Germany) and a cobalt standard solution from Dinâmica (São Paulo, Brazil) at a concentration of 1000 mg L^{-1}. All glassware, tubes, Pasteur pipettes and other utensils used in the experiments underwent a rigorous cleaning process. Initially, the materials were washed with water and neutral detergent, followed by immersion in water with detergent for 24 h. They were then rinsed with distilled water, subjected to a new immersion in distilled water for another 24 h and, subsequently, immersed in a 10% HCl solution (v v^{-1}) for the same period. After the cleaning process, the materials were rinsed with distilled water and dried at room temperature before use.

Solutions that required pH adjustment were prepared using dilute solutions of hydrochloric acid (HCl) and sodium hydroxide (NaOH). The reagents used were HCl P.A. (36% w w^{-1}) and NaOH P.A. in the form of beads. The determination of the metal ion concentration was performed by flame atomic absorption spectrometry (FAAS) in a PerkinElmer spectrometer, model AAnalyst 400. The multielement hollow cathode lamp (Co, Cu, Fe, Mn and Mo), also from PerkinElmer, operated at a wavelength of 240.73 nm and a deuterium lamp for background correction. The FAAS instrument was operated as recommended by the manufacturer: lamp current of 4 mA, slit width of 0.1 nm, burner height of 17 mm, acetylene flow rate of 2.0 L min^{-1}, and air flow rate of 13.5 L min^{-1}.

Preparation of the adsorbent

The plant material, known as the dehydrated calyx of the *Hibiscus sabdariffa* flower, was purchased from a health food store (Catalão, GO, Brazil), where it is sold for food purposes and often used in the preparation of teas. Initially, the material was washed with deionized water under agitation in a heated magnetic stirrer (C-MAG HS 7 IKA), simulating the tea infusion process. The water was renewed in 20 minutes cycles, repeating the procedure until the pigments were completely removed from the material.

The magnetization of the adsorbent was performed using a ferromagnetic fluid obtained from a mixture of 40.0 mL of ferric chloride ($FeCl_3$) at 1.0 mol L^{-1} and 10.0 mL of ferrous chloride ($FeCl_2$) at 2.0 mol L^{-1}, in an acidic medium containing HCl 1.0 mol L^{-1}. To this solution, 500.0 mL of ammonium hydroxide (NH_4OH) at 0.70 mol L^{-1} were added, resulting in the formation of a gelatinous precipitate, which was separated magnetically using a magnet. After separation, the precipitate was subjected to successive washings with ultrapure water and kept under stirring in the presence of perchloric acid ($HClO_4$) at 2.0 mol L^{-1}.[41] The solid phase was isolated by centrifugation and, to complete the peptization process, water was added to the precipitate, forming the ferrofluid.

For the modification of the adsorbent, 6.0 mL of the ferrofluid were added to a container containing 40.0 mL of methanol (CH_3OH) and 3.0 g of the adsorbent (hibiscus), being kept under stirring for 1 h.[41] The final material was filtered using a solvent filtration system, washed with methanol and dried at room temperature.

Characterization of the adsorbent material

The adsorbent was characterized by energy dispersive X-ray fluorescence (EDXRF) and determination of the point of zero charge (pH_{PZC}). The incorporation of the magnetic material into the natural adsorbent was evaluated through the application of a magnetic field generated by a magnet, as well as by X-ray diffraction (XRD). The analysis was carried out using a Shimadzu XRD-6100 diffractometer with Kα radiation (λ = 1.5418 Å). The diffractograms were obtained at room temperature, with a scanning rate of 2° min^{-1} and a 2θ range from 10° to 80°. The results were compared with standard patterns available in the ICDD-PDF database (International Centre of Diffraction Data – Powder Diffraction File).

The surface electrical behavior of the adsorbent was evaluated by determining the point of zero charge (pH_{PZC}). The determination was performed by adding 20 mg of the adsorbent to capped flasks containing 15 mL of ultrapure water, with the pH adjusted between 1 and 12 using a portable pH meter (Akso, model AK90). After 24 hours rest, pH measurements were repeated, and the pH_{PZC} was calculated based on the difference between the initial and final pH values.

Evaluation of pH influence in the adsorption of cobalt ions

Adsorption experiments were carried out using 20 mg of the adsorbent in 10 mL of an aqueous solution containing Co(II) ions (2 mg L^{-1}). The experiments were conducted in triplicate at room temperature. The adsorbent was added to the aqueous solution containing cobalt ions and kept under agitation using a vortex mixer (IKA VORTEX 3) for 15 minutes. After agitation, the material was filtered using glass wool, discarded, and the supernatant was stored in Falcon tubes for subsequent analysis.

The choice of solution pH is essential for optimizing the adsorption process, as this parameter affects the surface charge of the adsorbent and the distribution of metallic ion species. Therefore, the influence of the medium's pH was evaluated individually to observe the behavior of the adsorption process. The adsorption of the metal ion was evaluated at different pH values (2, 7, and 8).

Optimization of adsorption and desorption parameters

The optimization of the experimental conditions for desorption and adsorption was performed using a 2^4 full factorial design, considering the following variables: adsorbent mass (20 mg and 80 mg), extraction time (2 min and 10 min), eluent concentration (0.1 mol L^{-1} and 1.0 mol L^{-1}), and elution time (2 min and 10 min). Sixteen experiments were performed, in which the adsorbent was brought into contact with a Co(II) solution at 2 mg L^{-1} in pH 7.0, and subjected to an ultrasonic bath (Q3.8) for the predetermined time. All factorial design experiments were performed in triplicate. The energy released by the ultrasonic bath promotes better interaction between the solid phase and the metal ion, eliminating the need for mechanical stirring. After this period, magnetic separation was carried out, the supernatant was discarded, and the adsorbent was subjected to elution with 2 mL of the eluent solution, again placed in the ultrasonic bath under specified conditions.

The experimental design included the calculation of primary, secondary, tertiary, and quaternary effects using Octave software, aiming to maximize the absorbance obtained.

The variables that had the greatest influence on the extraction/elution process were optimized using an experimental design based on the Doehlert matrix, with two experimental variables. For the variables adsorbent mass and extraction time, the matrix consists of a central point accompanied by six regularly distributed points, forming a hexagon. This approach provides a better estimation of the response as a function of the evaluated variables. The experimental points were defined based on the coded values of the matrix.[42] Equation (1) gives the relationship between the coded values and the actual variables.

$$Xi = \left(\frac{Zi - Zi_0}{\Delta Zi}\right) \beta d \qquad (1)$$

Where Xi represents the coded value, Zi the actual value of the variable, Zi_0 the central value, ΔZi the variation range, and βd an adjustment coefficient.[42]

Analytical parameters

To evaluate the analytical performance of the developed extraction method, the limits of detection and quantification, linear range, and sensitivity were determined. These parameters were established by constructing a calibration curve after the preconcentration step of cobalt ions, considering the concentrations and replicates described in Table I.

Table I. Concentrations used for the construction of the calibration curve for evaluating the performance of the extraction method

Concentration (mg L^{-1})	Number of replicates
Blank	16
0.25	6
0.5	6
1	10
2.5	6
5	6
10	6

The accuracy of the method was evaluated through recovery tests using different aqueous samples. Recovery, a fundamental criterion in the validation of analytical methods, represents the amount of cobalt recovered by the developed technique in relation to the actual concentration present in the samples. For this evaluation, samples of coconut water, tap water, swimming pool water, calcium-rich hard water, and cachaça, were spiked with known concentrations of cobalt ions, covering the linear working range of the method. The experiments were carried out after parameter optimization, as illustrated in Figure 1.

Individual calibration curves were constructed for each sample to compensate possible matrix effects. The recovery experiments were carried out in triplicate by subjecting the spiked samples to the magnetic solid phase extraction (MSPE) procedure using magnetized *Hibiscus sabdariffa* calyx under optimized conditions. The resulting eluates were analyzed by FAAS. Recovery was calculated by comparing the concentration of Co(II) quantified in the spiked samples with the concentrations added, allowing the evaluation of the method's efficiency and accuracy in the presence of different matrices.[43]

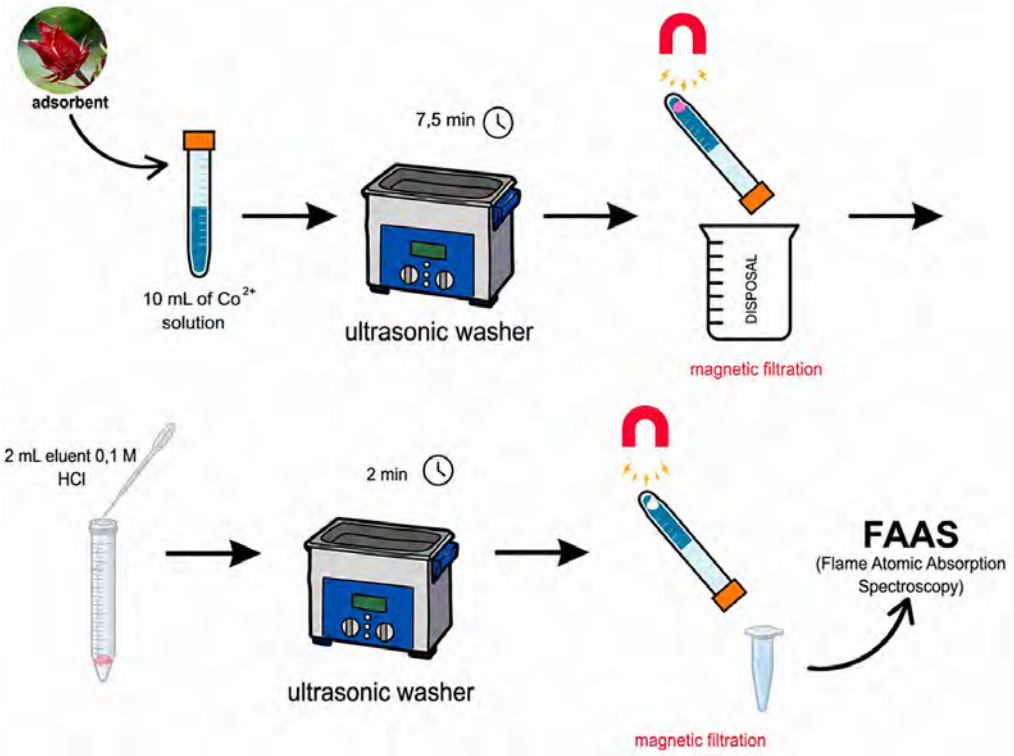

Figure 1. Flowchart of the experimental procedure for the extraction of cobalt ions using hibiscus calyx by magnetic solid-phase microextraction.

RESULTS AND DISCUSSION

Adsorbent material characterization

To verify the effectiveness of the adsorbent's magnetization and to understand the elemental composition of *Hibiscus sabdariffa* in its natural form and after the magnetization process, analyses were performed using energy dispersive X-ray fluorescence spectroscopy (EDXRF).

EDXRF is a non-destructive analytical technique that enables the identification and semiquantitative determination of the chemical elements present in a sample, based on the emission of characteristic X-rays after excitation by an X-ray source.

The results of the semiquantitative analysis, expressed as mass percentages, are presented in Table II. In addition to the EDXRF analysis, magnetization was evidenced by the attraction of the material dispersed in water by a magnetic field generated by a magnet. The results of the semiquantitative analysis, expressed as mass percentages, are presented in Table II.

Table II. Semiquantitative EDXRF results for natural and magnetized hibiscus materials

Elements	*In natura* hibiscus (%)	Magnetized hibiscus (%)
Ca	76.78	6.40
K	40.29	0.55
Si	2.27	0.47
Fe	–	87.62

The analysis reveals that natural hibiscus contains a high percentage of calcium (Ca), potassium (K), and silicon (Si), elements commonly found in plant-based materials; calcium and potassium are essential macronutrients, while silicon contributes to the structural integrity of the plant. Iron was not detected, indicating that its concentration is below the detection limit of the technique used in the analysis.

In the magnetized material, a reduction in the percentage of calcium, potassium, and silicon is observed, which is expected due to the hot water washing step that removes soluble components. The main highlight is the significant incorporation of iron, reaching 87.62% of the elemental composition. This high value confirms the effective magnetization of the material, indicating a strong interaction.

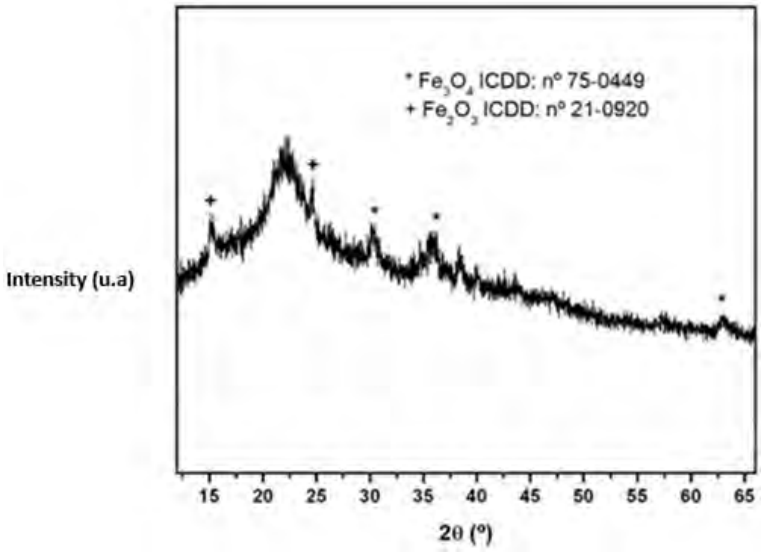

Figure 2. Diffractograms of the magnetized hibiscus sample.

Figure 2 presents the diffractogram of the magnetized *Hibiscus sabdariffa* sample. The diffractometric peaks observed at approximately 2θ = 30.3º, 35.8º, and 63.1º correspond to the crystalline phase of magnetite (Fe_3O_4), as identified in the ICDD crystallographic card No. 75-0449, confirming the obtention of the desired magnetic phase. However, according to ICDD card No. 21-0920, the peaks located at 2θ = 15.2º and 24.6º indicate the presence of a secondary hematite Fe_2O_3 phase.

The low intensity of the diffraction peaks and the presence of a diffuse band at approximately 2θ = 22º are attributed to the organic composition of the hibiscus, since amorphous materials promote X-ray scattering and reduce the diffraction of the crystalline phase.[44]

The point of zero charge (pH_{PZC}) provides essential information about the surface charge of the adsorbent material, representing the equilibrium between negative and positive charges.[45] This parameter helps understand the electrostatic interactions between the adsorbent and the adsorbate (cobalt ions), allowing us to predict the material's surface tendency to interact with cations or anions, depending on the medium's pH. Figure 3 shows the pH_{PZC} results for the natural hibiscus and magnetized hibiscus samples.

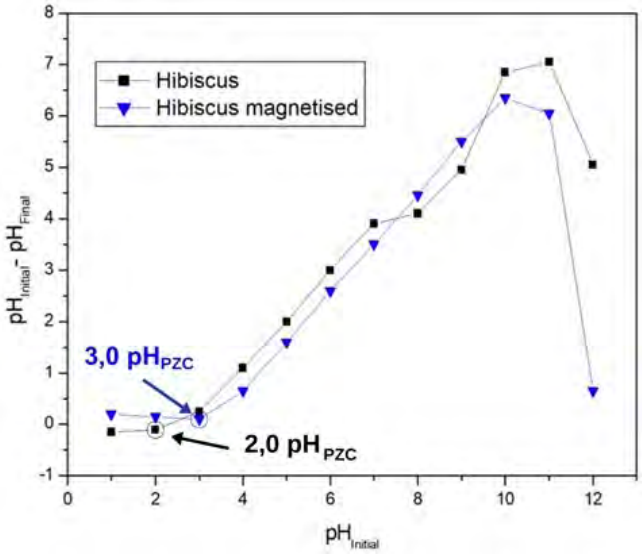

Figure 3. Study of the point of zero charge (pH_{PZC}) for *in natura* hibiscus and magnetized hibiscus.

The pH_{PZC} of *in natura Hibiscus sabdariffa* was determined to be approximately 2.0, while the material subjected to the washing and magnetization process exhibited a value of 3.0. This increase can be attributed both to the washing of the material, which promotes the removal of various bioactive compounds from the plant, such as anthocyanins, ascorbic acid, organic acids, flavonoids, and polyphenols, and to the incorporation of the magnetic material.[46] Thus, the adsorption of cations in solutions tends to be more effective at pH values higher than the pH_{PZC}, since, in this range, the adsorbent surface acquires a negative charge, favoring interaction.

Evaluation of the influence of pH on cobalt ion adsorption by the adsorbent material

The pH is one of the most critical parameters in adsorption processes, as it governs two fundamental dimensions of the system. First, it controls the surface charge of the adsorbent, since the medium's pH can drastically alter the protonation/deprotonation state of functional groups on the adsorbent material, determining the surface charge and, consequently, its electrostatic affinity for metal species. Second, pH influences the equilibrium among the different chemical species of the metal ion (free, complexed, hydrolyzed etc.), directly affecting the availability of the adsorbable species. Because it simultaneously affects both the adsorbent and the adsorbate, pH plays a dominant role that, in most cases, surpasses the relative impact of other variables.

Therefore, the individual assessment of pH was adopted as an initial step, allowing the identification of the pH range in which significant adsorption occurs, avoiding regions where the metal ion may precipitate, and establishing a reliable starting point before evaluating other variables with a higher likelihood of interaction. To evaluate the influence of pH on cobalt ion adsorption by *Hibiscus sabdariffa*, experiments were conducted in solutions with pH 2, 7, and 8.

At pH 2, the *in natura Hibiscus sabdariffa* showed an average extraction rate of 5.13%, while the magnetized material exhibited a rate of 10.26%. The low adsorption at acidic pH is likely due to the protonation of functional groups on the adsorbent's surface, leading to electrostatic repulsion with Co(II) ions. The slight improvement observed with the magnetized material can be attributed to the introduction of functional groups during the magnetization process. These groups, such as the oxygen atoms present in the magnetite structure, interact with the cobalt ion even at low pH.

At pH 7, the *in natura* material showed an adsorption of 2.67%, which increased to 8.00% at pH 8. The magnetically functionalized material performed significantly better, with 57.33% adsorption at pH 7 and 58.00% at pH 8. The magnetic particles (MPs) of magnetite, incorporated into the adsorbent during

the magnetization process, possess functional FeOH groups on their surface in aqueous media. These groups can be either deprotonated (FeO^-) or protonated ($FeOH_2^+$) depending on the pH of the medium.[47] At pH values above the pH_{PZC}, magnetite will have groups that are predominantly deprotonated (FeO^-). This contributes to the removal of cationic species due to the electrostatic attraction between the Co^{2+} ions and the adsorbent.

The results, illustrated in Figure 4, demonstrate that the washing and magnetization processes significantly increased the material's adsorption capacity, especially at neutral and alkaline pH values.

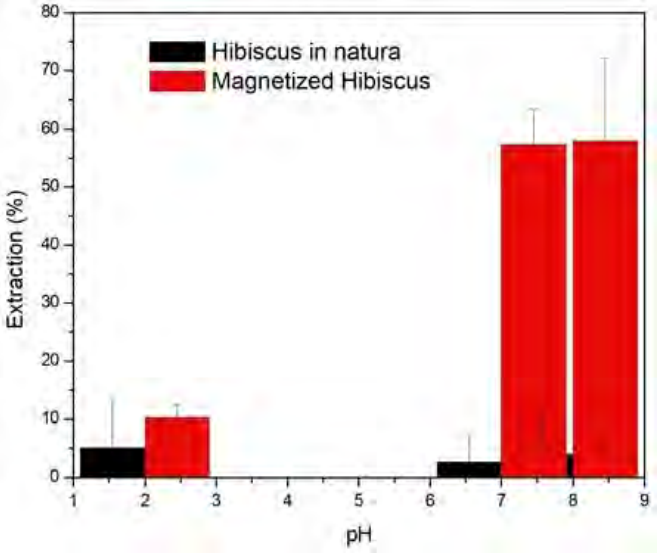

Figure 4. Effect of pH on cobalt ion adsorption by *in natura* and magnetized *Hibiscus sabdariffa*.

The magnetized material showed a slightly better extraction capacity, and additionally, the magnetic separation of the material makes the procedure easier and more efficient.

Optimization of adsorption and desorption parameters

Solid phase extraction (SPE) offers several advantages, including simplified procedures, short extraction times, and compatibility with various analytical techniques. Magnetic extraction emerges as a variation of SPE. Studies conducted by Pasupuleti and Huang (2023)[48] highlight the diverse applications of magnetic solid phase extraction (MSPE) in determining metal ions in environmental samples.

Despite its advantages, SPE requires the optimization of parameters that influence its efficiency, such as extraction time, agitation method, and pH.[49] To maximize the efficiency in extracting cobalt ions, a 2^4 full factorial design was used to evaluate the influence of previously selected factors.[50]

After conducting the experiments, the significance of the variables studied was evaluated using probability plots and percentage of effects plots, presented in Figures 5 and 6.

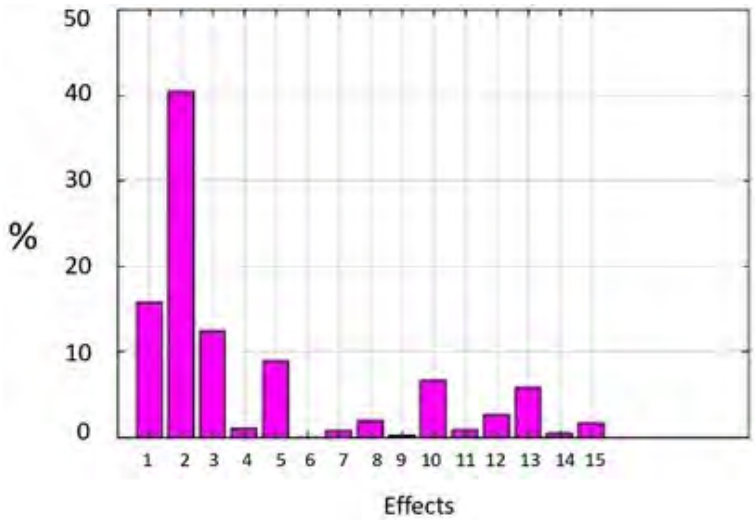

Figure 5. Percentage of effects for the 2^4 factorial design.

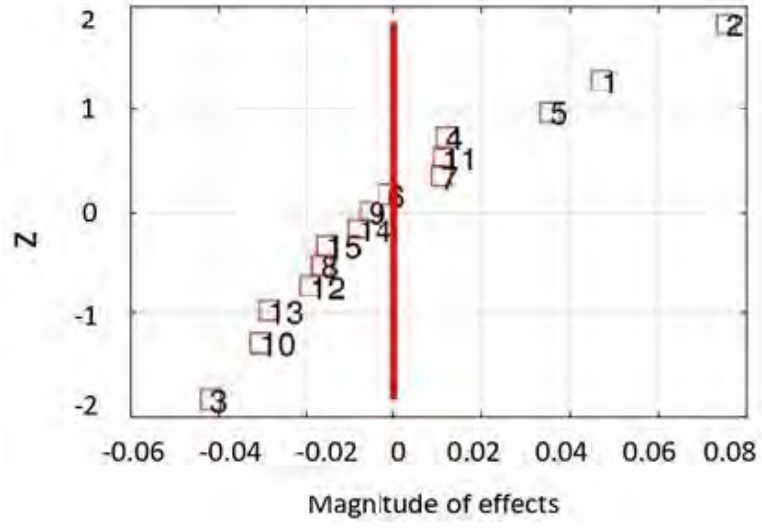

Figure 6. Probability of effects for the 2^4 factorial design.

In optimizing the extraction procedure, significant effects for the system are those furthest from zero on the probability plot, while non-significant effects are clustered near zero. The percentage of effects plot indicates the relative contribution of each effect to the extraction process.

Effects 1 and 2, corresponding to the adsorbent mass and extraction time, respectively, showed positive values and should therefore be kept at high levels (80 mg and 10 min, respectively). Effect 3, referring to the eluent concentration, showed a negative value on the probability plot of effects, indicating that it should be kept at a low level (0.1 mol L^{-1}).

Additionally, Figure 6 shows that effect 5, which is the interaction between the adsorbent mass and extraction time, is significant for the system. Its positive contribution means both variables should be kept at their high levels. Considering the most significant effects (1, 2, 3, and 5), the model explained approximately 79.03% of the data variability.

After identifying the most significant effects, a Doehlert design was used to optimize the variables with the highest impact: adsorbent mass (1) and extraction time (2). These variables were analyzed at five and three levels, respectively. To maximize cobalt ion extraction and evaluate the impact of the variables and their interactions, a response surface plot was constructed, as shown in Figure 7.

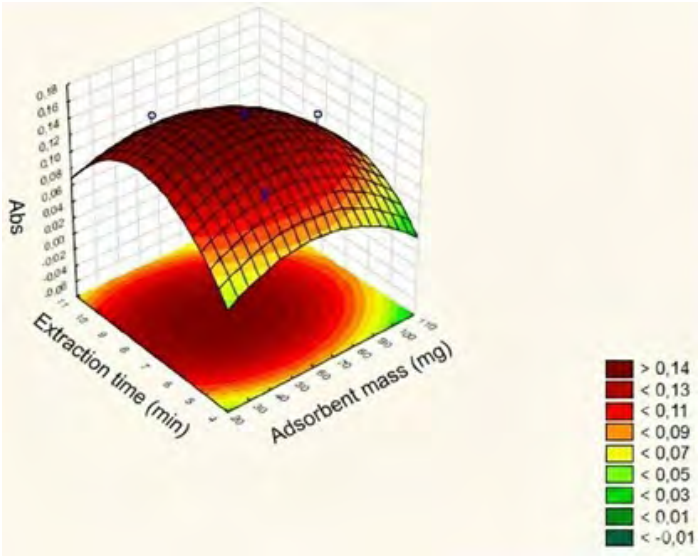

Figure 7. Response surface plot for the Doehlert design.

The critical values determined for maximum extraction efficiency were an adsorbent mass of 51.39 mg and an extraction time of 7.5 minutes.

The statistical parameters obtained were a coefficient of determination (R^2) of 0.7708 and a mean square of residuals (MS Residual) of 0.00104. The low MS Residual value suggests good agreement between the predicted and experimental values, demonstrating a good fit of the model to the experimental data. The coefficient of determination (R^2) indicates that approximately 77.08% of the data variability can be explained by the model, reinforcing its suitability for process optimization.

Evaluation of analytical parameters

Validating analytical methods is essential to ensure the reliability of results, especially when determining chemical species at low concentrations, such as in environmental, pharmaceutical, and food analyses. Validation demonstrates that the method is fit for its intended purpose.

After optimizing the experimental conditions, we evaluated the performance of the proposed method by assessing its limits of detection (LOD) and limits of quantification (LOQ). The linear working range defines the concentration interval where there's a linear relationship between the analytical signal (in this case, absorbance) and the analyte concentration, ensuring acceptable precision and accuracy.[43] Linearity was assessed using correlation coefficient (r) and residual analysis, with 5 concentration points (Table III).

The LOD (Limit of Detection) is defined as the lowest analyte concentration that can be reliably detected, though not necessarily quantified. The LOQ (Limit of Quantification) is the lowest concentration that can be quantified with acceptable precision and accuracy within pre-established confidence limits.[51]

Table III. Analytical parameters obtained for the developed method

Parameter	Value
Linear range (mg L^{-1})	0.440 - 10.0
Limit of detection (mg L^{-1})	0.132
Limit of quantification (mg L^{-1})	0.440
Correlation coefficient	0.990
Equation	Abs = 0.0215[Co^{2+}] – 0.015
Sensitivity (mg L^{-1})	0.0215

The results show an excellent correlation coefficient (r = 0.990), indicating a strong linear relationship between absorbance and analyte concentration within the studied range.

Table IV compares the performance of the proposed MSPE method in this study with other extraction methods reported in the literature for the determination of cobalt(II) ions, using limits of detection (LOD), limits of quantification (LOQ), and linear working ranges as parameters.

In a comparative analysis with other MSPE methodologies listed in Table IV, which use adsorbents such as zirconium nanoparticles (Zr-NPs) with polyaniline (PANI) and polythiophene, some methods show greater detection potential, with significantly lower LOD and LOQ values. A prominent advantage of the proposed method lies in its sustainable profile, specifically the use of plant-based adsorbent material (hibiscus calyces), which is an abundant and low-cost industrial byproduct.

Table IV. Comparison of the proposed method with methods from the literature

Method		LOD (mg L^{-1})	LOQ (mg L^{-1})	Linear range (mg L^{-1})	Sample	Ref.
MSPE	*Hibiscus sbariffa* calyx magnetized	0.132	0.440	0.440, 10.0	Hard water, pool water, tap water, cachaça	This work
MSPE	Zirconium nanoparticles (Zr-NPs)	0.0016	0.0053	0.2, 5.0	Diverse sodas, spices, vegetables, and water samples	52
MSPE	Polyaniline (PANI) and polythiophene (PTH) coated magnetic nanoparticles (MNPs)	0,00173	0,0058	–	Aqueous	53
SPE	Magnetic carboxyl-modified nanodiamonds (MCNDs)	0.0022	0.0072	0.0075, 0.075	Soil samples	54
SPE	C-18 modified silica	0.0019	0.0063	0.006, 5.0	Nutritional supplements: *Spirulina platensis* tablets and *Saccharomyces cerevisiae* yeast tablets	55

The method's accuracy, assessed through recovery tests, is crucial for verifying its analytical performance in different matrices. This parameter compares the found value with the added value (considered the true value in this type of assay), revealing potential interferences. For this study, were selected six distinct samples (coconut water, swimming pool water, tap water, calcium-rich hard water, and two types of cachaça), presumably with low or no initial cobalt concentration.

The samples were fortified with Co(II) ions at concentrations of 0.5, 2.5, and 6.5 mg L^{-1} and then subjected to the optimized MSPE procedure. Table V summarizes the results, showing the added concentrations, the experimentally found concentrations, and their respective recovery percentages.

Table V. Evaluation of recovery potential

Sample	0.5 mg L^{-1} Co^{2+} added		2.5 mg L^{-1} Co^{2+} added		6.5 mg L^{-1} Co^{2+} added	
	Found (mg L^{-1})	Recovery (%)	Found (mg L^{-1})	Recovery (%)	Found (mg L^{-1})	Recovery (%)
Coconut water	0.375 ± 0.008	75.0	2.44 ± 0.007	97.6	6.13 ± 0.002	94,2
Swimming pool water	0.541 ± 0.0004	108	2.24 ± 0.01	89.6	6.95 ± 0.03	107
Tap water	0.398 ± 0.003	99.6	2.28 ± 0.005	91.3	5.33 ± 0.007	82,1
Calcium-rich hard water	0.576 ± 0.003	115	1.18 ± 0.007	47.3	6.47 ± 0.002	99,6
Cachaça 1	0.419 ± 0.002	83.8	2.95 ± 0.02	118	5.83 ± 0.07	89,7
Cachaça 2	0.319 ± 0.004	63.9	2.91 ± 0.01	116	7.41 ± 0.04	114

Initially, it can be observed that the recovery values vary widely, ranging from a minimum of 47.3% (calcium-rich hard water) to a maximum of 118% (Cachaça 1). At the lowest concentration added (0.5 mg L^{-1}), notably low recoveries were observed for coconut water (75.0%) and Cachaça 2 (63.9%). Coconut water is a matrix naturally rich in electrolytes, containing high concentrations of ions such as Na^+, K^+, Ca^{2+}, Mg^{2+}, Cl^-, and HCO_3^-, among others. In solid phase extraction (SPE) processes, especially those based on adsorption onto materials with active functional groups, the presence of these ions can generate direct competition for the adsorption sites intended for the analyte. Ions present at high concentrations, such as K^+ and Mg^{2+}, may preferentially occupy adsorption sites due to their abundance. Since the number of active sites is limited, a portion of them may be occupied before cobalt ions interact with the material, thereby reducing their recovery.

Similarly charged ions, particularly divalent, such as Ca^{2+} and Mg^{2+}, also present at high concentrations in this matrix, can compete more effectively with Co(II) for negatively charged sites, decreasing selectivity and consequently reducing analyte recovery. These effects are more pronounced when the analyte is present at concentrations near the method's quantification limits.

At the intermediate fortification level (2.5 mg L^{-1}), most matrices, including coconut water (97.6%), swimming pool water (89.6%), and tap water (91.3%), showed recoveries within the commonly accepted range (80-120%). The most significant exception was observed in the calcium-rich hard water sample, with a low recovery (47.3%). This is likely due to the high concentration of Ca^{2+} and Mg^{2+} ions, which can compete with Co^{2+} for adsorption sites on the hibiscus or interfere with the elution/measurement step.

The low standard deviation values associated with the concentrations found (Table IV) indicate good precision (repeatability) of the final FAAS measurement. However, the wide variation in recovery percentages across different matrices and concentrations demonstrates that the accuracy of the overall method (MSPE-FAAS) is affected by matrix effects and/or procedural losses. The variability in recovery doesn't primarily originate from the FAAS reading step but rather from the preparation/extraction stages and specific interactions with each matrix.

CONCLUSIONS

This study successfully demonstrated the viability of using *Hibiscus sabdariffa* calyces, a low-cost natural material, as an adsorbent in a magnetic solid-phase extraction (MSPE) system for the extraction and determination of cobalt ions (Co^{2+}) by FAAS. The magnetization process was efficient, incorporating a high percentage of iron (confirmed by EDXRF and XRD as magnetites/hematites), which facilitated the adsorbent's separation. Characterization showed that magnetization altered the surface properties (increasing the pH_{PZC}) and significantly improved the Co^{2+} adsorption capacity at neutral and alkaline pH (pH 7-8) compared to the *in natura* material.

Optimizing the extraction and elution parameters using factorial and Doehlert designs helped define the optimal conditions (adsorbent mass ≈ 51 mg, contact time ≈ 7.5 min, 0.1 mol L^{-1} HCl eluent) to maximize the analytical response. The developed method showed satisfactory figures of merit, including good linearity ($r = 0.990$) in the range of 0.440 to 10.0 mg L^{-1}, and detection (0.132 mg L^{-1}) and quantification (0.440 mg L^{-1}) limits suitable for various applications.

The magnetized *Hibiscus sabdariffa*-based adsorbent shows promise as a sustainable and low-cost alternative for determining Co^{2+} ions. The proposed method is efficient, particularly for simpler aqueous matrices. However, its application in complex matrices requires caution and possibly additional optimizations or alternative calibration strategies (such as standard addition) to ensure accurate results.

Acknowledgements

The author Ana Alice Silva acknowledges the Conselho Nacional de Desenvolvimento Científico e Tecnológico (CNPq) for the Master's scholarship granted (Grant No. 131938/2025-8).

Conflicts of interest

The authors declare no conflicts of interest.

Use of artificial intelligence (AI) tools

The authors acknowledge the use of ChatGPT and Grammarly for language editing. The authors take full responsibility for the accuracy, integrity, and originality of the work and confirm that no AI tools were used to generate scientific ideas, independently analyze data, or replace the authors' critical role.

REFERENCES

(1) Radwan, A.; El-Sewify, I. M.; Azzazy, H. M. E. S. Monitoring of Cobalt and Cadmium in Daily Cosmetics Using Powder and Paper Optical Chemosensors. *ACS Omega* **2022**, *7* (18), 15739–15750. https://doi.org/10.1021/acsomega.2c00730

(2) Betancourt-Cantera, J. A.; Sánchez-De Jesús, F.; Bolarín-Miró, A. M.; Torres-Villaseñor, G.; Betancourt-Cantera, L. G. Magnetic Properties and Crystal Structure of Elemental Cobalt Powder Modified by High-Energy Ball Milling. *J. Mater. Res. Technol.* **2019**, *8* (5), 4995–5003. https://doi.org/10.1016/j.jmrt.2019.07.048

(3) Botelho Junior, A. B.; Dreisinger, D. B.; Espinosa, D. C. R. A Review of Nickel, Copper, and Cobalt Recovery by Chelating Ion Exchange Resins from Mining Processes and Mining Tailings. *Mining, Metall. Explor.* **2019**, *36* (1), 199–213. https://doi.org/10.1007/s42461-018-0016-8

(4) Adams, T. N.; Butt, Y. M.; Batra, K.; Glazer, C. S. Cobalt Related Interstitial Lung Disease. *Respir. Med.* **2017**, *129*, 91–97. https://doi.org/10.1016/j.rmed.2017.06.008

(5) Lauwerys, R.; Lison, D. Health Risks Associated with Cobalt Exposure - an Overview. *Sci. Total Environ.* **1994**, *150* (1–3), 1–6. https://doi.org/10.1016/0048-9697(94)90125-2

(6) Kosiorek, M.; Wyszkowski, M. Effect of Cobalt on the Environment and Living Organisms - A Review. *Appl. Ecol. Environ. Res.* **2019**, *17* (5), 11419–11449. https://doi.org/10.15666/aeer/1705_1141911449

(7) Schatkoski, V. M.; Montanheiro, T. L. A.; de Menezes, B. R. C.; Pereira, R. M.; Rodrigues, K. F.; Ribas, R. G.; da Silva, D. M.; Thim, G. P. Current Advances Concerning the Most Cited Metal Ions Doped Bioceramics and Silicate-Based Bioactive Glasses for Bone Tissue Engineering. *Ceram. Int.* **2021**, *47* (3), 2999–3012. https://doi.org/10.1016/j.ceramint.2020.09.213

(8) Ivanov, V. B.; Zhukovskaya, N. V. Effect of Heavy Metals on Root Growth and the Use of Roots as Test Objects. *Russ. J. Plant Physiol.* **2021**, *68*, (S1–S25). https://doi.org/10.1134/S1021443721070049.

(9) Singh, V.; Singh, N.; Rai, S. N.; Kumar, A.; Singh, A. K.; Singh, M. P.; Sahoo, A.; Shekhar, S.; Vamanu, E.; Mishra, V. Heavy Metal Contamination in the Aquatic Ecosystem: Toxicity and Its Remediation Using Eco-Friendly Approaches. *Toxics* **2023**, *11* (2), 147. https://doi.org/10.3390/toxics11020147

(10) Carter, S.; Clough, R.; Fisher, A.; Gibson, B. Atomic spectrometry update: review of advances in the analysis of metals, chemicals and materials. *J. Anal. At. Spectrom*. **2018**, *33* (11), 1802–1848. https://doi.org/10.1039/c8ja90039f

(11) Hemmati, M.; Rajabi, M.; Asghari, A. Magnetic nanoparticle based solid-phase extraction of heavy metal ions: A review on recent advances. *Microchim. Acta* **2018**, *185*. https://doi.org/10.1007/s00604-018-2670-4

(12) Meng, L.; Chen, C.; Yang, Y. Suspension Dispersive Solid Phase Extraction for Preconcentration and Determination of Cobalt, Copper, and Nickel in Environmental Water by Flame Atomic Absorption Spectrometry. *Anal. Lett.* **2014**, *48* (3), 453–463. https://doi.org/10.1080/00032719.2014.947537

(13) Carolin, C. F.; Kumar, P. S.; Saravanan, A.; Joshiba, G. J.; Naushad, Mu. Efficient techniques for the removal of toxic heavy metals from aquatic environment: A review. *J. Environ. Chem. Eng.* **2017**, *5* (3), 2782-2799. https://doi.org/10.1016/j.jece.2017.05.029

(14) Zahir, K. O.; Keshtkar, H. A Colorimetric Method for Trace Level Determination of Cobalt in Natural and Waste Water Samples. *Int. J. Environ. Anal. Chem.* **1998**, *72* (2), 151–162. https://doi.org/10.1080/03067319808035886

(15) Jamali, M. R.; Khodayar, P.; Rahnama, R. Ultrasound-assisted dispersive magnetic solid phase extraction using toner powder for the separation and preconcentration of cobalt in water and food samples and determination by flame atomic absorption spectrometer. *J. Dispersion Sci. Technol.* **2023**, *45* (11), 2103–2111. https://doi.org/10.1080/01932691.2023.2247064

(16) Liu, Y.; Han, Q.; Huo, Y.; Yang, X. Determination of Trace Cobalt in Water Samples by Ionic Liquid-Dispersive Liquid–Liquid Microextraction and Graphite Furnace Atomic Absorption Spectrometry. *J. Water Chem. Technol.* **2024**, *46*, 480–490. https://doi.org/10.3103/S1063455X24050102

(17) Zhen, Y.; Chen, H.; Zhang, M.; Hu, J.; Hou, X. Cadmium and cobalt ions enhanced-photochemical vapor generation for determination of trace rhenium by ICP-MS. *Appl. Spectrosc. Rev.* **2021**, *57* (4), 318–337. https://doi.org/10.1080/05704928.2021.1878368

(18) Mettakoonpitak, J.; Miller-Lionberg, D.; Reilly, T.; Volckens, J.; Henry, C. S. Low-cost reusable sensor for cobalt and nickel detection in aerosols using adsorptive cathodic square-wave stripping voltammetry. *J. Electroanal. Chem.* **2017**, *805*, 75-82. https://doi.org/10.1016/j.jelechem.2017.10.026

(19) Fumes, B. H.; Silva, M. R.; Andrade, F. N.; Nazario, C. E. D.; Lanças, F. M. Recent advances and future trends in new materials for sample preparation. *TrAC, Trends Anal. Chem.* **2015**, *71*, 9-25. https://doi.org/10.1016/j.trac.2015.04.011

(20) Płotka-Wasylka, J.; Szczepańska, N.; de la Guardia, M.; Namieśnik, J. Miniaturized solid-phase extraction techniques. *TrAC, Trends Anal. Chem.* **2015**, *73*, 19-38. https://doi.org/10.1016/j.trac.2015.04.026

(21) Moral, A.; Borrull, F.; Marcé, R. M.; Fontanals, N. Novel materials for sorptive extraction techniques for the analysis of environmental water samples. *TrAC, Trends Anal. Chem.* **2024**, *181*, Part A, 118005. https://doi.org/10.1016/j.trac.2024.118005

(22) Martínez-Pérez-Cejuela, H.; Gionfriddo, E. Evolution of Green Sample Preparation: Fostering a Sustainable Tomorrow in Analytical Sciences. *Anal. Chem.* **2024**, *96* (20), 7840-7863. https://doi.org/10.1021/acs.analchem.4c01328

(23) Chai, W. S.; Cheun, J. Y.; Kumar, P. S.; Mubashir, M.; Majeed, Z.; Banat, F.; Ho, S.-H.; Show, P. L. A review on conventional and novel materials towards heavy metal adsorption in wastewater treatment application. *J. Cleaner Prod.* **2021**, *296*, 126589. https://doi.org/10.1016/j.jclepro.2021.126589

(24) Bilal, M.; Ihsanullah, I.; Younas, M.; Shah, M. U. H. Recent advances in applications of low-cost adsorbents for the removal of heavy metals from water: A critical review. *Separation Purif. Technol.* **2021**, *278*, 119510. https://doi.org/10.1016/j.seppur.2021.119510

(25) Tomasin, G. S.; Silva, W. R.; Costa, B. E. dos S.; Coelho, N. M. M. Highly sensitive determination of Cu(II) ions in hemodialysis water by F AAS after disposable pipette extraction (DPX) using Moringa oleifera as solid phase. *Microchem. J.* **2021**, *161*, 105749. https://doi.org/10.1016/j.microc.2020.105749

(26) Alves, V. N.; Coelho, N. M. M. Selective extraction and preconcentration of chromium using *Moringa oleifera* husks as biosorbent and flame atomic absorption spectrometry. *Microchem. J.* **2013**, *109*, 16-22. https://doi.org/10.1016/j.microc.2012.05.030

(27) Silva, W.; Costa, B.; Batista, A.; Alves, V.; Coelho, N. Development of a Disposable Pipette Extraction Method Using Coffee Silverskin as an Adsorbent for Chromium Determination in Wastewater Samples by Solid Phase Extraction. *J. Braz. Chem. Soc*. **2022**, *33* (5), 498–507. https://doi.org/10.21577/0103-5053.20210171

(28) Khairiah, K.; Frida, E.; Sebayang, K.; Sinuhaji, P.; Humaidi, S. Data on characterization, model, and adsorption rate of banana peel activated carbon (*Musa acuminata*) for adsorbents of various heavy metals (Mn, Pb, Zn, Fe). *Data Brief* **2021**, *39*, 107611. https://doi.org/10.1016/j.dib.2021.107611

(29) Akar, S. T.; Balk, Y.; Sayin, F.; Akar, T. Magnetically functionalized alunite as a recyclable and ecofriendly adsorbent for efficient removal of Pb^{2+}. *J. Water Process Eng.* **2022**, *48*, 102867. https://doi.org/10.1016/j.jwpe.2022.102867

(30) Safari, M.; Yamini, Y. Application of magnetic nanomaterials in magnetic in-tube solid-phase microextraction. *Talanta* **2021**, *221*, 121648. https://doi.org/10.1016/j.talanta.2020.121648

(31) Ricardo, A. I. C.; Abujaber, F.; Bernardo, F. J. G.; Martín-Doimeadios, R. C. R.; Ríos, Á. Magnetic solid phase extraction as a valuable tool for elemental speciation analysis. *Trends Environ. Anal. Chem.* **2020**, *27*, e00097. https://doi.org/10.1016/j.teac.2020.e00097

(32) Alizadeh, M.; Peighambardoust, S. J.; Foroutan, R.; Azimi, H.; Ramavandi, B. Surface magnetization of hydrolyzed Luffa Cylindrica biowaste with cobalt ferrite nanoparticles for facile Ni^{2+} removal from wastewater. *Environ. Res.* **2022**, *212*, Part B, 113242. https://doi.org/10.1016/j.envres.2022.113242
(33) Prosen, H.; Zupančič-Kralj, L. Solid-phase microextraction. *TrAC, Trends Anal. Chem.* **1999**, *18* (4), 272-282. https://doi.org/10.1016/S0165-9936(98)00109-5
(34) Dias, F. de S.; Meira, L. A.; Carneiro, C. N.; Santos, L. F. M. dos; Guimarães, L. B.; Coelho, N. M. M.; Coelho, L. M.; Alves, V. N. Lignocellulosic materials as adsorbents in solid phase extraction for trace elements preconcentration. *TrAC, Trends Anal. Chem*. **2023**, *158*, 116891. https://doi.org/10.1016/j.trac.2022.116891
(35) Piovesana, A.; Rodrigues, E.; Noreña, C. P. Z. Composition Analysis of Carotenoids and Phenolic Compounds and Antioxidant Activity from Hibiscus Calyces (*Hibiscus sabdariffa* L.) by HPLC-DAD-MS/MS. *Phytochem. Anal.* **2019**, *30* (2), 208–217. https://doi.org/10.1002/pca.2806
(36) Zhen, J.; Villani, T. S.; Guo, Y.; Qi, Y.; Chin, K.; Pan, M. H.; Ho, C. T.; Simon, J. E.; Wu, Q. Phytochemistry, Antioxidant Capacity, Total Phenolic Content and Anti-Inflammatory Activity of *Hibiscus sabdariffa* Leaves. *Food Chem.* **2016**, *190*, 673–680. https://doi.org/10.1016/j.foodchem.2015.06.006
(37) Da-Costa-Rocha, I.; Bonnlaender, B.; Sievers, H.; Pischel, I.; Heinrich, M. *Hibiscus sabdariffa* L. - A Phytochemical and Pharmacological Review. *Food Chem.* **2014**, *165*, 424–443. https://doi.org/10.1016/j.foodchem.2014.05.002
(38) Hussein, H.; Ibrahim, S. S.; Khairy, S. A. Green Synthesis of ZnO Nanoparticles using *Hibiscus sabdariffa* L: Rapid Pb^{2+} Ion Removal, Photocatalytic Degradation of Methylene Blue, and Biomedical Applications. *J. Water Process Eng.* **2025**, *69*, 106649. https://doi.org/10.1016/j.jwpe.2024.106649
(39) Komalavalli, L.; Amutha, P.; Monisha, S. A facile approach for the synthesis of carbon dots from *Hibiscus sabdariffa &* Its Application as Bio-Imaging Agent and Cr (VI) Sensor. *Mater. Today Proc.* **2019**, *33*, 2279–2285. https://doi.org/10.1016/j.matpr.2020.04.195
(40) Ambi, A. A.; Isa, M. T.; Ibrahim, A. B.; Bashir, M.; Ekwuribe, S.; Sallau, A. B. Hexavalent Chromium Bioremediation Using *Hibiscus sabdariffa* Calyces Extract: Process Parameters, Kinetics and Thermodynamics. *Sci. African* **2020**, *10*, e00642. https://doi.org/10.1016/j.sciaf.2020.e00642
(41) Massart, R. Preparation of Aqueous Magnetic Liquids in Alkaline and Acidic Media. *IEEE Trans. Magn*. **1981**, *17* (2), 1247-1248. https://doi.org/10.1109/TMAG.1981.1061188
(42) Teófilo, R. F.; Ferreira, M. M. C. Quimiometria II: planilhas eletrônicas para cálculos de planejamentos experimentais, um tutorial. *Quím. Nova* **2006**, *29* (2), 338–350. https://doi.org/10.1590/S0100-40422006000200026
(43) Brito, N. M.; Amarante Junior, O. P.; Polese, L.; Santos, T. C. R.; Ribeiro, M. L. Validação de métodos analíticos: estratégia e discussão. *Pesticidas: Revista de Ecotoxicologia e Meio Ambiente* **2003**, *13*, 129–146. https://doi.org/10.5380/pes.v13i0.3173
(44) Mariano, N. A.; May, J. E.; Kuri, S. E. Ligas Finemet nanocristalizadas a partir de precursores amorfos. *REM, Rev. Esc. Minas* **2004**, *57* (2), 129–133. https://doi.org/10.1590/S0370-44672004000200010
(45) Nascimento, M. S. Aplicação de planejamento fatorial no estudo da adsorção de corante reativo azul 5G em quitosana. *Revista Processos Químicos* **2017**, *11* (21), 59–68. https://doi.org/10.19142/rpq.v11i21.713
(46) Izquierdo-Vega, J. A.; Arteaga-Badillo, D. A.; Sánchez-Gutiérrez, M.; Morales-González, J. A.; Vargas-Mendoza, N.; Gómez-Aldapa, C. A.; Castro-Rosas, J.; Delgado-Olivares, L.; Madrigal-Bujaidar, E.; Madrigal-Santillán, E. Organic acids from Roselle (*Hibiscus sabdariffa* L.)—A brief review of its pharmacological effects. *Biomedicines* **2020**, *8* (5), 100. https://doi.org/10.3390/biomedicines8050100
(47) Pasupuleti, R. R.; Huang, Y. L. Recent applications of atomic spectroscopy coupled with magnetic solid-phase extraction techniques for heavy metal determination in environmental samples: A review. *J. Chin. Chem. Soc.* **2023**, *70* (6), 1326–1337. https://doi.org/10.1002/jccs.202300029

(48) Spietelun, A.; Kloskowski, A.; Chrzanowski, W.; Namiésnik, J. Understanding solid-phase microextraction: key factors influencing the extraction process and trends in improving the technique. *Chem. Rev.* **2013**, *113* (3), 1667–1685. https://doi.org/10.1021/cr300148j
(49) Ferreira, S. L. C.; Lemos, V. A.; Carvalho, V. S.; Silva, E. G. P.; Queiroz, A. F. S.; Felix, C. S. A.; Silva, D. L. F.; Dourado, G. B.; Oliveira, R. V. Multivariate optimization techniques in analytical chemistry – an overview. *Microchem. J.* **2018**, *140*, 176–182. https://doi.org/10.1016/j.microc.2018.04.002
(50) Ministério da Agricultura, Pecuária e Abastecimento (MAPA). Guia de validação: controle de qualidade analítica. Brasília: MAPA; 2021. Available at: https://www.gov.br/agricultura/pt-br/assuntos/lfda/arquivos-publicacoes-laboratorio/guia-de-validacao-controle-de-qualidade-analitica.pdf/view (accessed 04/2026).
(51) Silva, C. A. S.; Silva, R. L. S.; Figueiredo, A. T.; Alves, V. N. Magnetic Solid-Phase Microextraction for Lead Detection in Aqueous Samples Using Magnetite Nanoparticles. *J. Braz. Chem. Soc.* **2020**, *31* (1), 109–115. https://doi.org/10.21577/0103-5053.20190134
(52) Elci, S. G. Determination of cobalt in food by magnetic solid-phase extraction (MSPE) preconcentration by polyaniline (PANI) and polythiophene (PTH) coated magnetic nanoparticles (MNPs) and microsample injection system - flame atomic absorption spectrometry (MIS-FAAS). *Instrum. Sci. Technol.* **2020**, *48* (6), 661–675. https://doi.org/10.1080/10739149.2020.1818577
(53) Khan, M.; Soylak, M. Magnetic Solid Phase Extraction of Lead, Cadmium, and Cobalt on Magnetic Carboxyl-Modified Nanodiamonds (MCNDs) from Natural Water Samples and Their Determination by Flame Atomic Absorption Spectrometry. *At. Spectrosc.* **2018**, *39* (2), 81–89. https://doi.org/10.46770/AS.2018.02.005
(54) Tekin, Z.; Borahan, T.; Özdoğan, N.; Bakırdere, S. Peristaltic pump-assisted zirconium nanoparticle-based pipette-tip solid phase extraction for the determination of cobalt by slotted quartz tube-flame atomic absorption spectrophotometry. *Anal. Methods* **2020**, *12*, 1244–1249. https://doi.org/10.1039/c9ay02762a
(55) Bartosiak, M.; Jankowski, K.; Giersz, J. Determination of cobalt species in nutritional supplements using ICP-OES after microwave-assisted extraction and solid-phase extraction. *J. Pharm. Biomed. Anal.* **2018**, *155*, 135–140. https://doi.org/10.1016/j.jpba.2018.03.058

Brazilian Journal of Analytical Chemistry
2026, Volume 13, Issue 52, pp 119-132
doi: 10.30744/brjac.2179-3425.AR-71-2025

BrJAC

ARTICLE

Laser-Induced Graphene Sensor for Electrochemical Determination of Nimesulide

Mylla Karliane Vera Cruz Fróz[1], Dianderson Cristiano Monteiro Ferreira[2], Matheus Barros Garcez[1], Gustavo Carvalho Diniz[3], Luiz Ricardo Guterres e Silva[1], Jéssica Santos Stefano[4], Auro Atsushi Tanaka[1], Iranaldo Santos da Silva[4], Luiza Maria Ferreira Dantas*[4]

[1]*Departamento de Química, Universidade Federal do Maranhão, São Luís, MA, 65080-805, Brazil*
[2]*Instituto de Química, Universidade Federal de Uberlândia, Uberlândia, MG, 38408-100 Brazil*
[3]*Instituto Federal de Educação, Ciência e Tecnologia do Maranhão, São Luís, MA, 65030-005, Brazil*
[4]*Departamento de Tecnologia Química, Universidade Federal do Maranhão, São Luís, MA, 65080-805, Brazil*

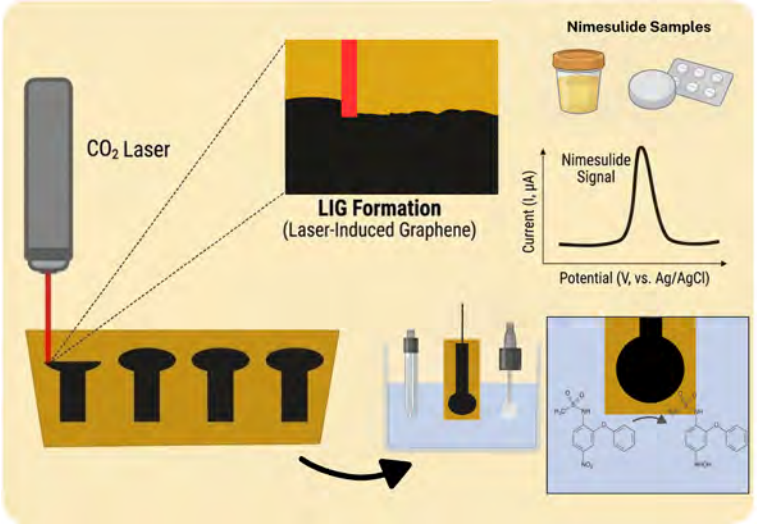

Part of this graphical abstract was generated with the assistance of the Google Gemini AI tool. The final figure was reviewed by the authors, who take full responsibility for its content.

Nimesulide (NMS) is a sulfonamide-class non-steroidal anti-inflammatory drug widely used in pharmaceutical formulations, whose reliable quantification is essential for quality control. In this work, an unmodified laser-induced graphene electrode (LIGe), fabricated by direct CO_2 laser ablation of polyimide, is proposed for the electrochemical determination of NMS using square-wave voltammetry (SWV). Voltammetric studies revealed that NMS oxidation is an irreversible, diffusion-controlled process that involves the transfer of two protons and two electrons. After systematic optimization of pH and instrumental parameters, the method exhibited a wide linear working range from 11.0 to 131 μmol L^{-1}, with a detection limit of 1.30 μmol L^{-1}. The sensor showed good repeatability (RSD < 5%, n = 10) and was successfully applied to the analysis of pharmaceutical tablets, yielding results consistent with the declared content. Accuracy was further evaluated in synthetic urine, with recovery rates between 97% and 111%. Interference studies demonstrated that common non-electroactive urinary constituents caused only minor signal variations (<3%). Although the detection limit is higher than that reported for heavily modified electrodes, the proposed approach offers simplicity of fabrication, rapid analysis, disposability,

Cite: Fróz, M. K. V. C.; Ferreira, D. C. M.; Garcez, M. B.; Diniz, G. C.; Guterres e Silva, L. R.; Stefano, J. S.; Tanaka, A. A.; da Silva, I. S.; Dantas, L. M. F. Laser-Induced Graphene Sensor for Electrochemical Determination of Nimesulide. *Braz. J. Anal. Chem.* 2026, *13* (52), pp 119-132. https://doi.org/10.30744/brjac.2179-3425.AR-71-2025

Submitted: August 18, 2025; **Revised:** February 4, 2026; **Accepted:** March 10, 2026; **Published online:** May 4, 2026.

This article is part of the BrJAC Special Issue dedicated to the 21st ENQA and 9th CIAQA.

and a broad linear range, which are notably advantageous for pharmaceutical quality control applications where analyte concentrations are relatively high. These results highlight unmodified LIG as a practical, cost-effective, and scalable sensing platform for routine nimesulide analysis.

Keywords: nimesulide, laser-induced graphene electrode, electrochemical detection, pharmaceutical analysis

INTRODUCTION

Nimesulide (NMS) is a non-steroidal anti-inflammatory drug (NSAID) belonging to the sulfonamide class, with analgesic and antipyretic properties.[1,2] It is widely prescribed in Brazil due to its superior efficacy compared to similar drugs such as diclofenac, ibuprofen, and piroxicam.[3] Despite its advantages, including low cost and rapid onset of action, indiscriminate administration, particularly at high doses or in combination with other drugs, can lead to severe side effects, including gastric, hepatic, and renal damage, as well as renal insufficiency and hepatotoxicity.[4-8] NSAIDs are one of the most widely used classes of drugs worldwide, employed in treating acute and chronic pain associated with inflammatory processes. These drugs possess anti-inflammatory, analgesic, and antipyretic properties, which stem from their ability to inhibit prostaglandin synthesis by blocking cyclooxygenase enzymes COX-1 and COX-2. This action has led to the creation of subgroups of selective and non-selective COX-2 inhibitors.[9] NSAIDs are primarily used to alleviate symptoms of osteoarthritis, rheumatoid arthritis, fever, and pain.[6]

Various analytical techniques, such as spectrophotometric and chromatographic methods with UV-vis or mass spectrometric detection[10,11] have been employed to determine NMS. However, these techniques are often associated with high costs, complex sample pre-treatment steps, and the generation of toxic waste.[12] In this regard, electroanalytical methods offer several advantages over conventional approaches, including lower reagent consumption, shorter analysis time, lower instrumentation costs, and fewer toxic reagents.[13]

In electroanalytical techniques, the choice of the working electrode is fundamental for the development of analytical methods.[13] Among carbon-based materials, graphene has emerged as a prominent option due to its high electrical conductivity, large surface area, and mechanical strength.[14] A particularly attractive form is laser-induced graphene (LIG), which is produced through a direct and rapid laser scribing process that converts sp^3 carbon into sp^2 carbon on polymeric substrates. This fabrication method is simple, cost-effective, and scalable, eliminating the need for complex synthesis steps and chemical treatments typically required for graphene production.[15,16]

Laser-induced graphene electrodes (LIGe) have shown promise in pharmaceutical detection. Recent studies have demonstrated its efficacy as a portable platform for the electrochemical detection of tyrosine[15] and ivermectin,[17] employing voltammetric techniques that exhibited broad linear ranges, low detection limits, and good selectivity against interferents. However, to our knowledge, no studies have reported the use of LIG for the analysis of NMS. In fact, only one work describes the use of LIG for the determination of NSAID. Wanjari et al. (2024)[18] report the use of two different LIGs (based on Poly(ether sulfone) – PES, and polyimide – PI substrates) for the analysis of diclofenac. The authors explored the adsorptive and spontaneous interaction of diclofenac with LIG and applied the sensors in the analysis of the NSAID in water samples.

Although laser-induced graphene (LIG) has been widely explored as a versatile platform for electrochemical sensing, most reported LIG-based sensors rely on chemical modification, nanoparticle decoration, or biofunctionalization to achieve enhanced sensitivity. Similarly, the majority of electrochemical methods reported for nimesulide determination employ multi-step electrode modification strategies, such as carbon paste formulation with modifiers, nanocomposite synthesis, or polymer electrodeposition, to reach ultralow detection limits. While these approaches are effective for trace-level analysis, they often increase fabrication complexity, preparation time, and batch-to-batch variability.

In this context, the present work addresses a practical gap by investigating the use of unmodified polyimide-based laser-induced graphene (LIG) electrodes for nimesulide determination. Rather than targeting the lowest possible detection limit, the proposed approach focuses on achieving a wide linear working range combined with minimal fabrication complexity, aiming at applications where analyte concentrations are relatively high and rapid, low-cost analysis is required. In this study, NMS was successfully determined in pharmaceutical formulations and synthetic urine using an unmodified disposable LIG electrode fabricated by CO_2 laser ablation of polyimide (Kapton). Square-wave voltammetry (SWV), fully optimized with respect to pH and instrumental parameters, provided fast voltammetric responses enabling straightforward NMS quantification without electrode modification or complex sample pretreatment. As a result, the sensor proved to be a reliable, cost-effective, and efficient tool for NMS determination in pharmaceutical and simulated biological matrices, highlighting its potential for routine quality control and preliminary clinical applications.

MATERIALS AND METHODS

Reagents and solutions

All reagents used in this work were of analytical grade and used as received. The aqueous solutions were prepared with high-purity deionized water with a resistivity of at least 18 MΩ cm, obtained from a Millipore Direct 8 water purification system (Millipore®, Germany). A stock solution containing 5.0 mmol L^{-1} NMS (Sigma-Aldrich®, USA) was prepared in 0.10 mol L^{-1} sodium hydroxide (Isofar®, Brazil). Prior to conducting the experiments, this solution was diluted using a suitable supporting electrolyte. A 0.12 mol L^{-1} Britton-Robinson (BR) buffer solution was formulated from acetic acid, boric acid, phosphoric acid, and potassium chloride reagents (Isofar®, Brazil). Additionally, a 0.10 mol L^{-1} phosphate buffer (PB) solution was prepared with monosodium phosphate and disodium phosphate (Isofar®, Brazil).

Preparation of the electrode

The LIGe was fabricated using a WorkSpecial WS4040 CO_2 laser cutter (São Paulo, Brazil) equipped with a 10.6 μm wavelength laser and a total power of 40 W. The electrode design was created using RDWorks 8.0 software and fabricated using a power of 0.9 W, a pulse duration of 14 μs, and a printing speed of 40 mm s^{-1}. The laser was positioned 10 mm above the polyimide substrate, and a batch of four electrodes was produced within 280 seconds. To delimit the working electrode area, a layer of commercial colorless nail polish was applied. After drying at room temperature, a copper tape was used to establish improved electrical contact.[17]

Electrochemical measurements

Experiments involving cyclic voltammetry (CV) and square wave voltammetry (SWV) were conducted using an Autolab PGSTAT-128N potentiostat/galvanostat (Metrohm Autolab, Utrecht, Netherlands). This equipment was connected to a microcomputer and operated with NOVA 2.2.1 software, in conjunction with a non-heating magnetic stirrer (Fisatom, São Paulo, Brazil). Baseline correction was applied to all experiments data using the moving average mode (window size 2) within the NOVA 2.2.1 software. Electrochemical tests were conducted in a cylindrical electrochemical cell with an internal volume of approximately 10 mL. A platinum wire served as the counter electrode, a miniaturized Ag|AgCl|KCl (3.0 mol L^{-1}) reference electrode was used, LIGe functioned as the working electrode, and magnetic stirring was employed between measurements.

Sample preparation

Pharmaceutical samples containing 100 mg of NMS per tablet were purchased from local drug stores in São Luís, MA, Brazil. Ten tablets were finely ground using a mortar and pestle. An accurately weighed portion of approximately 88.32 mg of the powdered sample was transferred to a 50.0 mL volumetric flask and dissolved in a 0.10 mol L^{-1} NaOH solution. The solution was placed in an ultrasonic bath for 20

minutes to ensure complete dissolution. In the final step, it was diluted to the required concentrations using a supporting electrolyte. The synthetic urine sample was prepared following the procedure described by Laube et al.[19] Specifically, 0.73 g of NaCl, 0.40 g of KCl, 0.28 g of $CaCl_2 \cdot 2H_2O$, 0.56 g of Na_2SO_4, 0.35 g of KH_2PO_4, 0.25 g of NH_4Cl, and 6.25 g of urea were dissolved in water in a 250.0 mL volumetric flask. This mixture was then diluted in a 0.10 mol L^{-1} NaOH solution at a 1:10 ratio and supplemented with three varying concentrations of NMS.

RESULTS AND DISCUSSION

Electrochemical behavior of NMS

The initial study focused on investigating the electrochemical behavior of NMS across a wide potential range, as this analyte contains two redox centers within its molecule: the $–NO_2$ group, which undergoes reduction at more negative potentials, and the –NH group, which oxidizes at less negative potentials. To ensure accurate measurements, oxygen was removed from the solution, as its presence could interfere at negative potentials. Figure S1 shows the cyclic voltammogram obtained over a potential range of +1.5 to -1.2 V. Two reduction peaks are observed at approximately 0.0 V and -0.5 V, corresponding to the reduction of the nitro group and its derivatives. These form two redox pairs with oxidation peaks around +0.06 V and +0.6 V. The oxidation peaks observed beyond these potentials are associated with the –NH group.[20-22]

This work focuses on developing a simple and rapid method for the determination of NMS. A potential range of +0.5 to +1.3 V was selected to avoid interference from oxygen reduction and the formation of byproducts at more negative potentials. As shown in Figure 1A, an anodic peak (Ipa) was observed at approximately +1.0 V, with no corresponding reduction peak, indicating that the electrode process in this potential window is irreversible. Similar behavior has been reported in previous studies on NMS oxidation,[1,13] and according to the literature, this anodic peak is attributed to the irreversible oxidation of the methylsulfonamide group in the NMS structure.[23,24] Although nimesulide exhibits multiple electrochemical processes, as evidenced in Figure S1, the analytical strategy adopted in this work was based on the selective use of this single redox process, which provides a well-defined, intense, and reproducible voltammetric signal within a safe potential window, thereby minimizing matrix interferences and electrode fouling. While the simultaneous exploration of multiple redox processes could, in principle, enhance selectivity, it generally increases methodological complexity and reduces robustness for routine analysis. Therefore, the selected anodic process represents the best compromise between sensitivity, selectivity, and operational simplicity for practical sensor applications.

The mass transport of the NMS molecule at the proposed electrode was investigated using a 0.12 mol L^{-1} PB solution containing 30.0 µmol L^{-1} NMS, with a scan rate range from 10 to 100 mV s^{-1} (see Figure 1B). The relationship between the peak current and the square root of the scan rate (Figure 1C) exhibited good linearity, with a correlation coefficient of 0.9978. This result suggests that the electron-transfer process governing mass transport occurs via diffusion. To validate this finding further, the relationship between the logarithm of the peak current and the logarithm of the scan rate (Figure 1D) was examined, leading to the equation $\text{Log } I_p = 0.426 \text{ Log } v – 0.514$. In such analyses, coefficients near 0.5 or 1.0 usually suggest that mass transfer is mainly governed by diffusion or adsorption, respectively.[25,26] The coefficient derived in this research suggests that the electron-transfer process controlling the mass transport of NMS at the proposed electrode is primarily diffusion-driven, consistent with existing literature.[27,28]

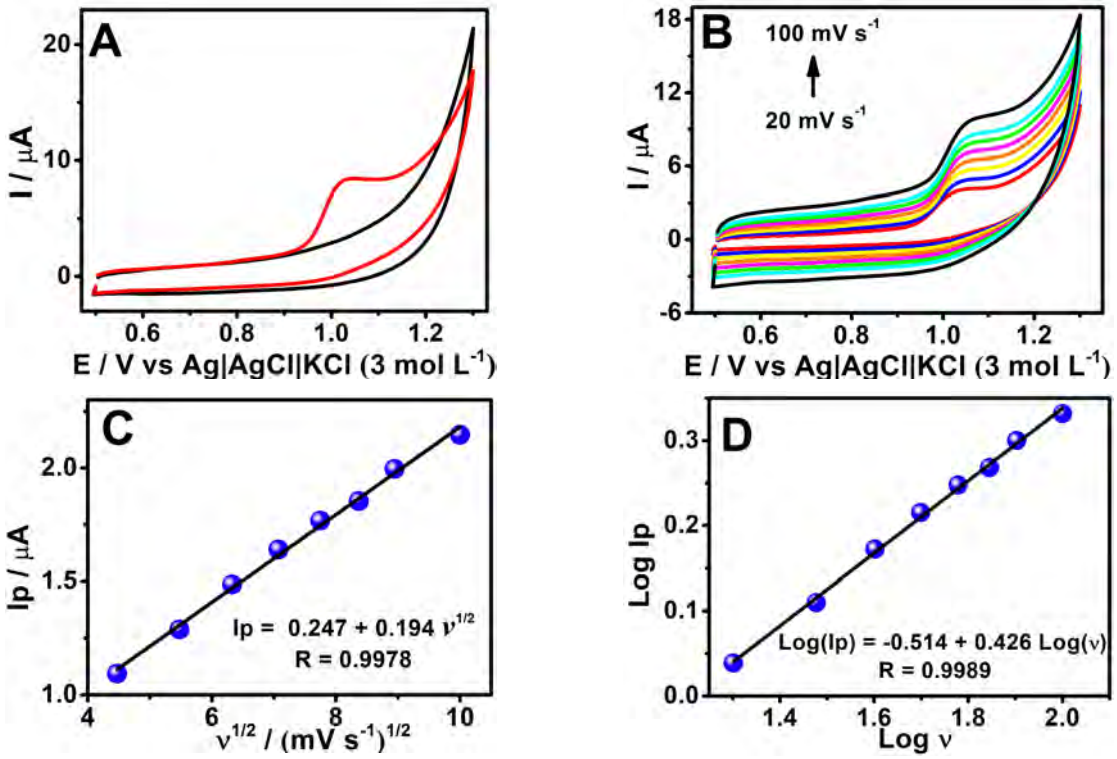

Figure 1. Cyclic voltammograms were obtained using LIGe in a 0.12 mol L^{-1} PB solution at pH 5.00. (A) The response is shown without (black line) and with (red line) 30.0 µmol L^{-1} NMS. The instrumental settings were a scan rate of 50 mV s^{-1} and a step potential of 5 mV s^{-1}. (B) Voltammograms at varying scan rates (v) from 10 to 100 mV s^{-1} in the presence of 30.0 µmol L^{-1} NMS. (C) The relationship between the peak current (Ip) and the square root of the scan rate ($v^{1/2}$). (D) The relationship between the logarithm of the peak current (log Ip) and the logarithm of the scan rate (log v).

The kinetic parameters of the electrode process were further investigated. Based on the Laviron theory for irreversible systems, the relationship between the peak potential (E_p) and the natural logarithm of the scan rate (ln(v)) was analyzed (Figure S2). From this analysis, the charge transfer coefficient (α) was determined to be 0.9, and the number of electrons (n) transferred in the process was calculated as 1.7. This value is close to 2, which is consistent with the NMS oxidation mechanism reported in the literature.[13,23,27,28]

Through the pH study (Figure 2), the Nernst equation was used to determine the proton-to-electron ratio involved in the oxidation of NMS on the LIGe surface.[29] The slope obtained was 63.4 mV/pH. This value is very close to the theoretical slope of 59.2 mV per pH unit at 25 °C for a 1:1 proton-to-electron ratio. These results suggest an oxidation mechanism involving the transfer of two protons and two electrons. Regarding the optimal pH for analysis, the maximum current was obtained at pH 2.00. However, this potential is undesirably high, as it increases the risk of interference from other electroactive species, potentially compromising selectivity. Consequently, pH 7.00 was selected for subsequent studies, as it provided a high current response at a more favorable potential.

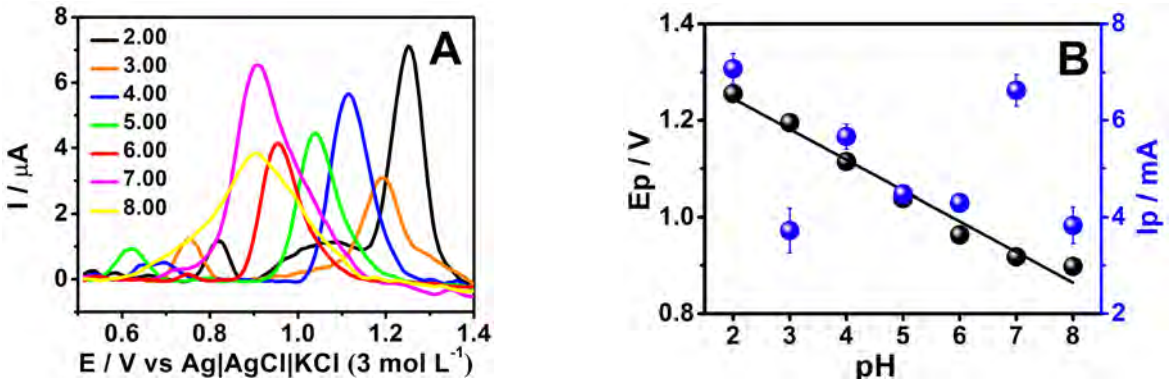

Figure 2. (A) Square wave voltammograms recorded with LIGe in the presence of NMS (10.0 µmol L^{-1}) in BR buffer solution (0.12 mol L^{-1}) at different pH values (2.00 – 8.00). (B) Dependence of the peak current (Ip) and peak potential (Ep) on the pH of the medium. Experimental conditions: amplitude = 60 mV; frequency = 10 Hz; potential increment = 5 mV.

SWV system optimization and analytical performance

To enhance the experimental conditions, the parameters of SWV, including pulse amplitude (20 to 100 mV), potential increment (2 to 10 mV), and frequency (5 a 25 Hz), were systematically optimized (Figure S3). These evaluations were conducted using a 10.0 µmol L^{-1} NMS solution prepared in 0.12 mol L^{-1} PB at pH 7.00. The selection of the optimal parameters was guided by criteria such as stability, reproducibility, current intensity, and peak resolution, ensuring robust and precise analytical performance. The optimal analytical parameters for NMS determination using SWV are summarized in Table I. Therefore, the optimal values of the SWV operational parameters chosen were frequency (*f*) = 15 Hz, amplitude (*a*) = 60 mV, and step potential (ΔE) = 10 mV.

Table I. Experimental parameters evaluated for SWV technique, and the corresponding values selected for determining NMS

Parameter	Range	Optimized
Frequency (Hz)	5 to 25	15
Amplitude (mV)	20 to 100	60
Step potential (mV)	2 to10	10

After optimizing the SWV parameters, the analytical curve was constructed by successively adding aliquots of the stock solution (1.0 mmol L^{-1}) of NMS into the electrochemical cell containing 0.12 mol L^{-1} PB (pH 7.00) using the LIGe. As shown in Figure 3, the analytical curve exhibited linearity in the concentration range of 11.0 to 131 µmol L^{-1}, following the linear regression equation: Ip (µA) = 5.00 + 0.181C_{NMS} (µmol L^{-1}), with r^2 = 0.999. The equations LOD = 3.3 s/b and LOQ = 10 s/b were employed to determine the limits of detection (LOD) and quantification (LOQ), where s represents the standard deviation of the blank and b denotes the slope of the analytical curve. The LOD and LOQ were found to be 1.30 and 4.30 µmol L^{-1}, respectively.

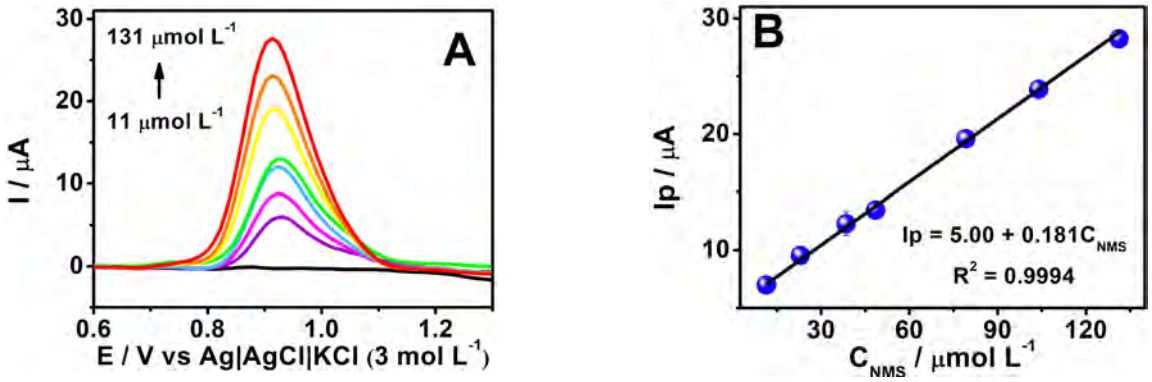

Figure 3. (A) Square wave voltammograms obtained using LIGe for NMS concentrations ranging from 11.0 to 131 μmol L^{-1} in 0.12 mol L^{-1} PB (pH 7.00). SWV parameters: *f* = 15 Hz, *a* = 60 mV, *ΔEs* = 10 mV. (B) Analytical curve (Ip *vs*. C_{NMS}).

The analytical performance of the proposed unmodified LIG sensor should be interpreted in the context of both its intended application and the fabrication strategy adopted. As summarized in Table II, electrochemical sensors for nimesulide span a broad spectrum of analytical characteristics. Methods based on nanocomposites or chemically modified electrodes typically achieve detection limits in the nanomolar range; however, they require complex multi-step fabrication procedures, including nanoparticle synthesis, polymer electrodeposition, or composite formulation, which substantially increase preparation time and experimental complexity.

In contrast, the unmodified LIG electrode developed in this work provides a wide linear range of 11–131 μmol L^{-1} (120 μmol L^{-1} span), which is comparable to or broader than that reported for many modified electrodes, despite the complete absence of chemical modification. Among unmodified electrodes reported in the literature, the present sensor exhibits one of the widest working ranges, while maintaining straightforward fabrication by direct CO_2 laser ablation.

Although the detection limit (1.30 μmol L^{-1}) is higher than those achieved by heavily modified sensors, this value is fully adequate for pharmaceutical quality control, where typical working concentrations after sample preparation are on the order of 50–200 μmol L^{-1}. In this application context, ultra-low detection limits are not a strict requirement, whereas a broad linear range, minimal sample dilution, and operational simplicity are highly advantageous. The results therefore demonstrate a deliberate trade-off between ultimate sensitivity and practical applicability, favoring simplicity, scalability, and reproducibility.

Table II. Comparison of analytical parameters obtained by different methods reported in the literature for NMS determination

Electrode	Technique	Linear Range (μmol L^{-1})	LOD (μmol L^{-1})	Samples	Ref.
BNC/CPE	SWV	0.01 – 0.55	11×10^{-3}	Urine / Pharmaceutical Samples	30
3D-printed CB/PLA	DPV	1 – 75	0.193	Wastewater	31
SiC-NPs/GCE	DPV	0.9 – 8.7	0,03	Human blood serum	32
GR/p(L-Cys)/GCE	DPV	1.0 – 55.0	0.3	Tap Water / River Water	28
LIGe	**SWV**	**11.0 – 131.0**	**1.29**	**Urine / Pharmaceutical Samples**	**This work**

BNC: bentonite clay; CPE: Carbon paste electrode; GR/p(L-Cys): poly(L-cysteine) and graphene composite; GCE: Glassy Carbon Electrode; SiC-NPs: Carbon silica nanoparticles; CB/PLA: carbon black/filled polylactic acid.

To assess the precision of the proposed method for the determination of NMS, a repeatability study was conducted based on the analytical signal obtained from 10 consecutive measurements in a standard solution of NMS (30.0 μmol L^{-1}) under optimized conditions. From the results presented in Figure S4, it can be observed that there was no significant variation in current values, as the relative standard deviation (RSD) of the analysis is below 5%. This indicates good stability in the electrode response and suggests that no significant decrease in electrode activity was observed.

An interference study was conducted using the SWV technique. The effect of potential interferents was evaluated at 1:10 ratio (NMS:interferents) by comparing the anodic peak currents obtained in absence and presence of each species (Table III). As observed, there was no significant interference in the determination of NMS, as the variations remained below 3.0%. Therefore, the methodology can be effectively applied for NMS detection even in the presence of these species.

Table III. Effect of potential interferents on the voltammetric determination of NMS at a concentration level of 1.0 mmol L^{-1}

Interferent	Interferent Ratio	Ip Variation (%)
Urea	1:10	2.24
Glicose	1:10	0.37
Oxalic Acid	1:10	2.66
Citric Acid	1:10	2.27

Sample analysis

To analyze the pharmaceutical sample, NMS determination was performed using the external calibration curve equation: $Ip(\mu A) = 5.00 + 0.181C_{NMS}$ (μmol L^{-1}). For the pharmaceutical samples, the result obtained was 101 mg/tablet of NMS. According to the information provided by the manufacturer, the declared NMS mass per tablet is 100 mg. This result aligns with the specifications presented in the pharmacopeia, which establishes a minimum of 95% and a maximum of 105% of the declared NMS content in tablets.[33] The determination of NMS was also carried out in synthetic urine samples at three different concentrations (44.4, 58.4, and 85.1 μmol L^{-1}), and the analysis was based on an external calibration curve (Figure S5), given by the equation $Ip(\mu A) = 5.28 + 0.196C_{NMS}$ (μmol L^{-1}), and the results were assessed in terms of percentage recovery, as summarized in Table IV.

It should be noted that the concentrations of nimesulide evaluated in synthetic urine were selected exclusively for analytical validation purposes and were not intended to reproduce physiological urinary levels. Under therapeutic conditions, nimesulide undergoes extensive hepatic metabolism, and less than 0.5% of the administered dose is excreted in urine as unchanged drug, with elimination occurring predominantly as hydroxylated and conjugated metabolites, especially 4′-hydroxynimesulide.[34,35] Radiolabeled studies further confirm that urinary excretion reflects metabolic products rather than the parent compound.[34,36] Therefore, the concentration levels employed in synthetic urine were chosen to fall within the linear working range of the sensor and to ensure reliable evaluation of accuracy and recovery in a complex matrix, rather than to simulate real urinary concentrations.

Table IV. Determination of NMS in synthetic urine samples

Sample	Spiked (μmol L^{-1})	Found (μmol L^{-1})	Recovery (%)
Synthetic urine	44.4	42.9 ± 1.5	97
	58.4	63.8 ± 5.4	109
	85.1	94.8 ± 9.7	111

CONCLUSION

This work demonstrates, for the first time, the potential of unmodified laser-induced graphene (LIG) electrodes for the electrochemical determination of nimesulide. Voltammetric studies showed that NMS oxidation is an irreversible, diffusion-controlled process involving the transfer of two protons and two electrons. Systematic optimization of experimental parameters (electrolyte pH and SWV conditions) resulted in reliable analytical performance, with a wide linear range of 11.0–131 μmol L^{-1} (120 μmol L^{-1} span) and a detection limit of 1.30 μmol L^{-1}. The sensor was successfully applied to pharmaceutical tablets, providing results consistent with the declared content (101 mg per tablet versus 100 mg per tablet). Recovery values in synthetic urine ranged from 97% to 111%, indicating acceptable accuracy in a complex matrix. Interference studies demonstrated that common non-electroactive urinary constituents, such as urea, glucose, oxalic acid, and citric acid, caused only minor signal variations (<3%), supporting adequate selectivity toward these species. Importantly, the main contribution of this work does not lie in achieving the lowest detection limit reported in the literature, but in combining a broad linear working range with extremely simplified fabrication, eliminating chemical modification and nanomaterial synthesis. Although the detection limit is higher than that of ultra-sensitive modified electrodes, it is fully adequate for pharmaceutical quality control applications, where analyte concentrations are typically much higher. The balance between analytical performance, fabrication speed, low cost, and disposability positions the proposed unmodified LIG sensor as a practical and attractive alternative for routine analysis and rapid screening, while further studies in real biological samples are encouraged to expand its clinical relevance. Further validation using multiple independent samples, statistical comparison tests, and reference analytical methods is required to fully establish the accuracy of the proposed sensor.

Acknowledgements

The authors are grateful for the financial support provided by the Brazilian agencies Fundação de Amparo à Pesquisa e ao Desenvolvimento Científico e Tecnológico do Maranhão – FAPEMA (00930/22, 00901/22); Coordenação de Aperfeiçoamento de Pessoal de Nível Superior – CAPES (Finance Code 001, 88887.658022/2021-00), and Conselho Nacional de Desenvolvimento Científico e Tecnológico – CNPq (444777/2024-5).

Conflicts of interest

The authors declare no competing financial interest.

Use of Artificial Intelligence (AI) tools

The authors acknowledge using the Grammarly tool exclusively for linguistic revision to improve clarity, grammar, spelling, and fluency. The AI tool Google Gemini was used to generate part of the graphical abstract. The authors take full responsibility for the accuracy, integrity, and originality of the work and confirm that no AI tools were used to generate scientific ideas, analyze data independently, or replace the authors' critical role.

REFERENCES

(1) de Oliveira, W. B. V.; Lisboa, T. P.; de Souza, C. C.; Matos, M. A. C.; Matos, R. C. Composite Material Immobilized in 3D-Printed Support, an Economical Approach for Electrochemical Sensing of Nimesulide. *Microchem. J.* **2023**, *188*, 108463. https://doi.org/10.1016/j.microc.2023.108463

(2) Ho, C. V.; Pazourek, J. Rapid Determination of Nimesulide by Capillary Zone Electrophoresis in Various Pharmaceutical Formulations. *Separations* **2025**, *12* (5), 132. https://doi.org/10.3390/separations12050132

(3) de Almeida, A. C.; Ferreira, P. O.; Porto, M. V.; Canotilho, J.; de Castro, R. A. E.; Caires, F. J.; Eusébio, M. E. S. Novel Nimesulide Multicomponent Solid Forms: Screening, Synthesis, Thermoanalytical Study and Characterization. *J. Therm. Anal. Calorim.* **2025**, *150*, 6885-6897. https://doi.org/10.1007/s10973-024-13189-2

(4) Regi, J. K.; Lalwani, K.; Pawar, S. Comparative Trends in the Usage of Nonsteroidal Anti-Inflammatory Drugs: Self-Administration versus Prescription. *MGM Journal of Medical Sciences* **2024**, *11* (1), 139–145. https://doi.org/10.4103/mgmj.mgmj_145_22

(5) Arfeen, M.; Srivastava, A.; Srivastava, N.; Khan, R. A.; Almahmoud, S. A.; Mohammed, H. A. Design, Classification, and Adverse Effects of NSAIDs: A Review on Recent Advancements. *Bioorg. Med. Chem.* **2024**, *112*, 117899. https://doi.org/10.1016/j.bmc.2024.117899

(6) Yue, X.; Xu, X.; Liu, C.; Zhao, S. Simultaneous Determination of Cefotaxime and Nimesulide Using Poly(L-Cysteine) and Graphene Composite Modified Glassy Carbon Electrode. *Microchem. J.* **2022**, *174*, 107058. https://doi.org/10.1016/j.microc.2021.107058

(7) Lavande, J. P.; Bais, S. K.; Kharat, V. Active Pharmaceutical Ingredient and Impurity Profiling Nimesulide. *International Journal of Advanced Research in Science, Communication and Technology* **2023**, 525–536. https://doi.org/10.48175/IJARSCT-9248

(8) Pandey, S. K.; Pudasaini, J.; Parajuli, H.; Singh, R. E.; Shah, K. P.; Adhikari, A.; Rokaya, R. K. Formulation and Evaluation of Floating Tablet of Nimesulide by Direct Compression Method. *Magna Scientia Advanced Research and Reviews* **2024**, *10* (1), 153–161. https://doi.org/10.30574/msarr.2024.10.1.0008

(9) Kamble, S.; Bangale, G.; Deshmukh, R.; Dawargave, K.; Shingare, D.; Suryawanshi, O.; Kadam, K. Development and Optimization of Nimesulide Loaded Transethosomal Gel. *Bionanoscience* **2025**, *15* (2), 223. https://doi.org/10.1007/s12668-025-01802-z

(10) Waheb, A. A.; Rasheed, A. S.; Hassan, M. J. M. Strategies for the Separation and Quantification of Non-Steroidal Anti- Inflammatory Drugs Using ZIC-HILIC-HPLC with UV Detection. *Curr. Pharm. Anal.* **2022**, *18* (10), 949–958. https://doi.org/10.2174/1573412918666220915090831

(11) Sheikholeslami, M. N.; Gómez-Canela, C.; Barron, L. P.; Barata, C.; Vosough, M.; Tauler, R. Untargeted Metabolomics Changes on Gammarus Pulex Induced by Propranolol, Triclosan, and Nimesulide Pharmaceutical Drugs. *Chemosphere* **2020**, *260*, 127479. https://doi.org/10.1016/j.chemosphere.2020.127479

(12) Łysoń, M.; Górska, A.; Paczosa-Bator, B.; Piech, R. Nimesulide Determination on Carbon Black-Nafion Modified Glassy Carbon Electrode by Means of Adsorptive Stripping Voltammetry. *Electrocatalysis* **2021**, *12* (6), 641–649. https://doi.org/10.1007/s12678-021-00676-5

(13) Deroco, P. B.; Rocha-Filho, R. C.; Fatibello-Filho, O. A New and Simple Method for the Simultaneous Determination of Amoxicillin and Nimesulide Using Carbon Black within a Dihexadecylphosphate Film as Electrochemical Sensor. *Talanta* **2018**, *179*, 115–123. https://doi.org/10.1016/j.talanta.2017.10.048

(14) Inlumphan, S.; Wongwiriyapan, W.; Khemasiri, N.; Rattanawarinchai, P.; Leepheng, P.; Luengrojanakul, P.; Wuttikhun, T.; Obata, M.; Fujishige, M.; Takeuchi, K.; et al. Laser-Induced Graphene Electrochemical Immunosensors for Rapid and Sensitive Serological Detection: A Case Study on Dengue Detection Platform. *Sensors and Actuators Reports* **2025**, *9*, 100276. https://doi.org/10.1016/j.snr.2024.100276

(15) Matias, T. A.; Rocha, R. G.; Faria, L. V.; Richter, E. M.; Munoz, R. A. A. Infrared Laser-Induced Graphene Sensor for Tyrosine Detection. *ChemElectroChem* **2022**, *9* (14). https://doi.org/10.1002/celc.202200339

(16) Matias, T. A.; de Faria, L. V.; Rocha, R. G.; Silva, M. N. T.; Nossol, E.; Richter, E. M.; Muñoz, R. A. A. Prussian Blue-Modified Laser-Induced Graphene Platforms for Detection of Hydrogen Peroxide. *Microchim. Acta* **2022**, *189* (5), 188. https://doi.org/10.1007/s00604-022-05295-5

(17) Ferreira, D. C. M.; Inoque, N. I. G.; Tanaka, A. A.; Dantas, L. M. F.; Muñoz, R. A. A.; da Silva, I. S. Lab-Made CO_2 Laser-Engraved Electrochemical Sensors for Ivermectin Determination. *Anal. Methods* **2024**, *16* (25), 4136–4142. https://doi.org/10.1039/D4AY00414K

(18) Wanjari, V. P.; Kumar, P.; Duttagupta, S. P.; Singh, S. P. Adsorption-Enhanced Sensitivity for Electrochemical Sensing of Diclofenac by Poly(Ether Sulfone)-Based Laser-Induced Graphene. *Langmuir* **2025**, *41* (1), 152–161. https://doi.org/10.1021/acs.langmuir.4c03229

(19) Laube, N.; Mohr, B.; Hesse, A. Laser-Probe-Based Investigation of the Evolution of Particle Size Distributions of Calcium Oxalate Particles Formed in Artificial Urines. *J. Cryst. Growth* **2001**, *233* (1–2), 367–374. https://doi.org/10.1016/S0022-0248(01)01547-0
(20) Moscoso, R.; Álvarez-Lueje, A.; Squella, J. A. Nanostructured Interfaces Containing MWCNT and Nitro Aromatics: A New Tool to Determine Nimesulide. *Microchem. J.* **2020**, *159*, 105361. https://doi.org/10.1016/j.microc.2020.105361
(21) Goularte, R. B.; Winiarski, J. P.; Latocheski, E.; Jost, C. L. Novel Analytical Sensing Strategy Using a Palladium Nanomaterial-Based Electrode for Nimesulide Electrochemical Reduction. *J. Electroanal. Chem.* **2022**, *920*, 116622. https://doi.org/10.1016/j.jelechem.2022.116622
(22) Miranda, L.; Pereira, V. C.; Machado, C. S.; Torres, Y. R.; dos Anjos, V. E.; Quináia, S. P. Direct Determination of Nimesulide in Natural Waters and Wastewater by Cathodic Stripping Voltammetry. *Arch. Environ. Contam. Toxicol.* **2017**, *73* (4), 631–640. https://doi.org/10.1007/s00244-017-0425-6
(23) Bukkitgar, S. D.; Shetti, N. P.; Kulkarni, R. M.; Halbhavi, S. B.; Wasim, M.; Mylar, M.; Durgi, P. S.; Chirmure, S. S. Electrochemical Oxidation of Nimesulide in Aqueous Acid Solutions Based on TiO2 Nanostructure Modified Electrode as a Sensor. *J. Electroanal. Chem.* **2016**, *778*, 103–109. https://doi.org/10.1016/j.jelechem.2016.08.024
(24) da Silva, I. S.; Capovilla, B.; Freitas, K. H. G.; Angnes, L. Strategies to Avoid Electrode Fouling for Nimesulide Detection Using Unmodified Electrodes. *Anal. Methods* **2013**, *5* (14), 3546. https://doi.org/10.1039/c3ay40463c
(25) Fatibello-Filho, O.; Silva, T.; Moraes, F.; Sitta, E. *Eletroanálises - Aspectos Teóricos e Práticos.* EDUFSCAR, Ed., São Carlos, SP, 2022.
(26) Pacheco, W. F.; Semaan, F. S.; Almeida, V. G. K.; Ritta, A. G. S. L.; Aucélio, R. Q. Voltammetry: A Brief Review About Concepts. *Rev. Virtual Quim.* **2013**, *5* (4). https://doi.org/10.5935/1984-6835.20130040
(27) Shetti, N. P.; Malode, S. J.; Nayak, D. S.; Bukkitgar, S. D.; Bagihalli, G. B.; Kulkarni, R. M.; Reddy, K. R. Novel Nanoclay-Based Electrochemical Sensor for Highly Efficient Electrochemical Sensing Nimesulide. *J. Phys. Chem. Solids* **2020**, *137*, 109210. https://doi.org/10.1016/j.jpcs.2019.109210
(28) Yue, X.; Xu, X.; Liu, C.; Zhao, S. Simultaneous Determination of Cefotaxime and Nimesulide Using Poly(L-Cysteine) and Graphene Composite Modified Glassy Carbon Electrode. *Microchem. J.* **2022**, *174*, 107058. https://doi.org/10.1016/j.microc.2021.107058
(29) Dai, C.; Crawford, L. P.; Song, P.; Fisher, A. C.; Lawrence, N. S. A Novel Sensor Based on Electropolymerized Substituted-Phenols for PH Detection in Unbuffered Systems. *RSC Adv.* **2015**, *5* (126), 104048–104053. https://doi.org/10.1039/C5RA22595G
(30) Prabhu, K.; Malode, S. J.; Veerapur, R. S.; Shetti, N. P. Clay-Based Carbon Sensor for Electro-Oxidation of Nimesulide. *Mater. Chem. Phys.* **2021**, *272*, 124992. https://doi.org/10.1016/j.matchemphys.2021.124992
(31) Cieślik, M.; Rucka, M.; Siqueira, G. P.; Koterwa, A.; Rycewicz, M.; Muñoz, R. A. A.; Bogdanowicz, R.; Ryl, J. Multi-Material Integrated 3D-Printed Electrochemical Detection Platform for Rapid on-Site Screening of Nimesulide in Industrial Sewage. *Microchim. Acta* **2025**, *192* (11), 757. https://doi.org/10.1007/s00604-025-07634-8
(32) Ghavami, R.; Navaee, A. Determination of Nimesulide in Human Serum Using a Glassy Carbon Electrode Modified with SiC Nanoparticles. *Microchim. Acta* **2012**, *176* (3–4), 493–499. https://doi.org/10.1007/s00604-011-0710-4
(33) *Farmacopeia Brasileira* (5th Ed.) 2010, *1*, 1–523.
(34) Bernareggi, A. Clinical Pharmacokinetics of Nimesulide. *Clin. Pharmacokinet.* **1998**, *35* (4), 247–274. https://doi.org/10.2165/00003088-199835040-00001
(35) Carini, M.; Aldini, G.; Stefani, R.; Marinello, C.; Facino, R. M. Mass Spectrometric Characterization and HPLC Determination of the Main Urinary Metabolites of Nimesulide in Man. *J. Pharm. Biomed. Anal.* **1998**, *18* (1–2), 201–211. https://doi.org/10.1016/S0731-7085(98)00172-1

(36) Macpherson, D.; Best, S. A.; Gedik, L.; Hewson, A. T.; Rainsford, K. D.; Parisi, S. The biotransformation and pharmacokinetics of 14C-nimesulide in humans following a single dose oral administration. *J. Drug. Metab. Toxicol.* **2012**, *4* (01). https://doi.org/10.4172/2157-7609.1000140

SUPPLEMENTARY MATERIAL

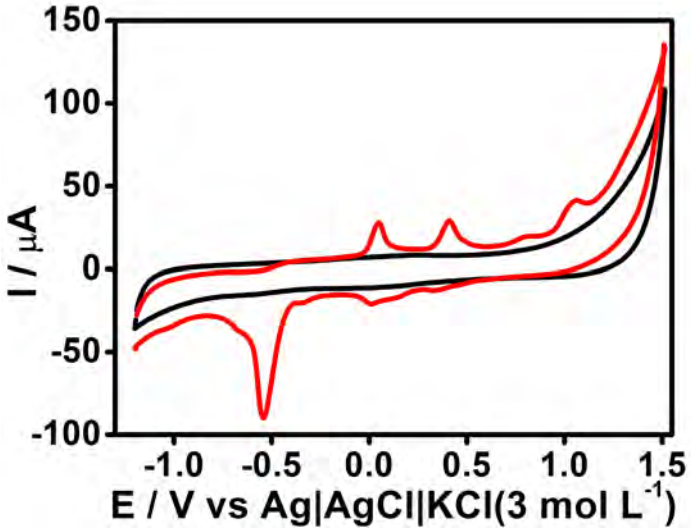

Figure S1. Cyclic voltammograms recorded in 0.12 mol L^{-1} PB solution pH 5.00 in the absence (black line) and presence (red line) of 100 µmol L^{-1} NMS. Instrumental conditions: scan rate = 50 mV s^{-1} and step potential = 5 mV s^{-1}.

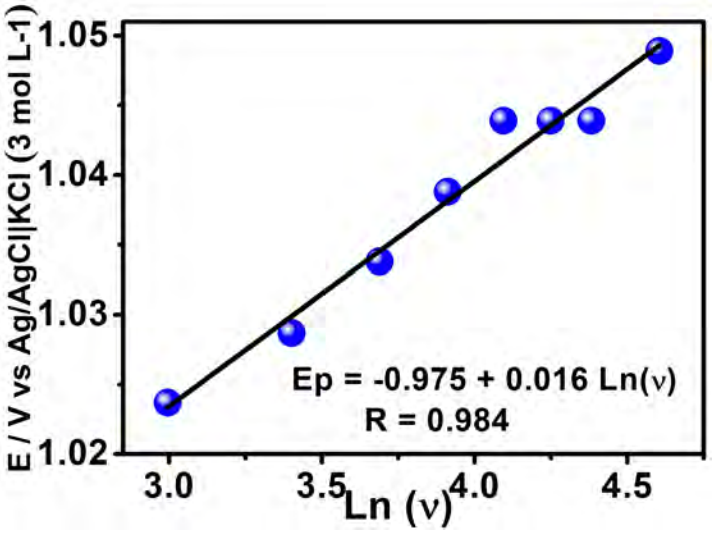

Figure S2. Dependence of the peak potential (Ep) on the natural logarithm of v in the presence of 30.0 µmol L^{-1} NMS. Experimental conditions: PB 0.12 mol L^{-1}; pH 5.00.

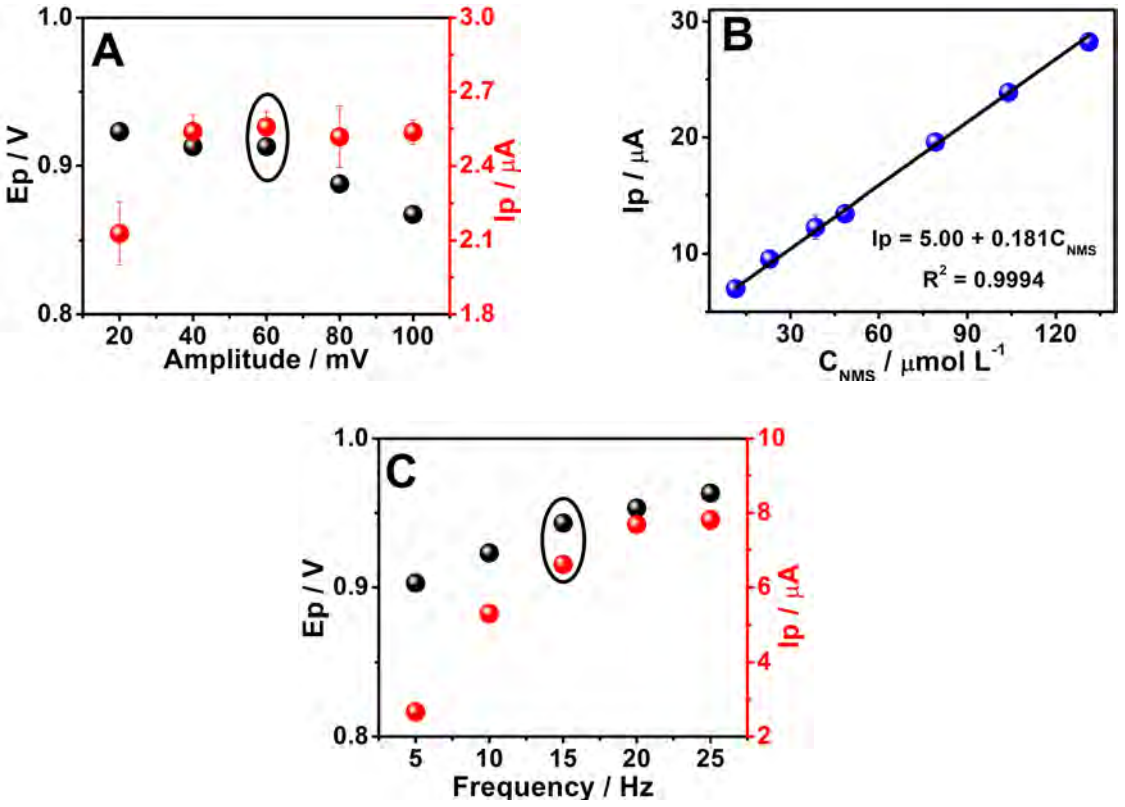

Figure S3. Optimizations of the SWV parameters: (A) amplitude (20.0 to 100 mV), (B) step potential (2.0 to 10.0 mV), and (C) frequency (5.0 to 25.0 Hz), in the presence of 10 μmol L^{-1} NMS. Experimental conditions: PB 0.12 mol L^{-1}; pH 7.00.

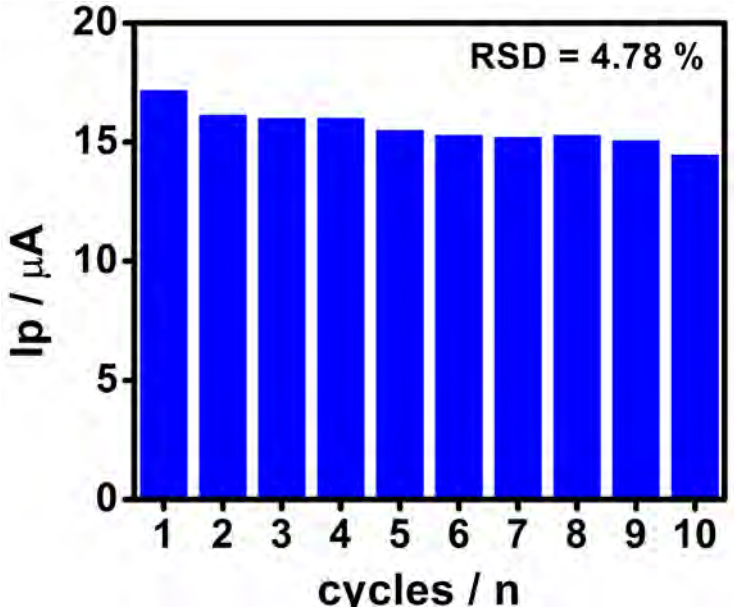

Figure S4. Repeatability study (*n*=10) of the LIGe electrode in the presence of NMS (30 μmol L^{-1}). Experimental conditions: 0.12 mol L^{-1} phosphate buffer; pH 7.0; a = 60 mV; f = 15 Hz; ΔEs = 10mV.

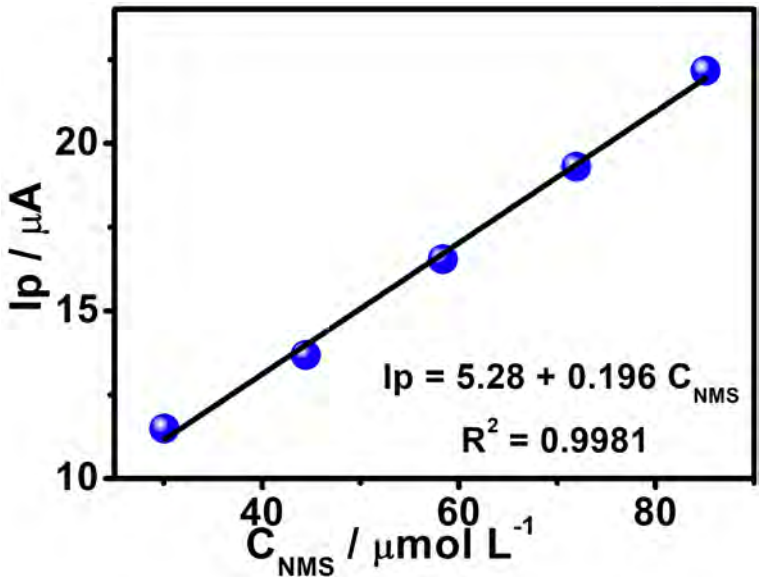

Figure S5. (A) Square wave voltammograms obtained using LIGe for NMS concentrations (44.4, 58.4, and 85.1 µmol L^{-1}) in synthetic urine. (B) External calibration curve (Ip vs. C_{NMS}). SWV parameters: *f* = 15 Hz, *a* = 60 mV, *ΔEs* = 10mV

Brazilian Journal of Analytical Chemistry
2026, Volume 13, Issue 52, pp 133-149
doi: 10.30744/brjac.2179-3425.AR-72-2025

BrJAC

ARTICLE

Evaluation of the Stability of Cannabidiol and delta-9-tetrahydrocannabinol in Cannabis-based Oily Product: Effects of Light, Temperature, Excipients and Antioxidant Additives

Aldo Sindulfo Barboza Valdez[1], Jeisson Brandway Blanco Castañeda[1], Nédice Borges Cardoso Rastely[1], Wagner Ferreira[1], Francisney Pinto Nascimento[2], Aline Theodoro Toci[1]*

[1]Laboratório de Estudos Interdisciplinares do Meio-Ambiente e Alimentos (LEIMAA), Universidade Federal da Integração Latino-Americana (UNILA) . Avenida Tancredo Neves, 6731, Foz do Iguaçu, PR, 85867-970, Brazil

[2]Laboratório de Cannabis Medicinal e Ciência Psicodélica (LCP), Universidade Federal da Integração LatinoAmericana (UNILA) . Avenida Tarquinio Santos Ave, 1000, Foz do Iguaçu, PR, 85870-650, Brazil

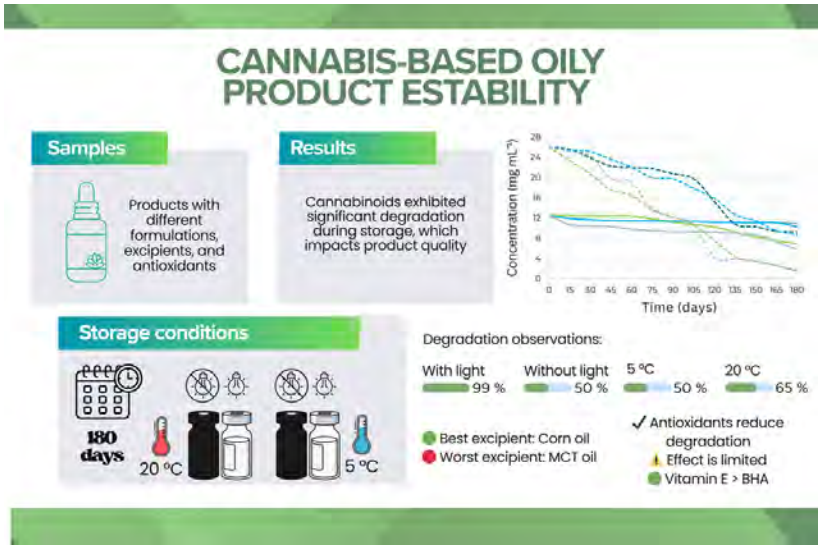

Due to the potential therapeutic effects of cannabis-based oily products and the increasing number of studies in this field, several producer associations have emerged in recent decades. Oral administration of formulations in oily excipients has been the most commonly used therapeutic route. However, the susceptibility of cannabinoids, such as delta-9-tetrahydrocannabinol (THC) and cannabidiol (CBD), to environmental factors is well known, and studies on the stability of cannabis-based oily products remain scarce. Therefore, research that supports associations in improving product quality and ensuring reliability is crucial. With these considerations, the objective of this study was to conduct a stability study of cannabis-based oil products containing CBD and THC under different storage conditions for 180 days. For the first time, the effects of temperature, light, excipients, and additives were evaluated together. Cannabinoid

Cite: Valdez, A. S. B.; Castañeda, J. B. B.; Rastely, N. B. C.; Ferreira, W.; Nascimento, F. P.; Toci, A. T. Evaluation of the Stability of Cannabidiol and delta-9-tetrahydrocannabinol in Cannabis-based Oily Product: Effects of Light, Temperature, Excipients and Antioxidant Additives. *Braz. J. Anal. Chem.* 2026, *13* (52), pp 133-149. https://doi.org/10.30744/brjac.2179-3425.AR-72-2025

Submitted: August 1, 2025; **Revised:** January 19, 2026; **Accepted:** January 30, 2026; **Published online:** March 5, 2026.

This article is part of the BrJAC Special Issue dedicated to the 21st ENQA and 9th CIAQA.

determination was performed using a validated HPLC-DAD methodology. Both CBD and THC were best preserved in corn and sesame oil, while medium-chain triglycerides were the worst excipient, reaching losses of 99%. Light was the most significant storage variable. In all samples, regardless of any other variable, the highest degradation rates were observed in the presence of light, for both CBD and THC. However, temperature exhibited less uniform behavior compared to light. Overall, the highest THC degradation occurred at 20 °C. The presence of antioxidants was not effective as expected. In sesame oil, lower degradation percentages of up to 10% were observed in samples containing butylhydroxyanisole. Regarding vitamin E, in general, the degradation rate was 2 to 11% and 3 to 22% lower than in samples without the vitamin, for CBD and THC, respectively. The addition of antioxidants shows promise but requires further study.

Keywords: cannabis-based oily products, cannabidiol, delta-9-tetrahydrocannabinol, photodegradation, cannabinoid stability

INTRODUCTION

In medicinal cannabis treatments, the predominant route of administration is oral, through oils, solutions, and formulated capsules.[1] This preference is due to its slow absorption, prolonged effect, precise dosing, and greater safety and convenience for the patient.[2] Given that cannabinoids are lipophilic compounds, their incorporation into oily vehicles is ideal, with vegetable oils being the most commonly used carriers. Among these, corn, sunflower, sesame, and olive oils are frequently employed, as well as medium-chain triglycerides (MCT), the latter derived from coconut oil.[3]

Beyond their pharmaceutical form, it is important to consider how these compounds act. Cannabinoids are bioactive compounds that interact with the endocannabinoid system, an endogenous signaling network present in various tissues, especially in the central nervous system, which regulates functions such as pain, inflammation, sleep, appetite, and mood.[4,5] Among the main cannabinoids, cannabidiol (CBD) and delta-9-tetrahydrocannabinol (THC) stand out, both found in high concentrations in the flowers of *Cannabis sativa* L.[6]

The growing interest in their clinical applications has also driven the advancement of scientific research. In Brazil, Dr. Elisaldo Carlini was a pioneer in clinical studies on medicinal cannabis, standing out with more than 30 publications in the field. In 1980, he led one of the first studies that demonstrated the potential of CBD in controlling seizures in epileptic patients.[7]

As science has progressed, regulatory frameworks have also been developed to allow access to these treatments. In Brazil, since 2015, the National Health Surveillance Agency (ANVISA) has authorized the import and domestic production of cannabis-based medications under medical prescription. In 2019, Resolution RDC No. 327 established a stricter regulatory framework, limiting THC content to 0.2% and setting high standards of quality and safety.[8] Even so, access remains limited, which has led to the emergence of patient associations that produce medicinal products through artisanal or semi-automated methods, with judicial authorization for cultivation, extraction, and distribution.

Once in the hands of the patient, another key aspect is the product's stability, as it determines its efficacy over time. Cannabinoid molecules are susceptible to isomerization and oxidation under various factors.[9] Variables such as light, temperature, humidity, and oxygen exposure can accelerate degradation, reducing potency and generating less active secondary products, such as cannabinol (CBN), a derivative of oxidized THC.[10]

This can be explained by the chemical structure of THC and CBD themselves (Figure 1), which feature regions highly sensitive to ultraviolet light and oxidation, such as conjugated double bonds and hydroxyl groups. Light exposure can cause bond breakage and the formation of free radicals, initiating chain reactions that degrade the original molecule. For this reason, protecting formulations from these factors is essential to preserve their integrity.[11]

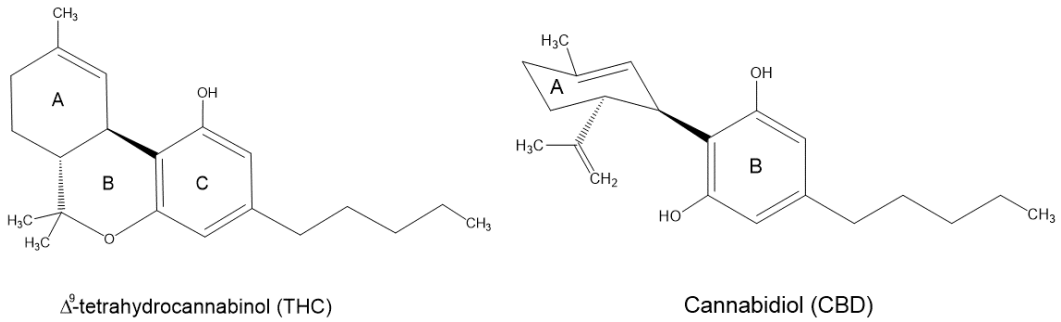

Figure 1. Chemical structures of THC and CBD.

Despite its relevance, the stability of cannabinoids in oily products based on medicinal cannabis has been scarcely studied. Nevertheless, some works have provided valuable information. Pacifici and collaborators[12] evaluated the stability of THC and CBD in olive oil over a 14-day period at 25 °C and 4 °C. They reported a degradation of 28% for THC and 20% for CBD at 25 °C, while at 4 °C the loss was 20% for both compounds.

Raslan-Jaramillo *et al*.,[13] in turn, studied oily extracts in coconut and sunflower oils. After 28 days of storage, both THC and CBD showed losses of less than 2% under refrigeration (4 ± 2 °C) or freezing (-20 ± 2 °C). Under room temperature (22 ± 2 °C) and light-protected conditions, CBD degraded by 5%, whereas THC degradation was 1.5%. In contrast, under light exposure at room temperature, THC lost 9% in three days, and CBD more than 19% in just one day, highlighting their instability under such conditions.

In oily extracts, Trofin *et al*.,[14] reported a 21.6% THC loss over one year under refrigeration and darkness, and 83.8% after four years. Under light and room temperature conditions, THC degraded by 23.2% in one year and by 89.9% over four years. CBD also degraded, with losses between 11.03% and 13.45% in the first year, depending on the storage conditions.[13]

In this context, the present study aimed to investigate the degradation of THC and CBD in cannabis-based oily products from Brazilian associations. The extracts were subjected to different storage conditions simulating real-life scenarios of temperature, light exposure, and storage time by patients. Additionally, the influence of the type of excipient and the presence of antioxidant additives on the stability of the compounds was evaluated.

MATERIALS AND METHODS

Samples

Twelve samples provided by Brazilian medicinal cannabis associations were analyzed. Their characteristics are described in Table I.

Table I. Chemical profile and characteristics of the Cannabis-based oily product analyzed

Sample	Company	Excipient	Additive	CBD (mg mL^{-1})	THC (mg mL^{-1})
1.a	A	MCT*	Vitamin E	12.5	12.4
1.b	A	MCT*	none	12.5	12.4
2.a	A	MCT*	Vitamin E	25.9	nd
2.b	A	MCT*	none	25.9	nd
3.a	A	MCT*	Vitamin E	nd	28.2
3.b	A	MCT*	none	nd	28.2
4.a	B	EVO**	Vitamin E	4.8	9.5
4.b	B	EVO**	none	4.8	9.5

(continued on next page)

Table I. Chemical profile and characteristics of the Cannabis-based oily product analyzed (continued)

Sample	Company	Excipient	Additive	CBD (mg mL^{-1})	THC (mg mL^{-1})
5.a	B	EVO**	Vitamin E	11.6	nd
5.b	B	EVO**	none	11.6	nd
6.a	B	EVO**	Vitamin E	nd	14.9
6.b	B	EVO**	none	nd	14.9
7	C	Corn oil	none	21.1	19.2
8	C	Corn oil	none	21.4	nd
9	D	Corn oil	BHA***	49.3	40.5
10	D	Corn oil	none	40.8	34.5
11	D	Sesame oil	BHA***	41.9	34.2
12	D	Sesame oil	none	42.5	37.0

Notes: *Medium-chain triglycerides; **Extra virgin olive oil (0.5% acidity); ***Butylated hydroxyanisole. Vitamine E was added for experimental purposes, while the samples containig BHA were obtained with the compound already incorporated.

Storage conditions

Sample storage was performed by placing 2 mL of each sample in 4 mL glass vials and storing them for 180 days, under controlled temperature conditions (5 and 20 °C) and in the presence or absence of light (Figure 2). In six samples (numbers 1a, 2a, 3a, 4a, 5a and 6a, as shown in Table I), 10 mg of vitamin E (equivalent to 1000 IU) was added.

Prepared sample vials were placed in custom-designed boxes under controlled temperature and light conditions. Boxes measuring 25 × 15 cm were made of pine plywood for 20 ± 1 °C storage (air-conditioned room) and cardboard for 5 ± 1 °C storage (refrigeration). Each box contained internal strips with 18 light-emitting diodes (LEDs) (3 mm) arranged within a 17 × 10 cm area, emitting white light in the 400–700 nm range. This illumination was selected for its common household use and low heat generation, minimizing interference with the system's internal temperature. Samples that were to be stored in the dark were covered with black tape to prevent light from reaching them. The samples were measured at the beginning of storage (time zero) and every 15 days, totaling 12 points.

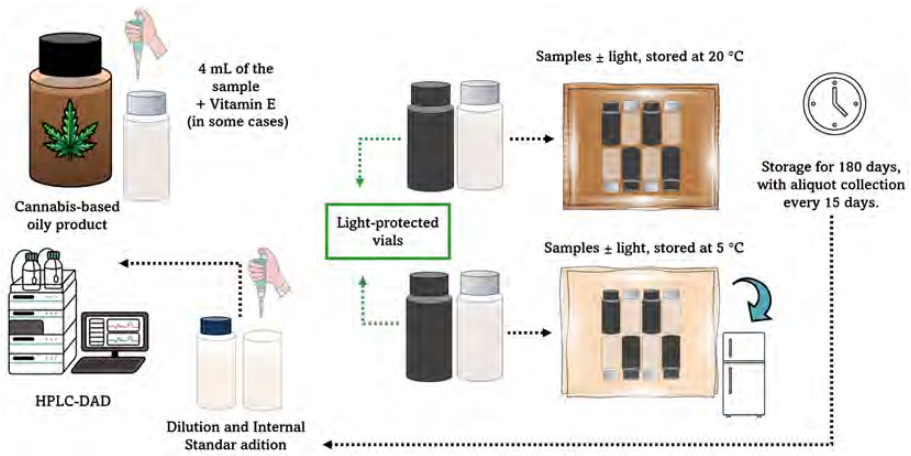

Figure 2. Experimental design to evaluate the stability of cannabinoids CBD and THC for 180 days.

CBD and THC quantification by HPLC-DAD

The determination of CBD and THC was performed according to the methodology proposed by Zivovinovic,[15] with some modifications. High-performance liquid chromatography (HPLC) coupled to a diode array detector (Ultimate 3000, Thermo®, Germany) was used, equipped with a quaternary pump 5600, an Accela 5600 autosampler, and a diode array detector (PDA Accela, 20 Hz, Thermo®, Germany). Data were processed using the Chromeleon 7.3.2 software (Thermo® Fisher Scientific). A C18 chromatographic column (250 × 4.6 mm, 5 µm particle size; ACE HPLC Columns, USA) was used at a constant temperature of 30 °C. Analytes were eluted in gradient mode with solvents (A) water with 0.1% formic acid and (B) acetonitrile with 0.1% formic acid, following the program: 30% A (2 min); 28.7% A from 2 to 4.5 min; 5% A from 4.5 to 6 min (held until 10 min); and back to 30% A from 10 to 20 min. The flow rate was 0.8 mL/min, and the injection volume was 5 µL. Detection was performed at a wavelength of 220 nm. THC and CBD were identified by comparing their spectra with those of reference standards and by their retention times.

Method validation

The quantification method for CBD and THC was validated prior to commencement of storage. The validation was conducted in accordance with the guidelines of the ICH (Harmonized Tripartite Guideline, 2005),[16] DOQ-CGCRE-008 from INMETRO[17] and ANVISA (RDC 166/2017 and RDC 899/2003)[18] through the determination of the selected parameters: selectivity, linearity, homoscedasticity, matrix effect, limits of detection (LOD), limits of quantification (LOQ) and precision.

Calibration curve

The following analytical standards were used: (−)-(6aR,10aR)-6,6,9-trimethyl-3-pentyl-6a,7,8,10a-tetrahydro-6H-benzo[c]chromen-1-ol with 2-[(1R,6R)-3-methyl-6-prop-1-en-2-ylcyclohex-2-en-1-yl]-5-pentylbenzene-1,3-diol (Dr. Ehrenstorfer, Germany). The calibration curve was prepared from an initial stock solution at a concentration of 200 µg mL^{-1}. The analytical curve was constructed by diluting the stock solution to obtain seven concentration points (0.5; 1; 2; 5; 10; 15 and 20 µg mL^{-1}). As the matrix effect was significant, the dilution solution contained 0.5% of a mix of oils in ethyl acetate and acetonitrile 1:1. The internal standard used was caffeine at a concentration of 100 µg mL^{-1} at each point of the calibration curve.

Sample preparation

At each storage period, 50 µL of sample was aliquoted and diluted in 1.5 mL vials, according to the initial sample concentration, generally 600 to 4000 times, with a 1:1 solution of ethyl acetate and acetonitrile, both HPLC grade. To each vial, 100 µL of the internal standard solution was added.

Statistical analysis

The normality of the data was verified by the Shapiro-Wilk test. The data were subjected to analysis of variance by ANOVA ($p \leq 0.05$), and in cases of significance, Tukey's test ($p \leq 0.05$) was used to compare the means. Both were performed with the Statistica software (StatSoft, version 14.1.0.8). To compare the slopes of the calibration curves, Student's *t*-test and F-test were used.

RESULTS AND DISCUSSION

The samples selected for the study are real samples available on the market for cannabis therapy in Brazil. In a pilot study conducted by our research group (unpublished data), it was found that the presence of more than one cannabinoid and the oily excipient used in the medicinal extract could influence the degradation rate. These hypotheses have also been raised in a few other studies.[14,19-21] Therefore, we selected real samples available on the market for cannabis therapy in Brazil, with different excipients, one or two cannabinoids, and the addition of an antioxidant. However, this last parameter was found in only a single collaborating company, or some samples may not have this information on their packaging. It should be noted that these extracts are controlled by regulatory agencies and are subject to controlled revenue,

so that, in order to carry out the research, it was necessary to prove the companies' collaboration and permission from ANVISA (No. 16/2023 and 18/2022).

Due to the numerous variables involved, controlled and inherent to the samples, the analysis of the results was divided into two sections. The first seeks to evaluate variables intrinsic to the samples, such as the excipient, number of cannabinoids, and antioxidants, and the second, controlled variables, such as temperature and light.

Method validation

Chromatography was employed in such a way that CBD and THC did not co-elute, thus ensuring the selectivity of each compound (Figure 3), in accordance with the guidelines followed.[16]

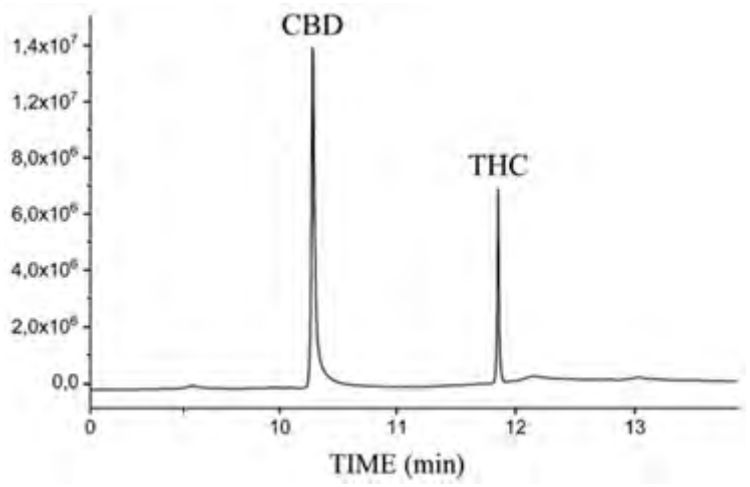

Figure 3. Chromatogram showing CBD and THC at 220 nm.

Suppression of the calibration curve slope was observed when the analysis was performed in the matrix (0.5% oil mixture), compared to the solvent, showing a slope ratio of 63.1% (see Figure S1 in the supplementary material). Consequently, statistical analyses using the F-Snedecor test and Student's *t*-test, applied to assess the equality of slopes based on the comparison of residual variances, indicated a statistically significant difference between the models ($p < 0.05$), evidencing the occurrence of a matrix effect (see Tables S2 and S3 in the supplementary material). Accordingly, all other analytical parameters were determined using matrix calibration. The calibration curves showed confirmed linearity for THC and CBD, based on the correlation coefficients obtained (R values) and the homoscedasticity of the system (residual dispersion) (see Table S4 in the supplementary material).

The limits of detection (LOD) and quantification (LOQ) ranged from 0.57 to 3.43 μg mL^{-1}, values well below the concentrations found in the analyzed extracts, indicating the adequacy of the method. Lower limits have previously been reported (LOD = 0.07 and LOQ = 0.22 μg mL^{-1} for CBD).[22] However, in this study, the determination of these parameters was performed from the analytical curve, making the values dependent on the chosen working range. Higher values than those obtained here have also been described in the literature, such as in the study by Carvalho *et al*.,[23] who reported LODs ranging from 0.20 to 0.22 mg mL^{-1} and LOQs of 0.59 to 0.66 mg mL^{-1} for CBD and THC, respectively.

Precision, evaluated through intraday repeatability, showed relative standard deviation (RSD%) values between 0.61% and 4.34% across the seven levels of the calibration curve, which is considered acceptable according to the established limits (up to 5.3%)[17] (see Table S5 in the supplementary material).

Effect of variables intrinsic to the cannabis-based oily products during storage

All samples showed degradation of the cannabinoids CBD and THC over 180 days (6 months) of storage, with percentages ranging from 13.1 to 94.6% and 9.1 to 99.7%, respectively (Table II). There was

no significant difference in the degradation profiles over the months among the excipients (Figure 4); only a more pronounced decrease in levels was observed at 45 days for sesame oil and at 15 days for corn oil (Figures 4c and 4d).

The highest degradation rates were found in the MCT excipient for both analytes (Table II). In these samples, both the pure CBD and the pure THC samples achieved degradation rates above 30% (samples 2 and 3, Table II). However, when the sample contains both analytes (sample 1), THC degradation is higher than CBD under specific conditions. For example, in sample 2b, under conditions without additive, with light and 20 °C, degradation reached 94.6% for CBD. However, in sample 1b, under the same conditions, degradation was 53.4% for CBD and 97.4% for THC (Table II). This behavior was also observed by Trofin *et al*.,[14] who carried out a study on the storage of two oily samples under two conditions: protected from light at 5 °C and with indirect natural light at 22 °C. They found that THC was more susceptible (approximately 9% and 11%, respectively) than CBD (approximately 5% and 6.5%, respectively) over 6 months of storage. Some other studies, with resinous products or in solvents, also report greater susceptibility to storage of THC compared to CBD.[19,20,21] The greater susceptibility of THC appears to be intrinsic to its chemical structure, as it has a cyclic ring (ring B, Figure 1) prone to oxidative processes.[24,25,26]

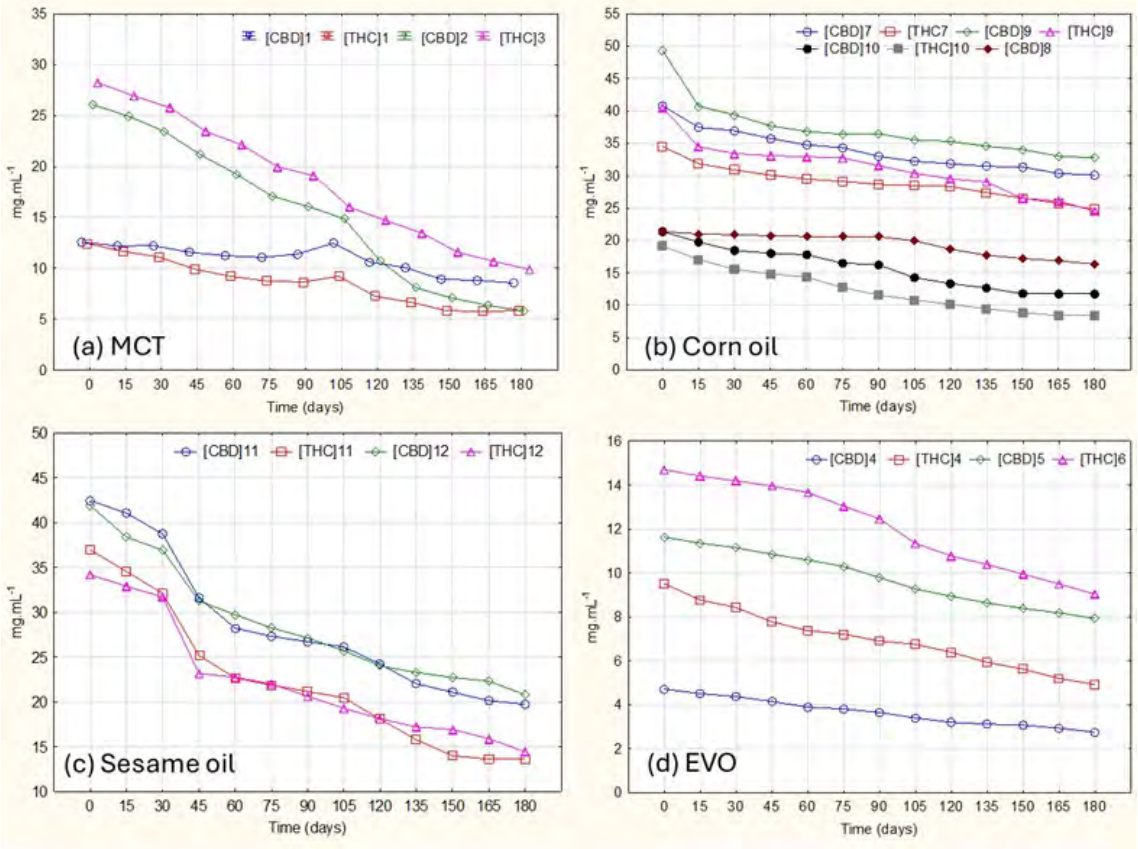

Figure 4. Least squares means for CBD and THC concentrations of cannabis-based oily products in different oils over 180 days.

Although the results reported by Troffin *et al*.[14] corroborate our findings, the degradation rates were much lower than ours. However, few sample characteristics were provided, except that the oil was very viscous. It is generally agreed that viscosity is a parameter that affects the rate of numerous reactions, and Grafström *et al*.,[20] evaluating the storage of resinous samples, also found lower rates, with 11.8% degradation for THC, and CBD remained stable over four years under ambient light and a temperature of 20-22 °C.

On the other hand, the lowest degradation rates were observed for corn oil, for both CBD and THC, with variations of 15% to 37.7% and 20% to 49.9% (samples 8, 9, and 10) (Table II), with the exception of sample 7, which was more outlier, reaching 54.8% and 74.5%. One possibility for this behavior could be the acidity of this sample, as acidity is known to increase the oxidative processes of cannabinoids[24]. However, due to the quantity of samples provided, we cannot verify this hypothesis.

Regarding the oil composition, MCT is a purified coconut oil that contains only saturated medium-chain triglycerides (100% capric and caprylic acid), while corn oil, among the four oils studied, has the highest percentage of polyunsaturated acids (linoleic acid), ranging from 53 to 60% (Table III). The high susceptibility of polyunsaturated fatty acids to oxidation is well reported in the literature and is primarily due to the greater number of double bonds in their structure, which facilitates free radical attack and the propagation of oxidative reactions, especially in the presence of light and heat.[27,28] Thus, comparing MCT with corn oil, we can assume that the polyunsaturated fatty acids in corn oil acted as sacrificial molecules, preventing the sharp degradation of CBD and THC. Or, in other words, we can say that the excipient itself acted as an antioxidant.

Sesame oil, in turn, showed the smallest variability in the degradation percentages between CBD and THC, ranging from 47.8 to 54.8% and 47.7 to 71.3%, respectively (samples 11 and 12) (Table II). In this oil, CBD also showed the most similar degradation percentages to THC, except for the most aggressive conditions for THC, with light and 20 °C. Our results diverge from a recent study by Orallo *et al*.,[29] who evaluated the stability of full-spectrum samples in sesame oil for 1 year at 25 °C and found no significant changes in the composition of CBD and THC. Sesame oil also has high levels of polyunsaturates (38-48% linoleic), but in lower quantities compared to corn oil (Table III), which explains why this oil showed a higher or equivalent degradation percentage compared to corn oil.

In olive oil, degradation rates ranged from 19 to 55% and 9 to 77% for CBD and THC, respectively (samples 4, 5, and 6; Table II). This oil showed the greatest variability across the various variables and samples. Unlike MCT oil, samples containing only CBD showed similar or even lower rates (19 to 48.8%, sample 5b) compared to samples containing both analytes (25.5 to 55.3%, samples 4a and 4b). However, THC, as in the other oils, showed the highest degradation rates, reaching 77.5%, although with considerable variability across storage conditions.

Table II. CBD and THC (mg mL^{-1}) at baseline and after 180 days of storage, with their respective % degradation, in cannabis-based oily products under different oil types and storage conditions

Sample	Excipient/ additive	Storage condition		Concentration (mg mL^{-1}) Begining (Time 0)		Concentration (mg mL^{-1}) After 180 days		Degradation (%)	
		Light	T (ºC)	CBD	THC	CBD	THC	CBD	THC
1.a	MCT/ Vitamin E	With	5.0±1	12.6 ± 0.03	12.5 ± 0.05	5.70^{c} ± 0.11	0.80^{c} ± 0.04	55.0	93.3
		None				10.3^{a} ± 0.08	10.0^{b} ± 0.11	17.8	19.9
		With	20±1			5.30^{d} ± 0.14	0.04^{d} ± 0.04	58.0	99.7
		none				10.5^{a} ± 0.10	10.5^{a} ± 0.12	16.5	15.7
1.b	MCT/ None	With	5.0±1	12.6 ± 0.03	12.5 ± 0.05	6.90^{c} ± 0.12	1.80^{b} ± 0.02	45.3	85.7
		none				10.9^{a} ± 0.15	10.6^{a} ± 0.74	13.1	14.7
		With	20±1			5.90^{d} ± 0.11	0.30^{c} ± 0.01	53.4	97.4
		none				10.3^{b} ± 0.05	10.1^{a} ± 0.11	18.4	19.3
2.a	MCT/ Vitamin E	With	5.0±1	26.1 ± 0.28	nd	2.90^{c} ± 0.01	nd	88.9	nd
		none				10.0^{a} ± 0.01		61.5	
		With	20±1			2.90^{c} ± 0.06		88.7	
		none				9.50^{b} ± 0.10		63.6	

(continued on next page)

Table II. CBD and THC (mg mL^{-1}) at baseline and after 180 days of storage, with their respective % degradation, in cannabis-based oily products under different oil types and storage conditions (continued)

Sample	Excipient/ additive	Storage condition		Concentration (mg mL^{-1}) Begining (Time 0)		Concentration (mg mL^{-1}) After 180 days		Degradation (%)	
		Light	T (°C)	CBD	THC	CBD	THC	CBD	THC
2.b	MCT/ None	With	5.0±1	26.1 ± 0.28	nd	1.70^{c} ± 0.08	nd	93.5	nd
		none				9.40^{a} ± 0.04		64.1	
		With	20±1			1.40^{d} ± 0.03		94.6	
		none				8.80^{b} ± 0.01		66.3	
3.a	MCT/ Vitamin E	With	5.0±1	nd	28.2 ± 0.04	nd	2.60^{c} ± 1.64	nd	90.7
		none					16.5^{b} ± 0.28		41.6
		With	20±1				1.40^{c} ± 0.06		95.0
		none					19.7^{a} ± 0.05		30.1
3.b	MCT/ None	With	5.0±1	nd	28.2 ± 0.04	nd	0.40^{d} ± 0.04	nd	98.5
		none					18.8^{a} ± 0.05		33.5
		With	20±1				1.70^{c} ± 0.13		93.9
		none					18.0^{b} ± 0.14		36.3
4.a	EVO/ Vitamin E	With	5.0±1	4.70 ± 0.12	9.50 ± 0.00	3.20^{b} ± 0.00	3.50^{b} ± 0.00	32.3	63.7
		none				2.30^{c} ± 0.40	7.10^{a} ± 0.10	50.6	26.0
		With	20±1			2.50^{c} ± 0.00	2.40^{c} ± 0.00	46.0	74.6
		none				3.50^{a} ± 0.15	7.10^{a} ± 0.00	25.5	25.3
4.b	EVO/ none	With	5.0±1	4.70 ± 0.12	9.50 ± 0.00	3.50^{a} ± 0.15	7.10^{a} ± 0.00	41.6	64.0
		None				2.70^{b} ± 0.33	3.40^{c} ± 0.00	55.3	33.0
		With	20±1			2.10^{c} ± 0.09	6.40^{b} ± 0.14	44.9	77.5
		none				2.60^{b} ± 0.00	2.10^{d} ± 0.00	34.3	21.8
5.a	EVO/ Vitamin E	With	5.0±1	11.6 ± 0.01	nd	3.10^{a} ± 0.13	nd	37.5	Nd
		none				7.30^{b} ± 0.16		22.1	
		With	20±1			9.10^{a} ± 0.09		34.5	
		none				7.60^{b} ± 0.12		23.1	
5.b	EVO/ none	With	5.0±1	11.6 ± 0.01	nd	8.90^{a} ± 0.11	nd	48.8	Nd
		none				5.90^{d} ± 0.02		19.4	
		With	20±1			9.40^{b} ± 0.08		44.7	
		none				6.40^{c} ± 0.01		23.3	
6.a	EVO/ none	With	5.0±1	nd	14.7 ± 0.28	nd	6.10^{c} ± 0.20	nd	58.5
		none					10.3^{b} ± 0.17		30.2
		With	20±1				5.00^{d} ± 0.15		65.7
		none					13.4^{a} ± 0.27		9.1
6.b	EVO/ none	With	5.0±1	nd	14.7 ± 0.28	nd	9.20^{c} ± 0.25	nd	37.6
		none					12.9^{a} ± 0.05		12.0
		With	20±1				5.40^{d} ± 0.14		63.6
		none					10.1^{b} ± 0.07		31.1

(continued on next page)

Table II. CBD and THC (mg mL⁻¹) at baseline and after 180 days of storage, with their respective % degradation, in cannabis-based oily products under different oil types and storage conditions (continued)

Sample	Excipient/ additive	Storage condition		Concentration (mg mL^{-1}) Begining (Time 0)		Concentration (mg mL^{-1}) After 180 days		Degradation (%)	
		Light	T (°C)	CBD	THC	CBD	THC	CBD	THC
7	Corn oil/ none	With		21.4 ± 0.39	19.1 ± 0.16	10.0^{c} ± 0.11	7.30^{c} ± 0.27	53.2	61.9
		none				11.9^{b} ± 0.17	9.90^{b} ± 0.07	44.4	48.5
		With				9.70^{c} ± 0.76	4.70^{d} ± 0.07	54.8	75.4
		none				15.5^{a} ± 0.00	12.0^{a} ± 0.07	27.4	37.6
8	Corn oil/ none	With	5.0±1	21.4 ± 0.39	nd	13.7^{d} ± 0.17	nd	35.7	
		none				17.2^{b} ± 0.23		19.3	
		With	5.0±1			16.3^{c} ± 0.23		23.8	
		none				18.1^{a} ± 0.08		15.1	
9	Corn oil/ BHA	With	20±1	49.3 ± 0.74	40.5 ± 0.49	31.7^{b} ± 0.29	23.1^{c} ± 0.04	35.8	42.9
		none				32.7^{ab} ± 0.85	26.0^{b} ± 0.47	33.6	35.9
		With	5.0±1			33.2^{a} ± 0.51	20.3^{d} ± 0.12	32.7	49.9
		none				33.5^{a} ± 0.13	28.8^{a} ± 0.48	32.0	29.0
10	Corn oil/ none	With	20±1	40.8 ± 0.31	34.5 ± 0.49	25.4^{c} ± 0.06	27.6^{a} ± 0.26	37.7	20.1
		none				30.4^{b} ± 0.58	26.9^{ab} ± 0.64	25.4	21.9
		With	5.0±1			30.3^{b} ± 0.58	18.7^{c} ± 0.18	25.8	45.8
		none				34.2^{a} ± 0.12	26.1^{b} ± 0.51	16.1	24.4
11	Sesame oil/ BHA	With	20±1	41.9 ± 0.37	34.2 ± 0.08	20.0^{b} ± 0.78	14.4^{c} ± 0.90	52.3	58.0
		none				21.9^{a} ± 0.45	17.9^{a} ± 0.32	47.8	47.7
		With	5.0±1			20.2^{b} ± 0.99	9.80^{d} ± 0.09	51.8	71.3
		none				21.2^{ab} ± 0.27	15.7^{b} ± 0.28	49.5	54.2
12	Sesame oil/ none	With	5.0±1	42.5 ± 0.28	37.0 ± 0.41	19.2^{b} ± 0.12	13.2^{c} ± 0.07	54.8	64.3
		none				20.5 ± 0.49	15.5 ± 1.76	51.6	58.0
		With	20±1			20.0 ± 1.02	11.8 ± 0.20	52.9	68.1
		none				19.2 ± 0.64	14.1 ± 0.13	54.8	62.0

Notes: Medium values with similar letters on the same column and sample showed no statistical difference according to the Tukey test at 5% probability; (nd= no detected).

Table III. Fatty acid composition of corn oil, olive oil, sesame oil, and MCT used as excipients in the cannabis-based oily products

Fatty acids	Corn	Sesame	Olive	MCT
SFA tot. (%)	12 – 13	14	14 – 20	100
C8:0 (caprylic)	–	–	–	50 – 60
C10:0 (capric)	–	–	–	40 – 50
C12:0 (lauric)	–	–	–	–

(continued on next page)

Table III. Fatty acid composition of corn oil, olive oil, sesame oil, and MCT used as excipients in the cannabis-based oily products (continued)

Fatty acids	Corn	Sesame	Olive	MCT
C16:0 (palmitic)	9 – 14	6 – 11	7.5 – 20	–
C18:0 (stearic)	1 – 4	2 – 7	0.5 – 5	–
C18:1 (oleic)	24 – 29	29 – 45	55 – 83	–
C18:2 (linoleic)	52 – 58	38 – 48	3.5 – 21	–
C18:3 (linolenic)	1 – 2	–	0 – 1.5	–

Adapted from Ref. 30 (licensed under CC BY 4.0) and Ref. 31 (Food and Agriculture Organization, public data).

Regarding the presence of the antioxidant in the samples, we observed that vitamin E (rich in tocopherols and tocotrienols) exerted a more effective preventive effect in some samples (samples 2, 4, and 5) than in others (samples 1, 3, and 6). In general, the degradation percentage was 2 to 11% and 3 to 22% lower than in samples without the vitamin, for CBD and THC, respectively. However, no similar behavior was observed regarding storage conditions (light and temperature) or the presence of one or two analytes. Although discreet in some conditions, the effect of the addition of the antioxidant BHA to sesame oil (sample 11) was also observed, with percentages reaching 5.3 and 10% lower than in samples without antioxidant (sample 12), for CBD and THC, respectively. However, for corn oil, BHA showed no effect (samples 9 and 10).

Effect of controlled storage variables on cannabis-based oily products

Both light and temperature influenced analytes degradation ($p < 0.05$). For all oils, the greatest losses, both for CBD and THC, occurred in the presence of light (Figure 5). For THC, this loss is much more prominent (reaching 99.7% at 20 °C, sample 1a, Table I) than for CBD, and can be clearly observed in the excipients MCT, corn, and sesame (Figures 5a, 5b, and 5c). The susceptibility to light of both molecules has been reported in some studies.[11,14,20,26,32,33] Trofin,[14] who also stored oil samples, found THC to be more susceptible than CBD. However, in resins, the results are more conflicting. Some authors report that light influences only THC.[20,32] Lydon,[26] in an accelerated study with ultraviolet irradiation, observed the degradation of CBD but not THC. The rate of photodegradation is also intrinsically associated with the extract composition, as demonstrated by Seccamani,[11] who conducted the study in different solvents. Probably for these reasons, studies are often contradictory.

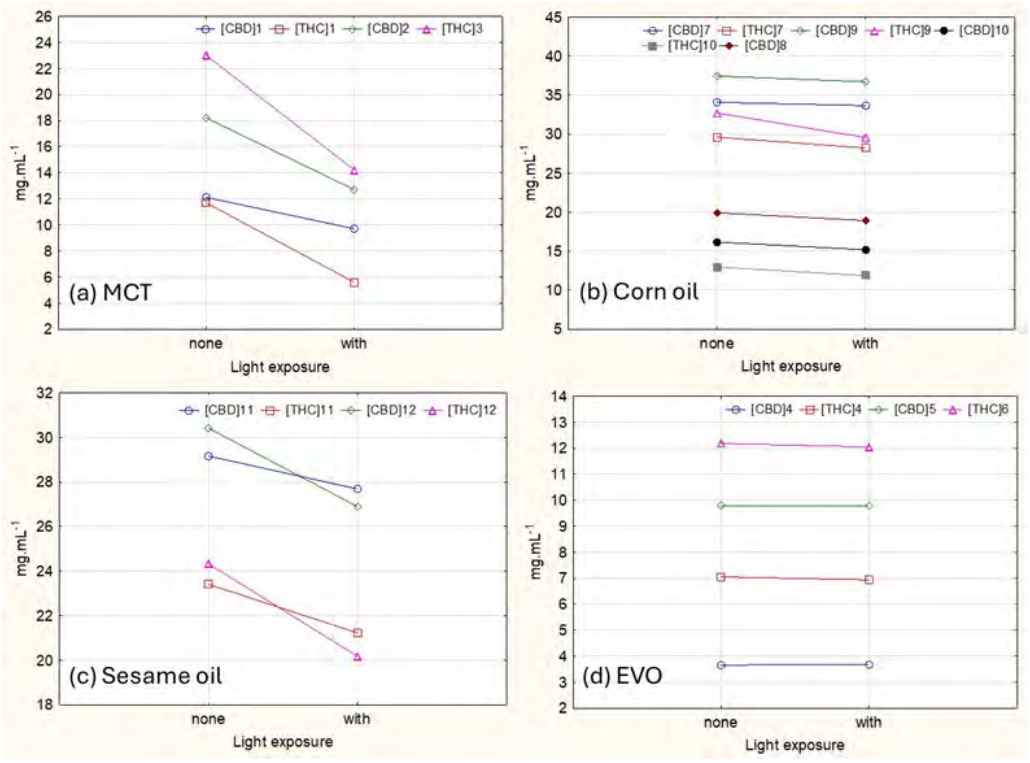

Figure 5. Effect of light (Least Squares Means) on CBD and THC in different cannabis-based oily products over 180 days.

Temperature has been shown to be a critical factor in the stability of cannabinoids.[10] When we analyzed the effect of temperature, we noticed that, although it was more discreet compared to light, it also had a significant effect on degradation for both analytes and all excipients ($p \leq 0.05$). Temperature exhibited less uniform behavior compared to light, neither with respect to a specific excipient nor with respect to a specific analyte. In general, it can be observed that for THC, the highest degradation percentages occurred at 20 °C, clearly evident in corn and sesame oils (Figures 6b and 6c). Interestingly, CBD presented, in all excipients, some samples where the greatest degradation occurred at 5 °C (Samples 2, 4, 7, and 12, Figure 6). This behavior could not be explained based on the data available in the present study. The observed variability may be related to subtle differences in sample composition, such as specific interactions between the cannabinoid, the excipient, and minor matrix components, or to combined effects of other storage factors. However, these hypotheses could not be confirmed and require further investigation. Trofin[14] also found greater degradation of THC at 22 °C compared to 4 °C, although this difference was not as pronounced. For CBD, however, temperature made no difference. However, Pacifici *et al*.[12] found similar degradation rates for THC and CBD in olive oil for 14 days at 25 °C and 4 °C, reaching 50% degradation. When analyzing our olive oil samples separately, we also observed the same behavior as the results of Pacifici *et al*.,[12] as the temperature did not show significant differences between CBD and THC (Figure 6d). In resin, Zamengo[32] reported average THC degradation of 11 to 13% at 22 °C in 100 days, and without significant changes in refrigerated samples, albeit in the dark. In the same study, CBD showed no changes. Very similar results were found by Grafström,[34] also in resinous materials.

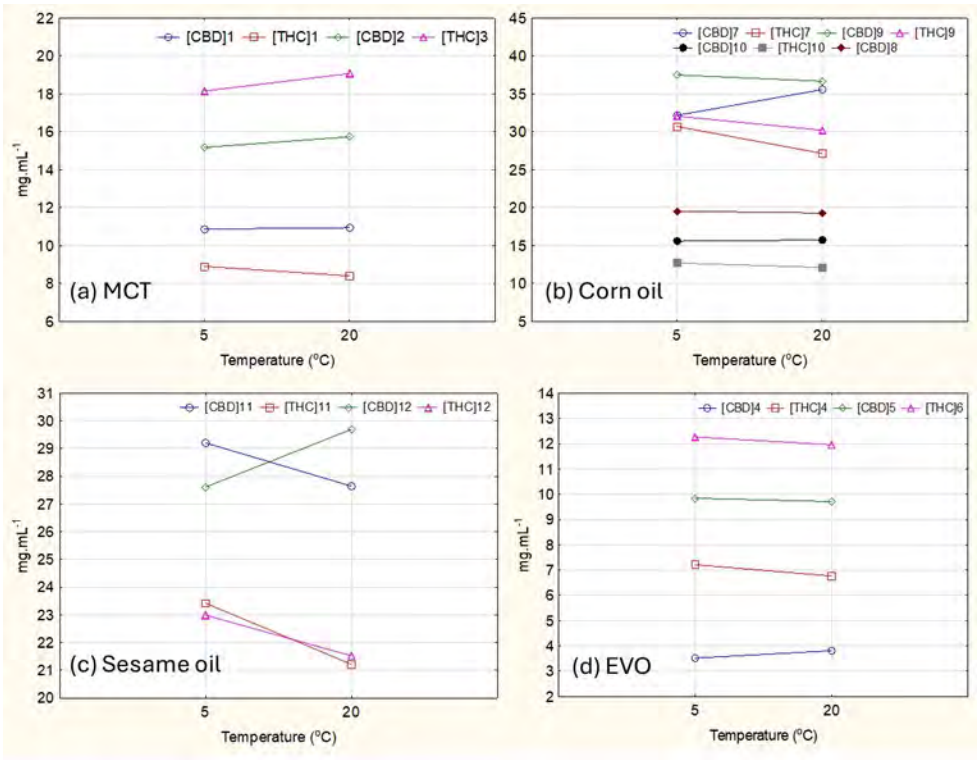

Figure 6. Effect of temperature (Least Squares Means) on CBD and THC in different cannabis-based oily products over 180 days.

Impact of results for companies and patients

Due to the potential therapeutic effects of cannabis-based oily products and the increasing number of studies in this field, several associations have emerged in Brazil over recent decades. Currently, more than 259 cannabis associations with active CNPJ registration operate in the country. However, despite this growth, many of these organizations lack adequate infrastructure to conduct analytical studies and perform quantitative analyses with the required accuracy, mainly due to the high costs of equipment and the need for specialized professionals.

Quality control of medicinal extracts, including stability studies, is based on chemical analyses of cannabinoids and the excipient used in the formulation, encompassing both the quantification of active compounds and the assessment of product purity. According to RDC No. 327,[8] cannabis extracts intended for human use must meet pharmaceutical quality standards, and associations are responsible for the technical documentation demonstrating product quality as well as for the operational capacity to perform quality control analyses, which may be outsourced. In this context, outsourcing quality control or establishing partnerships with universities represents viable and strategic alternatives, particularly for small- and medium-sized associations.

The results obtained in this study provide technical support that may assist these associations in improving extract stability and in developing more appropriate guidance for patients regarding the correct storage of medicinal products during treatment.

CONCLUSIONS

The results demonstrate the high sensitivity of CBD and THC to storage conditions, underscoring the importance of stability studies for cannabis-based products. Both sample composition and storage conditions significantly influenced cannabinoid degradation over a six-month period.

Among the excipients evaluated, corn oil and sesame oil showed the best stability performance, whereas MCT oil exhibited the highest degradation rates. Light exposure was the most critical factor, leading to

the greatest degradation percentages for both cannabinoids, regardless of other variables. Temperature showed a less uniform effect, with higher THC degradation at 20 °C and variable CBD behavior, which in some cases showed greater instability at 5 °C.

The addition of antioxidants had a statistically significant but limited effect. Vitamin E showed greater preventive potential than BHA; however, the results varied depending on the excipient, indicating the need for further studies to better understand these effects.

Overall, the most suitable strategy for cannabinoid preservation involves the use of corn or sesame oil, light-protective containers, the addition of antioxidants, and refrigerated storage. Nevertheless, even under these conditions, high degradation rates were observed, ranging from 19.3% to 51.6% for CBD and from 21.9% to 58% for THC. These values are clinically relevant and require dosage adjustments every two to three months during treatment.

Conflicts of interest

The authors declare that the research was conducted in the absence of any commercial or financial relationships that could be construed as a potential conflict of interest.

Acknowledgements

This study was financed by the Institutional Program “Agenda Tríplice” of UNILA [Edital No. 205/2021/PRPPG/UNILA] and “Laboratório de Ideias – LABID” [Edital No. 03/2021/IMEA/UNILA]. The authors would also like to thank the financial support granted by “Fundação Araucária” [Public Notice 23/2023 - Program of Scholarships for Productivity in Research and/or Technological Development].

REFERENCES

(1) Vinette, B.; Côté, J.; El-Akhras, A.; Mrad, H.; Chicoine, G.; Bilodeau, K. Routes of administration, reasons for use, and approved indications of medical cannabis in oncology: a scoping review. *BMC Cancer* **2022**, *22* (1), 1–19. https://doi.org/10.1186/s12885-022-09378-7

(2) Baratta, F.; Simiele, M.; Pignata, I.; Enri, L. R.; D’avolio, A.; Torta, R.; De Luca, A.; Collino, M.; Brusa, P. Cannabis-based oral formulations for medical purposes: Preparation, quality and stability. *Pharmaceuticals* **2021**, *14* (2), 1–16. https://doi.org/10.3390/ph14020171

(3) Romano, L. L.; Hazekamp, A. Cannabis Oil: chemical evaluation of an upcoming cannabis-based medicine. *Cannabinoids* **2013**, *1* (1), 1–11.

(4) Hanuš, L. O.; Mechoulam, R. Cannabinoid chemistry: an overview. In: Mechoulam, R. (Ed.) *Cannabinoids as Therapeutics.* Birkhäuser Basel, 2005, pp 23-46. https://doi.org/10.1007/3-7643-7358-x_2

(5) Prospéro-García, O.; Ruiz Contreras, A. E.; Ortega Gómez, A.; Herrera-Solís, A.; Méndez-Díaz, M. Endocannabinoids as Therapeutic Targets. *Arch. Med. Res.* **2019**, *50* (8), 518–526. https://doi.org/10.1016/j.arcmed.2019.09.005

(6) ElSohly, M. A.; Slade, D. Chemical constituents of marijuana: The complex mixture of natural cannabinoids. *Life Sci.* **2005**, *78* (5), 539–548. https://doi.org/10.1016/j.lfs.2005.09.011

(7) Zuardi, A. W.; Takahashi, R. N.; Guimarães, F. S.; Crippa, J. A. S. Prof. Elisaldo Araújo Carlini, Cannabis and Cannabinoids Research Pioneer (June 9, 1930–September 16, 2020). *Cannabis Cannabinoid Res.* **2020**, *5* (4), 272–273. https://doi.org/10.1089/can.2020.0121

(8) Agência Nacional de Vigilância Sanitária (ANVISA). Resolução da Diretoria Colegiada - RDC Nº 327, de 9 de dezembro de 2019. *Imprensa Nacional – Diário Oficial da União* **2019**, Ed. 239 (1), page 194. Available at: https://www.in.gov.br/en/web/dou/-/resolucao-da-diretoria-colegiada-rdc-n-327-de-9-de-dezembro-de-2019-232669072 (accessed: 12/2025).

(9) Fairbairn, J. W.; Liebmann, J. A.; Rowan, M. G. The stability of cannabis and its preparations on storage. *J. Pharm. Pharmacol.* **1976**, *28* (1), 1–7. https://doi.org/10.1111/j.2042-7158.1976.tb04014.x

(10) Strzelczyk, M.; Lochynska, M.; Chudy, M. Systematics and Botanical Characteristics of Industrial Hemp *Cannabis sativa* L. *J. Nat. Fibers* **2022**, *19* (13), 5804–5826. https://doi.org/10.1080/15440478.2021.1889443
(11) Seccamani, P.; Franco, C.; Protti, S.; Porta, A.; Profumo, A.; Caprioglio, D.; Salamone, S.; Mannucci, B.; Merli, D. Photochemistry of Cannabidiol (CBD) Revised. A Combined Preparative and Spectrometric Investigation. *J. Nat. Prod.* **2021**, *84* (11), 2858–2865. https://doi.org/10.1021/acs.jnatprod.1c00567
(12) Pacifici, R.; Marchei, E.; Salvatore, F.; Guandalini, L.; Busardò, F. P.; Pichini, S. Evaluation of cannabinoids concentration and stability in standardized preparations of cannabis tea and cannabis oil by ultra-high performance liquid chromatography tandem mass spectrometry. *Clin. Chem. Lab. Med.* **2017**, *55* (10), 1555–1563. https://doi.org/10.1515/cclm-2016-1060
(13) Raslan-Jaramillo, J. J.; Gisela, A. R.; Avello, M. A.; Diego, M. G. De. Determination of Cannabinoids in *Cannabis sativa* Oil and Infused Ice Cream by LC-DAD Method. *J. AOAC Int.* **2024**, *107* (1), 140–145. https://doi.org/10.1093/jaoacint/qsad122
(14) Trofin, I. G.; Dabija, G.; Váireanu, D. I.; Filipescu, L. The influence of long-term storage conditions on the stability of cannabinoids derived from cannabis resin. *Rev. Chim.* **2012**, *63* (4), 422–427.
(15) Zivovinovic, S.; Alder, R.; Allenspach, M. D.; Steuer, C. Determination of cannabinoids in *Cannabis sativa* L. samples for recreational, medical, and forensic purposes by reversed-phase liquid chromatography-ultraviolet detection. *J. Anal. Sci. Technol.* **2018**, *9* (1). https://doi.org/10.1186/s40543-018-0159-8
(16) Harron, D. W. G. Technical Requirements for Registration of Pharmaceuticals for Human Use: The ICH Process. In: Griffin, J. P.; Posner, J.; Barker, G. R. (Eds.). *The Textbook of Pharmaceutical Medicine*. Wiley, 2013. Chapter 23, pp 447-460. https://doi.org/10.1002/9781118532331.ch23
(17) Instituto Nacional de Metrologia (INMETRO). DOQ-CGCRE-008 Orientação sobre validação de métodos analíticos. *Inmetro* **2020**, 30.
(18) Agência Nacional de Vigilância Sanitária (ANVISA). Resolução da Diretoria Colegiada - RDC Nº 166: *Validação de Métodos Analíticos*. 2017. Available at: https://bvsms.saude.gov.br/bvs/saudelegis/anvisa/2017/rdc0166_24_07_2017.pdf (accessed: 12/2025).
(19) Lindholst, C. Long term stability of cannabis resin and cannabis extracts. *Aust. J. Forensic Sci.* **2010**, *42* (3), 181–190. https://doi.org/10.1080/00450610903258144
(20) Grafström, K.; Andersson, K.; Pettersson, N.; Dalgaard, J.; Dunne, S. J. Effects of long term storage on secondary metabolite profiles of cannabis resin. *Forensic Sci. Int.* **2019**, *301*, 331–340. https://doi.org/10.1016/j.forsciint.2019.05.035
(21) Smith, R. N.; Vaughan, C. G. The decomposition of acidic and neutral cannabinoids in organic solvents. *J. Pharm. Pharmacol.* **1977**, *29* (1), 286–290. https://doi.org/10.1111/j.2042-7158.1977.tb11313.x
(22) Tzimas, P. S.; Petrakis, E. A.; Halabalaki, M.; Skaltsounis, L. A. Effective determination of the principal non-psychoactive cannabinoids in fiber-type *Cannabis sativa* L. by UPLC-PDA following a comprehensive design and optimization of extraction methodology. *Anal. Chim. Acta* **2021**, *1150*, 338200. https://doi.org/10.1016/j.aca.2021.338200
(23) Carvalho, V. M.; Aguiar, A. F. L.; Baratto, L. C.; Souza, F. L. C.; Rocha, E. D. Cannabinoids quantification in medicinal cannabis extracts by high performance liquid chromatography. *Quim. Nova* **2020**, *43* (1), 90–97. https://doi.org/10.21577/0100-4042.20170457
(24) Golombek, P.; Müller, M.; Barthlott, I.; Sproll, C.; Lachenmeier, D. W. Conversion of Cannabidiol (CBD) into Psychotropic Cannabinoids Including Tetrahydrocannabinol (THC): A Controversy in the Scientific Literature. *Toxics* **2020**, *8*, 41. https://doi.org/10.3390/toxics8020041
(25) Vacek, J.; Vostalova, J.; Papouskova, B.; Skarupova, D.; Kos, M.; Kabelac, M.; Storch, J. Antioxidant function of phytocannabinoids: Molecular basis of their stability and cytoprotective properties under UV-irradiation. *Free Radic. Biol. Med.* **2021**, *164*, 258–270. https://doi.org/10.1016/j.freeradbiomed.2021.01.012

(26) Lydon, J.; Teramura, A. H. Photochemical decomposition of cannabidiol in its resin base. *Phytochemistry* **1987**, *26* (4), 1216–1217. https://doi.org/10.1016/S0031-9422(00)82388-2
(27) Ghnimi, S.; Budilarto, E.; Kamal-Eldin, A. The New Paradigm for Lipid Oxidation and Insights to Microencapsulation of Omega-3 Fatty Acids. *Compr. Rev. Food Sci. Food Saf.* **2017**, *16* (6), 1206–1218. https://doi.org/10.1111/1541-4337.12300
(28) Yin, H.; Porter, N. A. New insights regarding the autoxidation of polyunsaturated fatty acids. *Antioxid. Redox Signaling* **2005**, *7* (1–2), 170–184. https://doi.org/10.1089/ars.2005.7.170
(29) Orallo, D. E.; Fuentes, G. M.; Benavidez, M. G.; Suárez, P. A.; Nutter, D.; Fangio, M. F.; Ramirez, C. L. Long-term stability and bactericidal properties of galenic formulations of Cannabis sativa oils. *Fitoterapia* **2024**, *177*. https://doi.org/10.1016/j.fitote.2024.106128
(30) Matthäus, B.; Özcan, M. M. Fatty acid composition and tocopherol contents of some sesame seed oils. *Iran. J. Chem. Chem. Eng.* **2018**, *37* (5), 151–155. https://doi.org/10.30492/ijcce.2018.35427
(31) Food and Agriculture Organization (FAO). Standard for Named Vegetable Oils Codex Stan 210-1999. *Codex Alimentarius* 1999, 1–13.
(32) Zamengo, L.; Bettin, C.; Badocco, D.; Di Marco, V.; Miolo, G.; Frison, G. The role of time and storage conditions on the composition of hashish and marijuana samples: A four-year study. *Forensic Sci. Int.* **2019**, *298*, 131–137. https://doi.org/10.1016/j.forsciint.2019.02.058
(33) Bini, A.; Salerno, S.; Protti, S.; Pollastro, F.; Profumo, A.; Morini, L.; Merli, D. Photodegradation of cannabidiol (CBD) and Δ9-THC in cannabis plant material. *Photochem. Photobiol. Sci.* **2024**, *23* (7), 1239–1249. https://doi.org/10.1007/s43630-024-00589-4
(34) Grosso, A. F. Cannabis: from plant condemned by prejudice to one of the greatest therapeutic options of the century. *Journal of Human Growth and Development* **2020**, *30* (1), 94–97. https://doi.org/10.7322/jhgd.v30.9977

SUPPLEMENTARY MATERIAL

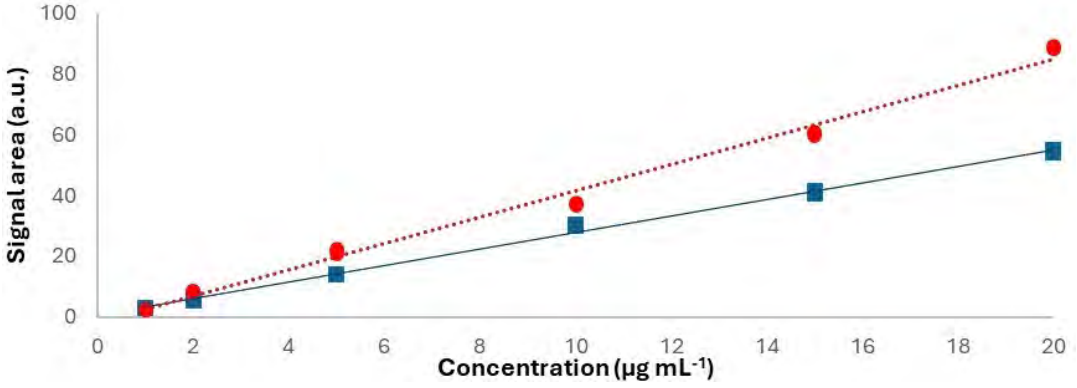

Figure S1. Calibration curves of THC obtained in solvent (red) and in matrix (blue).

Table S2. Regression parameters of THC calibration curves in solvent and matrix (n = 3)

Medium	Levels (µg mL^{-1})	Slope (a)	Intercept (b)	Linear regression (R^2)
Solvent	1-20	4.35	-1.95	0.991
Matrix	1-20	2.75	0.53	0.997

Table S3. Statistical analysis of the slopes of calibration curves in solvent and matrix

Parameters	Student's *t*-test			*F*-Snedecor test	
	***t* calculated**	***t* critical (90%)**	***t* critical (95%)**	***F* calculated**	***F* theorical (0.05; 10; 16)**
Results	59.7	1.74	2.11	7.58	2.70
Evaluation	*t* > *t* critical			*F* calculated > *F* theorical	
Conclusion	Slopes are different			Variances are different	

Table S4. Linearity range, R, Line equation, LOD and LOQ for the analytes

Analyte (µg mL^{-1})	Linearity (µg mL^{-1})	R	Line Equation	LOD (µg mL^{-1})	LOQ (µg mL^{-1})
CBD	1-20	0.9992	y = 1.6462x - 0.7436	0.98	3.43
THC	1-20	0.9991	y = 1.7134x + 0.0724	1.34	2.42

LOD: Limit of detection. LOQ: Limit of quantification.

Table S5. Values for Relative Standard Desviation (% RSD)

Analyte	Level (µg mL^{-1})	%RSD (n=3)	Analyte	Level (µg mL^{-1})	%RSD (n=3)
CBD	1	4.34	THC	1	2.45
	2	2.56		2	0.73
	5	0.92		5	0.65
	10	0.61		10	0.62
	15	1.56		15	1.23

Brazilian Journal of Analytical Chemistry
2026, Volume 13, Issue 52, pp 150-165
doi: 10.30744/brjac.2179-3425.AR-96-2025

BrJAC

ARTICLE

Evaluation of Closed-Vessel Conductively-Heated Digestion System with Diluted Acid for Analysis of Animal Feed by ICP-MS

Rayane Cristina Vieira Costa[1], Edilene Cristina Ferreira[1], Alex Virgílio[2], Elisabete Aparecida De Nadai Fernandes[2], José Anchieta Gomes Neto[1]*

[1]*Departamento de Química Analítica, Físico-Química e Inorgânica, Instituto de Química, Universidade Estadual Paulista (UNESP). Av. Prof. Francisco Degni, 55, Araraquara, SP, 14800-060, Brazil*

[2]*Centro de Energia Nuclear na Agricultura (CENA), Universidade de São Paulo (USP). Av. Centenário, 303, Piracicaba, SP, 13416-000, Brazil*

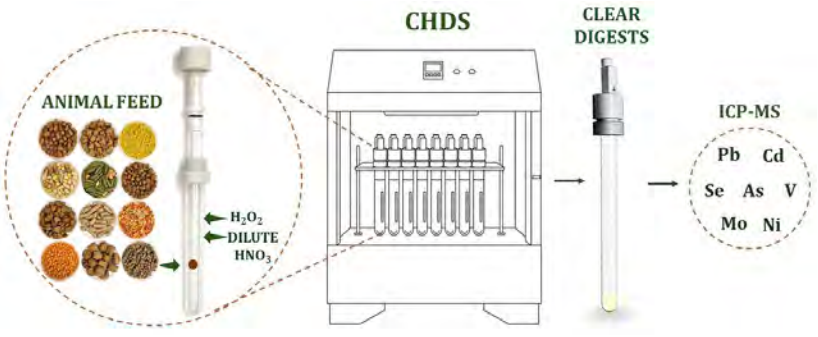

A conductively-heated digestion system (CHDS) with closed-vessel and diluted acid was evaluated for the preparation of animal feed for subsequent determination of As, Cd, Mo, Ni, Pb, Se and V by Inductively Coupled Plasma Mass Spectrometry (ICP-MS). The analytical performance of the digestor was checked by analyzing fish tissue, tuna and corn bran certified reference materials (CRMs) using 1 mL of 30% (w w^{-1}) hydrogen peroxide plus 2 mL of nitric acid at 3.5, 7 and 14 mol L^{-1} HNO_3. The recoveries of analytes in CRMs digested at different acid concentrations varied from 80 to 116% (3.5 mol L^{-1} HNO_3), 86 to 118% (7 mol L^{-1} HNO_3), and 80 to 123% (14 mol L^{-1} HNO_3). The method was applied to real animal feed samples, and the CHDS results were like those of comparative microwave digestion (MWD). Quantification limits of analytes found by CHDS and MWD were also similar, concerning different acid concentrations. However, the use of diluted nitric acid in the preparation of animal feed samples proved to be a viable and efficient approach, allowing lower residual acidity, reduction in reagent consumption and acid waste generation, in accordance with the principles of Green Chemistry.

Keywords: animal feed, nitric acid, sample preparation, conductively-heated digestion system, ICP-MS

INTRODUCTION

Animal feed is the mainstream option for animal nutrition due to its practicality, easiness of access. By adequately meet the nutritional and energy requirements of animals, a wide variety of feed formulations is available on the market and can be selected according to the breed, size, age, and health predispositions

Cite: Costa, R. C. V.; Ferreira, E. C.; Virgílio, A.; De Nadai Fernandes, E. A.; Gomes Neto, J. A. Evaluation of Closed-Vessel Conductively-Heated Digestion System with Diluted Acid for Analysis of Animal Feed by ICP-MS. *Braz. J. Anal. Chem.* 2026, *13* (52), pp 150-165. https://doi.org/10.30744/brjac.2179-3425.AR-96-2025

Submitted: October 9, 2025; **Revised:** December 10, 2025; January 5, 2026; **Accepted:** January 9, 2026; **Published online:** April 1, 2026.

This article is part of the BrJAC Special Issue dedicated to the 21st ENQA and 9th CIAQA.

of the animals.[1-3] The composition of these feeds can directly influence health, so accurately identifying certain elements is important since their presence at adequate concentrations can significantly contribute to preventing health problems. However, high levels of certain elements can lead to toxic effects on the body.[4] In this context, it is crucial to monitor the concentration of such elements like arsenic (As), cadmium (Cd), molybdenum (Mo), nickel (Ni), lead (Pb), selenium (Se), and vanadium (V). Although these elements are generally present at low concentrations, they can be toxic when accumulated at excessive levels. Controlling these elements is essential to ensuring the safety and well-being of animals.[4,5] Inductively coupled plasma mass spectrometry (ICP-MS) is a highly sensitive technique that enables the precise determination of trace and ultra trace elements. This technique is frequently used to identify potentially toxic elements in various samples. However, this technique is subject to polyatomic interference, which is caused by the combination of matrix ions and argon gas during ionization. This interference can compromise the accuracy of the results. One way to minimize this effect is to promote the complete decomposition of the matrix by employing an efficient digestion method.[6-8]

In 2014, Miranda, Pereira Filho, and Gomes Neto[9] developed a new conductively-heated digestion system (CHDS). The CHDS was successfully applied to various matrices, including plants,[9,10] feed,[11] meat,[12] agricultural materials,[13] and dog feed.[14] The instrument was commercially released two years ago with the launch of the Vert Simplify digestor, an evolution of that system. The performance of the Simplify model was evaluated by analyzing different matrices, including plant materials,[15] oil sludge,[16] biomass and biochar,[17] and animal feed samples.[18] The CHDS has demonstrated high efficiency in decomposing various types of samples. Using closed vials minimizes analyte loss and prevents contamination during digestion. Conductive heating via a thermal block ensures uniform and controlled temperature distribution. Additionally, the CHDS system is versatile, effectively decomposing different matrices with high reproducibility. Furthermore, the system's low operating and maintenance costs offer an economical and practical alternative for sample preparation.

Additionally, Costa et al. (2025) demonstrated that digesting animal feed samples with CHDS and diluted nitric acid efficiently decomposes the matrix, allowing for the subsequent determination of macronutrients and micronutrients via inductively coupled plasma optical emission Spectrometry (ICP OES).[18] Considering the sensitivity limitations of that work for determining analytes at trace and ultra-trace levels, the importance of animal feed quality control and the growing demand for more sustainable analytical methods, this study evaluated the performance of the Vert Simplify digestor to prepare bird, dog, horse, rabbit, cat and fish feed samples using diluted nitric acid for subsequent determinations of As, Cd, Mo, Ni, Pb, Se and V by ICP-MS.

MATERIALS AND METHODS

Reagents, analytical solutions and sample

Twelve feed samples, including two of each for birds, cats, dogs, fish, horses and rabbits, were purchased from a pet store in Araraquara, SP, Brazil. The samples were previously ground in a Spex 6750 cryogenic mill (Metuchen, NJ, USA) using a program with two grinding cycles, each lasting 3 minutes, and a 10-minute cooling ramp. This procedure yielded particles with an average diameter of less than 50 µm. The samples were then dried in an air-circulating oven (TE-394/2 Tecnal, Piracicaba, SP, Brazil) at 75 °C until constant mass. After drying, the samples were placed in appropriate containers and stored in a desiccator.

The performance of the CHDS digestion method was evaluated by digesting certified reference materials (CRMs) of Durum Wheat Flour (DUWF-1 8436) and Corn Bran (BRAN-1 8433) (National Research Council Canada),[19] and reference material (RM) of Tuna Fish (1101) (University of São Paulo, Brazil).[20] The particle sizes of CRMs and RM are approximately 50 µm.[19,20] The aqueous solutions were daily prepared by using deionized water (18.2 MΩ cm), produced by a reverse osmosis purification system (Gehaka Master System MS2000, São Paulo, Brazil). The digestion procedure used nitric acid (HNO_3, 69%, J.T. Baker, Deventer, Netherlands), which was previously purified by distillation in a boiling system, as well as hydrogen peroxide (H_2O_2, 30%, Merck, Darmstadt, Germany). The vessels were previously decontaminated by immersing them in a 10% (v/v) HNO_3 solution for 24 h. After the acid bath, they were thoroughly cleaned with deionized

water. The multi-element working standard solutions were prepared by appropriate dilution of 1000 mg L^{-1} single-element stock standards (SpecSol®, QUIMLAB, São Paulo, Brazil) with 5% HNO_3 (v v^{-1}) medium. The concentration range used in calibration curves for As, Cd, Se, Mo, Ni, Pb, and V was 0.01 – 500 µg L^{-1}.

Instrumentation

CHDS digestor (Simplify, Vert Technologies, São Paulo, Brazil) was used to digest animal feed samples, CRMs, and RM. The CHDS contains an aluminum heating block with 24 slot positions and a heating element of 1600 W, which enables temperatures up to 350 °C. The vessels are made of quartz, sealed with polytetrafluoroethylene (PTFE) lids, and tolerate a maximum pressure of 28 bar.[15] For comparison purposes, all samples were also digested using an Anton Paar model Multiwave 3000 microwave digestor (Graz, Austria). Dissolved organic carbon was determined using an inductively coupled plasma optical emission spectrometer (ICP-OES) (Thermo Scientific ICAP 7400, Waltham, USA). An 8900 Triple Quadrupole ICP-MS/MS (Agilent Technologies, Japan) inductively coupled plasma mass spectrometer (ICP-MS) was used to determine As, Cd, Mo, Ni, Pb, Se, and V in the samples. The instrumental parameters optimized for ICP-MS determinations are presented in Table I.

Table I. Instrumental operating parameters used for ICP MS data acquisition

Instrumental parameters	Operating conditions
RF Power	1500 W
Plasma gas-flow rate	15 L min^{-1}
Auxiliary gas-flow rate	0.68 L min^{-1}
Nebulizer gas-flow rate	0.5 L min^{-1}
Spray chamber	Double-pass Scott type
Nebulizer	Concentric
Operation mode	Single quad (He 5.5 mL min^{-1})
Isotope (*m/z*)	As (75), Cd (114), Mo (98), Ni (60), Pb (208), Se (78), and V (51)

Digestion procedures

For the CHDS digestions (n = 3), 200 mg of each sample was weighed into the digestion vessels. Then, 2.0 mL of nitric acid at 3.5, 7.0, or 14.0 mol L^{-1} and 1.0 mL of hydrogen peroxide were added, resulting in a total volume of 3.0 mL. Considering the dilution effect due to the addition of hydrogen peroxide, the final acid concentrations were 2.3, 4.7, and 9.3 mol L^{-1} HNO_3, respectively. The digestion procedure was performed using the following temperature program: (a) a temperature ramp of 10 °C min^{-1} from room temperature to 250 °C, (b) 20 min at 250 °C, and (c) a 25-min cooling period. Note that 250 °C corresponds to the temperature of the aluminum heating block while the internal temperature of the reaction medium was approximately 200 °C.[15] After digestion, the solutions were transferred to polypropylene tubes and diluted to a final volume of 25 mL with ultrapure water.

For microwave-assisted digestion (MW, n = 3), 200 mg of each sample was weighed into PTFE vessels. Then, 4.0 mL of nitric acid (3.5, 7, or 14 mol L^{-1}) and 2.0 mL of hydrogen peroxide were added. The microwave heating program consisted of three stages: (a) a 25-min ramp to 1200 W, reaching 200 °C; (b) a 15-min hold at 1200 W (200 °C); and (c) a 20-min cooling/venting period at 0 W. The final digests were transferred to polypropylene tubes and diluted to 25 mL with ultrapure water.

RESULTS AND DISCUSSION

To evaluate digestion efficiency using CHDS, the mass fraction (μg kg^{-1}) of As, Cd, Mo, Ni, Pb, Se, and V were determined by ICP-MS in CRMs and RMs. The CRMs and RM were selected based on their similarity to the animal feed samples to ensure comparable results. Digestions performed in closed vessels using HNO_3 and H_2O_2 allow the regeneration of nitric acid because when HNO_3 is used for oxidation of organic matter, the main product is $NO_{2(g)}$, which reacts with $O_{2(g)}$ (from H_2O_2) and $H_2O_{(g)}$, producing HNO_3 according to the following reactions:[6,13]

$$2\ H_2O_2 \rightarrow 2\ H_2O + O_{2(g)}$$

$$4NO_{2(g)} + 2\ H_2O_{(g)} + O_{2(g)} \rightarrow 4\ HNO_{3(aq)}$$

This regeneration is useful to reduce the amount of acid in the process of digestion, resulting in lower residual acidity.[6,13] Additionally, this method offers several advantages, including lower analytical blank values, reduced costs, and greater compliance with green chemistry principles.[6,13] Tables II show the results obtained for As, Cd, Mo, Ni, Pb, Se, and V by ICP-MS after digestion in CHDS with different HNO_3 concentrations.

The analyte recovery for the CRM and RM digested under different concentrations of nitric acid were 80 – 116% (3.5 mol L^{-1} HNO_3), 86 – 118% (7 mol L^{-1} HNO_3) and 80 – 123% (14 mol L^{-1} HNO_3). The digestion method using CHDS showed good trueness for all analytes, with recovery rates exceeding 80% under all evaluated conditions. It should be noted that the use of diluted HNO_3 (3.5 mol L^{-1}) was satisfactory to ensure accurate results, demonstrating the feasibility of using low concentrations of nitric acid in the digestion process of animal feed without compromising analytical performance. Precision (as relative standard deviation, RSD) were between 0.5 – 24% for 3.5 mol L^{-1} HNO_3, 0.1 – 29% for 7 mol L^{-1} HNO_3, and 0.1 – 29% for 14 mol L^{-1} HNO_3.

Statistical significance was evaluated by means of an unpaired *t*-test at 95% confidence level. In general, most of the results obtained with the CHDS digestion method using 3.5, 7, and 14 mol L^{-1} HNO_3 were not statistically different from the certified values. Notably, in some cases, significant differences were observed. However, trueness was close to 100% and this discrepancy can be attributed to small standard deviations resulting in shorter confidence intervals that do not overlap at a 95% confidence level.

Evaluating the influence of HNO_3 concentration variation in CRM and RM digests using the CHDS system revealed that each sample and analyte responded differently to changes in acid concentration. However, the trueness data did not show a clear trend in association with the HNO_3 concentration (3.5, 7, or 14 mol L^{-1}), suggesting that variation is random and the acidity does not significantly affect the results. Therefore, diluted nitric acid can be used for digesting these samples in CHDS without affecting trueness.

Table II. Results (mean ± standard deviation, n = 3) and recoveries (%) for trace and ultra-trace elements determined in CRMs and RM digested by CHDS using different nitric acid concentrations

CRM	HNO_3 (mol L^{-1})	Mass Fraction (µg kg^{-1})													
		As	%	Cd	%	Mo	%	Ni	%	Pb	%	Se	%	V	%
Tuna Fish (1101)	Certified	4680**		34**		*		20**		48**		5500**		*	
	3.5	4682 ± 51	100	33 ± 1	96	116 ± 1	-	18 ± 4	92	51 ± 3	106	5869 ± 80	107	78 ± 1	-
	7	5005 ± 280	107	39 ± 3	114	161 ± 1	-	23 ± 3	113	51 ± 7	106	5202 ± 800	95	75 ± 0	-
	14	5003 ± 4	107	40 ± 2	119	129 ± 1	-	16 ± 2	80	46 ± 3	95	5095 ± 89	93	70 ± 8	-
DUWF-1 (8436)	Certified	30*		110 ± 50		700 ± 12		170 ± 12		23 ± 6				21 ± 6	
	3.5	26 ± 1	88	107 ± 12	97	710 ± 86	101	170 ± 16	100	23 ± 3	101	1128 ± 37	-	23 ± 5	109
	7	26 ± 1	88	111 ± 1	101	751 ± 1	107	178 ± 9	105	20 ± 1	88	1388 ± 37	-	23 ± 2	110
	14	32 ± 1	107	129 ± 10	117	659 ± 60	94	203 ± 12	120	28 ± 2	123	1498 ± 94	-	22 ± 4	105
BRAN-1 (8433)	Certified	2*		12 ± 5		252 ± 39		160*		140 ± 34		45 ± 8		5*	
	3.5	1.7 ± 0.4	83	13 ± 1	105	286 ± 6	114	161 ± 6	101	141 ± 15	101	47 ± 7	105	4 ± 1	80
	7	1.7 ± 0.5	86	12 ± 1	97	293 ± 3	116	183 ± 2	114	161 ± 3	115	53 ± 1	118	5 ± 1	109
	14	2.1 ± 0.6	103	12 ± 3	102	300 ± 13	119	182 ± 11	114	138 ± 13	98	50 ± 11	111	6 ± 1	117

*not available; **non-certified values.

Arsenic, Cd, Mo, Ni, Pb, Se, and V were determined by ICP-MS in bird, cat, dog, fish, horse and rabbit feed samples. The samples were digested using the CHDS and MWD methods with HNO_3 concentrations of 3.5, 7, and 14 mol L^{-1}. All final digests were clear, indicating the complete decomposition of organic matter. To ensure digestion efficiency, the residual carbon content (RCC) was determined. The RCC values in general ranged from 0.09 to 0.17% (3.5 mol L^{-1}), 0.06 to 0.14% (7 mol L^{-1}), and 0.01 to 0.13% (14 mol L^{-1} HNO_3), suitable for analysis by ICP-OES and ICP-MS,[21] Considering the high presence of protein and fat in the samples, which are rich in carbon, the residual carbon levels were consistently low, demonstrating the effectiveness of the CHDS digestion method.

Shown in Table III are results (in μg kg^{-1}) for As, Cd, Mo, Ni, Pb, Se and V obtained by ICP-MS for animal feed samples prepared in CHDS and MWD using 1 mL of H_2O_2 and 2 mL of HNO_3 3.5 mol L^{-1}. The data related to HNO_3 concentrations of 7 and 14 mol L^{-1} are provided in Tables SI and SII of the Supplementary Material, respectively. Significant variations in analyte mass fractions were observed in animal feed. The highest and lowest levels (μg kg^{-1}) of V, Ni, As, Se, Mo, Cd and Pb were respectively 2,920 (horse) and 247 (dog), 5,020 (fish) and 1,203 (dog), 824 (fish) and 205 (bird), 700 (fish) and 196 (rabbit), 1580 (bird) and 413 (fish), 331 (fish) and 114 (cat), 928 (fish) and 275 (cat). These variations may be related to the composition of the ingredients used in each type of animal feed, the specific raw materials used, or possible environmental contamination associated with the production process. Identifying higher levels is particularly relevant for assessing toxicological risks, especially with potentially toxic elements such as arsenic, cadmium, and lead. In general, all analyte mass fractions found in animal feed were consistently below the established toxicity and tolerance limits.[4,22,23]

The mass fractions (μg kg^{-1}) of As, Cd, Mo, Ni, Pb, Se and V found in all samples digested by the proposed and comparative methods were similar. Figure 1 illustrates correlation plots of the mass fractions of analytes in animal feed samples determined by ICP-MS after digestion in CHDS and MWD using different concentrations of nitric acid. Typical linear correlations were ≥ 0.997 (3.5 mol L^{-1}), ≥ 0.996 (7 mol L^{-1}) and ≥ 0.996 (14 mol L^{-1}). Statistical tests were performed on all results to assess precision and accuracy by *F*-test and paired *t*-test, respectively. A comparison between CHDS and MWD results indicated that 99%, 93%, and 94% of the *F*-test results and 89%, 88% and 93% of the paired *t*-test results for 3.5, 7 and 14 mol L^{-1} HNO_3, respectively, exhibited no significant difference at a 95% confidence level.

The analyte determinations using CHDS showed relative standard deviations (RSDs) found to range from 0.2 to 18.3% at 3.5 mol L^{-1}, 0.1 to 18.9% at 7 mol L^{-1}, and 0.1 to 18.3% at 14 mol L^{-1}. The RSDs obtained using MWD were 0.1 – 17.7%, 0.1 – 13.2%, and 0.1 – 16.3% for the same samples.

Table III. Results (mean ± standard deviation, n = 3) for trace and ultra-trace element determined (μg kg^{-1}) in feed samples after digestion in CHDS and MWD using diluted nitric acid (3.5 mol L^{-1})

Sample	Digestion method	Mass Fraction (μg kg^{-1})						
		V	Ni	As	Se	Mo	Cd	Pb
Bird 1	CHDS	2007 ± 12	1797 ± 134	226 ± 1	501 ± 46	1580 ± 25	167 ± 0	390 ± 35
	MWD	2043 ± 31	1754 ± 56	247 ± 3	551 ± 41	1568 ± 34	165 ± 2	355 ± 54
	t-value	1.9	0.5	10.5	1.4	0.5	1.5	0.9
Bird 2	CHDS	274 ± 6	1219 ± 114	205 ± 1	195 ± 9	1261 ± 21	142 ± 1	297 ± 19
	MWD	300 ± 6	1294 ± 68	217 ± 1	210 ± 22	1279 ± 11	142 ± 0	294 ± 14
	t-value	5.2	1.0	12.2	1.2	1.3	0.5	0.2
Dog 1	CHDS	253 ± 6	1203 ± 65	212 ± 4	349 ± 9	1012 ± 27	134 ± 0	397 ± 3
	MWD	247 ± 3	1196 ± 21	222 ± 2	342 ± 4	1053 ± 29	138 ± 1	387 ± 8
	t-value	1.6	0.2	3.7	1.3	1.8	9.0	1.9
Dog 2	CHDS	327 ± 12	1290 ± 39	257 ± 3	407 ± 14	608 ± 4	157 ± 3	384 ± 9
	MWD	318 ± 6	1275 ± 94	270 ± 5	404 ± 9	620 ± 7	157 ± 10	388 ± 3
	t-value	1.1	0.3	3.7	0.3	2.5	0.1	0.6
Horse 1	CHDS	2023 ± 308	4615 ± 41	778 ± 16	324 ± 59	846 ± 44	132 ± 18	636 ± 48
	MWD	2120 ± 22	4316 ± 133	732 ± 24	332 ± 59	843 ± 97	146 ± 2	639 ± 49
	t-value	0.5	3.7	2.7	0.2	0.1	1.4	0.1
Horse 2	CHDS	2920 ± 14	4425 ± 42	716 ± 8	353 ± 11	1053 ± 12	163 ± 10	707 ± 129
	MWD	3482 ± 26	4550 ± 86	729 ± 2	508 ± 28	1073 ± 26	151 ± 3	705 ± 51
	t-value	33.2	2.3	2.8	9.0	1.2	2.0	0.02
Cat 1	CHDS	928 ± 24	2118 ± 97	430 ± 25	451 ± 11	1384 ± 27	114 ± 4	614 ± 37
	MWD	952 ± 61	2078 ± 64	444 ± 14	461 ± 35	1313 ± 87	115 ± 1	641 ± 12
	t-value	0.6	0.6	0.8	0.5	1.4	0.5	1.2

(continued on next page)

Table III. Results (mean ± standard deviation, n = 3) for trace and ultra-trace element determined (μg kg^{-1}) in feed samples after digestion in CHDS and MWD using diluted nitric acid (3.5 mol L^{-1}) (continued)

Sample	Digestion method	Mass Fraction (μg kg^{-1})						
		V	Ni	As	Se	Mo	Cd	Pb
Cat 2	CHDS	389 ± 30	1208 ± 58	251 ± 4	663 ± 22	567 ± 35	127 ± 6	275 ± 31
	MWD	397 ± 43	1296 ± 60	263 ± 5	654 ± 21	564 ± 14	122 ± 3	260 ± 4
	t-value	0.3	1.8	3.2	0.5	0.2	1.3	0.8
Fish 1	CHDS	1597 ± 14	5020 ± 998	728 ± 10	700 ± 41	1038 ± 54	119 ± 1	928 ± 14
	MWD	1514 ± 10	5384 ± 87	771 ± 8	690 ± 45	1135 ± 40	117 ± 0	951 ± 17
	t-value	8.4	0.6	6.0	0.3	2.5	4.3	1.9
Fish 2	CHDS	427 ± 11	1263 ± 41	824 ± 27	554 ± 24	413 ± 19	331 ± 17	307 ± 37
	MWD	419 ± 18	1253 ± 82	875 ± 30	566 ± 56	408 ± 10	327 ± 11	349 ± 15
	t-value	0.7	0.2	2.2	0.3	0.4	0.4	1.8
Rabbit 1	CHDS	953 ± 32	2591 ± 100	263 ± 7	196 ± 5	1075 ± 49	153 ± 3	522 ± 80
	MWD	1007 ± 23	2514 ± 136	282 ± 4	195 ± 15	1025 ± 48	154 ± 2	548 ± 8
	t-value	2.4	0.8	4.1	0.1	1.2	0.7	0.6
Rabbit 2	CHDS	380 ± 14	1599 ± 120	354 ± 12	439 ± 59	962 ± 38	138 ± 3	321 ± 13
	MWD	394 ± 48	1565 ± 79	349 ± 8	445 ± 23	946 ± 30	128 ± 0	340 ± 12
	t-value	0.5	0.4	0.6	0.2	0.6	6.6	1.8

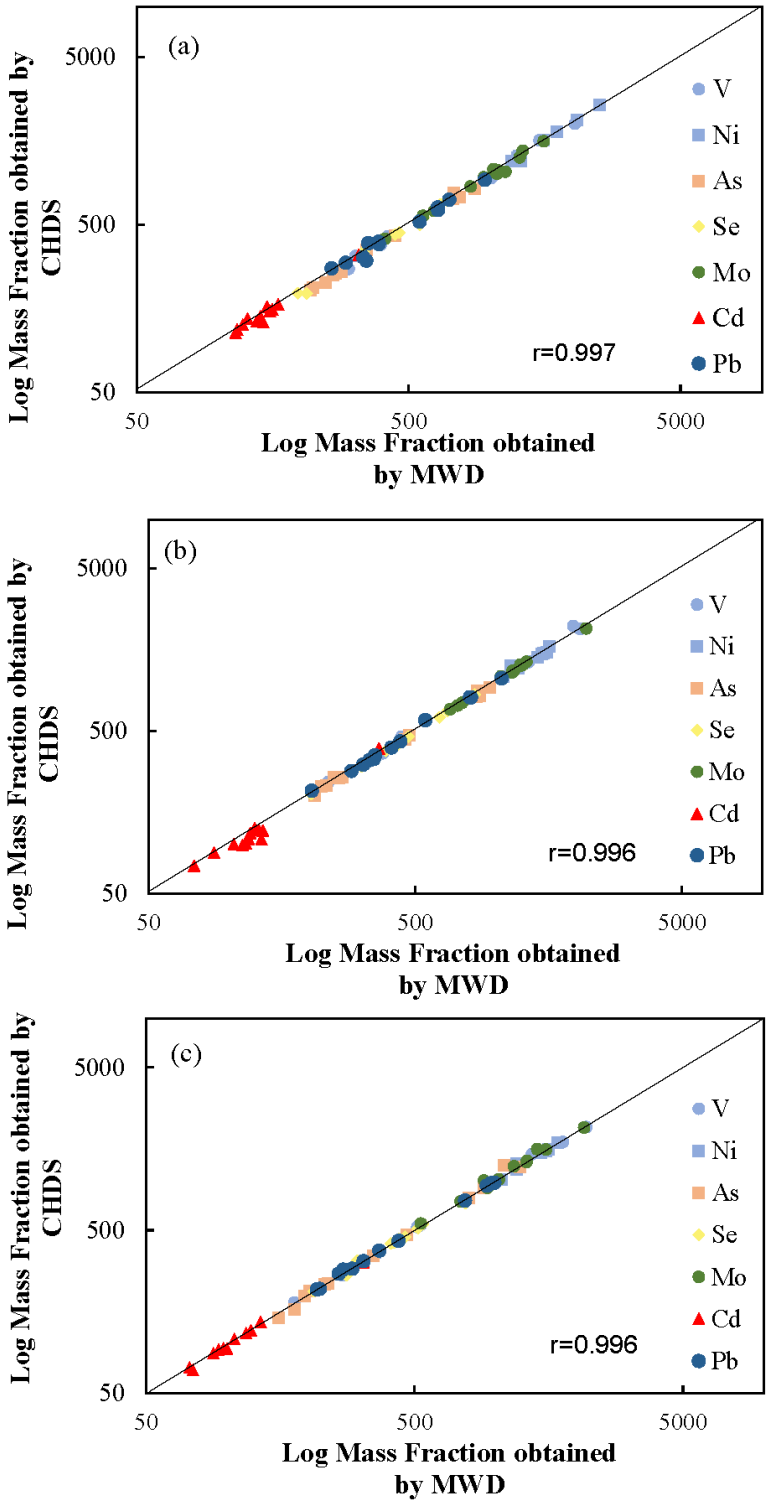

Figure 1. Correlation plot of the log of the Mass fraction (μg kg^{-1}) of trace and ultra trace elements in animal feed samples, as determined by ICP-MS after digestion in CHDS (y-axis) and MWD (x-axis), with the use of HNO_3 at concentrations of (a) 3.5 mol L^{-1}, (b) 7 mol L^{-1}, and (c) 14 mol L^{-1}.

The limits of quantification (LOQ) were calculated according to IUPAC recommendations.[24] Table IV presents data for As, Cd, Mo, Ni, Pb, Se and V obtained using CHDS and MWD. In general, the LOQ observed for CHDS and MWD using HNO_3 at 3.5, 7 and 14 mol L^{-1} were similar. These data demonstrate the effectiveness of the CHDS system to prepare animal feed for determining trace and ultra-trace elements using ICP-MS. Furthermore, variation in HNO_3 concentration showed no observable trend and did not influence the LOQ results. This demonstrates that the use of diluted acid is feasible for preparing animal feed samples.

Table IV. Limits of quantification (in μg kg^{-1}) for analytes determined by ICP-MS after digestion in CHDS and MWD methods using different nitric acid concentrations

Element	Method	Nitric acid, mol L^{-1}		
		3.5	**7**	**14**
V	CHDS	31	36	33
	MWD	48	25	19
Ni	CHDS	286	211	186
	MWD	245	164	122
As	CHDS	52	55	51
	MWD	44	59	38
Se	CHDS	66	47	51
	MWD	55	59	76
Mo	CHDS	186	214	398
	MWD	156	221	361
Cd	CHDS	5	13	15
	MWD	9	10	18
Pb	CHDS	52	61	86
	MWD	75	77	59

CONCLUSIONS

The application of diluted nitric acid in sample preparation using CHDS has shown promise for the digestion of animal feed for different species, including birds, cats, dogs, horses, fish, and rabbits. Determining As, Cd, Mo, Ni, Pb, Se, and V in CRMs and RMs demonstrated the high accuracy of the proposed method even using diluted nitric acid. The results showed that CHDS performs similarly to MWD digestion. Additionally, the limits of quantification obtained with CHDS were similar to those of MWD, independent of the HNO_3 concentration used, which contributes to reduced waste generation. Furthermore, the present study demonstrated not only the efficiency of the diluted acid digestion process, but also its potential to promote a more sustainable and environmentally responsible approach to animal feed quality control.

Conflicts of interest

There are no conflicts of interest to declare.

Acknowledgements

This study was supported by the São Paulo Research Foundation-FAPESP (grant 2024/02879-4) and Conselho Nacional de Desenvolvimento Científico e Tecnológico-CNPq (grant 303607/2021-1).

REFERENCES

(1) Costa, S. S. L.; Pereira, A. C. L.; Passos, E. A.; Alves, J. P. H.; Garcia, C. A. B.; Araujo, R. G. O. Evaluation of the Chemical Composition of Dry Feeds for Dogs and Cats. *J. Braz. Chem. Soc*. **2018**, *23* (12), 2616–2625. https://doi.org/10.21577/0103-5053.20180142

(2) Zicker, S. C. Evaluating Pet Feeds: How Confident Are You When You Recommend a Commercial Pet Feed? *Topics in Companion Animal Medicine* **2008**, *23* (3), 121–126. https://doi.org/10.1053/j.tcam.2008.04.003

(3) Costa, S. S. L.; Pereira, A. C. L.; Passos, E. A.; Alves, J. P. H.; Garcia, C. A. B.; Araujo, R. G. O. Multivariate Optimization of an Analytical Method for the Analysis of Dog and Cat Feeds by ICP-OES. *Talanta* **2013**, *108*, 157–164. https://doi.org/10.1016/j.talanta.2013.03.002

(4) National Research Council. *Mineral Tolerance of Animals* (2nd Ed.). The National Academies Press: Washington, DC, 2005.

(5) Association of Official Agricultural Chemists (AOAC). Official Methods of Analysis: *Guidelines for Standard Method Performance Requirements*. AOAC International: Gaithersburg, MD, 2016.

(6) Krug, F. J.; Rocha, F. R. P. *Métodos de Preparo de Amostras para Análise Elementar*. (2nd Ed.). EditSBQ: São Paulo, SP, 2019.

(7) de la Rocha, S. R.; Sánchez-Muniz, F. J.; Gómez-Juaristi, M.; Marín, M. T. L. Trace Elements Determination in Edible Seaweeds by an Optimized and Validated ICP-MS Method. *J. Feed Compos. Anal*. **2009**, *22* (4), 330–336. https://doi.org/10.1016/j.jfca.2008.10.021

(8) Evans, E. H.; Giglio, J. J. Interferences in inductively coupled plasma mass spectrometry - A Review. *J. Anal. At. Spectrom*. 1993, *8*, 1–18. https://doi.org/10.1039/JA9930800001

(9) Miranda, K.; Pereira-Filho, E. R.; Gomes Neto, J. A. A New Closed-Vessel Conductively Heated Digestion System: Fostering Plant Analysis by Inductively Coupled Plasma Optical Emission Spectroscopy. *J. Anal. At. Spectrom*. **2014**, *9*, 825–831. https://doi.org/10.1039/C3JA50369K

(10) Miranda, K.; Vieira, A. L.; Gomes Neto, J. A. High-Throughput Sugarcane Leaf Analysis Using a Low Cost Closed-Vessel Conductively Heated Digestion System and Inductively Coupled Plasma Optical Emission Spectroscopy. *Anal. Methods* **2014**, *6*, 9503–9508. https://doi.org/10.1039/C4AY01841A

(11) Miranda, K.; Vieira, A. L.; Bechilin, M. A.; Fortunato, F. M.; Virgilio, A.; Ferreira, E. C.; Gomes Neto, J. A. Determination of Ca, Cd, Cu, Fe, K, Mg, Mn, Mo, Na, Se, and Zn in Feedstuffs by Atomic Spectrometry After Sample Preparation Using a Low-Cost Closed-Vessel Conductively Heated Digestion System. *Feed Anal. Methods* **2015**, *9*, 1887–1894. https://doi.org/10.1007/s12161-015-0371-8

(12) Vieira, A. L.; Miranda, K.; Virgilio, A.; Ferreira, E. C.; Gomes Neto, J. A. Evaluation of an Improved Closed-Vessel Conductively Heated Digestion System for the Analysis of Raw Meat Samples by ICP Techniques. *J. Anal. At. Spectrom*. **2018**, *33*, 1354–1362. https://doi.org/10.1039/C8JA00121A

(13) Traversa, L. C.; Santiago, J. V. B.; Oliveira, E. M.; Ferreira, E. C.; Virgilio, A.; Gomes Neto, J. A. Closed-Vessel Conductively Heated Digestion System for the Elemental Analysis of Agricultural Materials by High-Resolution Continuum Source Flame Atomic Absorption Spectrometry (HR-CS FAAS). *Anal. Lett*. **2023**, *56*, 2443–2456. https://doi.org/10.1080/00032719.2023.2174133

(14) Costa, R. C.; Santiago, J. V. B.; Ferreira, E. C.; Virgilio, A.; Gomes Neto, J. A. Closed-Vessel Conductively Heated Digestion of Dry Dog Feed for Spectrometric Determination of Essential Nutrients. *Braz. J. Anal. Chem*. **2023**, *11*, 41–54. https://doi.org/10.30744/brjac.2179-3425.ar-4-2023

(15) Vieira, A. L.; Carvalho, G. G. A.; Gomes Neto, J. A.; Oliveira, P. V.; Kamogawa, M. Y.; Virgilio, A. A Convective Heated Digestion System with Closed Vessels: A New Digestor for Elemental Inorganic Analysis. *J. Anal. At. Spectrom*. **2024**, *39*, 356–363. https://doi.org/10.1039/D3JA00328K

(16) Pinto, A. L. M.; Souza, A. L.; Araujo, L. G.; Marumo, J. T.; Cotrim, M. E. B.; Guilhen, S. N. Innovative Sample Preparation Method Using a Conductively Heated Digestion System for Trace Element Analysis of Radioactive Oil Sludge by ICP-OES. *J. Anal. At. Spectrom*. **2026**, *296* (1), 128488. https://doi.org/10.1039/D5JA00042D

(17) Oliveira, E. M.; Ferreira, E. C.; Gomes Neto, J. A.; Virgilio, A. Closed-Vessel Conductively Heated Digestion System with Diluted Nitric Acid for the Preparation of Biomass and Biochar Samples. *Talanta* **2026**, *296* (1), 128488. https://doi.org/10.1016/j.talanta.2025.128488
(18) Costa, R. C. V.; Ferreira, E. C.; Gomes Neto, J. A.; Virgilio, A. Evaluation of a Cost-Effective and Environmentally Friendly Digestion Method for Preparing Animal Feed Samples for Elemental Analysis. *Anim. Feed Sci. Technol*. **2025**, *329*, 116511. https://doi.org/10.1016/j.anifeedsci.2025.116511
(19) National Research Council Canada (NRCC). Certified Reference Materials: *Wheat Flour (8436) and BRAN-1 (8433)*. Ottawa, Canada, 2022. Available at: https://nrc-digital-repository.canada.ca/eng/view/object/?id=d092223f-4000-49df-93c1-b6e901f33fbe (accessed 10/2025).
(20) Carioni, V. M. O.; Chelegão, R.; Naozuka, J.; Nomura, C. S. Feasibility Study for the Preparation of a Tuna Fish Candidate Reference Material for Total As Determination. *Accredit. Qual. Assur*. **2011**, *16*, 453–458. https://doi.org/10.1007/s00769-011-0796-8
(21) Bizzi, C. A.; Flores, E. L. M.; Nóbrega, J. A.; Oliveira, J. S. S.; Schmidt, L.; Mortari, S. R. Evaluation of a Digestion Procedure Based on the Use of Diluted Nitric Acid Solutions and H_2O_2 for the Multielement Determination of Whole Milk Powder and Bovine Liver by ICP-OES Based Techniques. *J. Anal. At. Spectrom*. **2014**, *29*, 332–338. https://doi.org/10.1039/c3ja50330e
(22) National Research Council. *Nutrient Requirements of Dogs and Cats*. The National Academies Press: Washington, DC, 2006. https://doi.org/10.17226/10668
(23) Dzanis, D. A. The Association of American Feed Control Officials Dog and Cat Feed Nutrient Profiles: Substantiation of Nutritional Adequacy of Complete and Balanced Pet Feeds in the United States. *The Journal of Nutrition* **1994**, *124* (suppl 12), 2535S–2539S. https://doi.org/10.1093/jn/124.suppl_12.2535S
(24) Currie, L. A. Nomenclature in Evaluation of Analytical Methods Including Detection and Quantification Capabilities (IUPAC Recommendations 1995). *Anal. Chim. Acta* **1999**, *391*, 105–126. https://doi.org/10.1016/S0003-2670(99)00104-X.

SUPPLEMENTARY MATERIAL

Table SI. Results (mean ± standard deviation, n = 3) for trace and ultra-trace element determined (μg kg^{-1}) in animal feed samples digested by CHDS and MW using HNO_3 7 mol L^{-1}

Sample	Digestion method	Mass Fraction (μg kg-1)						
		V	Ni	As	Se	Mo	Cd	Pb
Bird 1	CHDS	2221 ± 1	1525 ± 32	233 ± 12	385 ± 23	2138 ± 28	122 ± 1	332 ± 11
	MWD	1954 ± 24	1551 ± 5	232 ± 2	392 ± 27	2186 ± 15	134 ± 7	336 ± 10
	t-value	19.3	1.4	0.1	0.3	2.6	2.8	0.5
Bird 2	CHDS	244 ± 3	1643 ± 154	201 ± 1	205 ± 5	1262 ± 9	102 ± 0	338 ± 10
	MWD	236 ± 10	1111 ± 45	209 ± 0	203 ± 10	1235 ± 33	116 ± 0	349 ± 4
	t-value	1.3	5.7	9.0	0.3	1.4	253.0	1.8
Dog 1	CHDS	288 ± 20	1218 ± 49	229 ± 1	406 ± 12	1148 ± 12	101 ± 4	285 ± 46
	MWD	283 ± 35	1216 ± 31	222 ± 4	424 ± 37	1153 ± 31	104 ± 1	288 ± 2
	t-value	0.2	0.04	2.9	0.8	0.3	1.4	0.1
Dog 2	CHDS	365 ± 21	1082 ± 13	258 ± 1	378 ± 19	748 ± 15	100 ± 2	355 ± 22
	MWD	377 ± 28	1069 ± 44	258 ± 1	387 ± 6	748 ± 5	112 ± 0	352 ± 23
	t-value	0.6	0.5	0.5	0.8	0.03	12.6	0.1
Horse 1	CHDS	2910 ± 101	4723 ± 70	885 ± 9	306 ± 4	1085 ± 17	89 ± 0	806 ± 21
	MWD	2909 ± 125	4746 ± 32	854 ± 45	311 ± 8	1048 ± 9	88 ± 11	808 ± 62
	t-value	0.02	0.5	1.2	1.0	3.3	0.2	0.1
Horse 2	CHDS	3018 ± 239	4788 ± 10	824 ± 12	483 ± 77	1278 ± 14	109 ± 5	808 ± 2
	MWD	3008 ± 12	4765 ± 22	870 ± 39	489 ± 25	1263 ± 8	132 ± 1	801 ± 25
	t-value	0.1	1.7	1.9	0.1	1.6	7.5	0.5
Cat 1	CHDS	1321 ± 113	1658 ± 43	443 ± 25	464 ± 13	1336 ± 40	75 ± 1	586 ± 10
	MWD	1316 ± 127	1593 ± 68	457 ± 24	472 ± 39	1305 ± 103	74 ± 9	545 ± 31
	t-value	0.05	1.4	0.7	0.4	0.5	0.1	2.2

(continued on next page)

Table SI. Results (mean ± standard deviation, n = 3) for trace and ultra-trace element determined (μg kg^{-1}) in animal feed samples digested by CHDS and MW using HNO_3 7 mol L^{-1} (continued)

Sample	Digestion method	Mass Fraction (μg kg-1)						
		V	Ni	As	Se	Mo	Cd	Pb
Cat 2	CHDS	464 ± 18	1258 ± 108	263 ± 4	664 ± 14	683 ± 12	124 ± 5	311 ± 22
	MWD	445 ± 2	1139 ± 16	247 ± 4	661 ± 87	674 ± 12	130 ± 2	318 ± 20
	t-value	1.8	1.9	4.4	0.1	0.9	1.9	0.4
Fish 1	CHDS	2127 ± 45	5210 ± 444	934 ± 6	841 ± 16	1286 ± 20	109 ± 2	1060 ± 37
	MWD	2079 ± 95	5255 ± 35	948 ± 7	835 ± 47	1240 ± 2	118 ± 1	1052 ± 55
	t-value	0.8	0.2	2.5	0.2	3.9	7.9	0.2
Fish 2	CHDS	445 ± 17	1503 ± 91	819 ± 2	607 ± 13	717 ± 7	392 ± 9	433 ± 6
	MWD	443 ± 14	1506 ± 75	849 ± 15	615 ± 19	720 ± 8	365 ± 4	439 ± 3
	t-value	0.2	0.1	3.5	0.6	0.5	4.9	1.5
Rabbit 1	CHDS	1345 ± 101	1487 ± 17	262 ± 1	303 ± 57	1171 ± 12	126 ± 2	415 ± 27
	MWD	1335 ± 25	1486 ± 14	267 ± 2	314 ± 15	1169 ± 2	125 ± 1	404 ± 9
	t-value	0.2	0.1	3.0	0.3	0.3	1.2	0.6
Rabbit 2	CHDS	438 ± 13	1430 ± 95	470 ± 11	427 ± 11	1174 ± 3	118 ± 2	397 ± 2
	MWD	437 ± 10	1440 ± 32	474 ± 12	429 ± 3	1157 ± 60	120 ± 0	406 ± 1
	t-value	0.03	0.2	0.4	0.3	0.5	2.1	7.3

Table SII. Results (mean ± standard deviation, n = 3) for trace and ultra-trace element determined (μg kg^{-1}) in animal feed samples digested by CHDS and MW using HNO_3 14 mol L^{-1}

Sample	Digestion method	Mass Fraction (μg kg^{-1})						
		V	Ni	As	Se	Mo	Cd	Pb
Bird 1	CHDS	2148 ± 105	1563 ± 245	163 ± 15	419 ± 8	2133 ± 71	121 ± 5	217 ± 2
	MWD	2180 ± 31	1577 ± 34	178 ± 0	419 ± 16	2140 ± 105	123 ± 3	216 ± 4
	t-value	0.5	0.1	1.7	0.02	0.1	0.4	0.1
Bird 2	CHDS	180 ± 8	1360 ± 91	144 ± 4	211 ± 6	1314 ± 91	88 ± 1	270 ± 9
	MWD	178 ± 4	1358 ± 29	156 ± 1	210 ± 13	1304 ± 48	89 ± 2	261 ± 11
	t-value	0.5	0.03	5.4	0.1	0.2	0.8	1.2
Dog 1	CHDS	364 ± 39	1177 ± 16	197 ± 3	415 ± 51	1571 ± 104	107 ± 11	291 ± 9
	MWD	250 ± 19	1197 ± 2	195 ± 1	409 ± 26	1429 ± 30	106 ± 0	292 ± 10
	t-value	4.6	2.2	1.5	0.2	2.3	0.2	0.2
Dog 2	CHDS	265 ± 9	1220 ± 103	212 ± 5	546 ± 9	752 ± 40	116 ± 9	286 ± 17
	MWD	269 ± 5	1184 ± 21	203 ± 1	538 ± 31	742 ± 4	117 ± 1	270 ± 30
	t-value	0.5	0.6	3.0	0.4	0.4	0.2	0.8
Horse 1	CHDS	3637 ± 138	4520 ± 1196	1250 ± 36	443 ± 26	987 ± 77	93 ± 6	762 ± 27
	MWD	3644 ± 73	4322 ± 388	1078 ± 3	436 ± 29	971 ± 63	93 ± 2	769 ± 53
	t-value	0.1	0.3	8.3	0.3	0.3	0.1	0.2
Horse 2	CHDS	4534 ± 282	5081 ± 278	1224 ± 48	322 ± 9	1570 ± 44	136 ± 3	979 ± 76
	MWD	4521 ± 30	5814 ± 77	1236 ± 147	346 ± 34	1544 ± 29	133 ± 3	991 ± 59
	t-value	0.1	4.4	0.1	1.2	0.9	1.2	0.2
Cat 1	CHDS	1464 ± 89	1714 ± 148	346 ± 7	325 ± 18	1334 ± 98	72 ± 10	672 ± 13
	MWD	1366 ± 28	1708 ± 61	352 ± 7	306 ± 34	1312 ± 53	72 ± 4	661 ± 72
	t-value	1.8	0.1	0.9	0.9	0.4	0.1	0.2
Cat 2	CHDS	523 ± 83	1027 ± 115	234 ± 34	732 ± 53	1011 ± 138	136 ± 1	218 ± 0
	MWD	511 ± 83	1057 ± 20	238 ± 9	771 ± 57	905 ± 14	133 ± 4	221 ± 2
	t-value	0.2	0.4	0.2	0.9	1.3	1.2	2.1
Fish 1	CHDS	1614 ± 59	5876 ± 182	784 ± 10	757 ± 20	1239 ± 22	69 ± 1	936 ± 57
	MWD	1653 ± 109	5203 ± 37	799 ± 6	755 ± 31	1172 ± 99	74 ± 1	928 ± 7
	t-value	0.5	6.3	2.2	0.1	1.1	7.5	0.2

(continued on next page)

Table SII. Results (mean ± standard deviation, n = 3) for trace and ultra-trace element determined (μg kg^{-1}) in animal feed samples digested by CHDS and MW using HNO_3 14 mol L^{-1} (continued)

Sample	Digestion method	Mass Fraction (μg kg^{-1})						
		V	Ni	As	Se	Mo	Cd	Pb
Fish 2	CHDS	358 ± 14	1499 ± 20	909 ± 28	515 ± 13	551 ± 7	318 ± 4	323 ± 10
	MWD	359 ± 7	1476 ± 1	908 ± 24	513 ± 7	527 ± 23	322 ± 3	322 ± 10
	t-value	0.1	1.9	0.02	0.2	1.7	1.5	0.1
Rabbit 1	CHDS	1747 ± 136	1284 ± 188	233 ± 14	265 ± 25	914 ± 119	93 ± 8	430 ± 42
	MWD	1780 ± 117	1198 ± 105	230 ± 6	278 ± 3	932 ± 34	100 ± 1	435 ± 19
	t-value	0.3	0.7	0.3	0.9	0.3	1.4	0.2
Rabbit 2	CHDS	542 ± 40	1533 ± 73	469 ± 37	456 ± 9	1026 ± 10	94 ± 6	375 ± 34
	MWD	527 ± 27	1545 ± 9	467 ± 6	460 ± 20	1029 ± 18	97 ± 1	368 ± 22
	t-value	0.5	0.3	0.1	0.3	0.3	0.7	0.3

inscrições e informações:
82 98193.0529 / 98821.4091

REALIZAÇÃO

UNIVERSIDADE FEDERAL DE ALAGOAS

APOIO

IQB PPGQB Programa de Pós-Graduação em Química e Biotecnologia

FAPEAL FUNDAÇÃO DE AMPARO À PESQUISA DO ESTADO DE ALAGOAS

CNPq Conselho Nacional de Desenvolvimento Científico e Tecnológico

SECRETARIA EXECUTIVA

PRIME EVENTOS

Brazilian Journal of Analytical Chemistry
2026, Volume 13, Issue 52, pp 167-168

FEATURE

Science and Technology in Focus: Pittcon 2026 Concludes Historic Edition in Texas with a Focus on AI and Sustainability

Pittcon 2026, one of the world's largest conferences dedicated to laboratory science and analytical instrumentation, was held from March 7 to 11 at the Henry B. González Convention Center in Texas, bringing together thousands of researchers, academics, and industrial leaders. The central themes of discussions and product launches revolved around workflow automation, laboratory sustainability, and the integration of Artificial Intelligence into chemistry.

Pittcon is renowned for its exhibition hall. Photo: Pittcon 2026

With 45 short courses, 375 speakers, 1,200 presentations, and 500 exhibitors, Pittcon 2026 undoubtedly offered something for every scientist and researcher.

Pittcon 2026 opened with the Wallace H. Coulter Keynote Lecture, which traditionally features a speaker whose work has had a transformative impact on laboratory science. Nobel Prize laureate Professor Frances H. Arnold delivered the Coulter Lecture entitled "Innovation by Evolution: Bringing a New Chemistry to Life".

Another highly impactful moment was the lecture by Omar Yaghi, who introduced "AIMATRY," a new field that merges Artificial Intelligence with the design of complex molecular structures. Parallel symposia also addressed the future of biomedicine, with an emphasis on wearable sensors and devices designed for clinical analyses outside the traditional laboratory environment.

In addition to a strong technical program, Pittcon offered a wide range of short courses. These intensive, hands-on courses provide specialized training in dozens of subjects, ranging from fundamental concepts in chromatography and mass spectrometry to emerging areas such as data analysis and advanced materials characterization.

Among the event's honors, the prestigious Pittcon Heritage Award was presented to Alexandra Knauer, CEO of Knauer. The German executive was recognized for her leadership in the global expansion of high-performance liquid chromatography (HPLC) purification systems, essential for mRNA vaccine production, as well as for her pioneering corporate policies promoting pay equity.

Scientific advances in forensic medicine were also recognized with the Pittsburgh Spectroscopy Award, granted to Dr. Igor Lednev for his groundbreaking application of Raman spectroscopy in rapid medical diagnostics.

The Pittcon exhibition hall is the largest single showcase of instrumentation, services, and technology for laboratory sciences in North America. It serves as a dynamic hub for innovation and technology transfer, where abstract concepts discussed during technical sessions are transformed into tangible products and tools.

The exhibition's major commercial highlight was the announcement of the Pittcon Excellence Awards winners. In the large-company category, Xylem Lab Solutions earned the gold medal with the launch of the N-REALYZER, a high-speed nitrogen and protein analyzer based on the Dumas combustion method. Hoefer, Inc. received the silver medal for an automated laser engraving machine for biobank tubes, while Rigaku Americas Corporation took bronze for the XSPA-200 ER two-dimensional detector designed for X-ray diffraction.

As tradition dictates, the closing of the event also marked the announcement of plans for the following year. The organization confirmed that Pittcon 2027 will return to its geographical roots in Pittsburgh between April 24 and 28, 2027. The official calendar for scientific abstract submissions for the next edition will begin on June 1, 2026.

Text: Lilian Freitas – BrJAC Publisher
Source: Pittcon 2026

Authors

Richard Law,[1] Cristian Cojocariu,[1] Daniela Cavagnino[2]

[1]Thermo Fisher Scientific, Runcorn, UK

[2]Thermo Fisher Scientific, Milan, Italy

Keywords

GC-MS, Helium Saver, EPA 8270, SVOC, SVOA, semivolatile organic compound, BNA, base neutral acids, organic contaminants.

Introduction

The United States Environmental Protection Agency (U.S. EPA) released the first Semivolatile Organic Compounds (SVOC) method by Gas Chromatography-Mass Spectrometry (Method 8270) at the end of 1980. It is a common method used in almost all environmental laboratories looking to analyze semivolatile organic compounds in extracts prepared from many types of solid waste matrices, soils, air sampling media, and water.[1] Since then, single quadrupole mass spectrometers have become much more sensitive and the source fragmentation has changed. Many original assumptions[2] about the origin and nature of the ion species have proven to be wrong or require correction, while the new generations of the mass spectrometers have proven to provide more response in the high-mass region,[3] resulting in adjustment of the tuning criteria to be met.[4] To adjust to these changes, the EPA has changed the ion abundance criteria for the passing of DFTPP ion ratio criteria in EPA Method 8270D.

This application note shows how the Thermo Scientific™ ISQ™ 7000 single quadrupole GC-MS system can meet Method 8270D requirements with the extended dynamic range detection system. The working method range was shown to be 0.2–200 ppm using the same column. Particular attention has been posed on maximizing the uptime of the instrument, as required by high-throughput laboratories. The innovative Thermo Scientific™ NeverVent™ technology available on the ISQ 7000 GC-MS system is a unique solution for speeding up the routine maintenance operations, saving the time typically required to vent the MS system and re-establish the vacuum conditions.

The new Thermo Scientific™ Instant Connect Helium Saver Injector was also assessed in this application

to show that significant financial costs savings can be realized throughout the lifetime of a GC-MS instrument without compromising the instrument's performance.

Experimental

The method was tested on five ISQ 7000 GC-MS systems equipped with the Thermo Scientific™ ExtractaBrite™ ion source to assess method transferability and instrument-to-instrument variability. Both ranges (0.2–50 ppm and 2–200 ppm) were validated using the Instant Connect Helium Saver Injector (P/N 19070013) and the Thermo Scientific™ Instant Connect Split-Splitless (SSL) Injector module (P/N 19070010). The column used was a Thermo Scientific™ TraceGOLD™ TG-5MS GC Column with 5 m guard, 30 m × 0.25 mm × 0.25 µm (P/N 26098-1425). A Thermo Scientific™ Injection Port Deactivated Liner 4 mm ID × 105 mm (P/N 453A1925) was selected for the Split-Splitless injection port. The ISQ 7000 GC-MS system operated in full-scan mode and the Thermo Scientific™ Chromeleon™ Chromatography Data System (CDS) software was used to acquire, process, and report data. The operating parameters for the Thermo Scientific™ TRACE™ 1310 GC system are reported in Table 1a (splitless method, range 0.2–50 ppm) and Table 1b (split method, range 2–200 ppm). The ISQ 7000 single quadrupole MS operating conditions are detailed in Tables 2a and 2b.

Table 1a. TRACE 1310 GC system parameters for splitless method.

Injection Volume (µL)	1.0
Liner	Deactivated Splitless Liner
Inlet Temp (°C)	270
Inlet Module and Mode	SSL in Surge Splitless at 345 kPa for 0.6 min
Splitess Time (min)	0.6
Split Flow (mL/min)	50
Oven Temperature Program	
Initial Temperature 1 (°C)	35
Hold Time (min)	2.25
Rate (°C/min)	25
Temperature 2 (°C)	100
Hold Time (min)	0.1
Rate (°C/min)	30
Temperature 3 (°C)	280
Hold Time (min)	0.1
Rate (°C/min)	10
Temperature 4 (°C)	320
Hold Time (min)	5.00

Table 1b. TRACE 1310 GC system parameters for split method.

Injection Volume (µL)	1.0
Liner	Deactivated Splitless Liner
Inlet Temp (°C)	310
Inlet Module and Mode	SSL in Split Mode
Split Ratio	10:1
Split Flow (mL/min) Carrier Gas (mL/min)	15 He, 1.5
Oven Temperature Program	
Initial Temperature 1 (°C)	35
Hold Time (min)	2.25
Rate (°C/min)	25
Temperature 2 (°C)	100
Hold Time (min)	0.1
Rate (°C/min)	30
Temperature 3 (°C)	280
Hold Time (min)	0.1
Rate (°C/min)	10
Temperature 4 (°C)	320
Hold Time (min)	5.00

Table 2a. ISQ 7000 Single Quadrupole MS parameters for splitless method.

Transfer Line Temp (°C)	300
Ion Source	ExtractaBrite
Ion Source Temp (°C)	300
Ionization Mode	EI
Electron Energy (eV)	70
Acquisition Mode	Full-scan
Scan Range (*m/z*)	35–500
Emission Current (mA)	10
Dwell Time	0.1

Table 2b. ISQ 7000 Single Quadrupole MS parameters for split method.

Transfer Line Temp (°C)	310
Ion Source	ExtractaBrite
Ion Source Temp (°C)	300
Ionization Mode	EI
Electron Energy (eV)	70
Acquisition Mode	Full-scan
Scan Range (*m/z*)	35–500
Emission Current (mA)	15
Dwell Time	0.1

Tuning for DFTPP

The ISQ 7000 MS system was tuned with a built-in EPA 8270D specifically designed tune (DFTPP Tune). This assures fulfillment of all method requirements in terms of ion abundance criteria. A tune verification DFTPP solution was injected to verify that the ISQ 7000 GC-MS system met the tuning requirements shown in Figure 1. Chromeleon CDS software has a dedicated reporting package for environmental laboratories, and automatically reports tune evaluation performance with a Pass/Fail indicator (Table 3).

Standard and sample preparation

Standards (Restek 8270 MegaMix Cat. No. 31850, AccuStandard Internal Standard Cat. No. Z-014J, AccuStandard Surrogate Cat No. M-8270-SS) were prepared in methylene chloride, and the internal standards were spiked at a concentration of 5 ppm for both the splitless and split methods. Spiking the range of 0.2 to 200 ppm with the same concentration of internal standards eliminated the necessity of preparing two different sets of calibration standards. Table 4 contains the calibration levels of both methods.

A volume of 1 µL of the calibration standards was injected for all methods. Figure 2 shows the chromatogram of the 5 ppm calibration standard acquired in splitless mode.

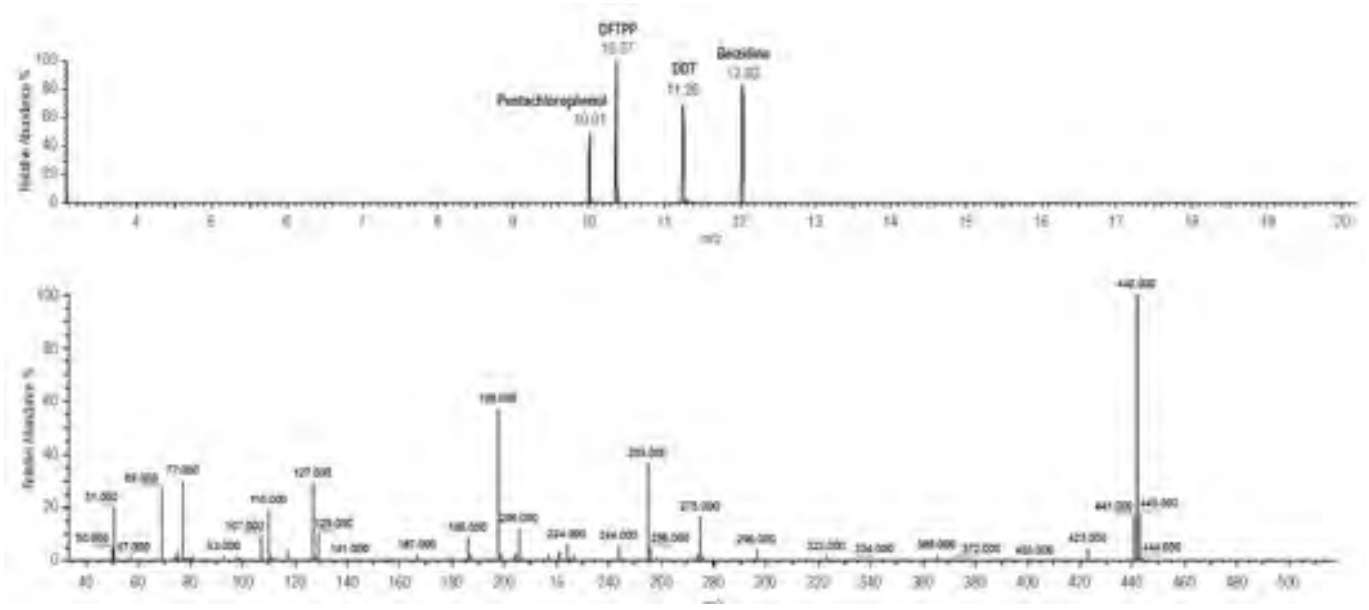

Figure 1. Acquired DFTTP mass spectrum using the ISQ 7000 single quadrupole GC-MS system operated in full-scan at 70 eV ionization energy.

Table 3. DFTPP spectrum check for ion abundance criteria.

Eval Mass (*m/z*)	Ion Abundance Criteria	Measured % Relative Abundance	Criteria Pass/ Fail
51	Greater than or equal to 10% AND less than or equal to 80% of Base Peak	20.7	Pass
68	Less than 2% of *m/z* 69	0.7	Pass
70	Less than 2% of *m/z* 69	0.5	Pass
127	Greater than or equal to 10% AND less than or equal to 80% of Base Peak	29.4	Pass
197	Less than 2% of *m/z* 198	0.1	Pass
198	Greater than 50% AND less than or equal to 100% of Base Peak	57.5	Pass
199	Greater than or equal to 5% AND less than or equal to 9% of *m/z* 198	5.9	Pass
275	Greater than or equal to 10% AND less than or equal to 60% of Base Peak	17.2	Pass
365	Greater than 1% of *m/z* 198	4.6	Pass
441	Greater than 0% AND less than 24% of *m/z* 442	17.4	Pass
442	Greater than 50% AND less than or equal to 100% of Base Peak	100.0	Pass
443	Greater than or equal to 15% AND less than or equal to 24% of *m/z* 442	18.1	Pass

Table 4. Calibration standards used for testing the splitless and split methods.

Calibration Standard	Splitless Conc. (ppm)	Split Conc. (ppm)
Cal 1	0.2	2.0
Cal 2	0.5	5.0
Cal 3	1.0	10.0
Cal 4	2.0	20.0
Cal 5	5.0	35.0
Cal 6	10.0	50.0
Cal 7	20.0	100.0
Cal 8	35.0	200.0
Cal 9	50.0	–

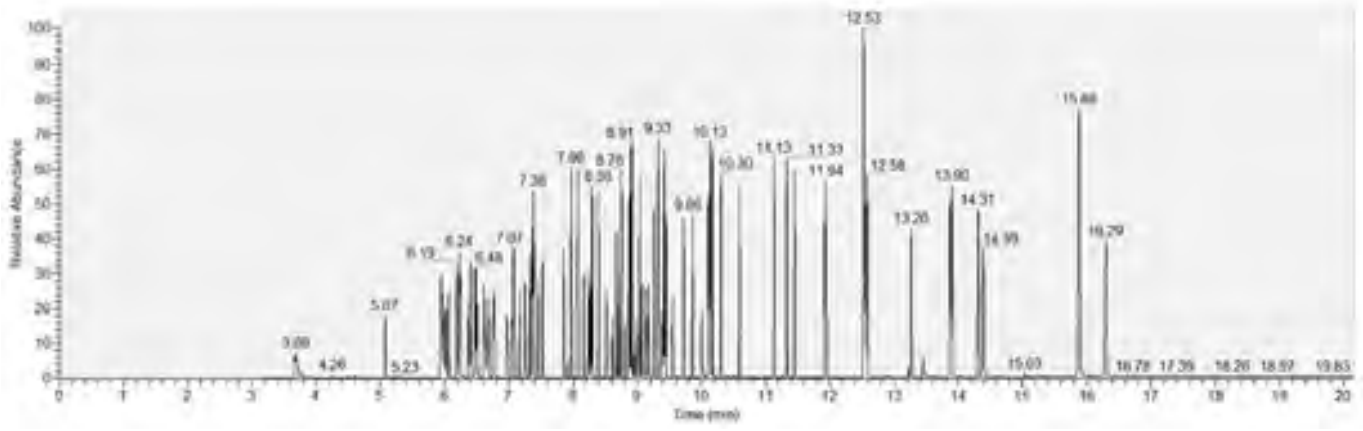

Figure 2. Total ion current (TIC) chromatogram of the 5 ppm EPA 8270 semivolatile calibration standard injected in splitless mode.

Results and discussion

Splitless method 0.2–50 ppm calibration

The average relative response factors of the 76 targeted compounds and six surrogates were calculated by analyzing the nine calibration standards from 0.2 ppm to 50 ppm in methylene chloride. Six compounds had Response Factors %RSD >20% and required an alternative curve fit. The %RSDs of those compounds calibrated using average response factors and r^2 values for the six alternative fit compounds are shown in Table 5.

Split method 2–200 ppm calibration

The average response factors of the 76 targeted compounds and six surrogates were calculated by analyzing eight calibration standards with concentrations ranging from 2 ppm to 200 ppm prepared in methylene chloride. Seven compounds had Response Factors %RSD >20% and required an alternate curve fit. The %RSDs of those compounds calibrated using average response factors and r^2 values for the seven alternative fit compounds are shown in Table 6.

Instant Connect Helium Saver module

Method 8270D was also tested with the Instant Connect Helium Saver module (P/N 19070013). Depending on the experimental conditions, the Helium Saver module allows up to 14 years of GC and GC-MS operation from a single helium cylinder. The inlet is supplied with two different gases: nitrogen is used for the septum purge and split flows with only helium supplying the analytical column. Because of this innovative and patented solution, helium consumption is dramatically reduced.

After time for equilibration, the GC-MS tuning mixture was injected and passed the criteria for EPA Method 8270D. Standards for a calibration curve (0.2–50 ppm and 2–200 ppm) were injected, and the data processed. Table 7(a) shows the results for splitless method and Table 7(b) reports split method. In both configurations (SSL and Helium Saver) and for both methods (split and splitless), less than 10% of compounds required an alternative curve fit. All the others had RSD% less than 20% with linear fit.

Minimum response factors

EPA Method 8270D requires a minimum relative response factor (RRF) for any point of the calibration curve for several compounds in the targeted list. Table 8 presents those minimum relative response factor requirements

and the minimum RRF across all curves performed on the ISQ 7000 single quadrupole GC-MS system.

Retention times

The four methods: splitless, splitless with Helium Saver, split, and split with Helium Saver, were developed over a period of three weeks. Table 9 demonstrates the stability of the retention times over this period of time. During this time, the liner and septa were changed and the analytical column trimmed. Still, the retention times are reproducible using different methods and different inlet modules. Table 9 shows a comparison of the retention times obtained using different methods and inlet modules.

NeverVent technology

Specifically designed to simplify the routine maintenance procedures and to maximize the GC-MS instrument uptime, the proprietary Vacuum Probe Interlock (VPI) and the V-lock solution available on the ISQ 7000 single quadrupole GC-MS system allow ion source cleaning or column replacement to be performed quickly without breaking the MS vacuum, saving up to 98% of the time typically required to perform those operations. Thanks to the VPI, the ion source can be fully removed—including all of the lenses and the repeller—through the front vacuum interlock, without venting the system. This allows cleaning the source, swapping it, or changing ionization type, and being ready to run samples within minutes, not hours or days. Additionally, the V-lock technology allows the MS under vacuum to be fully isolated from the GC system, permitting not only a quick replacement of the analytical column when necessary, but also quick and safe performance of regular maintenance at the injector side, like replacing the septum or the liner or trimming the analytical column, without the use of any additional postcolumn or auxiliary gas flow into the MS.

Table 5. Response factors %RSDs as well as coefficient of determination values (r^2) determined from the calibration curve acquired over a concentration range of 0.2–50 ppm (splitless injections).

Compound	%RSD	r^2	Compound	%RSD	r^2
N-Nitrosodimethylamine	11.53	—	Acenaphthylene	8.24	—
Pyridine	10.23	—	1,2-Dinitrobenzene	14.85	—
2-fluorophenol (surrogate)	5.57	—	3-Nitroaniline	8.09	—
Phenol-d6 (surrogate)	4.99	—	Acenaphthene-d10	5.78	—
Aniline	6.39	—	Acenaphthene	7.57	—
Phenol	7.30	—	2,4-dinitrophenol	—	0.9867
Bis(2-chloroethyl) ether	7.95	—	Phenol, 4-nitro-	18.15	—
Phenol, 2-chloro-	6.19	—	Dibenzofuran	6.78	—
Benzene, 1,3-dichloro-	6.29	—	2,4-dinitrotoluene	12.32	—
1,4-Dichlorobenzene-d4	4.90	—	Phenol, 2,3,5,6-tetrachloro-	—	0.9957
Benzene, 1,4-dichloro-	7.57	—	Phenol, 2,3,4,6-tetrachloro-	—	0.9965
Benzyl alcohol	7.33	—	Diethyl Phthalate	5.60	—
Benzene, 1,2-dichloro-	7.43	—	4-chlorophenylphenylether	6.50	—
Phenol, 2-methyl-	6.27	—	Fluorene	7.31	—
Bis(2-chloroisopropyl) ether	6.31	—	4-nitroaniline	7.88	—
Phenol, 3&4-methyl-	6.52	—	4,6-Dinitro-2-methylphenol	—	0.9945
N-Nitroso-di-n-propylamine	6.63	—	Diphenylamine	9.61	—
Ethane, hexachloro-	5.80	—	Azobenzene	7.06	—
Nitrobenzene-D5 (surrogate)	5.90	—	2,4,6-tribromophenol (surrogate)	—	0.9963
Benzene, nitro-	3.20	—	4-bromophenylphenylether	4.30	—
Isophorone	3.90	—	Hexachlorobenzene	8.18	—
Phenol, 2-nitro-	13.14	—	Phenol, pentachloro-	—	0.9960
Phenol, 2,4-dimethyl-	4.52	—	Phenanthrene	10.88	—
Bis (2-chloroethoxy) methane	5.17	—	**Phenanthrene-d10-**	3.54	—
Phenol, 2,4-dichloro-	4.76	—	Anthracene	11.38	—
Benzene, 1,2,4-trichloro-	6.17	—	Carbazole	9.69	—
Naphthalene	8.26	—	Di-n-butyl phthalate	8.10	—
Naphthalene-d8	5.02	—	Fluoranthene	10.94	—

Boldface indicates Internal Standards

(continued on next page)

Table 5 (cont.). Response factors %RSDs as well as coefficient of determination values (r^2) determined from the calibration curve acquired over a concentration range of 0.2–50 ppm (splitless injections).

Compound	%RSD	r^2	Compound	%RSD	r^2
p-Chloroaniline	4.95	—	Pyrene	10.68	—
1,3-Butadiene, 1,1,2,3,4,4-hexachloro-	5.36	—	p-Terphenyl-d14 (surrogate)	6.76	—
Phenol, 4-chloro-3-methyl-	4.14	—	Benzyl butyl phthalate	8.69	—
Naphthalene, 2-methyl	7.54	—	Bis (2-ethylhexyl) adipate	6.08	—
Naphthalene, 1-methyl-	7.00	—	Benz[a]anthracene	9.68	—
Hexachlorocyclopentadiene	9.80	—	Chrysene	9.38	—
Phenol, 2,4,5-trichloro-	8.21	—	**Chrysene-d12**	4.02	—
Phenol, 2,4,6-trichloro-	5.90	—	Bis (2-ethylhexyl) phthalate	7.42	—
2-fluorobiphenyl (surrogate)	4.99	—	Di-n-octylphthalate	6.30	—
Naphthalene, 2-chloro-	7.24	—	Benzo[b]fluoranthene	6.70	—
2-Nitroaniline	10.43	—	Benzo[k]fluoranthene	8.48	—
1,4-Dinitrobenzene	16.05	—	Benzo[a]pyrene	6.11	—
Dimethyl phthalate	5.66	—	**Perylene-d12**	5.73	—
Benzene, 1,3-dinitro-	13.75	—	Indeno[1,2,3-cd]pyrene	6.36	—
2,6-dinitrotoluene	6.11	—	Dibenzo[a,h]anthracene	6.39	—
			Benzo[g,h,i]perylene	7.75	—

Boldface indicates Internal Standards

Table 6. Response factors %RSDs as well as coefficient of determination values (r^2) determined from the calibration curve acquired over a concentration range of 0.2–200 ppm (10:1 split injections).

Compound	%RSD	r^2	Compound	%RSD	r^2
N-Nitrosodimethylamine	6.31	—	Acenaphthylene	6.59	—
Pyridine	10.80	—	1,2-Dinitrobenzene	15.11	—
2-fluorophenol (surrogate)	4.30	—	3-Nitroaniline	14.42	
Phenol-d6 (surrogate)	4.19	—	Acenaphthene-d10	7.23	—
Aniline	4.89	—	Acenaphthene	7.98	—
Phenol	5.48	—	2,4-dinitrophenol	—	0.9984
Bis(2-chloroethyl) ether	4.45	—	Phenol, 4-nitro-	—	0.9982
Phenol, 2-chloro-	4.94	—	Dibenzofuran	8.91	—
Benzene, 1,3-dichloro-	5.03	—	2,4-dinitrotoluene	18.65	—
1,4-Dichlorobenzene-d4	6.01	—	Phenol, 2,3,5,6-tetrachloro-	17.58	—
Benzene, 1,4-dichloro-	5.09	—	Phenol, 2,3,4,6-tetrachloro-	12.33	—
Benzyl alcohol	9.21	—	Diethyl Phthalate	7.83	—
Benzene, 1,2-dichloro-	4.76	—	4-chlorophenylphenylether	7.93	—
Phenol, 2-methyl-	6.77	—	Fluorene	9.13	—
Bis(2-chloroisopropyl) ether	4.85	—	4-nitroaniline	13.30	—
Phenol, 3&4-methyl-	5.92	—	4,6-Dinitro-2-methylphenol	-	0.9983
N-Nitroso-di-n-propylamine	6.23	—	Diphenylamine	8.13	—
Ethane, hexachloro-	4.85	—	Azobenzene	9.24	—
Nitrobenzene-D5 (surrogate)	10.59	—	2,4,6-tribromophenol (surrogate)	13.23	—
Benzene, nitro-	10.24	—	4-bromophenylphenylether	6.37	—
Isophorone	5.18	—	Hexachlorobenzene	5.72	—
Phenol, 2-nitro-	19.20	—	Phenol, pentachloro-	—	0.9981
Phenol, 2,4-dimethyl-	4.92	—	Phenanthrene	6.32	—

(continued on next page)

Table 6 (cont.). Response factors %RSDs as well as coefficient of determination values (r^2) determined from the calibration curve acquired over a concentration range of 0.2–200 ppm (10:1 split injections).

Compound	%RSD	r^2	Compound	%RSD	r^2
Bis (2-chloroethoxy) methane	8.67	—	**Phenanthrene-d10-**	6.95	—
Phenol, 2,4-dichloro-	5.68	—	Anthracene	7.23	—
Benzene, 1,2,4-trichloro-	5.74	—	Carbazole	11.25	—
Naphthalene	5.74	—	Di-n-butyl phthalate	6.69	—
Naphthalene-d8	6.53	—	Fluoranthene	7.64	—
p-Chloroaniline	6.02	—	Pyrene	6.93	—
1,3-Butadiene, 1,1,2,3,4,4-hexachloro-	5.54	—	p-Terphenyl-d14 (surrogate)	6.38	—
Phenol, 4-chloro-3-methyl-	8.26	—	Benzyl butyl phthalate	6.97	—
Naphthalene, 2-methyl	6.97	—	Bis (2-ethylhexyl) adipate	6.16	—
Naphthalene, 1-methyl-	7.35	—	Benz[a]anthracene	7.43	—
Hexachlorocyclopentadiene	—	0.9991	Chrysene	6.17	—
Phenol, 2,4,5-trichloro-	10.39	—	**Chrysene-d12**	10.49	—
Phenol, 2,4,6-trichloro-	7.92	—	Bis (2-ethylhexyl) phthalate	4.95	—
2-fluorobiphenyl (surrogate)	6.45	—	Di-n-octylphthalate	8.70	—
Naphthalene, 2-chloro-	8.16	—	Benzo[b]fluoranthene	7.06	—
2-Nitroaniline	17.03	—	Benzo[k]fluoranthene	6.26	—
1,4-Dinitrobenzene	—	0.9980	Benzo[a]pyrene	6.81	—
Dimethyl phthalate	8.30	—	**Perylene-d12**	14.99	—
Benzene, 1,3-dinitro-	—	0.9976	Indeno[1,2,3-cd]pyrene	6.15	—
2,6-dinitrotoluene	11.55	—	Dibenzo[a,h]anthracene	6.91	—
			Benzo[g,h,i]perylene	7.06	—

Boldface indicates Internal tandards

Table 7(a). Response factors %RSDs for the 76 targeted compounds and internal standards, as well as r^2, for alternative fit calibrations using the Instant Connect Helium Saver module in splitless mode.

Compound	%RSD	r^2	Compound	%RSD	r^2
N-Nitrosodimethylamine	6.62	—	Acenaphthylene	7.34	—
Pyridine	10.56	—	1,2-Dinitrobenzene	16.57	—
2-fluorophenol (surrogate)	6.37	—	3-Nitroaniline	19.06	—
Phenol-d6 (surrogate)	4.82	—	Acenaphthene-d10	3.99	—
Aniline	13.52	—	Acenaphthene	4.68	—
Phenol	5.41	—	2,4-dinitrophenol	—	0.9938
Bis(2-chloroethyl) ether	17.24	—	Phenol, 4-nitro-	—	0.9950
Phenol, 2-chloro-	6.34	—	Dibenzofuran	6.21	—
Benzene, 1,3-dichloro-	5.80	—	2,4-dinitrotoluene	—	0.9942
1,4-Dichlorobenzene-d4	2.53	—	Phenol, 2,3,5,6-tetrachloro-	—	0.9962
Benzene, 1,4-dichloro-	5.17	—	Phenol, 2,3,4,6-tetrachloro-	14.62	—
Benzyl alcohol	18.38	—	Diethyl Phthalate	5.69	—
Benzene, 1,2-dichloro-	5.36	—	4-chlorophenylphenylether	5.32	—
Phenol, 2-methyl-	6.17	—	Fluorene	9.43	—
Bis(2-chloroisopropyl) ether	4.53	—	4-nitroaniline	19.69	—
Phenol, 3&4-methyl-	7.17	—	4,6-Dinitro-2-methylphenol	—	0.9893
N-Nitroso-di-n-propylamine	7.58	—	Diphenylamine	6.12	—
Ethane, hexachloro-	6.39	—	Azobenzene	6.01	—

(continued on next page)

Table 7a (cont.). Response factors %RSDs for the 76 targeted compounds and internal standards, as well as r^2, for alternative fit calibrations using the Instant Connect Helium Saver module in splitless mode.

Compound	%RSD	r^2	Compound	%RSD	r^2
Nitrobenzene-D5 (surrogate)	8.67	—	2,4,6-tribromophenol (surrogate)	16.16	—
Benzene, nitro-	8.86	—	4-bromophenylphenylether	8.54	—
Isophorone	5.52	—	Hexachlorobenzene	5.49	—
Phenol, 2-nitro-	17.07	—	Phenol, pentachloro-	—	0.9971
Phenol, 2,4-dimethyl-	8.44	—	Phenanthrene	7.12	—
Bis (2-chloroethoxy) methane	8.87	—	**Phenanthrene-d10-**	2.95	—
Phenol, 2,4-dichloro-	8.56	—	Anthracene	12.18	—
Benzene, 1,2,4-trichloro-	5.36	—	Carbazole	6.86	—
Naphthalene	5.91	—	Di-n-butyl phthalate	6.59	—
Naphthalene-d8	2.41	—	Fluoranthene	8.46	—
p-Chloroaniline	5.82	—	Pyrene	7.82	—
1,3-Butadiene, 1,1,2,3,4,4-hexachloro-	4.82	—	p-Terphenyl-d14 (surrogate)	7.49	—
Phenol, 4-chloro-3-methyl-	8.96	—	Benzyl butyl phthalate	5.81	—
Naphthalene, 2-methyl	5.95	—	Bis (2-ethylhexyl) adipate	9.11	—
Naphthalene, 1-methyl-	6.54	—	Benz[a]anthracene	5.79	—
Hexachlorocyclopentadiene	—	0.9959	Chrysene	6.90	—
Phenol, 2,4,5-trichloro-	13.52	—	**Chrysene-d12**	4.59	—
Phenol, 2,4,6-trichloro-	9.81	—	Bis (2-ethylhexyl) phthalate	7.06	—
2-fluorobiphenyl (surrogate)	6.00	—	Di-n-octylphthalate	7.84	—
Naphthalene, 2-chloro-	5.66	—	Benzo[b]fluoranthene	8.98	—
2-Nitroaniline	17.31	—	Benzo[k]fluoranthene	11.28	—
1,4-Dinitrobenzene	—	0.9962	Benzo[a]pyrene	7.47	—
Dimethyl phthalate	5.88	—	**Perylene-d12**	5.38	—
Benzene, 1,3-dinitro-	17.90	—	Indeno[1,2,3-cd]pyrene	8.02	—
2,6-dinitrotoluene	11.80	—	Dibenzo[a,h]anthracene	5.99	—
			Benzo[g,h,i]perylene	7.43	—

Boldface indicates Internal Standards

Table 7(b). Response factors %RSDs for the 76 targeted compounds and internal standards, as well as r^2, for alternative fit calibrations using the Instant Connect Helium Saver module in split mode.

Compound	%RSD	r^2	Compound	%RSD	r^2
N-Nitrosodimethylamine	6.62	—	Acenaphthylene	7.25	—
Pyridine	13.09	—	1,2-Dinitrobenzene	17.76	—
2-fluorophenol (surrogate)	6.02	—	3-Nitroaniline	18.05	—
Phenol-d6 (surrogate)	5.71	—	Acenaphthene-d10	4.15	—
Aniline	6.13	—	Acenaphthene	7.36	—
Phenol	6.52	—	2,4-dinitrophenol	—	0.9965
Bis(2-chloroethyl) ether	5.69	—	Phenol, 4-nitro-	—	0.9978
Phenol, 2-chloro-	7.17	—	Dibenzofuran	6.90	—
Benzene, 1,3-dichloro-	7.28	—	2,4-dinitrotoluene	18.32	—
1,4-Dichlorobenzene-d4	3.26	—	Phenol, 2,3,5,6-tetrachloro-	—	0.9957
Benzene, 1,4-dichloro-	8.13	—	Phenol, 2,3,4,6-tetrachloro-	17.05	—
Benzyl alcohol	14.15	—	Diethyl Phthalate	6.09	—
Benzene, 1,2-dichloro-	6.95	—	4-chlorophenylphenylether	8.11	—

(continued on next page)

Table 7b (cont.). Response factors %RSDs for the 76 targeted compounds and internal standards, as well as r^2, for alternative fit calibrations using the Instant Connect Helium Saver module in split mode.

Compound	%RSD	r^2	Compound	%RSD	r^2
Phenol, 2-methyl-	6.68	—	Fluorene	8.51	—
Bis (2-chloroisopropyl) ether	6.28	—	4-nitroaniline	19.17	—
Phenol, 3&4-methyl-	6.42	—	4,6-Dinitro-2-methylphenol	—	0.9987
N-Nitroso-di-n-propylamine	7.31	—	Diphenylamine	7.24	—
Ethane, hexachloro-	9.32	—	Azobenzene	7.28	—
Nitrobenzene-D5 (surrogate)	10.02	—	2,4,6-tribromophenol (surrogate)	14.93	—
Benzene, nitro-	11.59	—	4-bromophenylphenylether	7.06	—
Isophorone	6.70	—	Hexachlorobenzene	7.82	—
Phenol, 2-nitro-	14.78	—	Phenol, pentachloro-	—	0.9991
Phenol, 2,4-dimethyl-	5.90	—	Phenanthrene	8.55	—
Bis (2-chloroethoxy) methane	5.64	—	**Phenanthrene-d10-**	3.85	—
Phenol, 2,4-dichloro-	5.96	—	Anthracene	6.87	—
Benzene, 1,2,4-trichloro-	6.67	—	Carbazole	8.99	—
Naphthalene	4.81	—	Di-n-butyl phthalate	7.05	—
Naphthalene-d8	3.84	—	Fluoranthene	7.25	—
p-Chloroaniline	5.55	—	Pyrene	6.05	—
1,3-Butadiene, 1,1,2,3,4,4-hexachloro-	7.15	—	p-Terphenyl-d14 (surrogate)	6.25	—
Phenol, 4-chloro-3-methyl-	7.32	—	Benzyl butyl phthalate	5.92	—
Naphthalene, 2-methyl	5.92	—	Bis (2-ethylhexyl) adipate	6.32	—
Naphthalene, 1-methyl-	6.15	—	Benz[a]anthracene	7.37	—
Hexachlorocyclopentadiene	—	0.9985	Chrysene	6.90	—
Phenol, 2,4,5-trichloro-	12.06	—	**Chrysene-d12**	4.81	—
Phenol, 2,4,6-trichloro-	12.35	—	Bis (2-ethylhexyl) phthalate	6.27	—
2-fluorobiphenyl (surrogate)	7.30	—	Di-n-octylphthalate	6.56	—
Naphthalene, 2-chloro-	7.68	—	Benzo[b]fluoranthene	6.55	—
2-Nitroaniline	17.72	—	Benzo[k]fluoranthene	9.18	—
1,4-Dinitrobenzene	19.53	—	Benzo[a]pyrene	7.40	—
Dimethyl phthalate	7.46	—	**Perylene-d12**	8.17	—
Benzene, 1,3-dinitro-	18.89	—	Indeno[1,2,3-cd]pyrene	8.23	—
2,6-dinitrotoluene	13.59	—	Dibenzo[a,h]anthracene	7.15	—
			Benzo[g,h,i]perylene	6.50	—

Boldface indicates Internal Standards

Table 8 (Part 1). EPA Method 8270D minimum relative response factors and those produced by the ISQ 7000 single quadrupole system.

Compound	EPA 8270D Minimum Response	Thermo Minimum		Thermo Minimum	
		Splitless	Splitless Helium Saver	Split (10:1)	Split Helium Saver
Phenol	0.8	1.990	2.895	2.603	2.767
Bis(2-chloroethyl) ether	0.7	1.499	2.225	1.929	2.134
Phenol, 2-chloro-	0.8	1.516	1.884	1.882	1.869
Phenol, 2-methyl-	0.7	1.412	1.802	1.719	1.771
Phenol, 3&4-methyl-	0.6	1.495	1.933	1.767	1.897
N-Nitroso-di-n-propylamine	0.5	1.110	1.886	1.254	1.579
Ethane, hexachloro-	0.3	0.530	0.439	0.716	0.690

(continued on next page)

Table 8 (Part 1) (cont.). EPA Method 8270D minimum relative response factors and those produced by the ISQ 7000 single quadrupole system.

Compound	EPA 8270D Minimum Response	Thermo Minimum		Thermo Minimum	
		Splitless	Splitless Helium Saver	Split (10:1)	Split Helium Saver
Benzene, nitro-	0.2	0.316	0.469	0.404	0.471
Isophorone	0.4	0.708	0.989	0.869	0.995
Phenol, 2-nitro-	0.1	0.160	0.170	0.152	0.157
Phenol, 2,4-dimethyl-	0.2	0.389	0.453	0.430	0.465
Bis(2-chloroethoxy)methane	0.3	0.432	0.589	0.530	0.586
Phenol, 2,4-dichloro-	0.2	0.282	0.269	0.313	0.288
Naphthalene	0.7	1.085	1.247	1.176	1.260
p-Chloroaniline	0.01	0.464	0.493	0.497	0.546
1,3-Butadiene, 1,1,2,3,4,4-hexachloro-	0.01	0.112	0.118	0.175	0.116
Phenol, 4-chloro-3-methyl-	0.2	0.342	0.394	0.382	0.418
Naphthalene, 2-methyl	0.4	0.785	0.730	0.726	0.724
Hexachlorocyclopentadiene	0.05	0.236	0.128	0.213	0.044
Phenol, 2,4,6-trichloro-	0.2	0.345	0.322	0.372	0.298
Phenol, 2,4,5-trichloro-	0.2	0.324	0.286	0.368	0.300
Naphthalene, 2-chloro	0.8	1.232	1.388	1.314	1.349
2-Nitroaniline	0.01	0.335	0.406	0.339	0.455
Dimethyl phthalate	0.01	1.361	1.511	1.442	1.482
2,6-dinitrotoluene	0.2	0.229	0.259	0.258	0.242
Acenaphthylene	0.9	1.899	2.216	2.063	2.165
3-Nitroaniline	0.01	0.298	0.336	0.428	0.541
2,4-dinitrophenol	0.01	0.055	0.042	0.045	0.025
Acenaphthene	0.9	1.312	1.574	1.383	1.417
2,4-dinitrotoluene	0.2	0.304	0.327	0.316	0.330
Dibenzofuran	0.8	1.840	1.907	1.811	1.863
Phenol, 4-nitro-	0.01	0.167	0.042	0.124	0.055
Diethyl Phthalate	0.01	1.335	1.676	1.508	1.518
4-chlorophenylphenylether	0.4	0.740	0.609	0.692	0.621
4-nitroaniline	0.01	0.306	0.360	0.315	0.296
Fluorene	0.9	1.434	1.647	1.471	1.470
4,6-Dinitro-2-methylphenol	0.01	0.079	0.057	0.063	0.047
Diphenylamine	0.01	0.683	0.897	0.750	0.799
4-bromophenylphenylether	0.1	0.477	0.332	0.241	0.206
Hexachlorobenzene	0.1	0.324	0.256	0.283	0.267
Phenol, pentachloro-	0.05	0.131	0.077	0.064	0.049
Phenanthrene	0.7	1.125	1.335	1.289	1.275
Anthracene	0.7	1.270	1.138	1.272	1.347
Carbazole	0.01	1.070	1.407	1.006	1.156
Di-n-butyl phthalate	0.01	1.314	1.856	1.517	1.626

Table 8 (Part 2). EPA Method 8270D minimum relative response factors and those produced by the ISQ 7000 single quadrupole system.

Compound	EPA 8270D Minimum Response	Thermo Minimum		Thermo Minimum	
		Splitless	Splitless Helium Saver	Split (10:1)	Split Helium Saver
Fluoranthene	0.6	1.263	1.123	1.268	1.234
Pyrene	0.6	1.072	1.326	1.296	1.487
Benzyl butyl phthalate	0.01	0.496	0.906	0.677	0.847
Bis(2-ethylhexyl)phthalate	0.01	0.741	1.225	0.941	1.144
Chrysene	0.7	1.025	1.110	1.164	1.102
Benz[a]anthracene	0.8	1.068	1.228	1.171	1.124
Di-n-octylphthalate	0.01	1.465	2.673	2.084	2.413
Benzo[b]fluoranthene	0.7	1.364	1.417	1.592	1.432
Benzo[k]fluoranthene	0.7	1.292	1.185	1.586	1.396
Benzo[a]pyrene	0.7	1.353	1.420	1.500	1.414
Indeno[1,2,3-cd]pyrene	0.5	1.600	1.794	1.727	1.866
Dibenzo[a,h]anthracene	0.4	1.393	1.645	1.472	1.617
Benzo[g,h,i]perylene	0.5	1.302	1.560	1.406	1.636

Table 9 (Part 1). Retention times (RT) for the four methods.

Compound	Splitless RT (min)	Split (10:1) RT (min)	Split (10:1) Helium Saver RT (min)	Splitless Helium Saver RT (min)
Pyridine	3.66	3.71	3.66	3.29
N-Nitrosodimethylamine	3.71	3.74	3.68	3.33
2-fluorophenol (surrogate)	5.08	5.07	5.04	4.98
Phenol-d6 (surrogate)	5.96	5.93	5.91	5.92
Phenol	5.97	5.94	5.93	5.92
Aniline	5.98	5.95	5.94	5.92
Bis(2-chloroethyl) ether	6.04	6.00	5.98	5.97
Phenol, 2-chloro-	6.08	6.05	6.03	6.02
Benzene, 1,3-dichloro-	6.20	6.17	6.15	6.14
1,4-Dichlorobenzene-d4	6.23	6.20	6.18	6.17
Benzene, 1,4-dichloro-	6.25	6.21	6.20	6.19
Benzyl alcohol	6.39	6.36	6.34	6.34
Benzene, 1,2-dichloro-	6.42	6.38	6.37	6.36
Phenol, 2-methyl-	6.49	6.46	6.45	6.46
Bis(2-chloroisopropyl)ether	6.51	6.48	6.47	6.46
Phenol, 3&4-methyl-	6.63	6.60	6.59	6.59
N-Nitroso-di-n-propylamine	6.67	6.62	6.60	6.61
Ethane, hexachloro-	6.68	6.65	6.64	6.63
Nitrobenzene-D5 (surrogate)	6.77	6.73	6.72	6.72
Benzene, nitro-	6.79	6.75	6.74	6.74
Isophorone	7.00	6.96	6.94	6.95
Phenol, 2-nitro-	7.06	7.03	7.02	7.02
Phenol, 2,4-dimethyl-	7.09	7.06	7.05	7.06
Bis(2-chloroethoxy)methane	7.18	7.14	7.13	7.13
Phenol, 2,4-dichloro-	7.27	7.23	7.22	7.23
Benzene, 1,2,4-trichloro-	7.33	7.30	7.29	7.29
Naphthalene-d8	7.37	7.34	7.33	7.33

Table 9 (Part 2). Retention times (RT) for the four methods.

Compound	Splitless RT (min)	Split (10:1) RT (min)	Split (10:1) Helium Saver RT (min)	Splitless Helium Saver RT (min)
Naphthalene	7.39	7.36	7.35	7.35
p-Chloroaniline	7.46	7.43	7.42	7.42
1,3-Butadiene, 1,1,2,3,4,4-hexachloro-	7.53	7.50	7.49	7.49
Phenol, 4-chloro-3-methyl-	7.87	7.84	7.83	7.84
Naphthalene, 2-methyl	7.99	7.95	7.94	7.95
Naphthalene, 1-methyl-	8.08	8.04	8.03	8.04
Hexachlorocyclopentadiene	8.17	8.13	8.12	8.13
Phenol, 2,4,6-trichloro-	8.25	8.21	8.21	8.22
Phenol, 2,4,5-trichloro-	8.28	8.25	8.24	8.25
2-fluorobiphenyl (surrogate)	8.31	8.27	8.26	8.27
Naphthalene, 2-chloro-	8.41	8.37	8.36	8.37
2-Nitroaniline	8.53	8.49	8.49	8.50
1,4-Dinitrobenzene	8.63	8.59	8.58	8.60
Dimethyl phthalate	8.70	8.66	8.64	8.66
Benzene, 1,3-dinitro-	8.74	8.69	8.68	8.70
2,6-dinitrotoluene	8.77	8.72	8.71	8.73
Acenaphthylene	8.77	8.73	8.72	8.73

Conclusion

The Thermo Scientific ISQ 7000 single quadrupole GC-MS system with the ExtractaBrite ion source and the innovative NeverVent technology is the perfect solution to perform the EPA 8270D Method.

Thanks to the extended dynamic range detection system, the ISQ 7000 GC-MS system allows covering a 0.2–200 ppm range with the same column and liner. Seventy-six compounds were reported, and each fulfilled the EPA 8270D requirements in terms of minimum response factors and linearity.

Chromeleon CDS software, with the Environmental Reporting package, offers unparallel flexibility, scalability, and compliance. It provides compliance with EPA 8270D Method requirements offering a full complement of standard reports including DFTPP Tune Check report, Breakdown report, Internal Standard Summary report, Tentatively Identified Compounds report, various quality control reports for check standards, laboratory control samples, matrix spikes, surrogate recoveries, and more.

The Thermo Scientific Instant Connect Helium Saver Module is a unique tool that can be used to reduce the cost per analysis, without compromising the analytical results. The Helium Saver Module makes laboratories more efficient and environmentally friendly, saving 90% of helium during each run.

The ExtractaBrite ion source design, as integrated in the ISQ 7000 GC-MS system, keeps the system cleaner, longer. With heat throughout the ion optics and the patented RF lens, the ISQ 7000 GC-MS system has been proven to be capable to analyze more dirty samples per day, with maximum uptime. Even better, when the instrument finally requires cleaning, the column needs to be replaced or trimmed, or maintenance is required at the injector side, the NeverVent technology offers the user the possibility to operate without venting the MS system, in a very fast and simple way. Why break your workflow when you can have unstoppable productivity?

References

1. United States Environmental Protection Agency (U.S. EPA). Method 8270D (SW-846): *Semivolatile Organic Compounds by Gas Chromatography/ Mass Spectrometry (GC/MS)*, Revision 5, July **2014**. https://www.epa.gov/sites/production/files/2015-12/documents/8270d.pdf [Accessed February 11th, 2018].

2. Eichelberger, J. W.; Harris, L. E.; Budde, W. L. *Anal. Chem.*, **1975**, *47* (7), pp 995–1000.

3. Donnelly, J. R. *J. Assoc. Off. Anal. Chem.*, **1988**, *71* (2), pp 434–439.

4. Tondeur, Y.; Niederhutl, W. J.; Campana, J. E.; Mitchum, R. K.; G. Sovocool, W.; Donnelly, J. R. *Biological Mass Spectrometry*, **1988**, *15* (8), pp 429–439.

Find out more at **thermofisher.com/ISQ7000**

thermo scientific

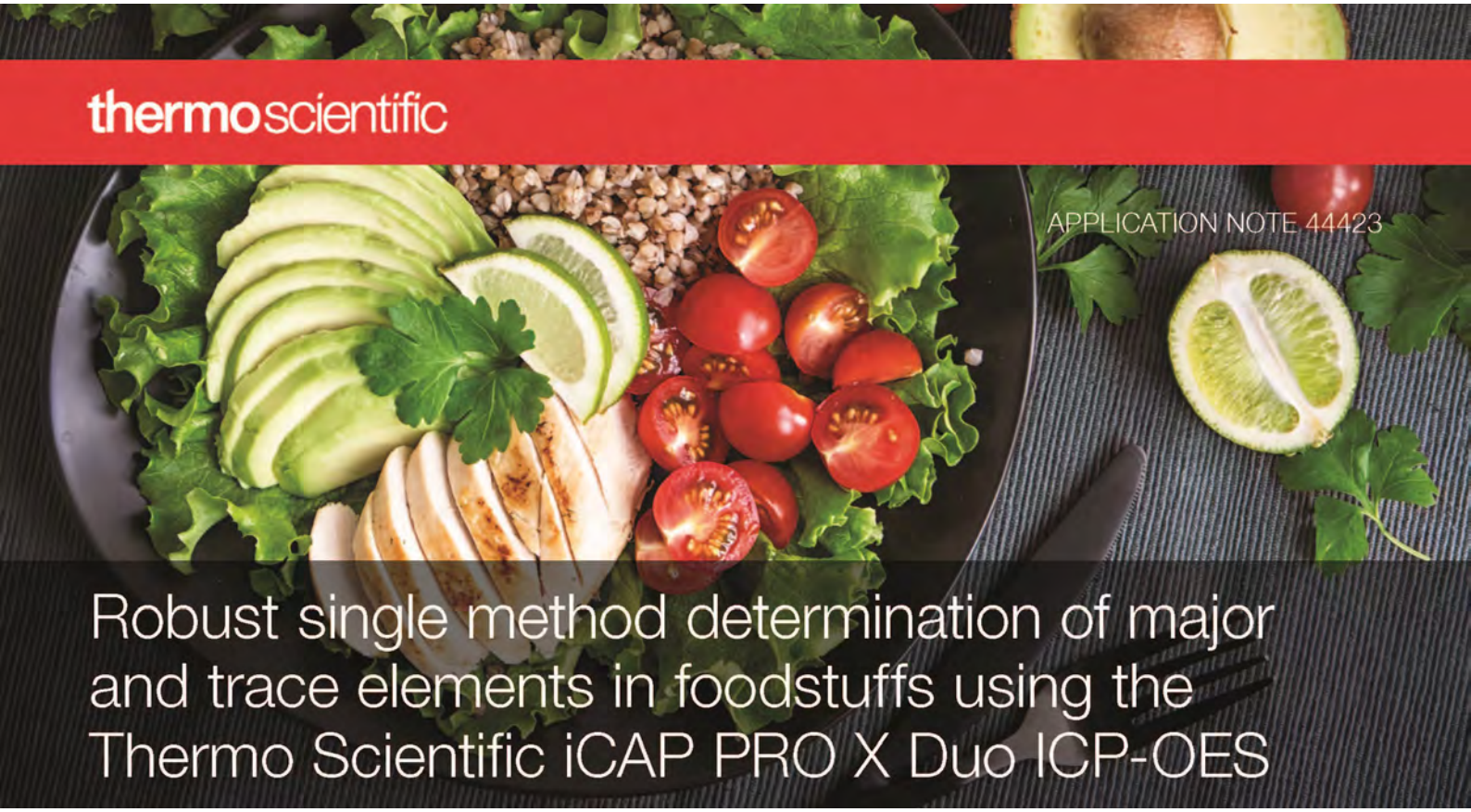

Robust single method determination of major and trace elements in foodstuffs using the Thermo Scientific iCAP PRO X Duo ICP-OES

Author
Nora Bartsch,
Application Specialist,
Thermo Fisher Scientific,
Bremen, Germany

Keywords
Foodstuffs, Micronutrients, Microwave digestion, Toxic elements

Goal

This application note demonstrates the ability of the Thermo Scientific™ iCAP™ PRO Series ICP-OES to determine trace elements and major components in foodstuffs to comply with regulations.

Introduction

Food protection from potentially hazardous contaminants has become a major topic of public interest. As well as the standard regulatory testing, it is necessary to account for contaminants, which may enter the food chain via many means, such as industrial pollution or environmental contamination, i.e., polluted rainfall on crops. Once toxic elements are in the food chain, they can pose significant health risks. With this in mind and the increasing number of micronutrients requiring determination, it is critical that the method of testing is a rigorous and reliable one. The organization charged with the development of the Codex standards (worldwide food and consumer regulations) is the Codex Alimentarius Commission, which is an intergovernmental body jointly sponsored by the Food and Agriculture Organization and the World Health Organization.

Instrumentation

The Thermo Scientific iCAP PRO Series ICP-OES employs a high-resolution Echelle spectrometer with a charge injection device (CID) detector. Advancements in CID technology allow this detector to feature lower noise and better separation of spectral orders than any of its predecessors. With the new optical design,

the full spectrum from 167 nm up to 852 nm can be measured with a single exposure. A Thermo Scientific™ iCAP™ PRO X Duo ICP-OES was chosen for this analysis as this enables maximum sensitivity using axial view whilst maintaining excellent matrix tolerance in radial viewing mode. The instrument parameters used are listed in Table 1.

Table 1. Instrument parameters.

Parameters	Setting	
Pump tubing	Sample Tygon® orange/white Drain Tygon® white/white	
Spray chamber	Glass cyclonic	
Nebulizer	Glass concentric	
Center tube	2.0 mm	
Pump speed	45 rpm	
Nebulizer gas flow	0.6 L·min^{-1}	
Auxiliary gas flow	0.5 L·min^{-1}	
Coolant gas flow	12.5 L·min^{-1}	
RF power	1150 W	
Exposure time	Axial	Radial
	15 s	15 s

Method development and analysis

Initially, more than one wavelength was selected for each element (using both axial and radial view). The subarrays for each wavelength were then examined and the most appropriate wavelength for the application was chosen (Table 2) based on the presence of interferences, calibration curve quality, QCs, and CRMs and the required linearity for the element. The subarray plots for each element can be easily manipulated by the analyst, allowing the optimum peak integration and background correction points to be selected. The Thermo Scientific™ Qtegra™ Intelligent Scientific Data Solution™ (ISDS) Software was used for data acquisition and provides easy options for post-analysis data manipulation.

Qtegra ISDS Software has integrated Quality Control (QC) checks that allows the user to define automatically controlled actions to ensure data integrity, as well as a Flags and Limits function which flags samples according to user specifications.

Table 2. Element, wavelength and plasma view used.

Element	Wavelength (nm)	Plasma view
Ca	317.933	Radial
Cu	324.754	Axial
Fe	259.940	Axial
Mg	285.213	Radial
Mn	257.610	Axial
Ni	231.604	Axial
P	178.284	Radial
Pb	220.353	Axial
Zn	206.200	Axial

Sample preparation

Samples were prepared using certified reference material (CRM) standards. 0.5 g aliquots of rice flour (NBS1568b) and bovine liver (NBS1577c) were digested in 9 mL TraceMetal™ grade nitric acid (Fisher Chemicals, Loughborough, UK) using a standard food method program in a high pressure microwave system. The final digests were made up to 50 mL with deionized water before analysis.

Standard preparation

High purity standards (1000 mg·kg^{-1} single element standards) were used to prepare the calibration standards for this method. All samples and standards were acid matched. Table 3 indicates the concentration of each of the standards, selected to cover the concentration range of the samples.

Table 3. Standard concentrations in mg·kg^{-1}.

Element	STD 1	STD 2	STD 3	STD 4
Pb	0.01	0.05	0.2	0.5
Mn, Ni, Zn, Cu	0.1	0.5	2	5
Ca, P, Fe, Mg	1	5	20	50

Results

The instrument was calibrated using a blank and at least two standards for each element. After inspection, a linear fit was applied to all elements. The calibration standards and samples were analyzed in a single sequence with an acid rinse between samples. The sample data was measured by interpolation and results are shown in Table 4. Suitable dilutions were made to over-range elements to ensure they fell within the calibration range. Method detection limits (MDLs) were also established by analyzing the acid matched calibration blank using a 10 replicate analysis and multiplying the standard deviation of

the analysis by 3. This was repeated three times and the average values for method detection limits are also summarized in Table 4.

Table 4. Results of measurement, CRM and MDLs in mg·kg^{-1} and calculated recoveries in %.

Element	SRM1577c			SRM1568b			MDL
	CRM	Measured	Recovery (%)	CRM	Measured	Recovery (%)	µg·kg^{-1}
Ca	131	124	95	118.4	107	90	1.90
Cu	275.2	272.3	99	2.35	2.13	91	0.4
Fe	197.94	205.97	104	7.42	7.78	105	1.5
Mg	580	579	100	549	478	87	1.23
Mn	10.46	10.12	97	19.2	18.1	94	0.04
Ni	0.0353	0.0325	92	-	-	-	0.52
P	-	-	-	1490	1302	87	12
Pb	0.0628	0.0623	99	< MDL	-	-	2.9
Zn	179.1	163.3	91	19.16	15.59	81	0.28

Conclusion

The results table shows that major and trace elements were measured with equal success. Precise, accurate results for digested foodstuff samples are easily attained on the Thermo Scientific iCAP PRO X Duo ICP-OES. The full wavelength coverage of the unique CID detector allowed the optimum wavelengths to be selected and the whole spectrum to be measured with one exposure, while the sensitivity of the axial view provided the low detection limits for this application.

Find out more at **thermofisher.com/icp-oes**

AN44423-EN 0320C

thermo scientific

Tech Note

Simplifying Mixed-Food Microwave Sample Preparation for ICP-MS Analysis

Utilizing Single Reaction Chamber (SRC) Technology for Trace Metals Analysis for Food Samples.

Summary

Low-level analysis of food matrices has placed a demand on manufacturers, testing laboratories, and instrumentation vendors worldwide. Stricter regulations, better analytical instrumentation, and greatly improved sample preparation (pre-analytical) techniques have focused eff orts to simplify and standardize these analyses. Often overlooked, the preanalytical step determines the quality of the resulting data and requires careful attention to a number of details, including sample size, digestion parameters, and the level of detection needed. This article describes the selection of critical factors used in the optimization and simplification of food and mixed-batch food microwave digestion.

Food and contract testing laboratories are in an uphill battle in determining the best approach in processing foodstuffs.

Regulatory bodies such as the Food and Drug Administration (FDA), United States Department of Agriculture (USDA), and European Commission (EC) have established element concentration limits on food and agricultural products. A recent addition to the methods menu from the FDA provides a guideline for the pre-analytical step for microwave sample digestion followed by inductively coupled plasma mass spectrometry (ICP-MS) analysis of trace metals in food (1). Many publications and the Association of Analytical Communities (AOAC) performance methods have validated microwave digestion as a standard approach to food analysis. In fact, Method 4.7 from the FDA is an example of an internal validation exceeding standards set forth by the AOAC. The USDA has also recently updated their chemistry laboratory guidebook for the analysis of food utilizing inductively coupled plasma optical emission spectrometry (ICP OES) and ICP-MS following sample microwave digestion (2). The important feature in many of these methods relates to the choice of analytical tools and sample preparation technique, which leads to the questions: What is the best way to perform sample preparation and which instrument is best for multi-element analysis within a lab setting?

Sample preparation is given little attention in the overall process for the analysis of trace metals, and for many sample types it turns out to be routine. Normally,

scientists simply look at the detection limits for an ICP OES or ICP-MS system and calculate back from a detection level or interferences to determine the instrument of choice. Unfortunately, with highly organic sample types and the breadth of complexity increasing, the need for a good quality digestion process is more critical. A list of pre-analytical contributing factors that can affect the backend analysis includes sample size, acid digestion volume, sample fat and organic content, contamination, throughput, and post-digestion residual carbon content. Each of these will play a role in the methods chosen for processing a food sample.

Larger samples sizes have been used because of the limits of analytical detection and sample inhomogeneity. The consideration on what to use for the sample preparation then becomes a choice between ashing and microwave digestion. Ashing is complicated by the loss of critical elements such as Cd, Pb, and Hg along with contamination issues (3). Microwave digestion also historically has been a concern with the lack of vessel temperature and pressure capability for complete digestion of reasonably sized sample amounts. This picture becomes even more opaque with incomplete digestions causing problems for the ICP OES or ICP-MS analysis with a resulting high residual carbon content (4–6). While ICP OES dominates the testing laboratory environment, there is consistent movement toward ICP-MS with all of the advantages and trace metal regulations it offers (7).

Conventional closed-vessel microwave digestion has been recognized for the past two decades as the most effective technique for the digestion of the widest range of sample types in metals analysis, largely because of its ability to operate at high temperatures and pressures. Because the digestions are in a closed vessel, cross-contamination and the loss of volatile elements are eliminated (8). Additionally, microwave sample preparation techniques have overcome challenges of poor digestion quality by providing better digests with low residual acidity, lower carbon content, and lower concentrations of dissolved solids, a critical feature necessary for back-end ICP-MS and ICP-OES analysis (9). It was recently suggested that an ideal sample preparation procedure would be capable of digesting large sample amounts, provide high throughput, be compatible with multi-element analysis, and be safe, green, and easy to use (9). A recent publication illustrates the importance of sample size, lower acid consumption, complete digestion with low residual carbon, and the effects of temperature and pressure with a variety of food samples in a conventional microwave and a new single reaction chamber technology (10). This research goes a long way into the basic understanding of how to think about sample preparation as a process. To further illustrate the completeness of sample preparation, we used a single reaction chamber (SRC) microwave digestion approach for processing mixed-batch and large food samples.

Methods and Materials

SRC microwave digestion has been utilized extensively in the last several years. The operation, specification, sequence of operation, and application have been published for further reading (11,12). The SRC uses a large, pre-pressurized chamber where multiple independent sample types are digested simultaneously up to 300 °C and 199 bar (including multiple acid combinations for determining the right digestion chemistry). By choosing different size racks to fit inside the chamber, different sample sizes and throughput can be performed, depending on internal needs. Pre-pressurizing the chamber allows a single microwave method to be chosen for all types without the need for extensive method development.

All digestions were developed using an UltraWAVE based on the SRC design. The microwave delivers 1500 W of microwave power to a 1L stainless-steel reinforced PTFE chamber that can hold sample racks of 5, 15, or 22 vessels depending on sample and acid volume. Direct temperature and pressure control provide direct control of each sample (all samples reach the same temperature and pressure). The experiments described in this article were performed using a 15-position rack with 15 mL disposable glass vials and a 5-position rack with quartz vials for large sample sizes. An Agilent 7700x ICP-MS system was used for the analysis of all elements. The operating conditions for the ICP-MS system were as follows: RF applied power to the torch, 1.55 kW; carrier gas flow, 0.95 L/min; dilution gas flow rate, 0.15 L/min; plasma mode normal, He cell gas flow, 4 mL/min. Operating in He collision mode for samples allowed for routine robust analysis.

Microwave Sample Preparation

Samples were selected to include a variety of food types along with standardized reference materials. The primary "big four" toxic metal profiles were used to establish a microwave method and instrument baseline numbers. Following this approach, an expanded set of metals was determined using the same microwave method. The final experiment examined a set of samples with sizes greater than 2 g to illustrate the feasibility of processing larger food samples with an identical microwave method established in the previous experiments (expands the capability to use ICP OES in the well-established food industry).

Typical food samples (0.5 g) were placed in disposable glass test tubes and placed in a 15-position rack for microwave operation. The samples were treated with a 4 mL nitric acid and 0.5 mL hydrochloric acid combination (for Cd, Pb, As, and Hg stabilization) or 5 mL of nitric acid for the expanded list of elements and placed in the microwave chamber (note: the PTFE liner contains 100 mL of water, 10 mL of hydrogen peroxide, and 3 mL of sulfuric acid as the microwave load for parameter control) Following pre-pressurization of the chamber with nitrogen to 40 bar, the samples were digested using the following time–temperature microwave method: Ramp to 240 °C over 30 min, hold at 240 °C for 15 min, cool to 60 °C, and depressurize the chamber for analysis. The total time was 55 min. It should be noted that pressures can reach 100 bar or greater during the course of a digestion and sample decomposition, illustrating one of the critical

needs to have a system capable of higher temperatures and pressures for quality digestions. Systems or vessels venting during the course of these conditions would preclude development with the loss of volatile elements at a partial digestion point during a method.

Table 1. ICP-MS Analysis of Mixed-Food Samples following SRC Digestion (0.5 g, 4 mL HNO_3, 0.5 mL HCl; 30 min to 240 °C with 15 min at 250 °C)

Quality Control Summary				
	Concentration (ppb)			
	Arsenic	Cadmium	Mercury	Lead
Blank	0.001	0	<0.005	0.089
Spike Concentration	100	100	100	100
Spike Result	103	103	105	106
Spike Recovery %	97	97	5	94
Spike Dup Result	101	100	103	106
Duplicate recovery %	99	100	97	94
Detection Limit (ppt)	11.9	2.9	1.2	1.3
Sample Summary				
	Concentration (ppm)			
Apple Certified Values	0.038	0.013	0.044	0.47
Apple SRM 1515	0.041	0.011	0.04	0.45
Apple SRM 1515 dup.	0.044	0.01	0.038	0.44
Olive Leaves	0.01	0.009	0.02	0.097
Apple Leaves	0.021	0.088	0.023	0.09
Cheese	0.052	0.062	0.054	0.132
Candy Bar	0.008	0.008	0.028	0.084
Yogurt	0.055	0.089	1.46	0.12

Results

Three separate microwave digestion runs were performed with a variety of food sample types and sizes. Each microwave method formed clear digestates with lower acid volumes, that were diluted with water to 25 mL, followed by a 2 mL aliquot diluted to 40 mL, and analyzed using ICP-MS. The first sample set was analyzed for As, Cd, Hg, and Pb. The second set was expanded to include Mg, Mn, Cu, Fe, and Zn. Last, larger sample sizes were digested and analyzed for Se and Hg. For quality control (QC) an acid blank, spikes, and duplicates were analyzed as part of ongoing instrument calibration verification. Quantitative data, detection limits, and QC data are shown in Tables 1, 2, and 3.

Table 2. ICP-MS Analysis of Mixed-Batch Samples Following SRC Digestion (2-25 g 10 mL HNO_3, 4 mL H_20, 1 mL HCL; 30 min to 240 °C w/ 15 min at 240 °C)

Quality Control Summary					
	Concentration (ppb)				
	Mg	Fe	Mn	Cu	Zn
Blank	0	0	0	0	0
Spike Concentration	100	100	100	100	100
Spike Result	98	100	96	106	95
Spike Recovery %	98	100	96	100	95
Spike Dup Result	96	101	94	98	100
Duplicate recovery %	96	100	94	98	100
Detection Limit (ppt)	2.8	14.8	8.5	2.7	14
Sample Summary					
	Concentration (ppm)				
Tomato 1573 Certified	-	368	246	4.7	30.9
Tomato 1573a	-	365.1	241.6	4.35	29.5
Tomato 1573a dup	-	367.8	243.6	4.4	30.1
Apple Leaves	2.051	92.9	79.3	9.2	43.1
Olive Leaves	1.917	88.2	28.2	31.3	18.5
Cheese	6.5	124.2	38.1	45.08	65.35
Peanut Butter	6.27	67.5	12.4	16.7	31.5
Milk Powder	ND	1.75	0.251	0.68	45.2

Table 3. ICP-MS Analysis of Large Sample Sizes Following SRC Digestion (2-25 g 10 mL HNO_3, 4 mL H_20, 1 mL HCL; 30 min to 240 °C 15 min at 240 °C)

Sample Summary		
	Concentration (ppb)	
	Selenium	Mercury
Tomato 1573 Certified	54	34
Tomato 1573a	52.48	35.609
Rice	294.53	27.56
Candy Bar	33.106	26.897
Cheese	31.865	50.695
Yogurt	134.65	1.463.775
Instrument QC	52.011	0.9939

Conclusion

Given the high-throughput nature of testing labs, the standardization of the SRC microwave method aligns well with the use of ICP OES or ICP-MS analysis for all sample types. SRC microwave digestion in food, testing, and manufacturing labs for the analysis of trace metals provided a single optimized sample prep method. To achieve complete digestions for multiple sample types simultaneously, an optimized temperature of 240 °C was used; disposable glass vials were used to eliminate the need for vessel cleaning in subsequent digestion runs. With a 15-position rack and a 55 min digestion time start to finish, a series of multiple samples can be processed

for multi-element trace metals. Standardizing the SRC method provided a way to scale the process to larger sample sizes without the need for extensive method development, batching, vessel cleaning, and assembly.

References

1. P. Gray, W. Mindak, and J. Cheung FDA Elemental Analysis Manual for Food and Related Products, Section 4.7, (2013).
2. USDA, Determination of Metals by ICP-MS and ICP-OES (Optical Emission Spectrometry) USDA, Food Safety and Inspection Service (2013).
3. J.S. Barin, B. Tischer, R.S. Picoloto, F.G. Antes, F.E.B. Silva, F.R. Paula, E.M.M. Flores, J. Anal. At. Spectrom, 29, 352–358. (2013) .
4. M. Wurfels, E. Jackwerth, and M. Stoeppler, Anal. Chim. Acta, 26, 1-16 (November, 1989).
5. P. Fecher and G. Ruhnke, At. Spectrosc. 19, 204–206 (1998).
6. G. Grindlay, L. Gras, J. Mora, and M.T.C. de Loos-Vollebregt. Spectrochim. Acta Part B, 63, 234–243 (2008).
7. S. McSheehy, M. Hamester, and M. Godula, Food Qual. Saf. (2010).
8. D. Gunn, Spectroscopy: Applications of ICP & ICP-MS Techniques for Today's Spectroscopists 28 (s11), 8–16 (2013).
9. J.A. Nobrega, C. Pirola, L.L. Fialho, G. Rota, C.E.K.M.A. Campos Jordão, and F. Pollo, Talanta 98, 272–276 (2012).
10. C.C. Mueller, A.L.H. Muller, C. Pirola, F.A. Duarte, E.M.M. Flores, and E.I. Muller, Microchem. J. 116, 255–260 (2014).
11. T. Michel, Amer. Lab. 42, 32–35 (2010).
12. T. Michel and S. Hussain, Spectroscopy supplement: Applications of ICP & ICP-MS Techniques for Today's Spectroscopists 27(s11), 30–35 (2012).

MILESTONE HELPING CHEMISTS

MILESTONE Srl - Via Fatebenefratelli, 1/5 - 24010 Sorisole (BG) - Italy Tel: +39 035 573857 - Fax: +39 035 575498
www.milestonesrl.com - email: analytical@milestonesrl.com

SPONSOR RELEASE

ISQ™ 7610 Single Quadrupole GC-MS

Produce results more rapidly and experience unstoppable efficiency in your analysis with the Thermo Scientific™ ISQ™ 7610 Single Quadrupole GC-MS system

To stay ahead, analytical testing laboratories need the ultimate confidence of a GC-MS system that easily and reliably produces trusted results, day after day. For this, you can count on the Thermo Scientific™ ISQ™ 7610 Single Quadrupole GC-MS System. Simplified operation, automated workflows, and extended dynamic range deliver consistent results from system to system in every laboratory. Thermo Scientific™ NeverVent™ technology, extended-life detector, and intelligent software eliminate unnecessary downtime to maximize sample throughput. To ensure you are ready for any analytical challenge, the system is upgradeable from entry-level to advanced configurations. Now you can take the lead with rapid return on investment (ROI) for your regulated GC-MS analyses

Increase instrument uptime

Eliminate unnecessary, unplanned instrument downtime and maximize productivity to achieve unprecedented efficiency, day after day. The ISQ 7610 Single Quadrupole GC-MS System combines robustness with the ability to change the GC column and clean the ion source without interrupting your analytical workflows.

Monitor key aspects of your GC-MS system

With Thermo Scientific™ SmartStatus™ instrument tracking within Chromeleon CDS, quickly see whether instruments are ready to run samples, if maintenance is required or if consumables should be replaced. The fully customizable software enables you to make data-driven decisions on when to perform maintenance and avoid unnecessary downtime.

Maximize sample throughput

When high sample throughput is essential, the system delivers results on time and with ease. Automated workflows and simplified instrument operation ensure every user produces consistent results, sample after sample. Extended linear range enables method consolidation so you can analyze more compounds at varying concentrations in a single run.

Realize rapid return on investment

Ensuring your system delivers results as soon as it's installed is necessary to achieve rapid ROI. With built-in intelligence that simplifies instrument setup, analytical methods, and everyday operation, the ISQ 7610 Single Quadrupole GC-MS System is designed for accelerated deployment. Reduced needs for operator training and faster time to full productivity together with maximum sample throughput provide fast return on your instrument investment.

Thermo Fisher Scientific is working to provide more information about our products' environmental impact by stepping up to participate in the ACT Label program with selected products.

Find out more at **thermofisher.com/ISQ7610**

ThermoFisher SCIENTIFIC

Thermo SCIENTIFIC

ISQ™ 7610 Single Quadropole GC-MS

Produce results more rapidly and experience unstoppable efficiency in your analysis with the Thermo Scientific™ ISQ™ 7610 Single Quadrupole GC-MS system.

VIDEO **WEBSITE**

Thermo SCIENTIFIC

Perform like a PRO

Thermo Scientific™ iCAP™ PRO X ICP-OES system delivers Simplicity, Speed and Robustness

Deliver robust, uncomplicated trace elemental analysis for your laboratory with the Thermo Scientific™ iCAP™ PRO X ICP-OES system. This system combines powerful multi-element capability with flexibility, so your lab is ready for any challenge. Produce consistent, reliable data quickly and easily. Experience enhanced sample throughput, matrix tolerance, and flexibility to produce results you can trust.

The iCAP™ PRO X ICP-OES offers fast start-up, easy-to-use software and incredible speed with pre-optimized method conditions, providing multi-element detection technology far superior to that of single-element AAS and multi element microwave plasma techniques. This system is ideal for laboratories with low sample throughput requirements. For ease of use a number of optimized settings are defined as standard, making them ideal for users new to the technique or those who require a simple solution for multi elemental analysis.

Experience more simplicity without compromising on detail

- Flexibility to fulfil demanding projects
- Long-term stability through gas MFCs and temperature control
- Full frame view immediately after measurement
- Intelligent monitoring of analytes with Qtegra ISDS Software
- Plasma optimization tool with tune sets and auto-tune for automated method development

Fast, powerful performance

- Advanced, high-speed charge injection device detection technology produces results in the fastest possible time
- A small optical tank ensures fast start up time and reduced purge gas requirements. With start up times of just 30 minutes from power off and 5 minutes from standby (model dependent)
- Detect from % range to sub ppb detection limits with a high dynamic range detector

Optimized vertical torch for ultimate robustness

- Both duo and radial view configurations of the instruments feature vertical torch orientation. When combined with the unique plasma interface, a new level of robustness is achieved
- Adjustable radial viewing height on both duo and radial view instruments, enabled by the vertical plasma interface
- Increase robustness further with dedicated accessories and analyze the most challenging samples, such as saturated brine solutions.

Accurately quantify the elemental composition of a wide range of samples in: Agricultural screening, Food production and safety, Environmental analysis, Pharmaceutical and nutraceutical compliance, Chemical QA and QC, Petrochemical, Metals and materials

Find out more at **thermofisher.com/icp-oes**

thermo scientific

iCAP PRO Series ICP-OES

Perform like a PRO
Simplicity, robustness and speed

Analyze even the most challenging sample matrices
The Thermo Scientific™ iCAP™ PRO Series ICP-OES combines powerful multi-element capability with flexibility so your lab is ready for any challenge.

Produce consistent, reliable data quickly and easily. Experience enhanced sample throughput, matrix tolerance and flexibility to produce results you can trust.

Achieve precise results first time, every time with the innovative Get Ready feature. This automated technology sets up the instrument for you and checks performance. Manage instrument processes using a logical dashboard interface. Trust in ICP-OES technology driven by Thermo Scientific™ Qtegra™ Intelligent Scientific Data Solution™ (ISDS) Software.

VIDEO **WEBSITE**

ThermoFisher SCIENTIFIC

SPONSOR RELEASE

ultraWAVE 3

Taking Productivity and Performance to New Heights

The new ultraWAVE 3 is the latest generation of SRC technology that further elevates the value of this technology for elemental analysis in terms of performance, time, workflow, and cost of ownership.

Single Reaction Chamber Technology
Updated construction that includes several technology advances further enhances the well-proven benefits of the SRC technology.
The new features of ultraWAVE 3 merge with those already intrinsic in the technology, so that labs will experience higher performance, greater productivity, and more streamlined workflow, providing them with improved competitiveness and a lower cost of ownership.
Thanks to its superior digestion capabilities that result from its higher temperature and pressure features, ultraWAVE's unique SRC technology provides greater digestion efficiency.
Several aspects of the system, such as reduced handling and cleaning and the ability to process any samples simultaneously, reduce turnaround time and increase lab efficiency.

BENEFITS
Rugged construction
Designed with all wetted components made of PTFE-TFM, fully compatible with any acid mixture and ensuring minimal maintenance to lower the cost of ownership.

High-pressure lines
Made of acid-resistant stainless steel, the two pressure lines, one for inlet and one for outlet, ensure high safety and lower blanks.

Racks
Available with racks of 7, 20, 27 and 40 vials to provide even higher throughput than previous generations.

easyTEMP Temperature control
True contactless temperature sensor to directly control the digestion of the samples from the inside out, without reading delays.

Advanced heating technology
The noiseless water-cooled magnetron ensures higher heating efficiency along with superior working conditions.

User interface
Equipped with the most up-to-date features to bring all digestion information within easy reach of the operator.

Find out more at **milestonesrl.com**

MILESTONE
HELPING CHEMISTS

MILESTONE
HELPING CHEMISTS

ultraWAVE 3

Single Reaction Chamber Technology

Updated construction that includes several technology advances further enhances the well-proven benefits of the SRC technology.
The new features of **ultraWAVE 3** merge with those already intrinsic in the technology, so that labs will experience higher performance, greater productivity, and more streamlined workflow, providing them with improved competitiveness and a lower cost of ownership.
Thanks to its superior digestion capabilities that result from its higher temperature and pressure features, ultraWAVE's unique SRC technology provides greater digestion efficiency.
Several aspects of the system, such as reduced handling and cleaning and the ability to process any samples simultaneously, reduce turnaround time and increase lab efficiency.

VIDEO WEBSITE

www.milestonesrl.com/products/microwave-digestion/ultrawave-3

New Books & Upcoming Events & Trusted Sources for Analytical Chemistry

Notices of Books on Analytical Chemistry

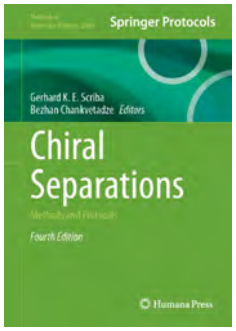

Chiral Separations – Methods and Protocols, 4th Edition

Gerhard K. E. Scriba, Bezhan Chankvetadze, Editors

2026, Humana New York, NY

This fully updated volume focuses on analytical separations by chromatographic and electrophoretic techniques, providing some overview along with a multitude of practical applications. Examination of the application of sensors for enantiodifferentiation as well as chapters on the analysis of analyte-selector complexes by NMR spectroscopy and molecular modeling have been included. Authoritative and practical, this book serves as a helpful guide for analytical chemists working on stereochemical problems in the fields of pharmacy, chemistry, biochemistry, food chemistry, molecular biology, forensics, environmental sciences, or cosmetics in academia, government, or industry.

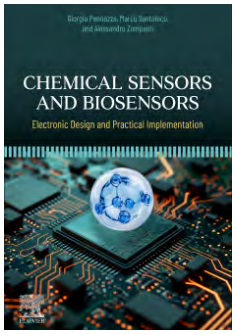

Chemical Sensors and Biosensors – Electronic Design and Practical Implementation

Giorgio Pennazza, Marco Santonico, Alessandro Zompanti, Authors

November, 2026, Elsevier

This book covers both foundational concepts and practical applications across various scientific disciplines to outline the development of chemical sensors. Section I, Fundamentals, explains sensor working principles, including key elements such as sensitivity, resolution, LOD, selectivity, repeatability, and reproducibility, along with calibration procedures. Section II, Practical Implementation, introduces application driven design and conceptual models for sensor development, including troubleshooting and common solutions across various sensors and their myriad applications. **Read more**

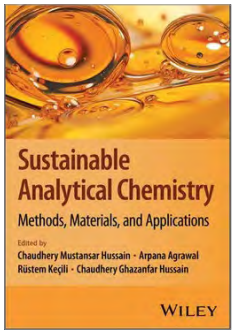

Sustainable Analytical Chemistry: Methods, Materials, and Applications

Chaudhery M. Hussain, Arpana Agrawal, Rüstem Keçili, Chaudhery G. Hussain, Eds.

March 2026, Wiley

This book provides a comprehensive overview of sustainable practices in analytical chemistry with a focus on reducing the environmental impact of analytical processes by using sustainable materials and techniques. The book reviews the latest advances in materials, sample preparation processes, extraction techniques, and sensor platforms, while also highlighting novel approaches such as smartphone-based detection and next-generation microfluidics. Emphasis is placed on the importance of nanotechnology and miniaturization in achieving sustainability goals and provides practical applications in fields such as environmental monitoring, healthcare, and food safety

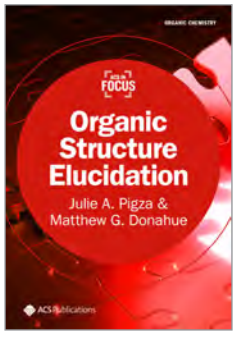

Organic Structure Elucidation *II* ACS In Focus

Julie A. Pigza, Matthew G. Donahue, Authors

May, 2026, American Chemical Society

This digital primer assists readers in developing the chemical logic required to interpret analytical data for the structural elucidation of small organic molecules. This primer focuses on elucidating organic compounds, and three main spectrometric techniques will be explored: infrared spectroscopy (IR), mass spectrometry (MS), and nuclear magnetic resonance spectroscopy (NMR). Some non-spectrometric aspects of structure elucidation will be described initially, including molecular formula, degree of unsaturation, and isomers, as they are used throughout any further analyses.

Events on Analytical Chemistry in 2026

July 23 to 24
ANALYTICA ACTA 2026
Paris, France
https://analytical-bioanalytical.pharmaceuticalconferences.com/

August 22 to 28
26th International Mass Spectrometry Conference (IMSC)
Lyon, France
https://imsc26.com/

August 30 to September 3
European Symposium on Analytical Spectrometry (ESAS)
Budapest, Hungary
https://esas2026.hu/

September 15 to 18
22nd National Meeting on Analytical Chemistry (ENQA) & 10th Ibero-American Congress on Analytical Chemistry (CIAQA)
Ruth Cardoso Cultural and Exhibition Center, Maceió, AL, Brazil
https://enqa2026.com.br/

September 28 to October 1st
11th Eurachem Workshop on Proficiency Testing in Analytical Chemistry, Microbiology and Laboratory Medicine
Hotel Complejo San Juan, Alicante, Espanha
https://eurachem-ptalicante2026.org/

October 4 to 9
XIII International Mass Spectrometry Conference on Petrochemistry, Environmental and Food Chemistry (Petromass 2026)
Yerevan, Armenia
https://petromass2026.org/

October 13 to 16
20th International Symposium on Preparative and Industrial Chromatography and Allied Techniques (SPICA 2026)
Muttenz (Basel), Suíça
https://www.spica2026.org/

Pittcon Conference & Expo

Pittcon is a catalyst for the exchange of information, a showcase for the latest advances in laboratory science, and a venue for international connectivity.

Pittcon is a dynamic, transnational conference and exposition on laboratory science, a venue for presenting the latest advances in analytical research and scientific instrumentation, and a platform for continuing education and science-enhancing opportunity. Pittcon is for anyone who develops, buys, or sells laboratory equipment, performs physical or chemical analyses, develops analysis methods, or manages these scientists.

Pittcon Awards

Honoring scientists who have made outstanding contributions to Analytical Chemistry

Each year, Pittcon provides a venue where scientists who have made outstanding contributions to laboratory science, analytical chemistry, and applied spectroscopy are honored.

Among these awards is the **Pittcon Heritage Award** which honors those visionaries whose entrepreneurial careers shaped the instrumentation and laboratory supplies community and by doing so have transformed the scientific community at large.

The award has been presented jointly with Pittcon since 2002 and is given out each year at a special ceremony during the Pittcon Conference and Expo. The recipient's name and achievements are added to the Pittcon Hall of Fame, which conference attendees can visit at the show each year.

Pittcon 2027 – Conference on Analytical Chemistry and Applied Spectroscopy
April 24-28, 2027
David L. Lawrence Convention Center
Pittsburgh, Pennsylvania, USA

Pittcon®
Conference and Exposition

Why Pittsburgh?

From Roots in Steelmaking to Innovative Technology

Meet the New Pittsburgh

- Heavily driven by advanced manufacturing, emerging technologies, healthcare, higher education, and university start-ups
- Over 29 colleges and universities, anchored by highly ranked research institutes like Carnegie Mellon University (CMU), Duquesne University, and the University of Pittsburgh (Pitt).
- Major academic and industrial disciplines include AI, Chemistry, Computer Science, Engineering, Health & Life Sciences, Materials Science, Medical Devices, Nanotechnology, and Robotics
- Corporate R&D headquarters of industrial leaders: Alcoa, Arconic, Calgon Carbon, Covestro, Kraft Heinz, PPG, U.S. Steel, Vitro, and many others
- U.S. Department of Energy (DOE) Government Labs: National Energy Technology Laboratory (NETL) and Bettis Atomic Power Laboratory

Pittcon 2027 Tracks

- AI & Data Analytics
- Bioanalytical & Life Sciences
- Environmental & Energy
- Forensic Science & Toxicology
- Instrumentation Innovations & Applications
- Materials & Nanoscience
- Pharmaceuticals & Biologics
- Professional & Career Development

So What is Pittcon?

Pittcon is a dynamic, international conference and exposition on laboratory science, a venue for presenting the latest advances in analytical research and scientific instrumentation, and a platform for continuing education and science-enhancing opportunity.

WHO SHOULD ATTEND? | EXPLORE PITTCON

Pittcon®
Conference and Exposition

SelectScience® Pioneers online Communication and Promotes Scientific Success

SelectScience®
The Fastest Way to Expert Opinion™

SelectScience® promotes scientists and their work, accelerating the communication of successful science. Through trusted lab product reviews, virtual events, thought-leading webinars, features on hot scientific topics, eBooks and more, independent online publisher SelectScience® provides scientists across the world with vital information about the best products and techniques to use in their work.

Some recent contributions from SelecScience® to the scientific community

EDITORIAL FEATURES

Advances in Bioanalytical Method Development

Bioanalytical method development is undergoing a transformation, driven by the need for greater sensitivity, specificity, and speed in the analysis of complex biological matrices. As the demand for robust data grows across drug development, the pressure to deliver accurate, reproducible, and regulatory-compliant methods has never been higher.

This dedicated feature explores the technologies, strategies, and digital tools shaping the future of bioanalytical method development. Discover expert insights, emerging trends, and curated resources to support innovation and decision-making across the bioanalysis landscape. Access here

Integrating LC-MS and Ligand Binding Assays to Meet Bioanalytical Demands

How two CROs are uniting ligand-binding assays and LC-MS expertise to tackle the complexity of modern biologics.

In this guest editorial we explore how an emerging collaboration between two expert CROs, Svar Life Science and Lablytica Life Science, is designed to address common bioanalytical challenges and support drug development from discovery through the clinic. Access **here**

Tracking PFAS and Emerging Environmental Contaminants

This SelectScience® Editorial Feature serves as a high-authority intelligence hub for environmental scientists and analytical chemists. It brings together validated workflows, emerging technologies, and expert-driven insights to help you stay ahead of evolving PFAS challenges. Explore cutting-edge approaches to PFAS quantification in aqueous samples, innovative extraction strategies for complex solid matrices, and advanced digestion techniques for AOF determination in line with EPA Method 1621, equipping your laboratory with the tools needed to elevate PFAS monitoring programs. Access here

WEBINAR

Enhance your Sample Prep and Chromatography for Environmental Contaminant Analysis

This webinar will highlight sample preparation and chromatography considerations during both routine and advanced LC-MS/MS workflows, for trace level contaminants including PFAS and GenX compounds. Access here

SelectScience® is the leading independent online publisher connecting scientists to the best laboratory products and applications.

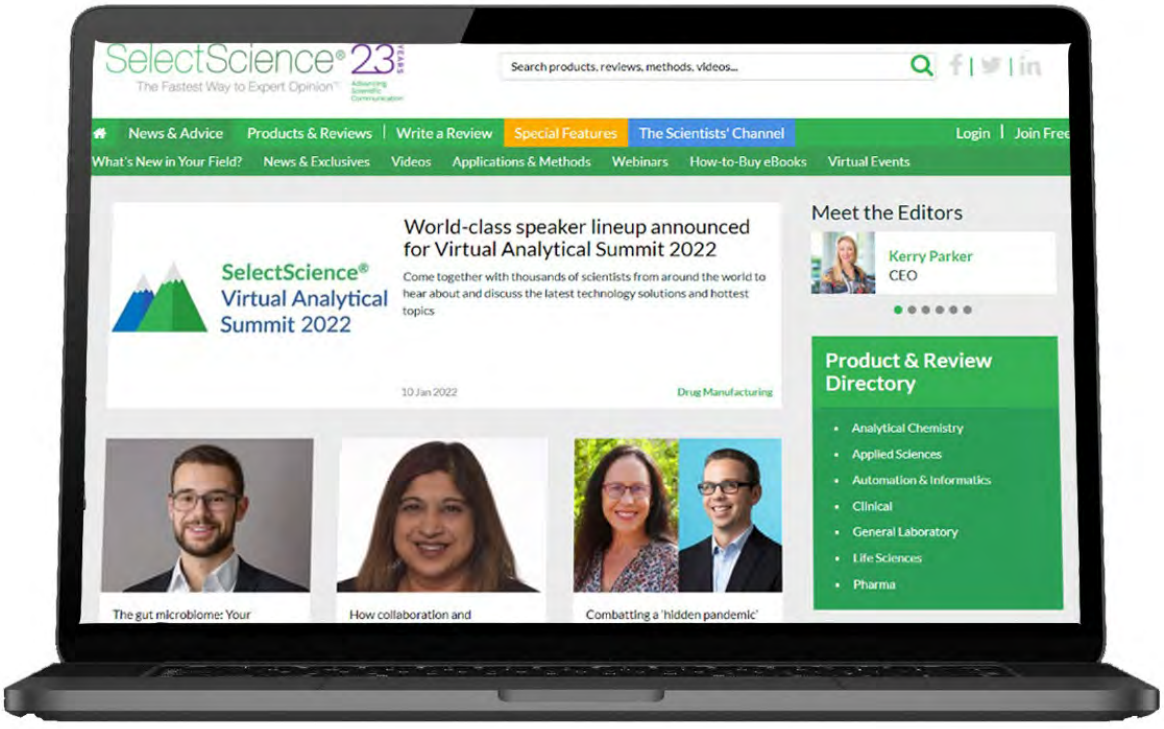

- Working with Scientists to Make the Future Healthier.
- Informing scientists about the best products and applications.
- Connecting manufacturers with their customers to develop, promote and sell technologies.

SelectScience®
The Fastest Way to Expert Opinion

CHROMacademy is the leading provider of eLearning for analytical science

CHROMacademy *helps scientific organizations acquire and maintain excellence in their laboratories*.

For over 10 years, CHROMacademy has increased knowledge, efficiency and productivity across all applications of chromatography. With a comprehensive library of learning resources, members can improve their skills and knowledge at a pace that suits them.

CHROMacademy covers all chromatographic applications – HPLC, GC, mass spec, sample preparation, basic lab skills, and bio chromatography. Each paradigm contains dozens of modules across theory, application, method development, troubleshooting, and more. Invest in analytical eLearning and supercharge your lab.

For more information, please visit www.chromacademy.com/

LC GC's **CHROMacademy**
powered by crawford scientific

CHROMacademy Lite members have access to less than 5% of our content. Premier members get so much more !

Video Training courses

Fundamental HPLC
Fundamental GC
Fundamental LCMS
Fundamental GCMS
HPLC Method Development
GC Method Development

Ask the Expert

We are always on hand to help fix your instrument and chromatographic problems, offer advice on method development, help select a column for your application and more.

To find out more about Premier Membership contact:

Glen Murry: +1 732.346.3056 | Glen.Murry@ubm.com
Peter Romillo: +1 732.346.3074 | Peter.Romillo@ubm.com

www.chromacademy.com

The worlds largest e-Learning website for analytical scientists

PERIODICALS & WEBSITES

American Laboratory® is a platform that addresses basic research, clinical diagnostics, drug discovery, environmental, food and beverage, forensics and other markets, and combines in-depth articles, news, and video to deliver the latest advances in their fields.
Featured Article: ***Q&A: Food Safety and Contamination Testing.*** As an analytical chemist at RTI Int., Walker-Franklin, uses a multitude of spectrometry and chromatography techniques to identify novel contaminants and metabolites in complex environmental and biological samples. In this Q&A, he outlines how these contaminants move, why their ubiquity makes prevention difficult and how limitations in sensitivity and reproducibility lead to a lack of standardized approaches for measuring microplastics. **Access here**

LCGC
Chromatographyonline delivers practical, nuts-and-bolts information to help scientists and lab managers become more proficient in the use of chromatographic techniques and instrumentation.
Article: ***Analytical Procedure Lifecycle Approaches in Accordance with ICH Q14 and ICH Q2(R2): Opportunity Knocks, or Just Another Challenge and Headache? Part 1.*** By Amanda G. Mahr, Jean-M. Roussel, Luis F. Ortiz, Adrian Clarke. This series addresses if this is a great opportunity to develop a greater understanding of method performance to ensure continuous improvement and regulatory flexibility, or if it is just additional challenges, complexity, and headaches.

Scientia Chromatographica
Scientia Chromatographica is the first and to date the only Latin American scientific journal dedicated exclusively to Chromatographic and Related Techniques. With a highly qualified and internationally recognized Editorial Board, it covers all chromatography topics in all their formats, in addition to discussing related topics such as “The Pillars of Chromatography”, Quality Management, Troubleshooting, Hyphenation (GC-MS, LC-MS, SPE-LC-MS/MS) and others. It also provides columns containing general information, such as: calendar, meeting report, bookstore, etc. **Read more**

Select Science
SelectScience® has transformed global scientific communications and digital marketing. It informs scientists about the best products and applications, connects manufacturers with their customers to develop, promote, and sell technologies, and promotes scientists and their work. This accelerates the communication of successful science. Scientists can make better decisions using independent expert information and easily access manufacturers. SelectScience® informs the global scientific community through editorial, feature, video, and webinar programs. **Read more**

Spectroscopy
With the *Spectroscopy* journal, scientists, technicians, and lab managers gain proficiency through unbiased, peer-reviewed technical articles, trusted troubleshooting advice, and best-practice application solutions. **Article:** ***New Product Advances in Vibrational and Atomic Spectroscopy (2025–2026).*** By Jerome Workman, Jr. Spectroscopy instrumentation and software are transitioning to intelligent, interconnected analytical “ecosystems.” Advances in detection, optics, and software across electronic, vibrational, atomic, and imaging spectroscopy have resulted in higher sensitivity, miniaturized and portable platforms, and multimodal capabilities. This review synthesizes major developments in spectroscopy systems and software from 2025–2026 and discusses emerging trends toward autonomous analytical laboratories. **Read more**

BrJAC AUTHOR GUIDELINES

Aims & Scope

Brazilian Journal of Analytical Chemistry is a double-blind peer-reviewed research journal dedicated to the diffusion of significant and original knowledge in all branches of Analytical and Bioanalytical Chemistry. It is addressed to professionals involved in science, technology, and innovation projects at universities, research centers and in industry. **BrJAC welcomes** the submission of research papers reporting studies devoted to new and significant analytical methodologies, putting in evidence the scientific novelty, the impact of the research and demonstrating the analytical or bioanalytical applicability. BrJAC **strongly discourages** those simple applications of routine analytical methodologies, or the extension of these methods to new sample matrices, unless the proposal contains substantial novelty and unpublished data, clearly demonstrating advantages over existing ones.

Additionally, there are other submission categories to BrJAC such as:

Reviews: They should be sufficiently broad in scope, but specific enough to permit an appropriate depth discussion, including critical analyses of the bibliographic references and conclusions. Manuscripts submitted for publication as Reviews must be original and unpublished. Reviews undergo double-blind full peer review and are handled by the Editor of Reviews.

Technical Notes: Concise descriptions of developments in analytical methods, new techniques, procedures, or equipment falling within the scope of the BrJAC. Technical notes also undergo double-blind full peer review.

Letters: Discussions, comments, and suggestions on issues related to Analytical Chemistry or Bioanalytical Chemistry. Letters are welcome and will be published at the discretion of the BrJAC Editor-in-Chief.

Points of View: This category is exclusively invited by the Editor-in-Chief.

See the next items for more information on the journal, the documents preparation, manuscript types, and how to prepare the submission.

Professional Ethics

Originality: manuscripts submitted for publication in BrJAC cannot have been previously published or be currently submitted for publication in another journal.

Preprint: BrJAC does not accept manuscripts that have been posted on preprint servers prior to the submission.

Integrity: the submitted manuscripts are the full responsibility of the authors. Manipulation/invention/omission of data, duplication of publications, the publication of papers under contract and confidentiality agreements, company data, material obtained from non-ethical experiments, publications without consent, the omission of authors, plagiarism, the publication of confidential data and undeclared conflicts of interests are considered serious ethical faults.
BrJAC discourages and restricts the practice of excessive self-citation by the authors.
BrJAC does not practice coercive citation, that is, it does not require authors to include references from BrJAC as a condition for achieving acceptance, purely to increase the number of citations to articles from BrJAC without any scientific justification.

Transparency: The use of artificial intelligence (AI) by authors must comply with the transparency guidelines below:

- Authors are responsible for all content submitted to BrJAC, including the accuracy of AI-generated content.

- The authors must provide a declaration regarding the use of artificial intelligence in preparing the submitted manuscript. A template for this declaration is available for download **here**. Authors must use this template when writing their declaration.
- For accepted articles, this declaration will appear in the published article as a section before the References, entitled "Use of Artificial Intelligence (AI) Tools".
- AI tools should not be listed as authors, as they cannot be held responsible for the published work.
- Any use of AI tools for text or image generation must be declared in the Methods section of the manuscript, with a description of how and for what purpose the AI tools were used.
- If AI is used to create graphics and the cover artwork, the name of the tool(s) used and a brief description of how the image was created should be included in the figure caption. Authors are responsible for ensuring that the terms of use of the tools used state that the result is not the property of the generating site.
- The Editor may, at his/her discretion, determine that the use of AI in a particular submission is too extensive. This determination may result in rejection of the manuscript or a request to remove or reduce the AI-generated portions of the manuscript.
- In the peer review process, the BrJAC states that the opinion of the reviewers consulted is solely that of the reviewer. The use of AI tools in the review of manuscripts is not accepted. This BrJAC standard is intended to protect the confidentiality of the manuscript.

Self-citation: BrJAC discourages and restricts the practice of excessive self-citation by the authors. The maximum percentage of self-citations acceptable by BrJAC is 20%.

Coercive citation: BrJAC does not practice coercive citation. That is, BrJAC does not require authors to include BrJAC references as a condition for acceptance, purely to increase BrJAC articles citations without scientific justification.

Similarities: Manuscripts submitted to BrJAC are analyzed for similarities using specialized software. The maximum total similarity index accepted by the BrJAC is 25%, with a maximum of 3% for each source.

Conflicts of interest: when submitting their manuscript for publication, the authors must include all potential sources of bias such as affiliations, funding sources and financial, management or personal relationships which may affect the work.

Copyright: will become the property of the Brazilian Journal of Analytical Chemistry, if and when a manuscript is accepted for publication. The copyright comprises exclusive rights of reproduction and distribution of the articles, including reprints, photographic reproductions, microfilms or any other reproductions similar in nature, including translations.

Request for permission to reuse figures and tables published in the BrJAC: researchers who want to reuse any document or part of a document published in the BrJAC should request reuse permission from the BrJAC Editor-in-Chief, even if they are the authors of such document. A template for requesting reuse permission can be downloaded **here**.

Misconduct will be treated according to the COPE's recommendations (https://publicationethics.org/) and the Council of Science Editors White Paper on Promoting Integrity in Scientific Journal Publications (https://www.councilscienceeditors.org/).

Manuscript submission

The BrJAC does not charge authors an article processing fee.

Manuscripts must be prepared according to the BrJAC manuscript template. Manuscripts in disagreement with the BrJAC guidelines are not accepted for revision.

The submission of manuscripts is done online by a submitting author through a digital manuscript manager system, which guides the author step by step through the entire submission process.

After the submitting author logs in to the system and enters his/her personal and affiliation details*, the submission can be started.

***Authors are required to provide an institutional e-mail address when creating or updating their registration in the manuscript management system.**

All co-authors must be added to the Authors section.

Five documents are mandatorily uploaded by the submitting author: Cover letter, Title Page, Declaration of AI usage, Novelty Statement and the Manuscript. Templates for these documents are available for download **here**.

The manuscript and the title page must be uploaded as Word files. The cover letter, declaration of AI usage, and novelty statement may be uploaded as PDF files. The manuscript Word file will be converted by the system to a PDF file which will be used in the double-blind peer review process.

All correspondence, including notification of the Editor's decision and requests for revision, is sent by e-mail to the submitting author through the manuscript manager system.

Documents Preparation

It is highly recommended that authors download and use the templates to create their five mandatory documents to avoid the suspension of a submission that does not meet the BrJAC guidelines.

Cover Letter
The cover letter template should be downloaded and filled out carefully.
Any financial conflict of interest or lack thereof and agreement with BrJAC's copyright policy must be declared.
It is the duty of the submitting author to inform his/her collaborators about the submission of the manuscript and its eventual publication.
The Cover Letter must be signed by the corresponding author.

Declaration on the Use of Artificial Intelligence
The Declaration on the AI Use template must be downloaded and filled out carefully.
The corresponding author must sign the Declaration on the AI Use.
In the declaration on the use of artificial intelligence, the corresponding author must indicate whether or not AI tools were used in preparing the manuscript.
If AI tools were used, the author must state which tools were used and for what purpose.

Title Page
The Title Page must contain information for each author: full name, affiliation and full international postal address, and information on the contribution of each author to the work. Acknowledgments must be entered on the Title Page. The submitting author must sign the Title Page.

Novelty Statement
The Novelty Statement must contain clear and succinct information about what is new and innovative in the study in relation to previously related works, including the works of the authors themselves.

Manuscript (all submission categories)

It is highly recommended that authors download the Manuscript template and create their manuscript in this template, keeping the layout of this file.

- **Language**: **English** is the language adopted by BrJAC. The correct use of English is of utmost importance. We highly recommend **Proof-Reading-Service.com**, a professional language editing service that specializes in **journal article proofreading** and **manuscript editing** for submissions to this journal. Upon completion of the proofreading, please provide a certificate confirming that the service has been carried out.

- **Required manuscript elements**: the manuscript must include a title, abstract, keywords, and the following sections: Introduction, Materials and Methods, Results and Discussion, Conclusion, and References.
- **Identification of authors**: as the BrJAC adopts a double-blind review, the manuscript file must **NOT** contain the authors' names, affiliations nor acknowledgments. Full details of the authors and their acknowledgements should be on the Title Page.
- **Layout**: the lines in the manuscript must be numbered consecutively and double-spaced.
- **Graphics and Tables**: must appear close to the discussion about them in the manuscript. For **figures** use **Arabic** numbers, and for **tables** use **Roman** numbers.
- **Figure files:** when a manuscript is approved for publication, the BrJAC production team will contact the corresponding author to request separate files of each figure and a graphical abstract. These files must have **good resolution** and the extension **PNG or JPG**. The graphical abstract should preferably be created in landscape format. In the article diagrammed in the journal, the graphical abstract will occupy a space of 8 to 9 cm in length and 6 cm in height. Chemical structures must have always the same dimensions.
- **Studies involving biological material**: for studies involving human and animal material for research purposes, authors must state in the manuscript that the research has been approved by the research ethics committee of the institution where the study was conducted.
- **Reuse of previously published material:** Authors must obtain permission from the copyright holder (publisher or scientific society) to reproduce or adapt figures, tables, or other material previously published in the scientific literature, including material originally published by the same authors. Documentation of the permission must be uploaded in the manuscript management system at the time of manuscript submission.
  Material published under Creative Commons licenses: Figures, tables, or other material distributed under a Creative Commons license may be reused or adapted in accordance with the terms of the applicable license. Authors are responsible for ensuring that all license conditions are met.
  Acknowledgment of the original source: The original source must be properly cited in the figure or table caption. When applicable, the type of license (e.g., CC BY 4.0) must also be indicated.
  Credit line: When permission is required, the credit line specified by the copyright holder must be included in the figure or table caption.
- **Chemical nomenclature, units and symbols**: should conform to the rules of the International Union of Pure and Applied Chemistry (IUPAC) and Chemical Abstracts Service. It is recommended that, whenever possible, the authors follow the International System of Units, the International Vocabulary of Metrology (VIM) and the NIST General Table of Units of Measurement. Abbreviations are not recommended except for those recognized by the International Bureau of Weights and Measures or those recorded and established in scientific publications. Use L for liters. Always use superscripts rather than /. For instance: use mg mL^{-1} and NOT mg/mL. Leave a space between numeric values and their units.
- **References throughout the manuscript:** the references must be cited as superscript numbers placed after the period at the end of the sentences. It is recommended that references older than 5 (five) years be avoided, except in relevant cases. Include references that are accessible to readers.
- **References section:** This section must be thoroughly checked for errors by the authors before submission. From 2022, BrJAC is adopting the American Chemical Society's Style in the Reference item. Mendeley Reference Manager users will find the Journal of American Chemical Society citation style in the Mendeley View menu. Non-users of the Mendeley Reference Manager may refer to the ACS Reference Style Quick Guide DOI: https://doi.org/10.1021/acsguide.40303

Review process

Manuscripts submitted to the BrJAC undergo an initial check for compliance with all of the journal's guidelines. Submissions that do not meet the journal's guidelines will be suspended and an alert sent to the corresponding author. The authors will be able to resend the submission within 30 days. If the submission

according to the journal's guidelines is not made within 30 days, it will be deleted from the BrJAC system on the first subsequent day, and an alert will be sent to the corresponding author.

Manuscripts that are in accordance with the journal's guidelines undergo a similarity analysis using specialized software.

The manuscript is then forwarded to the Editor-in-Chief who will check whether the manuscript is in accordance with the journal's scope and will analyze the similarity report. The maximum total similarity index accepted by the BrJAC is 25%, with a maximum of 3% for each source.

If the manuscript passes the screening described above, it will be forwarded to an Associate Editor who will also analyze the similarity report and invite reviewers.

Manuscripts are reviewed in double-blind mode by at least 2 reviewers. A larger number of reviewers may be used at the discretion of the Editor. As evaluation criteria, the reviewers employ originality, scientific quality, contribution to knowledge in the field of Analytical Chemistry, the theoretical foundation and bibliography, the presentation of relevant and consistent results, compliance with the BrJAC's guidelines, clarity of writing and presentation, and the use of grammatically correct English.

Note: In case the Editors and Reviewers consider the manuscript to require an English revision, the authors will be required to send an English proofreading certificate, by the ProofReading Service or equivalent service, before the final approval of the manuscript by the BrJAC.

The first-round review process usually takes around 5-6 weeks. If the manuscript is not rejected but requires corrections, the authors will have one month to submit a corrected version of the manuscript. In another 3-4 weeks, a new decision on the manuscript may be presented to the corresponding author.

The manuscripts accepted for publication are forwarded to the BrJAC production department. Minor changes to the manuscripts may be made, when necessary, to adapt them to BrJAC guidelines or to make them clearer in style, respecting the original content. The articles are sent to the authors for approval before publication. Once published online, a DOI number is assigned to the article.

Final Considerations

Whatever the nature of the submitted manuscript, it must be original in terms of methodology, information, interpretation or criticism.

With regard to the contents of published articles and advertisements, the sole responsibility belongs to the respective authors and advertisers; the BrJAC, its editors, editorial board, editorial office and collaborators are fully exempt from any responsibility for the data, opinions or unfounded statements.

Manuscript submission at www.brjac.com.br